Towards an effective vaccine against *Plasmodium vivax* malaria



Thomas Rawlinson

Lincoln College

University of Oxford

A Thesis submitted for the degree of

Doctor of Philosophy

Trinity 2018

Abstract

Over seventy vaccines are now licensed against more than thirty pathogens, but despite a century of effort, the malaria parasite is not among them. In the meantime, effective drugs and anti-mosquito measures notwithstanding, millions still suffer and die from of a disease which belongs in the history books. The reasons are largely political and economic, malaria is a neglected disease of the poor, but also scientific; a parasite as protean as *Plasmodium* is not easy to pin down with a vaccine.

It has been known for over a hundred years that almost a billion people on the world's most malarial continent are 'naturally immune' to *Plasmodium vivax* (*P. vivax*) malaria. I can think of no other human pathogen with such an ancient and continental-scale natural experiment to inspire research. The source of this immunity was discovered, over forty years ago, to be due to the lack of the Duffy antigen on the surface of red blood cells. The parasite must bind to this Duffy antigen, using its 'Duffy-binding protein' (DBP), in order to invade the erythrocyte. Despite this 'Achilles heel' of *P. vivax* being known about for decades, it was not until 2014 that it was first targeted in a human vaccine trial. This long overdue trial of a *P. vivax* DBP (PvDBP) vaccine provided the source material for, and the starting point of, this DPhil Thesis. The extreme polymorphism of malaria antigens, such as PvDBP, poses a great challenge to vaccine design, but new approaches are emerging to tackle this and it is one of these, known as 'epitope-focused vaccinology', that I pursue in this Thesis. I report the production of the first panel of vaccine-induced human monoclonal antibodies (mAb) against PvDBP and, through testing in functional assays using both *P. vivax* and a transgenic *Plasmodium knowlesi* line, the discovery of a broadly-neutralising mAb. X-ray crystallographic studies have identified its epitope on PvDBP and the process of re-engineering the PvDBP vaccine to place this conserved and critical epitope in the immune system's spotlight has begun.

Acknowledgements

My thanks to:

Simon Draper, my DPhil Supervisor, whose infectious enthusiasm made even binding ELISAs seem exciting and whose eagle eye never missed a wandering data point. Angela Minassian, who, when I asked her, in a corridor of the John Radcliffe Hospital four years ago, if she knew any good malaria researchers in Oxford, introduced me to her husband. My Co-Supervisor, Matt Higgins, and his student Natalie Barber, who through the dark art of crystallography unveiled the epitope of 'DB9' (see below).

All my Jenner Institute colleagues and in particular Dan, Florian, Jo, Dave, Sarah and Martino, who patiently taught a simple quack how to hold a pipette and guided me through a labyrinth of buffers and plasmids.

Rob Moon and Franziska Mohring from the London School of Hygiene and Tropical Medicine for their work on the transgenic *Plasmodium knowlesi*.

Bruce Russel, Laurent Renia, Francois Nosten, Jee Sun Cho and Varakorn Kosaisavee for making possible the *Plasmodium vivax* invasion assays in Thailand and Singapore.

Robert Victor Coxon, my Grandfather, whose 1950 DPhil Thesis sat on my desk and kept me writing when my spirits sagged. Though his Thesis and subsequent decades of medical research were in a very different field, I discovered that in 1945 he published a paper on malaria and it is in homage to him that I cite this as my first reference [102].

John, Sally, Kate and Susie, my clan, who never fail to encourage me in my meanderings.

And lastly, to L.B.J., my co-pilot, without whom nothing

Contents

List of Figures **xi**

List of Tables **xiii**

List of Abbreviations **xv**

1 Introduction **1**

1.1 Malaria; a brief history 1

1.1.1 Prehistory 1

1.1.2 On the Origin of Species 2

1.1.3 The Malaria Hypothesis 3

1.1.4 Out of Africa 4

1.1.5 Recorded History 5

1.2 *Plasmodium vivax* 11

1.2.1 Global public health significance 11

1.2.2 Biology and life-cycle 12

1.2.3 Red blood cell invasion 18

1.2.4 Clinical aspects of *Plasmodium vivax* 27

1.2.5 Natural immunity to *Plasmodium vivax* 30

1.3 The next generation of vaccines 35

1.4 Vaccines against *Plasmodium vivax* 37

1.5 Thesis outline and aims 42

2 Materials and Methods **45**

2.1 Materials 45

2.1.1 Reagents 45

2.1.2 Buffers and solutions 47

2.1.3 Primers 48

2.1.4 Lab consumables 50

2.1.5 Electronic Equipment 51

2.2 Chapter III methods 52

2.2.1 Production of mAbs 52

2.2.2 Recombinant protein expression 58

2.2.3 Screening the mAbs for antigen-specificity 60
2.2.4 Plasmid DNA preparation and *E. coli* culture 60
2.2.5 Expression of the PvDBPII-specific mAbs 61
2.2.6 Purification of the mAbs 61
2.2.7 Sequencing 61
2.2.8 Determination of antibody kinetics using SPR 61
2.2.9 Epitope binning by Bio-layer interferometry 62
2.2.10 PvDBPII-DARC binding inhibition assays 63
2.3 Chapter IV methods 64
2.3.1 Genetic modification of *Plasmodium knowlesi* parasites . . . 64
2.3.2 Assays of growth inhibitory activity (GIA) with *Plasmodium Knowlesi* 66
2.3.3 Statistical analysis 67
2.4 Chapter V methods 68
2.4.1 Short term *ex vivo* Pv invasion assays 68
2.4.2 Purification of reticulocytes from umbilical cord blood . . . 68
2.4.3 Purification of schizonts from *ex vivo* Pv samples 68
2.4.4 Sequencing of the PvDBPII gene from Thai isolates 70
2.5 Chapter VI methods 71
2.5.1 X-ray crystallography 71
2.5.2 Rabbit immunization 73
2.5.3 Quantification of antigen-specific antibody 75
2.5.4 GIA assays with rabbit serum 76
2.5.5 Statistical analysis 76
2.6 Chapter VII methods 76
2.6.1 AAV-expressed DB9 76
2.6.2 DB9-DARC immuno-adhesin 77
2.6.3 Pv-infected blood from returning travellers 78
2.6.4 Passive transfer mouse model 78

3 Isolation of a vaccine-induced panel of human monoclonal antibodies against *Plasmodium vivax* 81
3.1 Authorship statement 81
3.2 Introduction 81
3.3 Production of human mAbs to PvDBPII 84
3.4 Characterisation of the mAbs 93
3.4.1 Affinity and kinetics 93
3.4.2 Competition for epitopes 97
3.4.3 PvDBPII-DARC binding inhibition assays 99
3.5 Discussion 107

4 Transgenic *Plasmodium knowlesi* assays **111**
4.1 Authorship statement . . . 111
4.2 Introduction . . . 111
4.2.1 The assay of GIA . . . 112
4.2.2 *Plasmodium knowlesi* (Pk) . . . 113
4.3 *Plasmodium knowlesi* GIA . . . 117
4.3.1 Setting up the assay . . . 117
4.3.2 Controls . . . 119
4.3.3 Transgenic *Plasmodium knowlesi* . . . 123
4.3.4 Pk GIA assays with polyclonal rabbit serum . . . 126
4.3.5 Anti-PvDBPII mAbs in the Pk GIA assays . . . 128
4.3.6 Correlation between antibody kinetics and neutralisation . . . 132
4.4 Discussion . . . 134

5 *Plasmodium vivax* assays **137**
5.1 Authorship statement . . . 137
5.2 Introduction . . . 137
5.2.1 *Plasmodium vivax in vitro* . . . 137
5.2.2 The reticulocyte . . . 138
5.2.3 *Plasmodium vivax ex vivo* . . . 140
5.3 The human anti-PvDBPII mAbs in the *ex vivo* invasion assay . . . 143
5.3.1 Reticulocyte purification . . . 143
5.3.2 Schizont purification . . . 144
5.3.3 Controls . . . 145
5.3.4 The anti-PvDBPII human mAbs . . . 145
5.4 Sequencing the strains . . . 148
5.5 Combining the mAbs . . . 151
5.6 Discussion . . . 154

6 A broadly-neutralising epitope on PvDBPII **159**
6.1 Authorship statement . . . 159
6.2 Introduction . . . 159
6.2.1 Epitope mapping . . . 159
6.2.2 Epitope-focused vaccine design . . . 160
6.3 The crystal structure of DB9 bound to PvDBPII . . . 167
6.4 Subdomain three . . . 171
6.4.1 Immunising with SD3 . . . 175
6.5 Discussion . . . 178

7 Conclusions and future directions **183**
7.1 Summary of output . . . 183
7.1.1 Human mAbs against *Plasmodium vivax* . . . 183
7.1.2 Proof of concept of a transgenic *Plasmodium knowlesi* model for testing anti-*P. vivax* antibodies . . . 183
7.1.3 Isolating the first human broadly-neutralising antibody against *P. vivax* . . . 184
7.1.4 Mapping the broadly-neutralising epitope on PvDBPII . . . 184
7.2 Future directions . . . 185
7.2.1 *In vivo* data . . . 185
7.2.2 AAV-vectored DB9 . . . 186
7.2.3 Immuno-adhesins . . . 187
7.2.4 Other antigens . . . 188
7.3 Final thoughts . . . 189

Bibliography **191**

List of Figures

1.1 Phylogeny of malaria parasites . . . 3
1.2 Malaria mortality in the 20^{th} century . . . 8
1.3 Endemicity of *Plasmodium vivax* . . . 11
1.4 Life cycle of *Plasmodium vivax* . . . 15
1.5 Erythrocyte invasion . . . 18
1.6 The Duffy antigen receptor for chemokines (DARC) . . . 22
1.7 Overview of *P. vivax* merozoite interaction with the RBC membrane 24
1.8 Global frequencies of the Fy alleles . . . 26
1.9 National allele frequency of G6PD deficiency . . . 30
1.10 Impact of vaccination on mortality rates . . . 35
1.11 Malaria vaccine candidates in development . . . 38
1.12 Merozoite antigens . . . 40

2.1 Ig chain-specific vectors . . . 57

3.1 VAC051 clinical trial . . . 83
3.2 Antigen-specific ASC response after infection or vaccination . . . 85
3.3 Schematic of mAb production . . . 86
3.4 Protein gel electrophoresis of V_H, V_κ and V_λ exon inserts . . . 87
3.5 Screening ELISA for IgG and antigen-specific IgG . . . 88
3.6 Immunological data from clinical trial volunteers . . . 89
3.7 Sequencing of the mAbs . . . 92
3.8 Affinity of mAbs . . . 93
3.9 SPR sensorgram . . . 94
3.10 Binding kinetics of the mAbs . . . 96
3.11 Competition for binding sites on PvDBPII . . . 98
3.12 Cartoon of the PvDBPII-DARC binding inhibition assay . . . 100
3.13 PvDBPII-DARC binding-inhibition of the polyclonal clinical trial sera using the Sal1 PvDBPII . . . 101
3.14 PvDBPII-DARC binding inhibition of the clinical trial sera using variant alleles of PvDBPII . . . 102
3.15 PvDBPII allelic variants . . . 103

3.16 Polymorphic residues on the HMP013 variant of PvDBPII 103
3.17 Binding-inhibition of the mAbs against five variant alleles of recombinant PvDBPII 105
3.18 Summary histogram of the binding-inhibition of each mAb against the variant PvDBPII alleles 106

4.1 Schematic of the *P. knowlesi* GIA assay 118
4.2 Setting up the *P. knowlesi* GIA assay 119
4.3 Expression of DARC Fya 121
4.4 Testing controls for the *P. knowlesi* GIA assay 122
4.5 Schematic summary of the genetic modification of *P. knowlesi* . . . 123
4.6 CRISPR-Cas9 strategy for *P. knowlesi* 125
4.7 Polyclonal rabbit anti-PvDBPII IgG in the *P. knowlesi* assay 127
4.8 Rabbit anti-PkCyRPA and anti-PkMSP against Pk A1H1 128
4.9 Human anti-PvDBPII mAbs in the transgenic *P. knowlesi* GIA assays 129
4.10 Sequence alignment of region II of PvDBP and PkDBPα 131
4.11 Anti-PvDBPII mAb epitope binning by neutralisation phenotype . 131
4.12 Correlating mAb binding kinetics with GIA 133
4.13 Histogram showing the speed of merozoite invasion of erythrocytes . 135

5.1 Schematic of the *P. vivax ex vivo* invasion assays 142
5.2 Purification of reticulocytes from umbilical cord blood 143
5.3 Synchronisation of *P. vivax* schizonts 144
5.4 Smear microscopy of control wells in the *P. vivax ex vivo* invasion assays 145
5.5 Invasion inhibition of the mAbs in the Thai *ex vivo* invasion assays 147
5.6 Polymorphisms within PvDBPII of the Thai *P. vivax* isolates . . . 150
5.7 Synergy assays of the mAbs 153

6.1 Epitope-focused vaccine design 163
6.2 Structure of PvDBPII 165
6.3 X-ray crystal structure of DB9 Fab in complex with PvDBPII . . . 167
6.4 Contact amino acids in PvDBPII and DB9 Fab complex 170
6.5 Sequence alignments of subdomain III of PvDBPII 172
6.6 Binding of the panel of mAbs to PvDBPII subdomain III 174
6.7 Reactivity of rabbit anti-PvDBPII-SD3 sera 176
6.8 Rabbit anti-PvDBPII-SD3 IgG in the transgenic *P. knowlesi* GIA assay 177

7.1 Cartoon illustrating the binding of an anti-HIV immuno-adhesin. . 188

List of Tables

2.1 Reagents 47
2.2 Buffers and solutions 48
2.3 Primers 50
2.4 Lab consumables 51
2.5 Electronic equipment 51
2.6 RT Primer mix 52
2.7 RT-PCR reaction 53
2.8 PCR 1 53
2.9 Nested PCR Gamma Chain 54
2.10 Nested PCR Kappa Chain 54
2.11 Nested PCR Lambda Chain 55
2.12 Insert Digestion Reaction 56
2.13 Backbone digestion reaction 56
2.14 Colony screen PCR 58
2.15 Immunisation Schedule 75

3.1 Success rate of mAb production 90
3.2 Sequencing of the mAb variable regions 91
3.3 Affinity and kinetic rate constant values for each mAb 95

5.1 Summary of published *P. vivax ex vivo* invasion assays 141

6.1 Contact residues between DB9 and PvDBPII 168
6.2 Data collection and refinement statistics for the DB9 Fab:PvDBPII complex 169
6.3 Rabbit immunisation schedule 175

List of Abbreviations

AAV . . . . . Adeno-associated virus

Ab . . . . . Antibody

ADCC . . . . . Antibody-dependent cell-mediated cytotoxicity

APC . . . . . Antigen Presenting Cell

ASC . . . . . Antibody-secreting cell

AU . . . . . Arbitrary Units

BAP . . . . . Biotin Acceptor Peptide,

BCIP/NBT . 5-bromo-4-chloro-3'-indolyphosphate / nitro-blue tetrazolium

BCR . . . . . B cell receptor

BLI . . . . . Bio-Layer interferometry

bnAb . . . . . Broadly-neutralising antibody

BSA . . . . . Bovine Serum Albumin

CCR . . . . . Chemokine Receptor

CD . . . . . Cluster of differentiation

CDC . . . . . Complement-dependent cytotoxicity

CDR . . . . . Complementarity-determining regions

cDNA . . . . . Complementary deoxyribonucleic acid

CFCA . . . . . Calibration-free concentration analysis

ChAd63 . . . . Chimpanzee adenovirus serotype 63

CHMI . . . . . Controlled human malaria infection

COS cells . . . A simian cell line, carrying genetic material from SV40 virus

CPEC . . . . . Circular polymerase extension cloning

CYRPA . . . . Cysteine-rich protective antigen

DARC . . . . . Duffy antigen receptor for chemokines

DBL . . . . . Duffy binding-like

DBP . . . . . Duffy binding protein

DDT . . . . . Dichloro-Diphenyl-Trichloroethane

DMEM . . . . Dulbecco's modified Eagle medium

DMSO . . . . . Dimethyl sulphoxide

DNA . . . . . Deoxyribonucleic acid

EBA175 . . . . Erythrocyte Binding Antigen 175

EBL . . . . . Erythrocyte binding-like

EBV . . . . . Epstein-Barr Virus

EC50 . . . . . Effective concentration to achieve 50% of maximal effect

EDTA . . . . . Ethylenediaminetetraacetic acid

ELISA . . . . . Enzyme-linked immunosorbent assay

ELIspot . . . . Enzyme-linked immunospot (assay)

Fab . . . . . Fragment antigen binding

FACS . . . . . Fluorescence-activated cell sorting

Fc . . . . . Fragment crystallisable

FcR . . . . . Fc Receptor

FCS . . . . . Fetal calf serum

FDA . . . . . United States Food and Drug Administration

FPLC . . . . . Fast protein liquid chromatography

Fy . . . . . Gene encoding Duffy antigen

G6PD . . . . . Glucose-6-phosphate dehydrogenase

GIA . . . . . Growth inhibitory activity

GPI . . . . . Glycosylphosphatidylinositol

GP . . . . . Glycoprotein

HC . . . . . Heavy chain

Hct . . . . . Haematocrit

HDX-MS . . . Hydrogen-deuterium exchange mass spectrometry

HEK293 . . . Human embryonic kidney cell 293

HEPES . . . . (4-(2-hydroxyethyl)-1-piperazineethanesulfonic acid

His . . . . . Six histidine tag

HIV . . . . . Human immunodeficiency virus

hmAb . . . . . Human monoclonal antibody

ICM . . . . . Incomplete culture Medium

IEs . . . . . Infected Erythrocytes

IFA . . . . . Immunofluorescence assay

IFN-γ . . . . . Interferon-gamma

IgG . . . . . Immunoglobulin G

i.m. . . . . . Intramuscular

ITN . . . . . Insecticide-treated net

i.v. . . . . . Intravenous

iRBC . . . . . Infected red blood cell

kDa . . . . . Kilodalton

LB . . . . . Lysogeny broth

LC . . . . . Light chain

mAb . . . . . Monoclonal antibody

MACS . . . . . Magnetic-activated cell sorting

mBC . . . . . Memory B cell

MHC . . . . . Major histocompatibility complex

MSP1 . . . . . Merozoite surface protein 1

MVA . . . . . Modified vaccinia Ankara

MW . . . . . Molecular weight

NAI . . . . . Naturally acquired immunity

Ni . . . . . Nickel

NHP . . . . . Non-human primate

NHS . . . . . National Health service

NMR . . . . . Nuclear magnetic resonance

O.D . . . . . Optical density

OD405 . . . . . Optical density measured at 405 nm

ORF . . . . . Open reading frame

pAb . . . . . Polyclonal antibody

PABA . . . . . 4-aminobenzoic acid

PAGE . . . . . Polyacrylamide Gel Electrophoresis

PATH-MVI . Programme for Appropriate Technology in Health – Malaria Vaccine Initiative

PBMC . . . . Peripheral blood mononuclear cell

PBS . . . . . (Dulbecco's) phosphate-buffered saline

PBS-T . . . . . (Dulbecco's) phosphate-buffered saline + 0.005% Tween20.

PCR . . . . . Polymerase chain reaction

PEG . . . . . Polyethylene glycol

PEI . . . . . Polyethylenimine

PfCyRPA . . . *Plasmodium falciparum* cysteine-rich protective antigen

PfEBA-175 . . *Plasmodium falciparum* erythrocyte binding antigen 175

PfEBL-1 . . . *Plasmodium falciparum* erythrocyte binding-like (protein)

PfEMP-1 . . . *Plasmodium falciparum* erythrocyte membrane protein

PfRH5 . . . . . *Plasmodium falciparum* reticulocyte-binding protein homologue 5

PfRIPR . . . . *Plasmodium falciparum* RH5-interacting protein

Pfu . . . . . Plaque forming units

Pk . . . . . *Plasmodium knowlesi*

PkDBP$\alpha/\beta/\gamma$ *Plasmodium knowlesi* Duffy-binding protein alpha/beta/gamma

PkCyRPA . . *Plasmodium knowlesi* cysteine-rich protective antigen

PkMSP . . . . *Plasmodium knowlesi* merozoiite surface protein

PMR . . . . . Parasite multiplication rate

PNPP . . . . . p-Nitrophenyl phosphate

PR . . . . . Annual mean parasite rate

Pv . . . . . *Plasmodium vivax*

PvDBP . . . . *Plasmodium vivax* Duffy-binding protein

PvDBPII . . . *Plasmodium vivax* Duffy-binding protein region II.

PvRBP . . . . *Plasmodium vivax* reticulocyte-binding protein

PvCyRPA . . *Plasmodium vivax* cysteine-rich protective antigen

qPCR . . . . . Quantitative polymerase chain reaction

RBC . . . . . Red blood cell

RBL/RBP . . Reticulocyte binding-like proteins

RMSD . . . . . Root-mean-square deviation

RNA . . . . . Ribonucleic acid

RPM . . . . . Revolutions per Minute

RPMI medium Roswell Park Memorial Institute medium

rSAP . . . . . Recombinant shrimp alkaline phosphatase

RSV . . . . . Respiratory syncytial virus

RT . . . . . Room temperature

RT-PCR . . . reverse-transcriptase-polymerase chain reaction

SDS-PAGE . . Sodium dodecyl sulphate polyacrylamide gel electrophoresis

SEC . . . . . Size-exclusion chromatography

SHM . . . . . Somatic hypermutation

SNP . . . . . Single nucleotide polymorphism

SPR . . . . . Surface plasmon resonance

TBE . . . . . Tris/borate/ethylenediaminetetraacetic acid

TCR . . . . . T cell receptor

TEV . . . . . Tobacco etch virus protease

TFF . . . . . Tangential flow filtration

TFH cell . . . T follicular helper cell

Tm . . . . . Melting temperature

VH . . . . . Variable heavy region, used interchangeably with Vλ in less specific contexts

VHH . . . . . Single-domain heavy chain antibodies

VL . . . . . Variable light region. This is an umbrella term for Vκ and Vλ.

VLP . . . . . Virus-like particle

VSA . . . . . Variant surface antigen

Vγ . . . . . Gamma (heavy)-chain variable region

Vκ . . . . . Kappa (light)-chain variable region

Vλ . . . . . Lambda (light)-chain variable region

WHO . . . . . World health organization

WPRE . . . . Woodchuck hepatitis virus post-transcriptional regulatory element

WT . . . . . Wild type

1 Introduction

1.1 Malaria; a brief history

If cancer is heralded as 'The Emperor of all Maladies' then malaria has rightly been crowned 'The King of Diseases' [330]. No other infectious disease has shaped our species history and genome as ruthlessly as malaria.

1.1.1 Prehistory

Malaria-like parasites have infected and affected our ancestors since long before the origin of our human line. Molecular genetic evidence suggests that the malaria parasite's ancestor was a chloroplast-containing, free-living protozoan which adapted to live in the gut of aquatic invertebrates [422]. These unicellular organisms probably had obligate sexual reproduction, as, to this day, all known members of the phylum *Apicomplexa*, to which malaria parasites belong, retain an obligate sexual-stage in their life cycles and gamete fertilisation is always in the midgut lumen of their host [214]. At an early stage in their evolution, these "pre-malaria parasites" acquired an asexual, intracellular form of reproduction called 'schizogony' and became adapted to the aquatic larvae of early *Dipterans*; the taxonomic order which includes mosquitoes and first appeared about two hundred million years ago [144]. Following this period, certain parasite lines must have achieved two-host

life cycles adapted to the blood-feeding habits of their insect hosts. Contemporary human malaria parasites, alternating as they do between humans and blood-feeding female *Anopheles* mosquitos, are typical products of this line. In the two hundred million years since the appearance of these early biting insects, malaria-like parasites evolved, radiated and came to parasitise members of almost all major groups of land vertebrates. In current mammalian orders, more species of malaria parasite have been identified in primates than in all other mammals combined [144].

1.1.2 On the Origin of Species

Over twenty-five primate malaria species have been named and six of these are currently known to be human pathogens: *P. falciparum*, *P. vivax*, *P. malariae*, *P. ovale wallikeri*, *P. ovale curtisi* and *P. knowlesi*. Ideas about their evolutionary interrelatedness have been largely based on the morphology and biology of the parasites and on the geographic locations and relatedness of their various host species; in recent years however, molecular genetic analysis of the parasites themselves has added missing pieces to the puzzle [225, 226].

P. falciparum is very closely related to *P. reichenowi*, a parasite of chimpanzees, and molecular evidence shows that these two species are more closely related to the bird malaria species (Figure 1.1) than to those of other mammals [127]. The divergence that led to *P. falciparum* and *P. reichenowi* becoming distinct species has been placed at only four to ten million years ago [129], which overlaps the period in which the human line diverged from that of the African great apes [215]. The other species of human malaria fall within the single clade which includes all the mammalian malaria parasites so far analysed by molecular genetics [128]. Within this clade, all of the primate malaria parasites belong to one or other of the lineages represented by *P. malariae*, *P. ovale*, *P. knowlesi*, or *P. vivax* (Figure 1.1) and these four lines appear to have diverged over a hundred million years ago [12], long before the emergence of the lines leading to today's mammalian or primate orders.

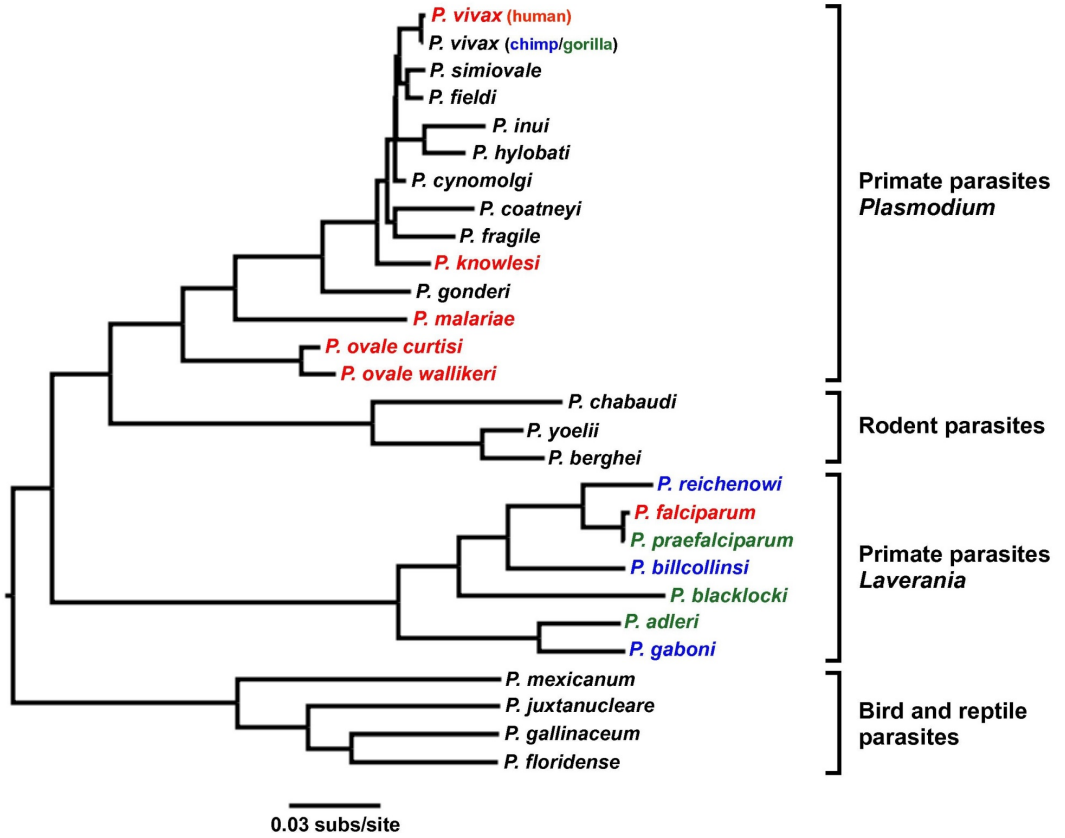


Figure 1.1: Evolutionary relationships of *Plasmodium* species. Species that infect humans are coloured in red, chimpanzees in blue, and gorillas in green. The phylogeny was estimated by maximum likelihood analysis of the mitochondrial genome; the scale bar indicates 0.03 substitutions per site. Taken from [227].

1.1.3 The Malaria Hypothesis

Malaria parasites have had a profound impact on human evolution. The 'Malaria Hypothesis', first proposed in the 1940s [161], posits that certain human genetic polymorphisms, especially those affecting red blood cells, have been selected to high frequencies because they protected against the effects of malarial infections. More currently known human genetic polymorphisms meet the expectations of the malaria hypothesis than can be attributed to selection by any other single agent [65]. There are now known to be many inherited mutations that fall within the terms of this hypothesis, the best known being; the thalassaemias; G6PD deficiency; sickle cell trait; ovalocytosis, haemoglobin C; haemoglobin E; and Duffy-negativity.

They are all fascinating conditions, whose current geographical spread tells us a lot about the evolutionary history of malaria and humans. The indigenous populations of northern Europe (except in parts of The Netherlands), northern parts of Asia, Australia and the Americas, from whom malaria has always been absent, or present only in recent centuries, are all without these polymorphisms in significant frequencies [65]. Today the genetic burden of these polymorphisms, in the form of the thalassaemias, sickle cell disease, G6PD deficiencies, and the ovalocytoses, is of the same order as the residual burden of malaria itself; up to half a million babies are born each year with severe forms of these inherited disorders [408]. Duffy-negativity is of special significance with regards to *P. vivax* malaria and will be considered in more detail later.

1.1.4 Out of Africa

P. falciparum and *P. vivax* each have a close biological relative (*P. reichenowi* and *P. schwetzi*, respectively) that is a parasite of African great apes, suggesting an African origin for both species. As the human and ape lines diverged, so did the parasites they carried; in one case, this led to *P. vivax* in the human line and to *P. schwetzi* in apes, and in the other case, to *P. falciparum* in humans and *P. reichenowi* in apes (Figure 1.1). Molecular genetic data on the present-day populations of *P. falciparum* support the proposition that they spread from an origin in sub-Saharan Africa [99]. Evidence from human genetic data imply a West African origin of *P. falciparum* within the past few thousand years, which is also the time within which modern populations of the parasites had their origin [400]. The case for an African origin of *P. vivax* rests largely on the evidence from the global distributions of RBC Duffy-negativity in humans. The extremely high frequencies of Duffy-negativity in Africa and its almost total absence outside those of African origin, is strong evidence that the greatest and longest burden of *P. vivax* disease was experienced by African populations [162].

If all human malaria parasites derive from Africa, how, why and when did they move out of Africa? One hypothesis is climate change. The warmer global climate, at the end of the last ice age that heralded the beginnings of agriculture and the entry of agricultural practice into Africa was pivotal to the subsequent evolution and history of human malaria [97]. In the Old World, prior to the agrarian revolutions, only *P. malariae*, by virtue of its transmission characteristics, might have been present among the low-density hunter-gatherer populations [97]. Around five thousand years ago, human populations in sub-Saharan Africa gradually switched from mobile hunter-gatherer life-styles, to communal living in settlements cleared in the tropical forest. In this new agricultural society, human densities increased greatly and the new practices generated numerous small water collections close to human habitations. These early farmers quickly transformed themselves into stable and accessible sources of blood surrounded by mosquito-breeding sites, thus providing a strong selective advantage to anthropophilic mosquito populations [97].

Gradually, the frequency of the mutation for Duffy-negativity would have risen until, as it approached fixation, *P. vivax* malaria itself declined to very low levels in West and Central Africa. It was not, however, and has not been, extinguished there [250]. Moreover, *P. vivax* was to spread beyond Africa and throughout almost all habitable zones of the world [250]. The fact that Duffy-negativity has not reached even moderately high frequencies outside of Africa argues against *P. vivax*'s long presence beyond this continent. Whenever it was that *P. vivax* spread beyond its African homeland, today, a gradient of declining RBC Duffy-negativity (Figure 1.8), marks its early contact with Arabia and the Near East [65].

1.1.5 Recorded History

The 'Nei Ching' describes repeated paroxysmal fevers associated with enlarged spleens and a tendency to epidemic occurrence [174]. This, almost five-thousand year old Chinese 'Canon of Medicine', is perhaps the earliest written record of malaria. Sumerian scripts from 3,500 to 4000 years ago also make frequent reference

to malaria-like illnesses and deadly epidemic fevers [349]; these may be descriptions of the first onslaughts of *P. falciparum* out of Africa. Over two thousand years later, in 323 B.C., Alexander the Great, while en route to India, is said to have died of malaria. If true, in a young, fit and healthy man, it would most likely have been *P. falciparum*. By this time, malaria had already appeared in the writings of the Greeks and its appearance characteristically coincided with the clearing of land for agriculture [335]. Works attributed to Hippocrates [193], leave no doubt about the presence of malaria in Greece in its benign tertian (*P. vivax*), quartan (*P. malariae*), and malignant subtertian (*P. falciparum*) forms. Malaria seems only to have reached mainland Italy in the second century B.C. [67], but when it did, the marsh-ridden countryside around Rome became a virtual desert.

By the beginning of the Christian era, malaria was widespread around the shores of the Mediterranean, the Arabian Peninsula, Central and Southeast Asia, China, Korea and as far North as Northern Japan [62]. When malaria began to spread into Northern Europe in the Middle Ages, its path would have lain via France and Britain to the countries of the North Sea seaboard. In Britain, potential malaria hot spots, such as the English Fens, were initially protected by Roman technology [119] and it wasn't until late medieval times that the Fens and other marshy areas, such as the Thames estuary, became blighted by the 'ague' [119]. The arrival of Europeans and West Africans in the New World at the end of the 15th century introduced *P. vivax* and *P. falciparum* for the first time [47]. European traders and colonisers suffered enormous losses of life from malaria; in the worst locations, such as West Africa, mortality rates often exceeded fifty percent of a company per year [107]. From the mid-19th century onward, quinine entered widespread use among Europeans and overall mortality rates plummeted to less than a quarter of their pre-quinine figures [107]. At some time during the 19th century, malaria reached its global limits. In absolute numbers and in the proportion of the humanity affected, it was exacting its highest ever toll of sickness and death; over half the world's population was at significant risk from malaria and of those directly affected

by malaria at least one in ten could expect to die from it [62]. Then, from the end of the 19th century, throughout North America and Northern and Western Europe, malaria entered an inexorable decline toward its present extinction in these regions.

The 20th Century

For over two millennia, the idea that malarial fevers were caused by miasmas rising from swamps had persisted. In the late 1800s, the integration of medicine and the sciences began, and following the development of germ theory by Pasteur and Koch in 1879, the search for the cause of malaria intensified. Scientific study of the disease first became possible after the discovery of the parasites by Laveran in 1880 [219] and the incrimination of mosquitoes as the vectors, first for avian malaria by Ross in 1897 [326] and then for human malarias by the Italian scientists Grassi, Bignami, Bastianelli, Celli, Golgi and Marchiafava between 1898 and 1900 [150].

Throughout the twentieth century, global malaria-related deaths never fell below half a million per year, but they were probably at least three million per year during most of its first half. These figures suggest that somewhere in the region of 150 to 300 million people died from the effects of malaria during the twentieth century [416]. As the century began, the malaria problem in Asia overwhelmed all others (Figure 1.2 A). In the same period in sub-Saharan Africa, with its intense, stable transmission, mainly of *P. falciparum*, the total malaria death toll was probably around 200,000 to 300,000 per year which, at the time, represented only about one tenth of the global malaria death toll. The annual malaria death toll for the whole of Europe and North America in the first decade of the 20th century was probably around 50,000 to 100,000 per year, as much as one-third of the total malaria deaths in sub-Saharan Africa at the time [416].

From shortly after the Second World War, a huge transformation in the global burden of malaria began to take place, giving rise to the common misperception that "malaria had gone away." With the relative political stability following the

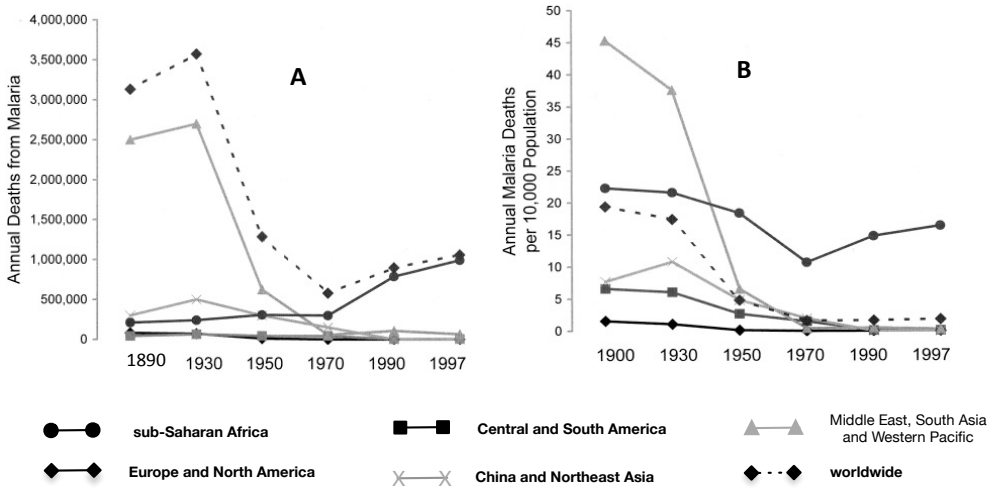


Figure 1.2: Malaria mortality in the 20th Century. (A) shows the total number of deaths due to malaria per year and (B) shows the number of malaria deaths per 10,000 population per year in the various regions indicated by the legend. Adapted from [62].

end of World War Two, the burden of malaria across most of Asia began a period of rapid decline (Figure 1.2).

In the late 1940s, national Malaria Control Campaigns were established in almost all affected Asian countries. Under the direction of the newly formed World Health Organization [415], and employing DDT to spray homes, they achieved remarkable reductions in malaria incidence and mortality [344]. Crucial to this success was the simultaneous deployment of highly effective antimalarial drugs, most notably chloroquine.

The anticipated goal, the eradication of malaria, was not achieved in any country of the region. The prohibitive economic and political costs of operating these 'Malaria Eradication Campaigns' [120], could not be sustained. Emerging resistance of both parasites and vectors led, from the early 1970s, to resurgences of malaria transmission throughout Southern Asia. Despite these setbacks, a return to the previous huge malaria toll in Asia has never been remotely approached (Figure 1.2). In the latter half of the 20th century, the risk of death from malaria plummeted in Asia and by the early 1960s, malaria in Europe and North America was extinct. For the world as a whole, outside Africa, the chances of dying from

malaria at the end of the 20th century were around one percent of what they were at the beginning. Thus, from around one death in ten at the century's start, malaria accounted for only about one in every thousand at its end [416].

The 21st Century

Since 1900, roughly half of all affected countries in the world have eliminated malaria and this includes nineteen countries since the year 2000 [274]. There has been a 47% reduction in global deaths from the disease since 2000 [418] and eradication has been back on the agenda for the last decade.

The Roll Back Malaria partnership has provided funds and direction for malaria surveillance and the deployment of modern malaria control tools, most importantly the antimalarial drugs known as artemisinins [121] and insecticide-treated bed nets [273]. These impressive successes have raised questions about the need for malaria vaccines [152]. Mathematical models have indicated that, used in combination with indoor residual spraying of insecticides, modern drugs and insecticide-treated bed nets have the potential to reduce the malaria prevalence rates to below one percent in low- and moderate-transmission settings [153]. The authors of this study accepted, however, that their model assumed unrealistically high coverage and even where models assume indefinitely sustained very high level coverage, as well as twice-yearly mass drug administration, parasite prevalence in high-transmission areas is not predicted to fall below ten percent [153]. In light of recent history it seems unwise to assume that these non-vaccine malaria control measures will retain their current levels of efficacy and financial support [9]. There are precedents for mosquitoes becoming resistant to insecticides [325] or changing their feeding habits to lessen the impact of bed nets [272]; and parasites becoming resistant to antimalarial drugs such as chloroquine [211, 312], and now the artemisinin-based therapies [11].

A strong case for malaria vaccine development is made by modelling studies which show the substantial benefit that would arise from deploying of a vaccine that is only partially protective [362, 363]. These models, which typically assume a vaccine efficacy of 50%, and a protective half-life of 3 years, predict variable impacts on mortality, morbidity and parasite prevalence, depending upon intensity of transmission, deployment of other control methods, rate of immune decay and access to healthcare [153, 362, 363]. They all, however, reach general agreement that even with modest levels of efficacy, a vaccine would facilitate reductions in parasite prevalence if used in combination with other strategies. This role for a vaccine is very different to the 'magic bullet' envisaged in the past; a vaccine would form one arm of an integrated programme consisting of indoor residual spraying, long-lived bed nets, draining of mosquito habitat and provision of artemisinin-based drugs [152]. The effect of a hypothetical vaccine with ninety-five percent efficacy and a protective half-life of ten years has also been modelled [153], and in this scenario a single mass administration of such a vaccine could; eliminate malaria from low-transmission zones; eliminate malaria from moderate-transmission zones if used in combination with other methods; and reduce prevalence to below five percent in high-transmission zones.

The recognition that the ability to prevent disease is not a necessary condition for a malaria vaccine intended to reduce prevalence [152], has led to development of vaccines aimed at interrupting parasite transmission from infected human to mosquito [311], with the course of human disease a secondary consideration.

If the very ambitious goal of malaria eradication by 2040 is to be achieved, all *Plasmodium* species infecting humans need to be targeted. In many regions of co-endemicity, there has been a relative increase in the proportion of infections due to the non-*falciparum* species, especially where PCR-based testing is performed [418]. These non-*falciparum* species pose problems of greater complexity, geographic range, and technical difficulty, with fewer tools available to tackle them and more unknowns.

1.2 *Plasmodium vivax*

1.2.1 Global public health significance

While elimination goals ostensibly address all human malarias, the allocation of funding and resources between the two parasites of greatest significance, *P. falciparum* and *P. vivax*, has been highly disparate. From 2007 to 2009, only about three percent of all malaria research and development funding was targeted at *P. vivax* [301]. *P. vivax* has the widest geographical distribution of the human malarias with approximately two and a half billion individuals living at risk of infection in 2010 [145].

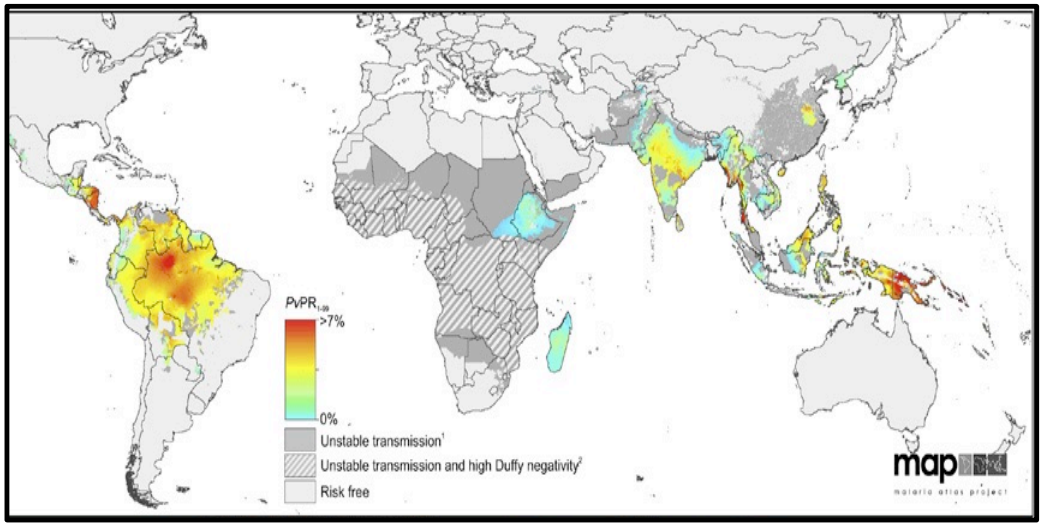


Figure 1.3: Predicted endemicity of Plasmodium vivax in 2010. PvPR is *Plasmodium vivax* Parasite Rate. Taken from [31].

The last decade has seen a dramatic reduction in the burden of malaria, with many countries in the Asia-Pacific and the Americas seeing reductions of over ninety percent in the number of clinical cases [1]. Thirty-four countries are now actively attempting to eliminate malaria and leaders of Central American and East Asian countries have declared their intention to eliminate malaria from their regions by 2020 and 2030, respectively [2]. In parallel to this reduction in overall incidence, a pronounced shift in species composition has been observed with *P. vivax* now the

predominant *Plasmodium spp.* in the vast majority of countries outside Africa [417]. *P. vivax* is epidemiologically and biologically different to *P. falciparum* and it cannot be assumed that control methods developed for *P. falciparum* are transferable to *P. vivax* malaria [16, 41, 45, 228]. These distinctive features of *P. vivax* present unique challenges to the control of the parasite [250, 412] and because of this, in elimination settings, *P. vivax* is often the 'last parasite standing' [131, 375]. The unique biological features of *P. vivax* that contribute to its stubborn persistence are discussed in the next section (Section 1.2.2).

Due to vector bionomics in regions where *P. vivax* is most prevalent, methods of mosquito control that are broadly effective in reducing *P. falciparum* transmission, such as insecticide-treated bed nets (ITNs), are less effective at controlling *P. vivax* [41].

1.2.2 Biology and life-cycle

In general terms, the life cycle of *P. vivax* is like that of all primate malaria species and requires an invertebrate and a vertebrate host; a female mosquito of a susceptible *Anopheles* species and a primate.

When the mosquito probes the dermis, sporozoites released from her salivary glands invade small blood vessels and are swept into the liver sinusoid vessels. There they penetrate phagocytes into the Space of Disse, before invading hepatocytes and beginning the liver-stage of their life-cycle. Once inside the hepatocyte, they round up, differentiate into trophozoites and grow in size over the next five days to become multinucleated schizonts. After approximately one week of growth and development, the fully mature liver schizont contains thousands of individual invasive single-nucleated merozoites surrounded by a parasitophorous membrane. The infected hepatocyte then breaks down, and blebs of the parasitophorous membrane, known as merosomes, break off. They flow first into the liver sinusoid vessels [377] and then into the faster flowing general circulation where the merozoites are released

[15] and rapidly invade reticulocytes.

Once inside the reticulocyte the merozoite differentiates into a trophozoite and remodels the host cell to provide a suitable environment for it to grow in and feed on for the next forty-eight hours. At about forty hours post-invasion, the parasite nucleus divides to create a schizont, which, over the next eight hours or so, continues to divide by 'schizogony' to form twelve to sixteen differentiated merozoites. The reticulocyte membrane then ruptures, releasing the merozoites to invade new RBCs and begin the blood-stage cycle again.

The merozoites in some schizonts are pre-programmed to differentiate into sexual male or female micro- and macro-gametocytes, respectively [322]. The sexual stage of the life cycle begins when a feeding female *Anopheles* mosquito ingests circulating gametocytes in a blood meal. Once inside her midgut the gametocytes shed their erythrocytic membrane and become sexually active. The nucleus of the male microgamete fractures, forming eight flagellating bodies [311]; when one of these penetrates a female macrogamete, the diploid zygote is formed which metamorphoses over twenty-four to thirty-six hours into an invasive ookinete. The ookinete penetrates the lining of the mosquito midgut to lodge under the basal membrane where it then transforms into an oocyst and undergoes multiple nuclear divisions.

At maturity, the cyst breaks open and thousands of sporozoites move through the haemocoel of the mosquito, penetrate the salivary glands and lodge in the glandular spaces, until the mosquito probes again.

The distinct life-cycle features of *P. vivax* and its sibling South-East Asian macaque monkeys species, *P. cynomolgi*, *P. simiovale* and *P. fieldi*, are illustrated in Figure 1.4 and include;

1. The dormant hypnozoite forms in the liver; which enables recurring blood-stage infections, termed relapses, to occur weeks or months after primary infection [212]. At about 4–5 μM, hypnozoites are a fraction of the size of a primary liver-stage schizont and very little is known about them, including what triggers their reactivation. What is known, however, is that *P. vivax* hypnozoites remain dormant for very variable time-periods, depending to some extent on geographical distribution but more so on the parasite strain [414]. In Northern latitudes the so-called "temperate" strains, exhibit a pattern of first relapse occurring eight, nine or twelve months after sporozoite infectio, and in these cases, there may be no preceding primary parasitaemia. The other basic type, known as "tropical" strains, have early and frequent relapse patterns at regular intervals of a few weeks and there is almost always an initial primary parasitaemia. The temperate form relapse pattern is thought to be a life-cycle strategy suited to climates with long winters and exists to infect mosquitoes emerging in late spring and early summer [414]. Most relapse parasites in individual patients with tropical strains, have been shown to be genetically heterogeneous, reflecting past and present infections with different genotypes of *P. vivax* [190].

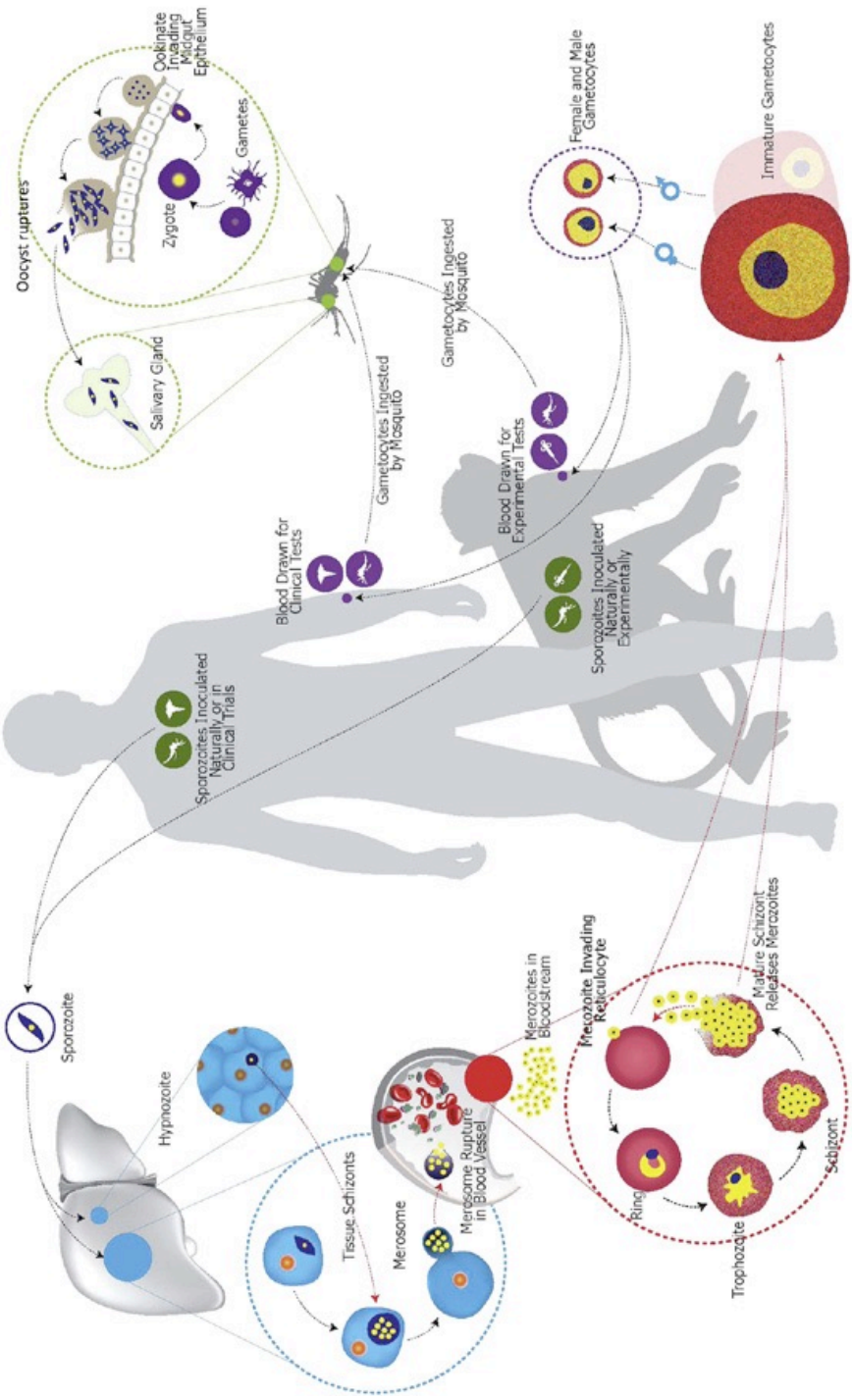


Figure 1.4: Schematic of the life cycle of *Plasmodium vivax* and comparable sibling simian species, depicted to represent the unique biological features of these species and the importance of clinical and experimental interventions. The unique biological features of *P. vivax* depicted are the hypnozoite, the preferential invasion of the merozoite into reticulocytes, the production of Caveola-vesicle Complexes (CVCs), represented as a mottled appearance of the infected RBCs, and the early and rapid development and circulation of gametocytes. Taken from [142].

2. Their preference for reticulocytes as host cells. Restriction to these immature RBCs, which typically represent 0.5–2% of the circulating RBCs, though it limits parasitaemia, may offer a survival advantage. *P. vivax* is thought to alter the infected reticulocyte to make it even more flexible and thus able to circulate through small capillary vessels and survive passage through the sinusoidal vasculature of the spleen [165]. This is the opposite strategy of *P. falciparum* which invades mature erythrocytes and increases the rigidity of its host cell. *P. falciparum* displays cytoadherence ligands, the variant antigens, at the surface of infected erythrocytes to allow the parasitised erythrocyte to sequester in small vessels by adhesion to endothelium and thus avoid passage through and destruction in the spleen. *P. vivax* does not have *var* genes encoding variant antigens like *P. falciparum* [27, 115, 360, 371] and because of the flexibility of its host cell does not need to sequester to avoid spleen passage.

3. The formation of elaborate flask-shaped and tubular membranous structures, known as caveola-vesicle complexes (CVC) and seen as Schüffner's stippling on Giemsa-stained blood smears. The metabolic functions served by the CVC remain the subject of speculation, but a role in the uptake and release of metabolites has been suggested [7].

4. *P. vivax* gametocytes develop quickly and circulate early in an acute infection; this allows transmission prior to patients feeling ill and seeking treatment. It has been shown that mosquitoes can become infected as early as eight days after human infection [50]. This very early gametocytogenesis, combined with the periodic renewal of blood infections by reactivating hypnozoites, makes *P. vivax* transmission fast, effective and persistent. The successful transmission of *P. vivax* in colder more northerly latitudes (unlike the other human malaria species), is enabled by the vivax sporozoite being able to develop over a larger temperature range and in an array of mosquito vector species that over winter, combined with the delayed relapse phenotypes.

For over a century scientists have been reporting attempts at the *in vitro* propagation of *P. vivax* blood-stages [281], but most have been little more successful than those first published in 1912 [28]. Nonetheless, attempts continue, with efforts mostly focused on the routine addition of fresh reticulocytes, either from umbilical cord blood, or produced *in vitro* from erythroid stem cell cultures [281], [28, 44, 148, 154]. Recently, a robust and reliable system for the short-term *in vitro* culture of *P. vivax* from *ex vivo* clinical samples has been developed [329] using umbilical cord blood RBCs (see Chapter V).

1.2.3 Red blood cell invasion

In 1978 this, now famous, picture was published, showing a *Plasmodium knowlesi* merozoite dragging itself into a red blood cell [6] (Figure 1.5).



Figure 1.5: *Plasmodium knowlesi* invasion of *Macaca mulatta* red blood cells. A *P. knowlesi* merozoite has commenced the invasion process through formation of gliding junctions involving merozoite and red cell membranes. This enables invagination of the erythrocyte membrane and movement of the parasite into the parasitophorous vacuole. R, rhoptry; M, micronemes; J, gliding junction; PV, parasitophorous vacuole; E, erythrocyte. Taken from [6].

This seminal paper described some of the distinct stages of erythrocyte invasion; attachment to the red cell membrane by the parasite's apical end, formation of a tight junction, invagination of the red cell membrane around the merozoite and sealing of the erythrocyte on completion of invasion. Identifying molecules involved in this attachment and junction formation is central to unravelling the mechanisms of RBC invasion, and understanding how to disrupt them is the focus of blood-stage

vaccinology and this DPhil Thesis.

Malariotherapy

Towards the close of the nineteenth century, malaria, tuberculosis and syphilis were the three most feared infectious diseases. All three were globally distributed and their causative agents were discovered within twenty-five years of each other; *Plasmodium* in 1880, *Mycobacterium tuberculosis* in 1882 and *Treponema pallidum* in 1905. Population estimates in early twentieth century Europe and the United States suggested that fifteen percent of the general population had syphilis [370]. The syphilitic origin of general paralysis of the insane (GPI) had first been suggested in the 1820's [10] and in the early decades of the twentieth century, patients with GPI accounted for ten to twenty percent of the inmates in mental institutions. In the nineteenth century, many psychiatrists espoused the view that a bout of fever can improve mental disorders, and in 1887, an Austrian Psychiatrist, Wagner-Jauregg, proposed infecting GPI patients with malaria to induce fever. Thirty years later, in 1917, he finally got his chance when a *P. vivax*-infected soldier returning from the Balkans was mistakenly admitted to his psychiatric ward in Vienna. Nine patients with GPI were infected with *P. vivax* malaria that summer and six of them improved significantly; an outcome so encouraging that by 1922 more than two hundred GPI cases had been treated [403]. There followed an extraordinary period when, from the early 1920s until the advent of penicillin in the mid-1940s, induced malaria became the standard treatment of neurosyphilis. Malariotherapy, as it was called, was a unique example of one pathogen being used to reverse pathology caused by another.

An observation made soon after the introduction of malariotherapy to the United States, was the refractoriness of most people of African origin to infection with *P. vivax*, as opposed to universal susceptibility of persons of other origins [49]. The basis for this resistance was not uncovered until the mid-1970s [254], when it was

demonstrated that Duffy blood group positivity was required for red blood cell invasion by *P. vivax*, and nearly all West Africans, and a majority of sub-tropical African populations, are Duffy-negative.

The Duffy blood group (Fy) and *P. vivax*

The Duffy blood group antigen (Fya) was first detected on erythrocytes in 1950 after a haemolytic transfusion reaction in a multiply-transfused haemophiliac [108] and named after this patient. The expected Fyb antisera was discovered the following year [187], but screening of blood samples from African-American donors in New York a few years later, showed that most samples did not react with either the Fya or Fyb antisera [333]. Based on the overlapping distribution of the Fy $(a-b-)$ phenotype with the very low prevalence of *P. vivax* in African populations [52] and the desire to identify 'receptors' used for invasion by malarial parasites, a series of experiments were performed which showed first that that *P. knowlesi* could not invade Fy $(a-b-)$ erythrocytes *in vitro* [255] and then that Fy $(a-b-)$ human volunteers could not be infected with *P. vivax* following mosquito bite challenge [254].

Later studies of the Duffy gene identified first a single nucleotide polymorphism (SNP) in codon 42 (Figure 1.6) causing a G to D switch associated with the Fya (G) and Fyb (D) antigens [71] and then a T to C SNP thirty three nucleotides upstream from the primary transcription starting position (-33) in the Duffy gene promoter [384], resulting in an Fyb^{ES} allele (ES = erythroid silent). Duffy-negative Africans were homozygous for this polymorphism and *in vitro* assays showed that the polymorphism blocked gene expression in erythroid lineage cells but not in non-erythroid cells [384]. This study provided the molecular genetic explanation for erythrocyte Duffy-negativity.

Further polymorphisms associated with variable DARC expression have since been described, including the Fya^{ES} and the Fy^{x} or Fy^{bweak} polymorphism which occurs within the first intracellular loop (Figure 1.6 on page 22) and is associated

with reduced cell surface expression of DARC [387]. There are currently five known Duffy alleles (Fya, Fyb, Fy^X, Fya^{ES} and Fyb^{ES}) giving rise to fifteen different genotypes with particular expression phenotypes. Additional observations that DARC expression is highest on reticulocytes [425] may contribute to the preferential invasion of these immature red cells by *P. vivax*.

DARC is referred to as a 'silent' 7-transmembrane receptor, due to the absence of a DRYLAIV amino acid motif in the second intracellular loop needed to couple with G-proteins that initiate intracellular signalling cascades [268]. On erythrocytes, DARC is proposed to act as a sink that binds excess chemokines and limits inflammation [111]. Reciprocally, DARC binding of chemokines prevents their diffusion into organs and peripheral tissue space and acts as a reservoir of chemokines in the circulating blood [139]. DARC is also expressed on a variety of non-erythroid cells including venular endothelial cells, where it has been proposed to act as a chemokine internalisation receptor by internalising and scavenging chemokines [275].

The merozoite ligands which interact with DARC are known as Duffy-binding proteins (DBP), and have been characterised for both *P. knowlesi* (PkDBP) [168] and *P. vivax* (PvDBP) [413]. PvDBP has a molecular weight of approximately 140 kDa and a 330-amino acid cysteine-rich region within it, known as region II (PvDBPII), is predicted to be the domain responsible for binding to DARC [317].

DBP, which are released from the micronemes and expressed on the surface of *P. knowlesi* and *P. vivax* merozoites, share a number of structural features with erythrocyte-binding proteins of other malarial parasites. These proteins, which have come to be known as Duffy-binding-like erythrocyte binding proteins (DBL-EBP) [5], have shared features which include two cysteine-rich regions (region II – containing twelve conserved cysteine residues and region VI containing eight conserved cysteine residues), highly polymorphic regions (regions III to V) and numerous aromatic amino acids [5].

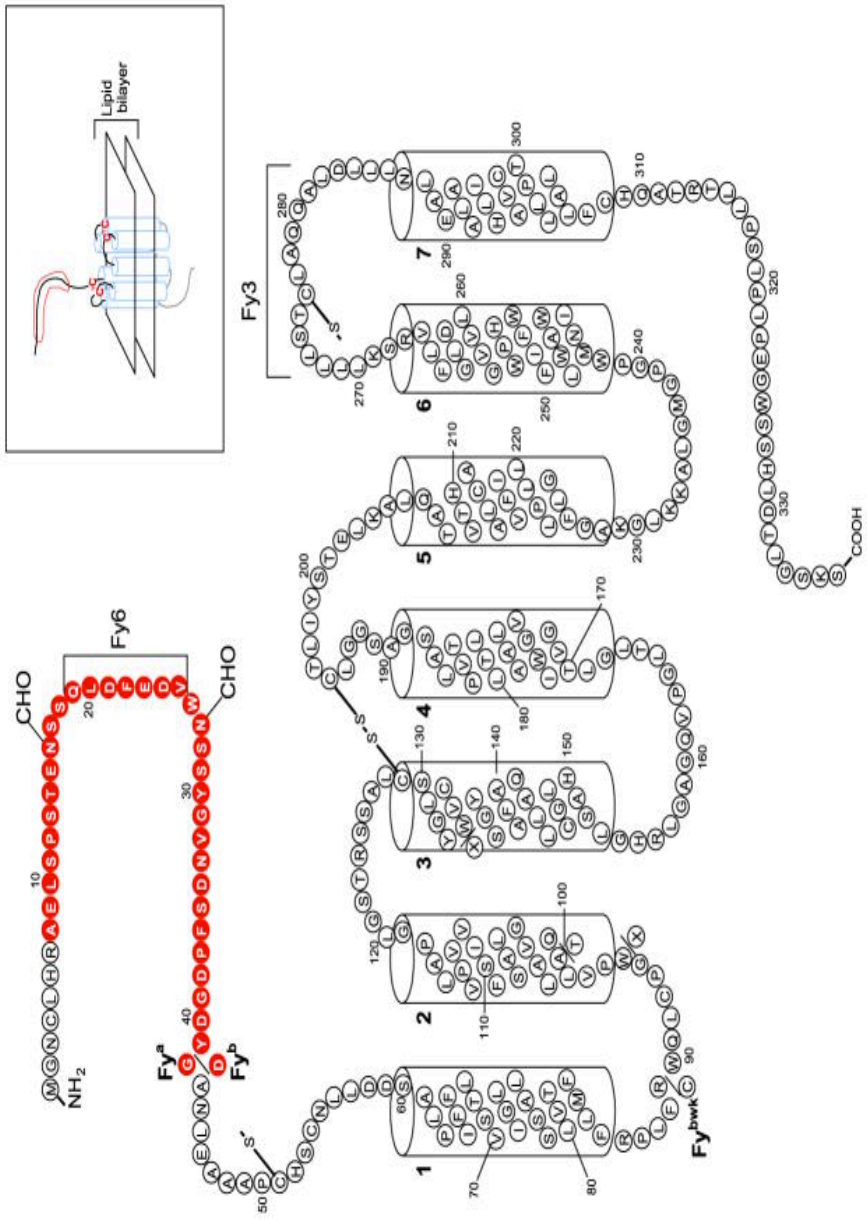


Figure 1.6: The Duffy Antigen Receptor for Chemokines (DARC), taken from [432], and illustrating the primary structure of the 236-amino-acid 36–46kDa Duffy antigen with seven predicted transmembrane domains and extracellular and intracellular domains. Amino acids comprising the Fy6 and Fy3 antibody-binding domains are marked by brackets. Amino acid sequence polymorphisms are identified at residues 42 (G vs. D; Fya vs. Fyb), 89 (R vs. C; Fyb vs. Fybweak) and 100 (A vs. T) and the two premature termination codons (W vs. X) at residue positions 96 and 134. Glycosylation sites are identified at amino acid residues N16 and N27. Disulphide bonds occurring between C129 (extracellular loop 2) and C195 (extracellular loop 3) and between C51 (amino terminal head) and C276 (extracellular loop 3) are predicted to contribute to further tertiary structure within the cell membrane as depicted in the inset. Amino acids predicted to comprise the *P. vivax* binding region are identified in red [78]

P. knowlesi merozoites have been shown to successfully contact and reorient their apical surfaces on the membranes of both Duffy-positive and Duffy-negative erythrocytes but the tight junction between merozoite and erythrocyte membranes (Figure 1.7) does not form with Duffy-negative cells [253]. Experiments focused on PvDBP have demonstrated competitive interference between recombinant PvDBP expressed on COS cells and the Duffy receptor on donor erythrocytes using; a 35-amino-acid peptide (amino acids 8–42) from the receptor's N-terminal domain (Figure 1.6), the anti-DARC monoclonal antibody anti-Fy6 (Figure 1.6) and the chemokine MGSA (CXCL1) [77].

These same studies also demonstrated that sulphation of tyrosine 41 (Figure 1.6) is critical for optimal DBP binding to the Duffy receptor *in vitro* [80]. Unlike *P. vivax* which has just one DBP gene, *P. knowlesi* has three; PkDBPα, PkDBPβ and PkDBPγ. *P. knowlesi* merozoites of PkDBPα knockout strain are not able to form a junction with or invade Duffy-positive human RBCs [350], however PkDBPα knockout parasites could successfully invade rhesus erythrocytes suggesting that the PkDBPβ and PkDBPγ proteins bind other receptors and enable Duffy-independent red cell invasion [317]. More recent studies have shown that both patient-derived and polyclonal rabbit antibodies specific for PvDBP are able to inhibit *P. vivax* invasion of human RBCs *in vitro* [154, 329].

Duffy-independent RBC invasion

With consistent observations of clinical resistance to *P. vivax* malaria associated with Duffy-negativity and reduced susceptibility to *P. vivax* associated with lower Duffy expression and/or reduced affinity between DARC and DBP [200], the Duffy antigen has come to be regarded as an essential receptor for *P. vivax* erythrocyte invasion. There have, however, been a number of studies reporting *P. vivax* PCR-positivity in Duffy-negative people; these include studies from Kenya [331], Brazil [66] and of European travellers returning from malaria areas [267]. However, a large-scale PCR-based survey covering nine different African countries detected only one *P.*

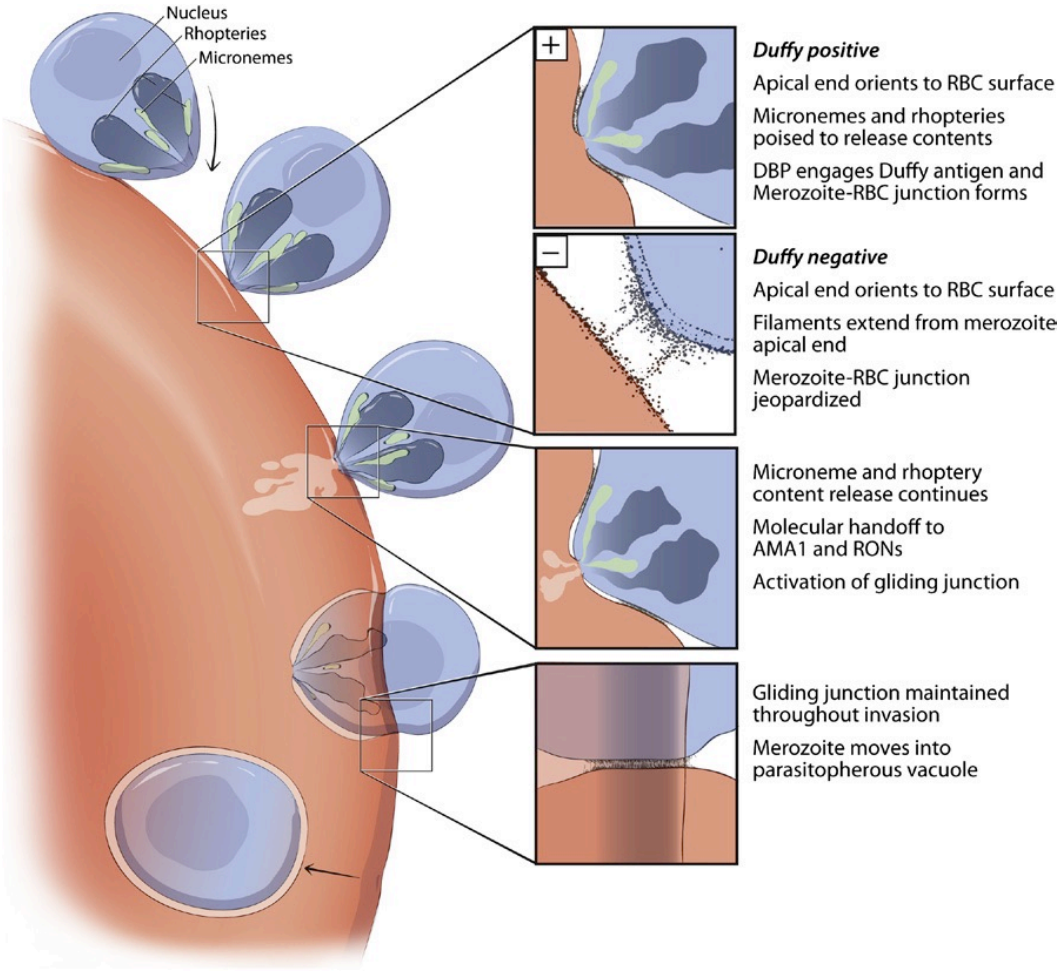


Figure 1.7: Overview of *P. vivax* merozoite interaction with the human red blood cell, taken from [432]. Initial attachment occurs between any part of the merozoite (blue) and erythrocyte (red). The merozoite reorients, positioning its apical end for attachment to the red cell membrane. A junction forms between the apical end of the merozoite and the erythrocyte membrane of Duffy-positive cells. In contrast, *P. knowlesi* electron microscopy has shown thin filaments between the merozoite apical end and the Duffy-negative red cell membrane; however, the merozoite is not drawn into contact with the red cell and the junction fails to form. This has implied that junction formation fails to occur between *P. vivax* and the Duffy-negative red cell membrane as well. Once a durable junction has formed between the merozoite and the red cell, micronemes (green) and rhopteries (dark blue) release their contents, the red cell membrane invaginates and the merozoite moves into the parasitophorous vacuole. Movement of the gliding junction is complete once the merozoite is engulfed within the parasitophorous vacuole and the orifice at the red cell membrane is sealed.

vivax-positive person in over two thousand five hundred samples, and that individual was Duffy-positive [106]. In 2010, surveys of school-aged children in Madagascar revealed *P. vivax* PCR positivity in 8.8% of asymptomatic Duffy-negative children

(n=476) and microscopy of some of these samples provided the first evidence to confirm Duffy-independent blood-stage infection and development by *P. vivax* [249].

Population-level observations showed that in the Malagasy communities with the highest frequencies of Duffy-negativity, there was little to no prevalence of *P. vivax* infection detected in either Duffy-positive or Duffy-negative people. In contrast, with an increase in the frequency of Duffy-positivity, *P. vivax* prevalence increased and was not significantly different between Duffy-positive and Duffy-negative people [249]; this suggested that high population levels of Duffy-negativity may act similarly to herd immunity to reduce transmission and consequently protect Duffy-positives from vivax malaria. Antibody reactivity against *P. vivax* merozoite proteins, PvDBP and PvMSP-1, indicate that liver-stage infection (and therefore hypnozoite formation) commonly occurs in Duffy-negative people [105]. A survey of clinical malaria from this Madagascar study did, however, suggest that Duffy-negativity was associated with protection from malarial illness [249]. Surveillance of *P. vivax* strains capable of Duffy-independent red cell invasion is clearly very important, given the major implications for the burden of clinical malaria in Africa and for *P. vivax* vaccine development.

A recently collated, geographically-referenced database of available Duffy phenotype and genotypes [182] is summarised in Figure 1.8.

Given that non-human primate studies provide evidence that Fyb (shown in green on the map) is the ancestral allele in the hominid line [290], the map suggests that Fyb^{ES} (shown in red to orange) originated in Africa and spread across a large area. Also apparent from this map is that Fya (shown in blue) reached genetic fixation in regions of the world where the non-human malaria parasite ancestors originated and dispersed [221] and from these potential Asian origins, Fya admixed with Fyb and spread into the Americas.

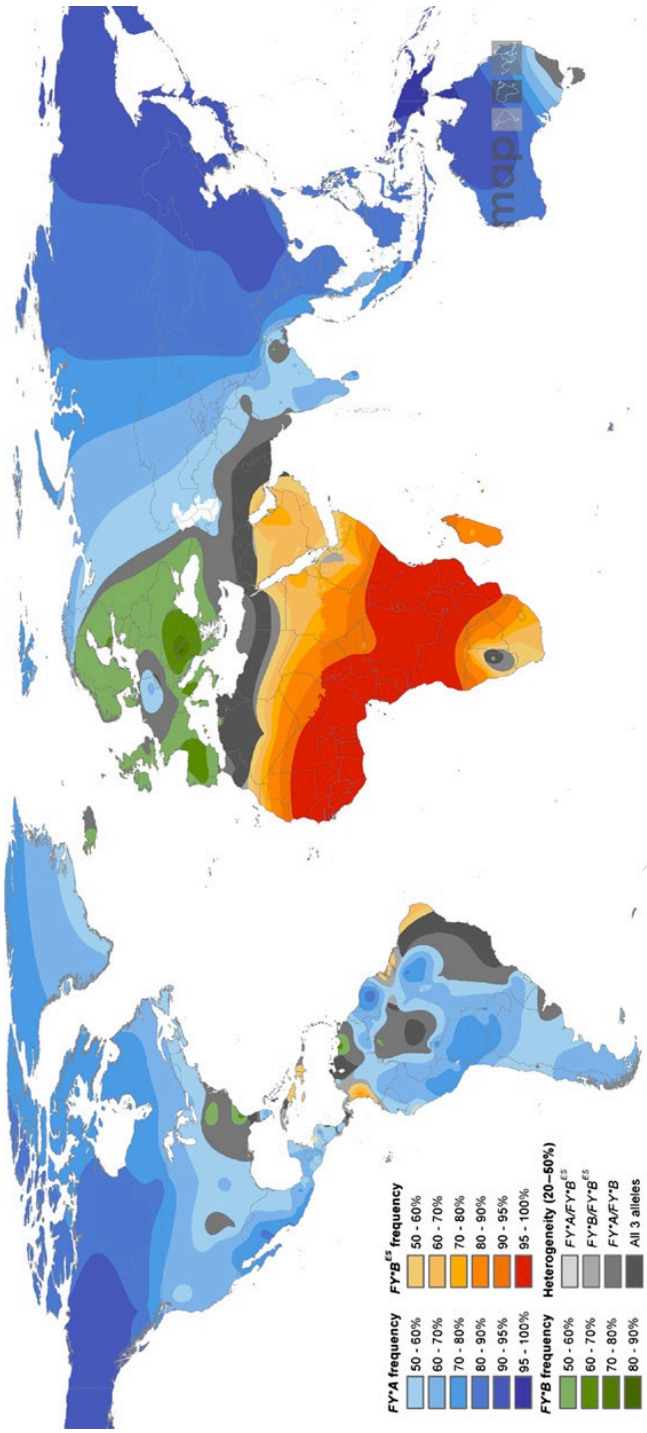


Figure 1.8: Global frequencies of the Fy alleles, taken from [432]. Areas predominated by a single allele (frequency $\geq 50\%$) are represented by a colour gradient (blue, Fya; green, Fyb; red/yellow, Fyb^{ES}). Areas of allelic heterogeneity where no single allele predominates, but two or more alleles each have frequencies $\geq 20\%$, are shown in grey-scale: palest for heterogeneity between the silent Fyb^{ES} allele and either Fya or Fyb (when co-inherited, these do not generate new phenotypes), and darkest being co-occurrence of all three alleles (and correspondingly the greatest genotypic and phenotypic diversity). Overall percentage surface area of each class is listed in the legend.

1.2.4 Clinical aspects of *Plasmodium vivax*

P. vivax malaria, historically described as 'benign tertian malaria' [236], because individual clinical episodes were less likely to cause severe illness than *P. falciparum* [40], is now recognised as major cause of morbidity, accounting for almost half of all malaria cases outside of Africa, and capable of causing severe disease [316]. Each year, there are between seventy and three-hundred and ninety million clinical vivax infections globally [313] with a disease spectrum ranging from asymptomatic parasitaemia to uncomplicated febrile illness, through to severe and fatal malaria [217]. As it is not the focus of this Thesis, I will just briefly outline some of the important clinical features of *P. vivax*.

Spectrum of disease Data from malariotherapy records, using the Madagscar strain of Pv in the immunologically naïve, showed the mean pre-patent period (time from infection to first appearance of parasites in peripheral blood) and incubation period (time from infection to first fever $> 37.8°C$) was 12.2 (range 8-23) and 13.4 (range 8-31) days respectively [203]. In contrast to these *P. vivax* strains of tropical origin, very prolonged incubation periods are often seen with temperate-zone strains, including a mean of 282 days for a Romanian strain [347] and up to 360 days for a Russian strain [277].

P. vivax is capable of inducing fever at levels of parasitaemia lower than those causing fever in *P. falciparum* infection. In Western Thailand, an area of low endemicity, the pyrogenic density was 180 parasites/μL, compared with 1000 parasites/μL observed in *P. falciparum* infection [229]. In keeping with this, the host inflammatory response is activated to a greater extent during *P. vivax* infections, with higher plasma levels of fever-inducing cytokines, such as TNF-α, in vivax malaria compared with *P. falciparum* infections of similar parasitaemia [170].

Clinical disease is associated with chills, vomiting, malaise, headache, fever, and myalgia. These non-specific symptoms cannot be distinguished reliably from other

febrile illnesses or other malarias [229]. High fever and rigors are more common in vivax than falciparum malaria, reflecting synchronicity of schizont rupture [170]. The classic paroxysms of fever, which last from four to eight hours and occur with forty-eight to fifty-six hour periodicity, take several asexual cycles to develop in primary infections, although relapses often start synchronously with rigors [95].

In the pre-antibiotic era, vivax malaria resulted in a chronic debilitating febrile illness associated with hypoproteinaemia, oedema and dramatic weight loss akin to kwashiorkor [203]. In the malariotherapy era, *P. vivax* infection was associated with significant risk of death, with five to ten percent of patients with neurosyphilis dying during therapy and up to fourteen percent when the Madagascar strain was used [133]. Even today, with access to effective antimalarials, severe and fatal infections occur with *P. vivax*. Most recent case series report PCR-exclusion of mixed infection with *P. falciparum*, but investigation for concurrent infections or co-morbidities is often incomplete. The strongest evidence for *P. vivax* being a major contributory factor is apparent for severe anaemia [312], acute respiratory distress syndrome [394] and acute kidney injury [358]. It has long been recognized that splenic rupture is a life-threatening, though rare, complication [100]; vivax malaria has also been associated with malnutrition [420] and possibly coma [35].

A fundamental clinical characteristic of *P. vivax* is its ability to relapse and cause repeated episodes of clinical and subclinical infections. The tiny and elusive dormant liver stages were not conclusively identified until 1980 [213] and the factors that trigger their activation are still not known. In tropical regions, *P. vivax* is characterized by frequent relapses three to six weeks apart [149] resulting in recurrent infections often with heterologous strains to which there is little cross-immunity [190]. These frequent recurrent infections prevent adequate time for the patient to achieve haematological recovery from each bout of haemolysis and the anaemia is cumulative. In contrast, in temperate areas, relapses are fewer and delayed, and the associated impact of each recurrence is less [149].

Diagnosis and treatment

Although microscopy remains the mainstay of diagnosis of vivax malaria, lack of access to good quality microscopy services in many endemic regions limits the reliability of diagnosis and contributes to the underestimation of cases. Even in the hands of expert microscopists, results can vary significantly depending on the species, parasite density and method of enumeration; this was demonstrated in a study of United Kingdom clinical laboratories, where microscopists correctly identified only 63% of confirmed *P. vivax*-positive blood films [256]. Aldolase-based and parasite lactic dehydrogenase-based rapid diagnostic tests (RDTs) have suboptimal sensitivity for *P. vivax* [302] which limits the utility of RDTs for vivax diagnosis [36].

The need to treat both liver- and blood-stages in *P. vivax* malaria, as opposed to blood-stages alone in falciparum malaria, amplifies the complexity of therapy. The poor state of vivax malaria chemotherapeutics derives from its historic neglect; the blood schizontocidals used against *P. vivax* today were first processed through drug-development programs targeting *P. falciparum* and while this approach worked well for drugs against blood-stage *P. vivax*, it did nothing to address the liver-stage. Chloroquine has been the mainstay of treatment of acute vivax malaria for over fifty years and has potent activity against asexual stages, but none against hypnozoites. Its long terminal elimination, however, ensures that plasma concentrations are sustained above the minimum inhibition concentration for at least a month and are thus capable of suppressing the first relapse, which in tropical zones occurs at about three weeks [17]. The first case of chloroquine-resistant *P. vivax* was reported in 1989 from Papua New Guinea [323] and resistant strains are now commonplace in Papua and Indonesia [138] with sporadic cases reported much further afield [366]. Most of the artemisinin-based combination therapies have proven efficacy against chloroquine-resistant strains of *P. vivax* [198, 314].

Primaquine, which was developed in the 1940s, long before hypnozoites were identified, remains the only licensed drug to clear the liver stage of *P. vivax*.

Unfortunately, it can cause severe, and sometimes life-threatening, haemolysis in patients with glucose-6-phosphate dehydrogenase deficiency (G6PDd). This risk is exacerbated by both a higher frequency of this trait where malaria is most common (Figure 1.9), and the absence of the laboratory capacities required to identify those at risk of haemolysis.

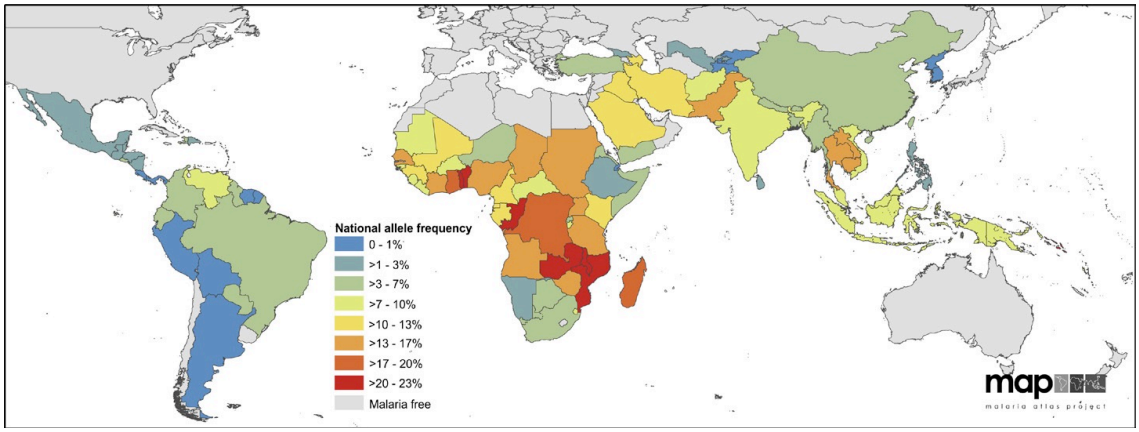


Figure 1.9: National allele frequency of G6PD deficiency, taken from [183].

1.2.5 Natural immunity to *Plasmodium vivax*

A major controlling force determining the incidence and prevalence of malaria infection and disease in endemic areas is the parasitological and clinical immunity collectively referred to as naturally acquired immunity (NAI). The basic elements of NAI were first described by Robert Koch after a visit to Indonesia in 1899 [206]. His observations can be summarised as:

- In endemic areas, malaria is most apparent in young children and the parasites may be absent from the blood of adults.
- Individuals constantly exposed to infection develop immunity to malaria, whereas immigrants from non-endemic areas, achieve an "unmistakable degree of immunity just as is the case in the children of natives" after 3–4 years of exposure.

- In people who have experienced numerous previous malaria attacks, infections will often present only with mild or no symptoms at all.
- Immunity against one *Plasmodium* species offers little protection against the other species.

Based on these observations he concluded;

"One may assume that anti-malarial immunity, which under ordinary conditions is acquired only in 4–6 years and after repeated attacks, could be conferred artificially and in a short time. Seeing, however, that as yet we have no idea how to obtain the toxins necessary for the immunizing process, chances of progress in this direction are small" [206].

Sadly, Koch's pessimistic prediction has proved true; almost 120 years after he wrote this, there is still no highly effective vaccine.

Although the human immune system will attack almost any stage of the parasite life cycle in the human host [175], NAI appears to primarily target blood-stage infections [90]. In *P. vivax* malaria, the development of NAI is achieved by, or dependent on, exposure to both primary blood-stage infections and relapse infections in the blood. NAI to *P. vivax*, manifested as protection against high-density parasitaemia and uncomplicated clinical disease, has the following characteristics: (1) adult residents of holoendemic areas show the highest degree of NAI, due to cumulative exposure to multiple infections and relapses over time, yielding a diverse repertoire of strain-specific immune responses of sufficient magnitude. (2) A significant degree of continuous or regular antigenic exposure, referred to as premunition, is generally thought to be required, and in some circumstances NAI is greatly diminished on cessation of infection (transmission). (3) NAI is relatively species specific (*P. vivax* versus *P. falciparum*), and relatively strain specific [48, 96, 265].

Premunition implies the maintenance of high levels of malaria-specific antibodies and T cells resulting from frequent priming by malarial infection. NAI to *P. vivax* has been noted without premunition, such as in individuals treated with malariotherapy [48], and in low transmission areas [167]. NAI to *P. vivax* may, therefore, develop with comparatively little exposure. Potential biomarkers for *P. vivax* immunity are not known, but there is some evidence that functional Abs to PvDBP [92] and PvMSP1 [280] correlate with protection; these immune responses are associations rather than causal relations of protective immunity.

Population studies in Papua New Guinea [224, 252], Thailand [306] and Sri Lanka [250] have shown that individuals acquire immunity to *P. vivax* more quickly than to *P. falciparum* irrespective of overall transmission intensity, resulting in younger age groups experiencing the peak burden of *P. vivax* malaria. In the study of children in Papua New Guinea [252], by five years of age most children had acquired an almost complete immunity to clinical *P. vivax* yet remained at considerable risk of *P. falciparum* illness; this was despite a similar burden of *P. vivax* blood-stage infections. This difference in the rate of natural acquisition of immunity between *P. vivax* and *P. falciparum* has also been described in other co-endemic areas of the world, including those with substantially lower transmission levels [250, 306].

Similarly, actively induced *P. vivax* infections in malariotherapy patients resulted in faster acquisition of immunity than *P. falciparum* infections [265]. About two to three months after clinical symptoms had disappeared, subjects were experimentally re-inoculated either by mosquito bite or intravenous blood-stage challenge with the same parasite strain. Up to two-thirds of the individuals were completely immune to clinical malaria upon re-challenge. By the third exposure with the same strain, almost 100% of the individuals were clinically immune [48]. Since subjects quickly developed clinical immunity to the same parasite strain, they were then infected with different *P. vivax* strains with the aim to continue the fever treatments and it

became apparent that immunity was strain-specific [95]. Experimental infections produced by inoculation with malaria-infected erythrocytes, compared to those induced by mosquito bites, induced similar patterns of immunity, indicating that the acquired immunity was directed to blood-stage infection [95].

Explanations that have been proposed to explain the more rapid acquisition of clinical immunity to *P. vivax*, include; blood-stage immunity can be boosted even when malaria transmission is absent, due to hypnozoite relapses; and that *P. vivax*'s dependance on critical interactions, such as that between DBP and DARC, as opposed to *P. falciparum*'s multiple redundant options, makes *P. vivax* more susceptible to antibody-blockade.

Adoptive transfer of serum from avian [237], murine [298], non-human primate [89] and human *P. falciparum* malarias with NAI [90] into naïve animals or humans, protected against clinical malaria or significantly attenuated the severity and burden of malaria [244] and established that antibodies are critical for NAI to malaria. It is possible, however, that cellular immunity contributes more to NAI against blood-stage *P. vivax* than has been previously appreciated. Reticulocytes, unlike mature erythrocytes, still express MHC-1 molecules, a remnant from the nucleated reticuloblast [55]. A recent *P. vivax* CHMI study showed an expansion of a CD8+ T cell population with cytotoxic potential following intravenous inoculation with *P. vivax*-infected RBCs [55]. Intravenous inoculation with *P. falciparum*-infected RBCs did not result in a similar CD8+ T cell expansion. If T cell-mediated killing of infected reticulocytes is a significant factor in controlling blood-stage vivax infection, this may contribute to the earlier acquisition of NAI and is further encouragement that blood-stage vaccines against *P. vivax* may show more efficacy than those targeting *P. falciparum*.

There are many gaps in our knowledge of the biology of *P. vivax* merozoites and only a small number of merozoite proteins have so far been identified with specific

localisations and confirmed functional roles. There remain many hypothetical proteins, some of which are likely to have critical biological functions and be important for the development of immunity. The *P. vivax* parasite has evolved a variety of mechanisms which impair development of protective immune responses. These include; antigenic variation, poor immunogenicity and masking of critical regions by non-essential immunogenic regions or expression of these critical regions only at essential points in parasite invasion.

There is a small group of *P. vivax* merozoite proteins that have been investigated with some consistency over the past two decades and these include; PvDBP, PvRBPs, PvAMA1 and several PvMSPs. PvDBP is a microneme protein associated with the decisive irreversible step of junction formation between merozoite and erythrocyte during invasion, making it a prime target for vaccine-induced Ab-mediated immunity. It is the only *P. vivax* blood-stage antigen to have made it to clinical trials and is the subject of this research project. The first human efficacy trial of a PvDBP vaccine is planned for next year (see Chapter VII).

As outlined above, there are reasons for tentative optimism as this first clinical trial of a blood-stage vaccine against *P. vivax* approaches. An ideal *P. vivax* vaccine would impact on all three life-cycle stages of the parasite, but finding an effective blood-stage antigen is a pre-requisite.

1.3 The next generation of vaccines

Vaccines have saved more lives than any other class of medicine [307]. Two major infections, smallpox and rinderpest, have been eradicated, polio is close to eradication and measles is being targeted for eradication. Today, more than seventy vaccines have been licensed for use against approximately thirty pathogens and most health economists agree that vaccination represents the most cost-effective means to save lives and preserve good health.

Disease	Estimated Prevaccine Cases in 20th Century	Deaths in 2002
	number	
Smallpox	4.81 million	0
Poliomyelitis	1.63 million	0
Diphtheria	17.60 million	2
Haemophilus influenzae	2.00 million	22
Measles	5.03 million	36
Mumps	1.52 million	236
Pertussis	1.47 million	6632
Rubella	4.77 million	20
Tetanus	0.13 million	13

Figure 1.10: Estimated cumulative number of cases of selected infectious diseases in the United States in the 20th century before the advent of a vaccine, as compared with mortality after utilisation [328]

For nearly all successful licensed vaccines, natural immunity to infection has been shown, and these vaccines mimic the protective immune response. In contrast, for more complex infections such as malaria, HIV and tuberculosis, it has been difficult to show preventive immunity and development of effective 'traditional' vaccines has been challenging. Protection against these pathogens requires a distinct approach to vaccine design; one based on a molecular understanding of immunopathogenesis informing the rational design of antigens [151, 269].

Understanding the steps related to the entry and survival of these complex pathogens serves to identify highly conserved structures and offers molecular targets for broadly neutralizing antibodies. The definition of these conserved sites of vulnerability and knowledge of their atomic structure can define the pathogen proteins that elicit broadly-neutralising antibodies; this is the idea behind structure-based vaccine design.

Many new monoclonal antibodies directed against many complex pathogens have identified critical structures and enabled such structure-based antigen design. For HIV infection, alternative forms of envelope glycoproteins, including trimers, monomers, subdomains, and specific peptide loops transplanted onto scaffolds have been designed [216]. These candidate vaccines have been further modified using protein-design algorithms based on bioinformatics [271] in an effort to stabilise the immunogen, better expose the conserved sites, and mask or remove undesired epitopes. Similar strategies are under development for influenza viruses, respiratory syncytial virus, group B meningococcal strains [126, 216, 247, 270, 339] and, as will follow in this DPhil, *Plasmodium vivax* malaria. The deep sequencing of heavy and light chain antibody genes has identified intermediates that are critical for the evolution of broadly neutralizing antibodies [162].

The overarching goal is to use knowledge of structural biology and antibody evolution to design vaccines that will elicit antibodies of known specificity [57]. To counter immune evasion, by pathogens such as *Plasmodium*, subdominant immune responses can be generated to highly conserved invariant regions that are vulnerable to the immune system. Vaccines of the future will need to go beyond mimicking natural immune responses and must generate unnatural immunity [270].

An increasing number of vaccine vectors are available which aim to induce stronger humoral or cellular immunity. Gene-based delivery of vaccine antigens effectively elicits immune responses by synthesizing proteins within antigen-

presenting cells for endogenous presentation on MHC class I and II molecules. DNA-expression vectors, replication-defective viruses, or prime-boost combinations of the two [184, 239, 382] have proved effective in eliciting broadly neutralizing antibodies [409]. Prime-boost vaccine regimens that use DNA and viral vectors [239] have increased both humoral immunity and memory CD8 T cell responses [59].

mAb production and bioavailability have improved greatly in recent years and growing consideration is now being given to using mAbs for passive protection. If current pilot studies show good efficacy, sustained delivery mechanisms could potentially be achieved with gene-based antibody delivery. Adeno-associated viral (AAV) vectors have shown efficacy in protecting rodents, nonhuman primates, and humanized mice from lentiviral infection [19, 192], but there remain major challenges with this approach, most notably the need to regulate or extinguish antibody gene expression in the event of unanticipated adverse events.

1.4 Vaccines against *Plasmodium vivax*

The recently revised Malaria Vaccine Technology Roadmap to 2030 recognises the severity of *P. vivax* malaria and calls for a vaccine intervention to achieve 75% efficacy over two years – equally weighted with *P. falciparum* [263]. However, despite this rallying call, efforts to develop interventions against *P. vivax* still lag far behind those for *P. falciparum* and few novel candidate vaccines are in the pipeline or have been progressed to the clinic [266].

Figure 1.11, taken from a recent review of malaria vaccines [124], shows all the vaccines currently in clinical development, grouped by the parasite lifecycle stage they target; of the twenty-five vaccines listed, only two are against *P. vivax*.

To date, two subunit vaccines targeting the pre-erythrocytic stage *P. vivax* circumsporozoite protein (PvCSP), based on recombinant protein- or long synthetic peptide–in-adjuvant formulations, have reached clinical trials [37, 171]. The soluble recombinant protein candidate, VMP001, delivered in a proprietary Adjuvant

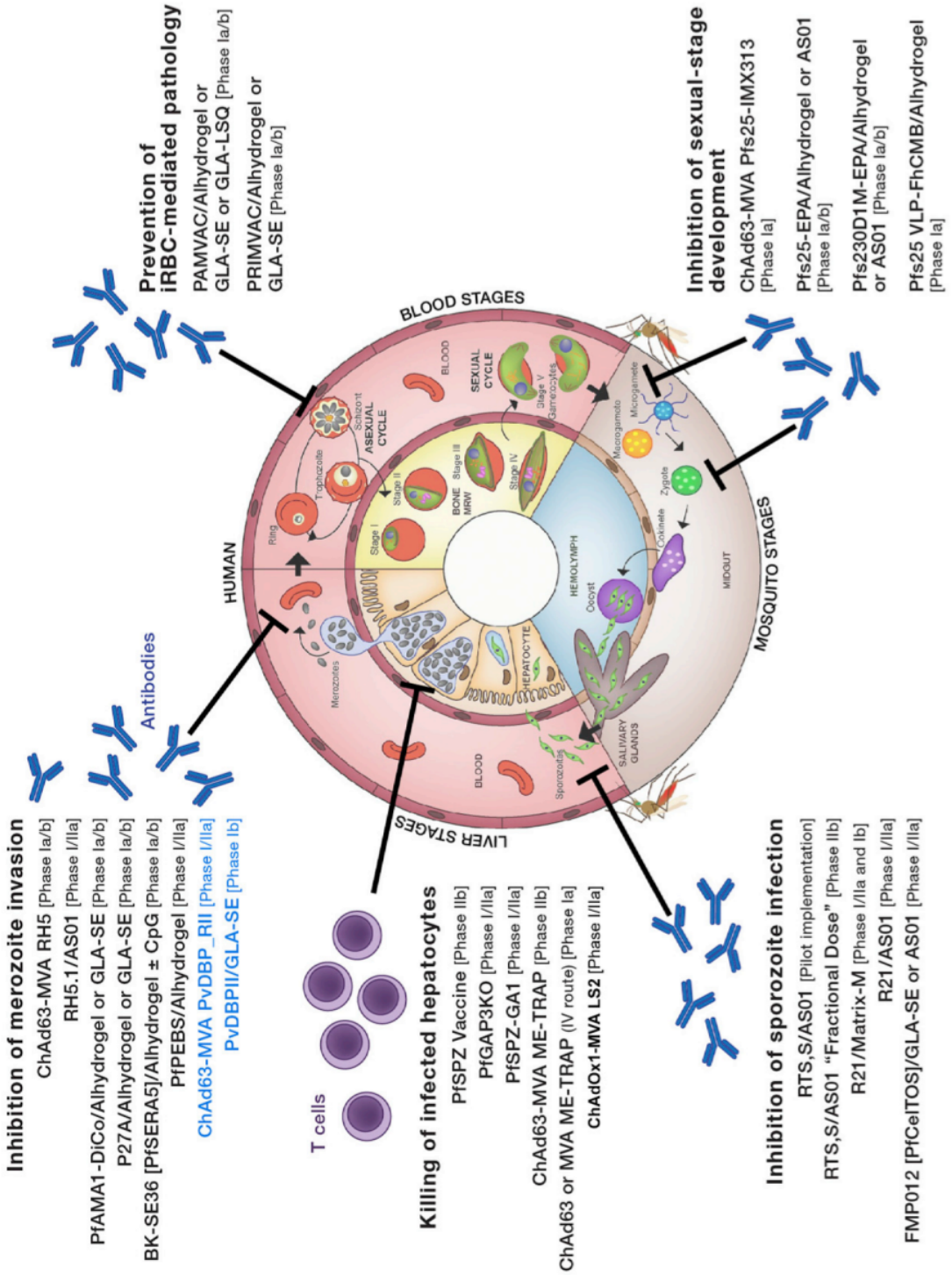


Figure 1.11: Malaria vaccine candidates in clinical development, taken from [124]. Data sources for this figure included the WHO Malaria Vaccine Rainbow Table and Clinicaltrials.gov. *P. vivax* vaccines are coloured blue.

System, AS01B, showed robust immunogenicity in healthy volunteers but failed to induce sterile protection following *P. vivax* controlled human malaria infection (CHMI) using a mosquito bite protocol. A small but significant delay in time to parasitaemia was seen in 16 of 27 vaccinated subjects compared with the control group [37]. A virus-like particle (VLP) using the same antigen fused to hepatitis B surface antigen (HBsAg), expressed in *Saccharomyces* cerevisiae and designated CSV-S,S, showed modest improvements in immunogenicity when tested in rhesus macaques with AS01 [399], but has not progressed to clinical testing.

In two other phase Ia clinical trials, a soluble recombinant protein vaccine targeting the sexual-stage ookinete surface protein Pvs25 was tested in two different adjuvants. This vaccine candidate, called Pvs25H, showed transmission-blocking activity in a direct membrane feeding assay when formulated with Alhydrogel [232], but vaccinations with Montanide ISA 51 were halted due to unexpected reactogenicity [427]. None of these pre-erythrocytic or transmission-blocking candidate subunit vaccines remain in active clinical development.

Vaccines targeting the asexual blood-stage infection (Figure 1.12) form an alternative and complementary approach to vaccines against the other life cycle stages, seeking to control and clear parasitaemia in order to prevent clinical disease and reduce onward transmission. As mentioned previously, epidemiological studies showing that under natural exposure, clinical immunity to *P. vivax* is acquired significantly more rapidly than to *P. falciparum*, both in high and low transmission settings [266], provides encouragement that the development of an effective blood-stage vivax vaccine may be feasible.

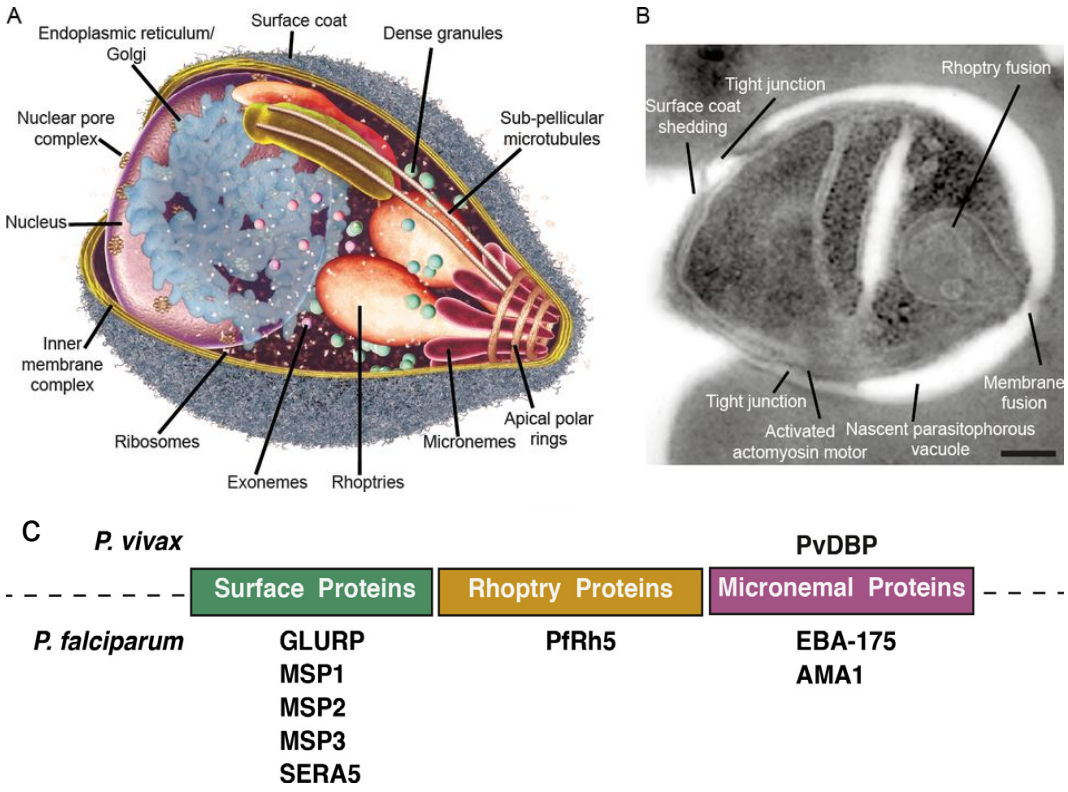


Figure 1.12: The *Plasmodium* merozoite. (A) Schematic showing several of the major structures and organelles of the merozoite. (B) A *P. falciparum* merozoite in the process of invading a human red blood cell (C) *Plasmodium vivax* and *Plasmodium falciparum* antigens currently in clinical development are shown according to their respective localisation to the surface coat, rhoptries or micronemes. PvDBP is *P. vivax* Duffy Binding Protein; EBA is erythrocyte-binding antigen; AMA is apical membrane antigen; PfRh5 is *P. falciparum* reticulocyte binding-like homologue 5, GLURP, glutamate-rich protein of *P.falciparum*; MSP, merozoite surface protein; SERA, serine repeat antigen. Figure is adapted from [376].

Although many candidates have been assessed over the years for *P. falciparum* [160], it was not until 2014 that the first clinical trial of a blood-stage vaccine against *P. vivax* took place [304]. This phase Ia trial of viral-vectored PvDBPII was conducted at The Jenner Institute here in Oxford and marked the starting point of this DPhil project.

Forty years after the discovery of Duffy-negativity as the source of natural immunity to Pv and twenty years after the parasite ligand, PvDBPII, which binds DARC had been described, this clinical trial was long overdue.

Despite not having progressed to human testing, PvDBP, and its interaction with DARC, has been subject to extensive pre-clinical scrutiny. It has been determined that a conserved, extracellular, cysteine-rich region known as region II (PvDBPII) contains the DARC-binding domain of PvDBP. Structural analyses of this domain showed that PvDBPII dimers bind either one or two DARC ectodomains, and proposed that distinct heterotrimeric and heterotetrameric architectures form on binding [30]. Immunization of mice, rabbits, and NHPs using PvDBPII–based vaccines induced binding-inhibitory antibodies [112, 264], and those raised against the *P. knowlesi* PkDBPα ortholog can block RBC invasion by this parasite *in vitro* [351]. In humans, naturally acquired high-titer binding-inhibitory antibodies against PvDBPII have been associated with reduced risk of *P. vivax* infection, lower *P. vivax* parasite densities following infection, and decreased risk of clinical malaria [201, 278].

All of these studies validated PvDBPII as a promising candidate antigen for a blood-stage vaccine and the 2014 phase Ia trial [304] showed that the viral-vectored (ChAd63-MVA) vaccine was well tolerated and demonstrated a favourable safety profile in malaria-naive adults. PvDBPII–specific *ex vivo* IFN-γ T cell, antibody-secreting cell, memory B cell, and serum IgG responses were all observed following the MVA boost immunization. Analysis of the antibody response to this trial formed the basis for this DPhil project and a Phase IIa proof-of-concept trial of this vaccine, using a blood-stage CHMI model, is planned for 2019.

1.5 Thesis outline and aims

An efficacious non-sterilising blood-stage malaria vaccine would suppress but not eliminate parasitaemia, thereby preventing disease and reducing transmission while allowing the development of protective NAI. Conceptually therefore, blood-stage malaria vaccines, have significant advantages over vaccines targeting other life-cycle stages; if pre-erythrocytic vaccines fail to provide sterilising immunity, the individual would be vulnerable to severe blood-stage disease and mosquito-stage vaccines would offer no protection to the individual once infected.

To date, however, efficacy from candidate blood-stage vaccines against *P. falciparum* has been disappointing and there is a general expectation that an effective blood-stage vaccine will need to target multiple parasite proteins to overcome redundancy and polymorphism.

This thesis aims to investigate the hypothesis that vaccine-induced protection against blood-stage *P. vivax* malaria might be achieved by focusing immune responses against a conserved region of one critical parasite protein.

The specific aims were to isolate a panel of human mAbs against the leading blood-stage *P. vivax* candidate antigen, PvDBPII, and to find ways of testing them for strain-transcendent neutralisation. The secondary aim, if a broadly-neutralising mAb could be found, was to map its epitope on PvDBPII, and thereby open up the possibility of re-engineering the vaccine to focus the immune response on a broadly-neutralising epitope. Another secondary aim, although ongoing and therefore not reported in this thesis, is to deliver such broadly-neutralising mAbs *in vivo* using viral vectored gene therapy.

Chapter II describes the experimental methods used.

Chapter III describes the process of isolating the antibody-coding genes of vaccine-induced B cells from the world's first clinical trial of a vaccine targeting the blood-stage of *P. vivax*. Ten mAbs were successfully isolated and expressed as recombinant proteins. I describe their binding kinetics, their competition for binding sites and their inhibitory profiles in biochemical assays using recombinant proteins.

Chapter IV describes the functional properties of the ten mAbs in terms of their ability to inhibit the growth of a transgenic *Plasmodium knowlesi* line expressing PvDBPII. This was the first time that a transgenic *P. knowlesi* parasite had been used to characterise anti-*P. vivax* antibodies. I review these initial functional data in light of the kinetic data and binding-inhibitory results reported in Chapter III.

Chapter V describes the neutralisation properties of the mAbs in short term *ex vivo* invasion assays using multiple clinical isolates of *P. vivax* in Thailand. Based on these assays, and sequencing of the PVDBPII gene region from the Thai isolates, I report the first broadly-neutralising human mAb against *P. vivax*. I compare the performance of the mAbs in the Thai *ex vivo* invasion assays to their performance in the transgenic *P. knowlesi* assays.

Chapter VI describes mapping the epitope of the broadly-neutralising mAb using an X-ray crystal structure of its Fab bound to PvDBPII, and the engineering of PvDBPII to focus immune response on the subdomain of this epitope. I also report the results of synergy assays between the broadly-neutralising mAb and other mAbs in the panel.

Chapter VII summarises the output of this thesis and discusses ongoing and future experiments with particular focus on (1) acquiring *in vivo* efficacy data for the newly-discovered broadly-neutralising mAb and (2) plans to deliver the mAb *in vivo* using viral-vectored gene therapy.

2
Materials and Methods

2.1 Materials

2.1.1 Reagents

Reagent	Company
2X ReddyMix PCR master mix	Thermo Scientific
4-nitrophenylphosphate-pNPP tablet	Sigma
Agarose	Sigma
Anti-CD71 MicroBeads	Miltenyi
Azide	Thermo Scientific
BCIP/NBT development buffer	Europa Bioproducts
Bovine serum albumin (BSA) 30%	Pierce
Carbenicillin	Sigma
Casein blocking buffer	Pierce
CD10 APC, clone HI10A Mouse anti-human	BD Bioscience
CD19 PE-Cy7 clone SJ25C1 Mouse anti-human	BD Bioscience
CD20 APC eFluor780 clone 2H7 Mouse anti-human	BD Bioscience
CD21 eFluor450 clone HB5 Mouse anti-human	BD Bioscience
CD27 Qdot65 clone CLB 27/1 mouse anti-human	BD Bioscience
CD38 PE-Cy5 clone HIT2 Mouse anti-human	BD Bioscience
DNeasy Blood and Tissue kit	Qiagen
IgG PE clone G18-145 Mouse anti-human	BD Bioscience
Diethanolamine 5x buffer	Fisher Scientific
Dimethyl sulphoxide (DMSO) 2.5%)	Sigma
Dulbecco's Modified Eagle Medium (DMEM)	Sigma
FastDigest buffer 10x	Fisher Scientific
FastDigest enzymes: Age1/ BshT1, Bsiw1/Pfl23II, Sal1, and Xho1	Fisher Scientific

Reagent	Company
Fetal calf serum (FCS)	Biotest Biosera
Field's Stain	Sigma
Formaldehyde 4%	Sigma
Gene ruler DNA ladder	Thermo Scientific
Glycerol	Sigma
Glycerolyte 57	Fenwal
Goat anti-human IgG (γ chain specific) -alkaline phosphatase conjugated	Sigma
Goat anti-human IgG γ-chain-HRP conjugate	Sigma
Goat anti-human IgG-Fluorescein Isothiocyanate (FITC) conjugate	Invitrogen
Goat anti-human IgG (Polyvalent)	Invitrogen
Goat anti-rabbit IgG Alkaline phosphatase	Sigma
GoTaq Master Mix	Promega
HEK293A cell line	In house (non-commercial)
HEK293E cell line	In house (non-commercial)
HEPES buffer (4-(2-hydroxyethyl)-1- piperazineethane-sulfonic acid)	Life Technologies
Expi293 complete expression media	Life Technologies
Freestyle media	Life Technologies
L-glutamine	Gibco
Loading dye 6x	New England Biolabs
Lysogeny broth (LB)	Sigma
McCoys 5A medium	Gibco
Nitro Blue Tetrazolium (NBT) solution	Sigma
Nuclease-free water	Qiagen
Papain beads (20341)	Thermo Fischer
Percoll	Sigma
Phusion polymerase	New England BioLabs
Protein G IgG elution buffer	Thermo Scientific
Polyethylenimine (PEI), Linear (MW 25,000)	Alfa Aesar
Qiagen Sensiscript RT kit	Qiagen
Qiagen Plasmid Plus Midi Kit	Qiagen
QIAprep Spin Miniprep Kit	Qiagen
QIAquick Gel Extraction Kit	Qiagen
Quick ligase	New England BioLabs
Quick ligase buffer 10x	New England BioLabs
Reticulocyte stain	Sigma
RNase Zap	Sigma
RNasin ribonuclease inhibitor	Promega
RPMI-1640	Sigma
Recombinant shrimp alkaline phosphatase (rSAP)	New England BioLabs
Super optimal broth (SOC)	Invitrogen
Stellar competent cells	Takara Bio Europe SAS

Reagent	Company
Sybr Safe DNA gel stain	Invitrogen
Thiazole Orange	Sigma
1M Tris-HCl pH 8.0	Sigma
TrypLE Express (trypsin)	Invitrogen
Tryphan blue	Sigma

Table 2.1: Reagents

2.1.2 Buffers and solutions

Name	Constituents
D0	500mL **DMEM** 5mL Pen/Strep (100U Penicillin, 100µg Strep/mL final concentration) 10mL L-glutamine (4mM final concentration)
D10	500mL **DMEM** 50mL **FCS** (10% final concentration) 5mL Pen/Strep (100U Penicillin, 100μg Strep/mL final concentration) 10mL L-glutamine (4mM final concentration)
R10	500mL **RPMI**-1640 media 50mL **FCS** (10% final concentration) 5mL Pen/Strep (100U Penicillin, 100µg Strep/mL final concentration) 5mL L-glutamine (4mM final concentration)
Development buffer	16mL deionised water 4mL 5x diethanolamine buffer 20mg 4-nitrophenylphosphate-pNPP tablet
***Plasmodium knowlesi* culture medium**	**RPMI** 1640 (Invitrogen) supplemented with: - 2.3 g/L sodium bicarbonate - 2.3 g/L sodium bicarbonate - 4 g/L dextrose - 5.957 g/L HEPES - 0.05 g/L hypoxanthine - 5 g/L Albumax II - 0.025 g/L gentamycin sulfate - 0.292 g/L L-glutamine - 10% (vol/vol) heat-inactivated human AB serum
***Plasmodium vivax* culture medium**	McCoys 5A medium (Gibco) supplemented with: - 2.4 g/L D-glucose - 40 mg/mL gentamycin sulfate - 20% (vol/vol) heat-inactivated human AB serum

Name	Constituents
Wash buffer	500mL PBS 1.66mL 30% BSA (0.1% final concentration) 0.1mL Azide (0.02% final concentration)

Table 2.2: Buffers and solutions

2.1.3 Primers

#	Name	Sequence 5' - %3'
	RT-PCR primers	
1	5' L VH1	ACAGGTGCCCACTCCCAGGTGCAG
2	5' L VH3	AAGGTGTCCAGTGTGARGTGCAG
3	5' L VH4/6	CCCAGATGGGTCCTGTCCCAGGTGCAG
4	5' L VH5	CAAGGAGTCTGTTCCGAGGTGCAG
5	3' Cγ CH1	GGAAGGTGTGCACGCCGCTGGTC
6	5' L VK1/2	ATGAGGSTCCCYGCTCAGCTGCTGG
7	5' L VK3	CTCTTCCTCCTGCTACTCTGGCTCCCAG
8	5' L VK4	ATTTCTCTGTTGCTCTGGATCTCTG
9	3' CK 543	GTTTCTCGTAGTCTGCTTTGCTCA
10	5' L Vλ1	GGTCCTGGGCCCAGTCTGTGCTG
11	5' L Vλ2	GGTCCTGGGCCCAGTCTGCCCTG
12	5' L Vλ3	GCTCTGTGACCTCCTATGAGCTG
13	5' L Vλ4/5	GGTCTCTCTCSCAGCYTGTGCTG
14	5' L Vλ6	GTTCTTGGGCCAATTTTATGCTG
15	5' L Vλ7	GGTCCAATTCYCAGGCTGTGGTG
16	5' L Vλ8	GAGTGGATTCTCAGACTGTGGTG
17	3' Cλ	CACCAGTGTGGCCTTGTTGGCTTG
	Screening/sequencing primers	
54	5'Ab sense	GCTTCGTTAGAACGCGGCTAC
55	AbVec IgG Rv	GGAAGTAGTCCTTGACCAGGC
56	AbVec Igκ Rv	GTTATTCAGCAGGCACACAACAG
57	AbVec Igλ Rv	TATCTGCCTTCCAGGCCAC
	Nested PCR primers	
58	VH1/5/7	CTTTTTCTAGTAGCAACTGCAACCGGT GTACATTCCGAGGTGCAGCTGGTGCAG
59	VH3	CTTTTTCTAGTAGCAACTGCAACCGGT GTACATTCTGAGGTGCAGCTGGTGGAG
60	VH4	CTTTTTCTAGTAGCAACTGCAACCGGT GTACATTCCCAGGTGCAGCTGCAGGAG
61	VH3-23	CTTTTTCTAGTAGCAACTGCAACCGGT GTACATTCTGAGGTGCAGCTGTTGGAG
62	VH4-34	CTTTTTCTAGTAGCAACTGCAACCGGT GTACATTCCCAGGTGCAGCTACAGCAGT
63	VH1–18	CTTTTTCTAGTAGCAACTGCAACCGGT GTACATTCCCAGGTTCAGCTGGTGCAG

64	VH1–24	CTTTTTCTAGTAGCAACTGCAACCGGT GTACATTCCCAGGTCCAGCTGGTACAG
65	VH3–9/30/33	CTTTTTCTAGTAGCAACTGCAACCGGT GTACATTCTGAAGTGCAGCTGGTGGAG
66	VH6–1	CTTTTTCTAGTAGCAACTGCAACCGGT GTACATTCCCAGGTACAGCTGCAGCAG
67	VH4–39	CTTTTTCTAGTAGCAACTGCAACCGGT GTACATTCCCAGCTGCAGCTGCAGGAG
68	VH3–33	CTTTTTCTAGTAGCAACTGCAACCGGT GTACATTCTCAGGTGCAGCTGGTGGAG
69	JH1/2/4/5	GATGGGCCCTTGGTCGACGCTGAGGAG ACGGTGACCAG
70	JH3	GATGGGCCCTTGGTCGACGCTGAAGAG ACGGTGACCATTG
71	JH6	GATGGGCCCTTGGTCGACGCTGAGGAG ACGGTGACCGTG
72	IPCR AbVecγ Fw	GTCGACCAAGGGCCCA
73	VK1	CTTTTTCTAGTAGCAACTGCAACCGGTG TACATTCTGACATCCAGATGACCCAGTC
74	VK1-9/1-13	CTTTTTCTAGTAGCAACTGCAACCGGTG TACATTCAGACATCCAGTTGACCCAGTCT
75	VK1D-43/1-8	CTTTTTCTAGTAGCAACTGCAACCGGTG TACATTGTGCCATCCGGATGACCCAGTC
76	VK2	CTTTTTCTAGTAGCAACTGCAACCGGTG TACATGGGGATATTGTGATGACCCAGAC
77	VK2-28/2-30	CTTTTTCTAGTAGCAACTGCAACCGGTG TACATGGGGATATTGTGATGACTCAGTC
78	VK3-11/3D-11	CTTTTTCTAGTAGCAACTGCAACCGGTG TACATTCAGAAATTGTGTTGACACAGTC
79	VK3-15/3D-15	CTTTTTCTAGTAGCAACTGCAACCGGTG TACATTCAGAAATAGTGATGACGCAGTC
80	VK3-20/3D-20	CTTTTTCTAGTAGCAACTGCAACCGGTG TACATTCAGAAATTGTGTTGACGCAGTCT
81	VK4-1	CTTTTTCTAGTAGCAACTGCAACCGGTG TACATTCGGACATCGTGATGACCCAGTC
82	JK1/2/4	ATGGTGCAGCCACCGTACGTTTGATYTCC ACCTTGGTC
83	JK3	ATGGTGCAGCCACCGTACGTTTGATATCC ACTTTGGTC
84	JK5	ATGGTGCAGCCACCGTACGTTTAATCTCC AGTCGTGTC
85	JK150/3	ATGGTGCAGCCACCGTACGTCTGA TTTCCACCTTGGTC
86	IPCR AbVec κ Fw	CGTACGGTGGCTGCAC
87	VL1	CTTTTTCTAGTAGCAACTGCAACCGGTT CCTGGGCCCAGTCTGTGCTGACKCAG
88	VL2	CTTTTTCTAGTAGCAACTGCAACCGGTT CCTGGGCCCAGTCTGCCCTGACTCAG
89	VL3	CTTTTTCTAGTAGCAACTGCAACCGGTT CTGTGACCTCCTATGAGCTGACWCAG

90	VL4/5	CTTTTTCTAGTAGCAACTGCAACCGGTT CTCTCTCSCAGCYTGTGCTGACTCA
91	VL6	CTTTTTCTAGTAGCAACTGCAACCGGTT CTTGGGCCAATTTTATGCTGACTCAG
92	VL7/8	CTTTTTCTAGTAGCAACTGCAACCGGTT CCAATTCYCAGRCTGTGGTGACYCAG
93	CL reverse	GGCTTGAAGCTCCTCACTCGAGGGYG GGAACAGAGTG
94	IPCR AbVec λ Fw	CTCGAGTGAGGAGCTTCAAG
95	IPCR AbVec λ Rv	ACCGGTTGCAGTTGCTACTA
mAb expression cassette primers		
96	J2620-mabK7Fw	GAGTCAGTGAGCGAGGAAG
97	J2621-mabK7Rev	GTTGCTGACTAATTGAGATGC

Table 2.3: Primers

2.1.4 Lab consumables

Consumable	Company
0.22μm syringe filter	Millipore
96-well U-bottom plate	Corning
96-well flat bottom cell culture plate	Corning
96-well PCR plate, non-skirted	Star Lab
96-well flat/half area tissue culture cluster plates	Appleton Woods
Amicon Ultra 15mL centrifuge filters	Millipore
CASYton tubes	Sedna Scientific
Centrifuge tubes, 150mL	Corning
F96 Maxisorp Nunc Immuno-Plate	Nunc
HiTrap Protein G HP 5mL column	GE Healthcare Life Sciences
CaptureSelect^{TM} C-tag column	Thermo Fisher
ELIspot Plates	Millipore
Erlenmeyer conical flasks, 250mL	Corning
Erlenmeyer conical flasks, 1000mL	Corning
HiLoad Superdex 75 16/60 GE	Healthcare
S200 HiLoad 16/60 column GE	Healthcare

Consumable	Company
MACS LS and LD columns	Miltenyi Biotec
Non-woven filters	Antoshin
PCR tubes strip domed 12 cap	Bio-Rad
Protein-A HiTrap column GE Healthcare	Life Sciences
T75 flat-bottom tissue culture flasks	Corning
Stericup 0.22μm vacuum filter	Millipore

Table 2.4: Lab consumables

2.1.5 Electronic Equipment

Equipment	**Company**	**Software**
Axiovert S100 inverted fluorescent microscope	Carl Zeiss	Axiovision digital microphotography software
ÄKTA Pure FPLC machine	GE Healthcare Bio-Sciences	
ÄKTA start FPLC machine	GE Healthcare Bio-Sciences	
Amaxa 4D electroporator	Lonza	
BIACore X100	GE Healthcare Bio-Sciences	Biacore X100 evaluation software
CASY cell Counter	Schärfe System	
CLARIOstar plate reader	BMG Labtech	CLARIOstar software
G Storm PCR Machine	Lab Tech	
Gel tank	Bi-Rad	
Infinite F50 Absorbance Microplate Reader	Tecan	Magellan reader
MoFlo cell sorter	Dako Cytomation	
Nanodrop ND-1000 Spectrophotometer	Labtech	ND-1000
OctetRED384	FortéBio	
P3 Primary cell 4D Nucleofector X Kit L	Lonza	
Sonicator S-400	Misonix, USA	

Table 2.5: Electronic equipment

2.2 Chapter III methods

2.2.1 Production of mAbs

Isolation of single antibody secreting cells

Peripheral blood samples were collected, in heparinised tubes, from volunteers in a phase Ia safety and immunogenicity trial [304] (clinicaltrials.gov identifier: NCT01816113) one week after the second immunisation with viral-vectored PvDBPII. PBMC were separated out by centrifugation in Leucosep tubes (Greiner Bio one) and enriched for B cells using a human pan-B cell enrichment kit (Easysep). These enriched B cells were then re-suspended in DMEM and stained with the following fluorophore-conjugated antibodies; $CD10^{-}$,$CD19^{+}$, $CD20^{-}$, $CD21^{-}$, $CD27^{+}$, $CD38^{+}$, IgG^{+}. The stained B cells were then single-cell sorted using a MoFlo cell sorter (Dako cytomation) into 96-well PCR plates containing 10μL of 10mM Tris HCl buffer and RNase inhibitor (Promega) at 40U/mL and stored at -80°C prior to RT-PCR.

Isolating the antibody variable regions

After thawing on ice, a one-step RT-PCR (Table 2.6) was carried out in each single cell well of the 96-well plate, using a panel of primers, 14 forward and 3 reverse, designed to cover the full diversity of antibody variable region sequences (Primers 1-17) and a Sensiscript RT kit (Qiagen).

	Total	
40μL each FWD primer 100μM stock	560μL	(3.57μM FWD primers in primer mix)
56μL each REV primer 100μM stock	168μL	(5.00μM REV primers in primer mix)
392μL nuclease-free water (Qiagen)	392μL	
	1120μL	

Table 2.6: RT Primer mix

The thermal cycle settings for the RT-PCR (Tabel 2.7 on the next page) were: 40 minutes at 37°C; 10 minutes at 43°C; 10 minutes at 50°C, with a holding temperature of 4°C.

	Total	
Nuclease-free water	3μL	
10x buffer	2μL	
RT primer mix	2μL	0.375μM FWD primers and 0.5µM REV primers in Sensiscript RT-PCR reaction
dNTP	2μL	
Sensiscript RT enzyme	1μL	
Well containing catch buffer and ASC	10μL	
	20μL reaction	

Table 2.7: RT-PCR reaction (Qiagen Sensiscript RT Kit)

The cDNA from the RT-PCR step was then amplified (PCR 1, Table 2.8) and subject to an Ig chain specific nested PCR. 1μL of cDNA was added to 19μL of PCR mix in the wells of a 96 well plate and run on the following PCR settings; 98°C for 30 seconds; then 15 cycles of alternating 98°C for 10 seconds and 72°C for 1 minute; 15 cycles of 98°C for 10 seconds alternating with 68°C for 30 seconds and 72°C for 1 minute; and finally 72°C for 10min, with a holding temperature of 4°C.

	Total	
Nuclease-free water	7.5μL	
RT primer mix	1μL	(0.375μM FWD primers and 0.5μM REV primers in PCR reaction)
DMSO (2.5%)	0.5μL	
Phusion polymerase (New England Biolabs)	10μL	
cDNA	1μL	
	20μL reaction	

Table 2.8: PCR 1

The PCR 1 product was diluted 1:100 in nuclease-free water and 1μL added to 19μL of PCR master mixes containing Phusion polymerase, DMSO and chain-specific primers were prepared for each Ig chain (Tables 2.9- 2.11). The thermal cycle for PCR2 was: 98°C for 30 seconds; 40 cycles of alternating 98°C for 10 seconds and 72°C for 1 minute; then 72°C for 10min, with a holding temperature of 4°C.

Heavy chain primer mix: 14 heavy primers, No. 58-71	
	Total:
7μL each heavy primer (100μM stock)	98μL (2.41μM each primers in primer mix)
42μL nuclease-free water	42μL
	140μL
Nested PCR Reaction:	
Nuclease-free water	8.25μL
Heavy chain primer mix	0.25μL (0.06μM of each primers)
DMSO (2.5%)	0.5μL
Phusion polymerase	10μL
cDNA (1:100 dilution in water)	1μL
	20μL reaction

Table 2.9: Nested PCR Gamma Chain

Kappa chain primer mix: 13 kappa primers, No. 73-85	
	Total:
7μL each kappa primer (100μM stock)	91μL (2.41μM each primers in primer mix)
49μL nuclease-free water	49μL
	140μL
Nested PCR Reaction:	
Nuclease-free water	8.25μL
Kappa chain primer mix	0.25μL (0.06μM of each primers)
DMSO (2.5%)	0.5μL
Phusion polymerase	10μL
cDNA (1:100 dilution in water)	1μL
	20μL reaction

Table 2.10: Nested PCR Kappa Chain

Lambda chain primer mix: 7 lambda primers, No. 87-93	
	Total:
21μL each lambda primer (100μM stock)	147μL (1.86μM each primers in primer mix)
273μL nuclease-free water	273μL
	420μL
Nested PCR Reaction:	
Nuclease-free water	8.25μL
Lambda chain primer mix	0.75μL (0.19μM of each primers)
Phusion polymerase	10μL
cDNA (1:100 dilution in water)	1μL
	20μL reaction

Table 2.11: Nested PCR Lambda Chain

The PCR product was run on a 1.8% agarose gel and screened for positive bands at approximately 440bp size, using Generuler DNA 1kb ladder (Thermofisher) with a range of 250-10,000bp. The positive bands were excised, purified using the Qiagen QIAquick gel extraction kit, and eluted in nuclease-free water. The cDNA concentrations were then measured using the NanoDrop 1000 spectrophotometer.

Restriction enzyme cloning

Antibody chain specific expression plasmids, AbVec-hIgG1/AbVec-hIgKappa/AbVec-hIgLambda, obtained from Patrick C. Wilson (University of Chicago), were digested and linearized using restriction enzyme BshTI at their 5' site and SalI, Pfl23II and XhoI respectively at their 3' sites (Table 2.12).

The Ig chain-specific vectors (Figure 2.1) were digested using the same enzyme combinations (Table 2.12 on the next page) as the insert digestions (FastDigest), but with the addition of rSAP. The backbones were digested at 37°C for 1 hour and then heat inactivated at 80°C for 10 minutes (Table 2.13 on the following page).

Ig chain	Chain-specific enzyme	Reaction
Heavy	0.5μL Sal1 FastDigest	0.5μL Age1/ BshT1 FastDigest enzyme +
Kappa	0.5μL Bsiw1/Pfl23II FastDigest	0.5μL Sal1/ Bsiw1/Pfl23II/ Xho1 FastDigest enzyme +
Lambda	0.5μL Xho1 FastDigest	3.4μL FastDigest buffer + 30 μL gel extraction

Table 2.12: Insert Digestion Reaction

Ig chain	Chain-specific enzyme	Reaction
Heavy	1μL Sal1 FastDigest	1μL Age1/ BshT1 FastDigest enzyme + 1μL Sal1/ Bsiw1/Pfl23II/ Xho1 FastDigest enzyme +
Kappa	1μL Bsiw1/Pfl23II FastDigest	4μL FastDigest buffer + 31μL water +
Lambda	1μL Xho1 FastDigest	2μLrSAP + 1μg (1μL) H/κ/ λ plasmid

Table 2.13: Backbone digestion reaction

Ligation, bacterial transformation and colony screening

2μL of digested insert was added to 2μL of digested insert-specific backbone, 15μL of nuclease-free water, 1.5μL Quick Ligase buffer and 0.5μL Quick Ligase. The 20μL ligation reaction took 10 minutes at room temperature. 2μL ligation product was then combined with 10μL Stellar competent cells in a 96-well PCR plate and left on ice for 30 minutes. The samples were heat shocked for 30 seconds in a 42°C water bath and placed on ice for a further 2 minutes. 50μL of SOC medium was added and samples were incubated for 10 minutes at 37°C. 30μL of the cell mixture was spread on warmed 0.1% Carbenicillin agar plates and left overnight in a 37°C

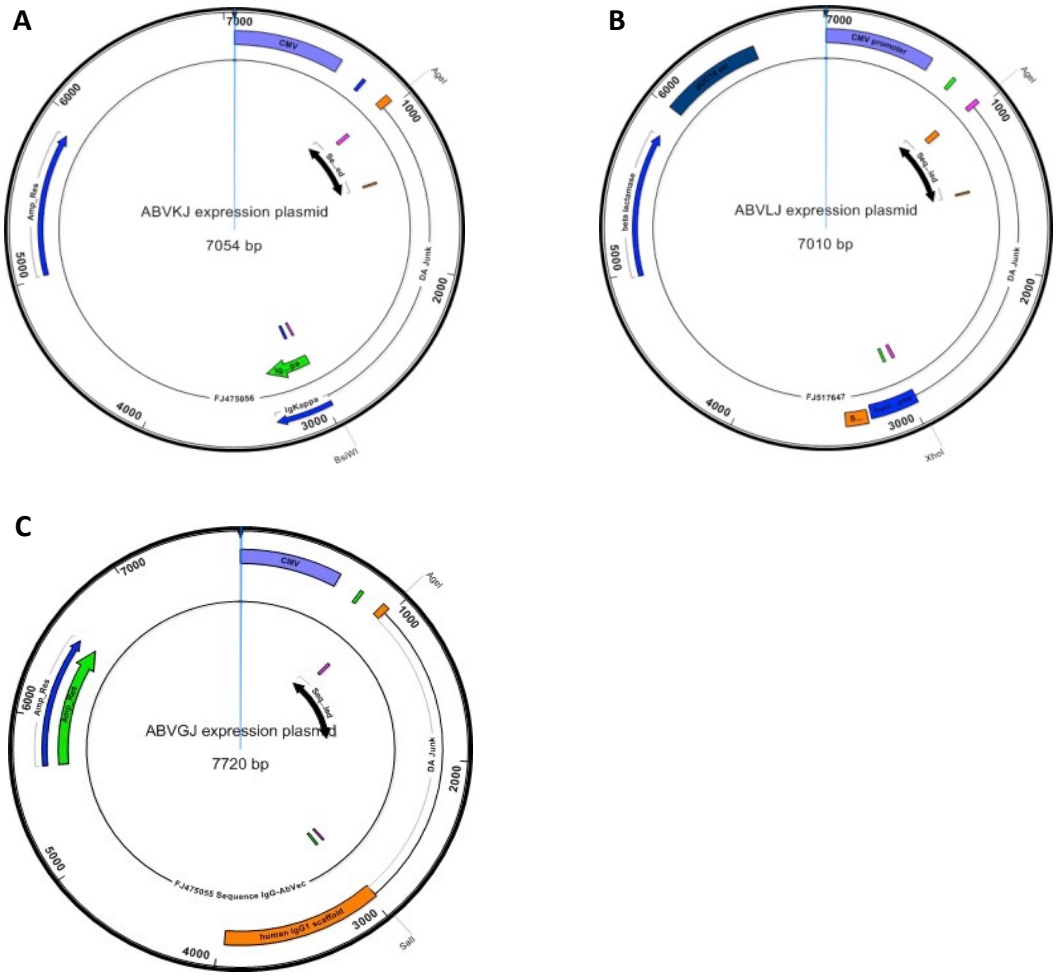


Figure 2.1: Ig chain-specific vectors. (A) ABVKJ expression plasmid (kappa backbone), (B) ABVLJ expression plasmid (lambda backbone), and (C) ABVGJ expression plasmid (heavy backbone). All expression vectors contained CMV promoter regions, Ampicillin resistance genes and specific enzyme restriction sites to which matching Ig insert digestions could be ligated. Plasmids were obtained from the Wilson group [426].

incubator.

Colonies were randomly selected from each agar plate and screened by PCR (Table 2.14) at the following thermal cycle settings; 98°C for 6 minutes; 10 cycles of alternating 95°C for 25 seconds, 68°C for 1 minute, 72°C for 90 seconds; 25 cycles of 95°C for 25 seconds, 68°C for 30 seconds, 72°C for 1 minute; 72°C for 5 minutes, with a holding temperature of 4°C.

The total volume of PCR product was run on a 1% agarose gel and screened for positive bands at approximately 600-700bp for heavy chains and 550bp for

Nuclease free water	4μL
ReddyMix 2xPCR Master mix	5μL
5′AbSense primer 10μM	0.5μL
AbVec IgG/K/L Rev primer 10μM	0.5μL
	10μL per reaction

Table 2.14: Colony screen PCR

light chains. Positive colonies were further bulked up in culture before purifying out their plasmid DNA.

Expression of the mAbs for antigen-specificity screening

Twenty four hours prior to transfection, exponential growth-phase adherent HEK293 cells (HEK293A) were re-suspended in DMEM (Sigma-Aldrich) supplemented with 2mM L-glutamine, 1mM sodium pyruvate, 100U/mL penicillin, 0.1mg/mL streptomycin and 10% ultra-low IgG foetal bovine serum (Thermofischer) and seeded at 40000 cells/well in 100μL in Costar 96-well cell culture plates (Corning).

The following day, 50μL of 60μg/mL linear 25kDa PEI (Alfa Aesar) was mixed with 200ng of matched heavy- and light-chain coding plasmid in a volume of 50μL and shaken at room temperature for 30 minutes. The DNA-PEI complexes were then added to the HEK293A cells. An additional 50μL of supplemented DMEM was added to each well the next day. All transfections were performed in triplicate wells and three wells were transfected with PEI but no DNA as a negative control. The supernatants were harvested 4 days after transfection.

2.2.2 Recombinant protein expression

PvDBPII

The production of recombinant PvDBPII from *Drosophila* S2 cells has been previously described [112]. In brief; the sequence used was identical to the VAC051 vaccine sequence; $\alpha\alpha$ D194–T521 of PvDBPII (SalI), with T257A, S353A and T422A substitutions to remove sites of possible N-linked glycosylation, followed by a shortened 9 $\alpha\alpha$ Pk/V5 epitope tag (IPNPLLGLD) and a 4 $\alpha\alpha$ C-tag (EPEA)[191]

for detection and purification, respectively.

Purification was performed on an AKTA Pure 25 system (GE Healthcare, UK), consisting of an affinity step with CaptureSelect™ C-tag column (Thermo Fisher Scientific, UK) and a polishing size exclusion chromatography (SEC) using Superdex 200 16/60 PG (GE Healthcare, UK) in 20 mM Tris-HCl, 150 mM NaCl, pH 7.4 (TBS). Purified protein was quantified by Nanodrop (Thermo Fisher Scientific, UK) and stored at -80°C until further use.

A gene encoding the PvDBPII HMP013 allele [243] (aa 194-521) was codon-optimized for human expression and synthesized (Genewiz, USA). This sequence, with a 5' KpnI site and 3' XbaI site, was cloned into a mammalian expression plasmid in frame with an N terminal mouse IgK light chain leader sequence and a C-terminal C-tag prior to the stop codon. Suspension EXPI293F cells (Thermo Fisher Scientific, UK) were transiently transfected and culture supernatants were harvested after 4 days. Purification was performed on an AKTA Pure 25 system (GE Healthcare, UK), consisting of an affinity step with CaptureSelect™ C-tag column (Thermo Fisher Scientific, UK) and a polishing SEC step using Superdex 200 Increase 10/300 GL (GE Healthcare, UK) in 20 mM Tris-HCl, 150 mM NaCl, 0.1% Tween 20, pH 7.4 (TBS). Purified protein was quantified by Nanodrop (Thermo Fisher Scientific, UK) and stored at -80°C until further use.

N-terminal DARC

The production of recombinant N-terminal DARC has been previously described [304]. In brief; a gene encoding the first 60 $\alpha\alpha$ of DARC Fyb allele (GenBank Accession # ABA10433.1) followed by a thrombin cleavage site (LVPRGS) and an AviTag (GLNDIFEAQKIEWHE) was codon-optimized for *E. coli* expression and synthesized (GeneArt, Life Technologies). Cysteines 4, 51 and 54 of DARC were mutated to alanine [30, 80]. This sequence with 5' KpnI site and 3' BamHI site was cloned into a mammalian expression plasmid [122] in-frame with an N-terminal human

tissue plasminogen activator (tPA) leader sequence [112] and a C-terminal hexa-histidine tag prior to the stop codon. Suspension HEK293E cells grown in EXPI293 expression medium (Thermo Fisher Scientific, UK) were transiently transfected with plasmid [122] and allowed to grow for three days before the supernatant was harvested, purified using a HisTrap Excel column (GE Healthcare, UK) and buffer exchanged into PBS. Purified protein was quantified by Nanodrop (Thermo Fisher Scientific, UK) and stored at -80°C until further use.

2.2.3 Screening the mAbs for antigen-specificity

Screening was by indirect ELISA of the HEK293A culture supernatant. PvDBPII was coated onto Maxisorp flat-bottom 96-well ELISA plates (Nunc) at 2μg/mL in 50μL at 4°C overnight. Wells were washed twice with PBS-T and blocked for an hour with 200μL of Blocker™ Casein (Thermofisher) before adding the neat HEK293A culture supernatant for 1 hour at room temperature. The plate was then washed 4 times with PBS-T before the addition of goat anti-human gamma-chain alkaline phosphatase-conjugated secondary antibody (Sigma-Aldrich) for 45 minutes at room temperature. After a final wash step, 6 times with PBS-T, the plates were developed with 100μL per well of PNPP substrate at 1mg/mL (Sigma-Aldrich) and read on an Infinity F50 plate reader at 405nm (Tecan).

2.2.4 Plasmid DNA preparation and *E. coli* culture

Plasmid DNA preparations of the PvDBPII specific mAbs were made with Plasmid *Plus* midi or maxi silica-based anion-exchange kits (Qiagen) as per the manufacturer's instructions. DNA was eluted in deionised water.

Transformed *E. coli* were seeded in appropriate volumes of LB with antibiotic and grown at 37°C in a shaking incubator at 225rpm for ≈18 hours.

2.2.5 Expression of the PvDBPII-specific mAbs

Twenty four hours prior to transfection, HEK293F cells were diluted to 1.10^6 cells/mL in Expi293 Expression medium (Thermofisher). The following day, 100μg of cognate heavy chain/light chain mix was mixed with Expifectamine 293 transfection reagent in 10mL of Gibco Opti-MEM™ I Reduced Serum Media (Thermofisher) for each 100mL of culture to transfect. This was incubated at room temperature for 20 min before adding it to the culture. 16 hours post transfection, enhancers 1 and 2 were added, as recommended in the manufacturer's instructions, and the culture was left to incubate in an orbital shaking incubator at 37°C for 72 hours. Supernatants were harvested by filtering the supernatant with a 0.22μm vacuum filter after centrifuging the culture at 2500g for 15 minutes.

2.2.6 Purification of the mAbs

The antibodies were purified using a 5mL Protein G HP column (GE Healthcare) on an ÄKTA start FPLC system (GE healthcare). Dulbecco's PBS was used for equilibration and wash steps before eluting in 0.1M glycine pH 2.7. The eluates were pH neutralized to 7.4 using 1.0M Tris HCl pH 9.0, buffer-exchanged into Dulbecco's PBS and concentrated using an Amicon ultra centrifugal concentrator (Millipore) with a molecular weight cut-off of 30kDa.

2.2.7 Sequencing

All sequencing was carried out by GATC-biotech using dye-terminator Sanger sequencing.

2.2.8 Determination of antibody kinetics using SPR

Recombinant PvDBPII was made as described above and data were collected on a Biacore X100 (GE healthcare) machine. Experiments were performed at 25°C in Dulbecco's PBS + 0.005% Polysorbate-20 (GE healthcare). A protein A-coated sensor chip (GE healthcare) was used to capture purified antibody diluted in SPR running buffer at a flow rate of 5μL/min. Next, a range (typically 20nM-0.625nM) of

six 2-fold dilutions of PvDBPII with one replicate was injected for 90s at 60μL/min and dissociation was measured for 1600s. Specific binding of the PvDBPII protein to mAb was obtained by reference-subtracting the response of a blank surface from that of the mAb-coated surface. Sensorgrams were fitted to a global Langmuir 1:1 interaction model, allowing the Biacore X100 evaluation software to determine the kinetic association and dissociation rate constants.

2.2.9 Epitope binning by Bio-layer interferometry

Assays, using streptavidin-coated biosensors (FortéBio) and black 96-well plates (Greiner), were carried out on an OctetRED384 (FortéBio).The biosensor assay followed six sequential steps:

- Baseline (PBS, 30s)
- Protein immobilisation (neat supernatant, 120s)
- Wash (PBS, 60s)
- mAb1 binding (300nM mAb1, 120s)
- Wash (PBS, 60s)
- mAb2 binding (150nM mAb2, 120s)

The antibodies were diluted in PBS. The PvDBPII protein sequence used was the Sal1 reference sequence (amino acids 194-521) with T257A, S353A and T422A substitutions to remove sites of possible N-linked glycosylation mutations. It also contained an AviTag™ biotin acceptor peptide followed by a Strep-Tag II™ at the 3' end of the PvDBPII-coding sequence. The PvDBPII was expressed as secreted protein in HEK293F cells, co-expressed with the bacterial BirA biotin ligase for efficient site-specific biotinylation. Supernatant was collected 3 days after transfection, centrifuged and filtered to remove cell material and extensively dialysed in PBS to remove free biotin.

2.2.10 PvDBPII-DARC binding inhibition assays

This assay was used initially to test the sera from the VAC051 trial and subsequently adapted for the anti-PvDBPII mAbs. The assay methodology for testing the trial sera has been previously reported [304]. In brief; recombinant N-terminal DARC protein was coated onto Nunc-Immuno Maxisorp plates at 1μg/mL in Dulbecco's PBS (DPBS – Sigma Aldrich, UK) overnight at 4°C. Plates were washed with PBS and PBS/T and blocked with 2% skimmed milk in PBS for 2 h at 37°C. mAb samples were diluted down in a 2-fold series (starting at 1mg/mL) in 0.25% milk in PBS and 50μL of each test sample (added at twice the final desired concentration) was then pre-incubated with 50μL of PvDBPII (at a concentration 0.1μg/mL in 0.25% skimmed milk in PBS) for 30 min at RT. The pre-incubated PvDBPII protein plus mAb mixture was then added to the DARC-coated plates (in duplicate wells). The plates were incubated for 1 h at 37°C, washed with PBS/T and then incubated for another hour with anti-PvDBPII polyclonal rabbit serum [112] diluted 1:1000 in 0.25% milk in PBS. After a further wash step in PBS/T, plates were incubated with a 1:1000 dilution of anti-rabbit IgG alkaline phosphatase (Sigma Aldrich, UK), washed once more with PBS/T and developed with 1 mg/mL p-nitrophenylphosphate in diethanolamine buffer (Pierce, UK).

OD_{405} was read using a Model 550 Microplate Reader (Bio-Rad, UK) when control wells containing PvDBPII protein and buffer only reached a value of 1.0. In one column of each 96 well plate, wells contained only mAb (1mg/ml) and buffer (no PvDBPII protein) and these 'background' OD_{405} values were subtracted from all test values. To calculate % binding-inhibition for each mAb sample the formula below was used:

1 – (OD_{405} value of d84 serum sample / OD_{405} value of corresponding d0 serum sample) x 100 %

Five allelic variants of recombinant PvDBPII were used in the assay; Sal1, which was made as described above; PvAH, PvO and PvP alleles, which were a kind gift from Chetan Chitnis; and PvHMP013, which was sequenced from a vivax-infected

patient in Australia [243]. The expression of recombinant PvDBPII HMP013 protein has been previously described [304] and is summarised above.
An in-house Ebola virus glycoprotein-reactive IgG1 mAb was used as a negative isotype control for mAb samples.

2.3 Chapter IV methods

2.3.1 Genetic modification of *Plasmodium knowlesi* parasites

The genetic modification of *Plasmodium knowlesi* was performed by colleagues at the London School of Hygiene and Tropical Medicine (*Mohring et al*, submitted for publication). The steps are summarised below.

Cloning of pDonor_PkDBPα

Recodonised sequences of PkDBPα and PvDBP of the *P. vivax* Salvador I strain with SpeI and NcoI restriction sites were obtained from Geneart (Thermo Fisher Scientific). 500 bp HRs in the 5'UTR and 3'UTR of PkDBPα were amplified with primers olFM062 and olFM063 adding SacII /SpeI and primers olFM064 and olFM065 adding NotI/NcoI restriction sites, respectively. HRs were cloned into the Geneart plasmid. In the next step either the recodonised PkDBPα or PvDBP gene was inserted with SpeI and NcoI restriction sites in between the HRs. The final vector was linearised with PvuI restriction enzyme and ethanol precipitated.

Cloning of pDonor_PkDBPα and γ

Transfection constructs were generated as described for pDonor_PkDBPα. A spacer sequence, to aid in subsequent diagnostic PCRs was generated by polymerase cycling assembly (PCA). Briefly, the spacer sequence was synthesised by using primers of 60 bp length with 20 bp homologous sequence to the adjacent primers on each side. Final concentrations of 0.6μM for outer primers (ol488 and ol492) and 0.03μM of inner primers (ol489, ol490, ol491 and ol762 (DBPβ) or ol503 (DBPγ) were used for PCA with the same cycle conditions as described for PCR. The final product

was inserted with SpeI and NcoI restriction sites between the HRs as described for pDonor_PkDBPα cloning, to replace the deleted DBPβ and DBPγ genes.

Parasite maintenance, transfection and dilution cloning

The *P. knowlesi* A1-H.1 parasite line [261] was used for all transfections. Parasites were maintained at 2% HCT in complete media, comprising RPMI 1640 (Invitrogen) with the following additions: 2.3g/L sodium bicarbonate, 4g/L dextrose, 5.957g/L HEPES, 0.05g/L hypoxanthine, 5g/L Albumax II, 0.025g/L gentamycin sulfate, 0.292g/L L-glutamine, and 10% (vol/vol) horse serum as described previously [262]. Parasites were synchronized by using gradient centrifugation with 55% nycodenz (Progen) in RPMI to enrich schizonts.

Tightly synchronized mature schizonts were transfected as described previously using the Amaxa 4D electroporator (Lonza) and the P3 Primary cell 4D Nucleofector X Kit L (Lonza) [261]. 10μl DNA including at 20μg repair template pDonor_p230p and 20μg pCas9/sg_p230p plasmid was used for transfections to generate eGFP expressing lines. 10μl DNA including 15μg repair template and 7μg pCas9/sg_p230p plasmid was used for transfections to integrate the eGFP expression cassette into the p230p locus with PCR repair templates. For generating tagged lines 10μg pCas/sg_GOI plasmid and 20μg PCR repair templates were used. After 24 h, and at daily intervals for 5 days, the medium was replaced with fresh medium containing 100 nM pyrimethamine (Sigma). Parasites were cloned out by limiting dilution. Parasites were diluted to 0.3 parasites/100μl and 100μl of 2% haematocrit culture was transferred to 96 flat-bottom plates in culture medium containing 200 mM L-glutamax (Sigma). After 7 days the media was changed and 0.2% fresh blood added. On day 11 the plate was screened for plaques, in an assay modified from *P. falciparum* [378]. Plaque positive cultures were transferred to 24 well plates containing 1 ml media with 2% haematocrit and used for genotyping.

DNA analysis

Genomic DNA from transfected parasite lines was extracted (QIAGEN) and analysed by PCR with GoTaq Master Mix (Promega) using the following conditions: 3 min at 96°C, then 30 cycles of 25 s at 96°C, 25 s at 52°C, and 1 min/kb at 64°C.

2.3.2 Assays of growth inhibitory activity (GIA) with *Plasmodium Knowlesi*

In vitro parasite culture and synchronization

Human RBC-adapted parasites were maintained in culture as previously described [261]. Briefly, parasites were grown at 2% hematocrit in O+ human red blood cells, which were prepared twice monthly. Culture medium contained 10% heat-inactivated pooled human serum mixed with RPMI 1640 supplemented with 25mM HEPES, 35μM hypoxanthine, 2mM L-glutamine and 20μg/mL gentamycin. Parasite cultures were synchronized at trophozoite/schizont stage by magnetic separation (MACS LS columns, Miltenyi Biotech).

In vitro assay of growth inhibitory activity (GIA assay)

Pk GIA assays were adapted from the protocol of the PATH-MVI international GIA Reference Centre [258]. Synchronised trophozoites were adjusted to 1.5% parasitaemia, and 20μL aliquots were pipetted into 96-well flat/half area tissue culture cluster plates (Appleton Woods). 20μL of test antibody or controls were added in duplicate or triplicate test over various concentration ranges (usually; 1, 0.5, 0.25, 0.125, 0.0625, 0.0312, 0.015 and 0.0075mg/mL) and incubated for one erythrocytic parasite cycle (26-30h). Parasitemia was measured using the lactate dehydrogenase (pLDH) activity assay following standard protocols [199]. Percent GIA was calculated following the equation below:

$$\%GIA = 100 - \frac{100(Sample_{A650} - Uninfected.RBC_{A650})}{(Infected.control_{A650} - Uninfected.RBC_{A650})}$$

An anti-DARC VHH nanobody [364] obtained from Dr Olivier Bertrand (INSERM, France), was included in the test plate as a positive control in every assay (at a final concentration of 6, 3 or 1.5μg/mL) and an Ebola virus glycoprotein-reactive IgG1 mAb as a negative isotype control for mAb samples.

The assays were performed using five different variants of transgenic Pk parasites made by CRISPR/CAS9 editing of the PkDBP locus (*Mohring F. et al*, submitted). For details of each Pk line see Chapter IV. As well as samples of recombinant human mAbs, the assay was also used to test purified polyclonal IgG from rabbit, human sera and various recombinant proteins for growth inhibition activity.

IgG was purified from sera, either rabbit or human, using protein G columns (Pierce) and then buffer-exchanged into RPMI 1640 medium, concentrated using ultra centrifugal devices (Millipore), filter sterilized through a 0.22μm filter (Millipore) and frozen at -20°C until use. Any recombinant proteins tested in the assay were buffered exchanged into RPMI 1640 medium and concentrated in ultra-centrifugal devices (Millipore).

2.3.3 Statistical analysis

All data analysis was carried out in Prism 5.0 (GraphPad). The threshold for statistical significance (α) was set at 0.05 and p-values were two-tailed. Nonlinear least-squares regression was used to approximate EC_{50} and EC_{30} values; these were interpolated by fitting a four-parameter dose-response curve to the relationship between Log10(dose, μg/mL)) and GIA (%). Correlations between EC_{30} values from the GIA assay and BLI epitope binning assay were assessed by calculating the Spearman rho coefficient (R). This nonparametric test was chosen due to the small sample sizes and because of its ability to detect non-linear relationships.

2.4 Chapter V methods

2.4.1 Short term *ex vivo* Pv invasion assays

These assays have been previously described [79, 329]. The major steps are outlined below.

2.4.2 Purification of reticulocytes from umbilical cord blood

The clinical samples used in this study were collected under the following ethical guidelines in the approved protocols: OXTREC 027-025 (Center for Clinical Vaccinology and Tropical Medicine, University of Oxford, Oxford, United Kingdom) and MUTM 2008-215 from the Ethics Committee of the Faculty of Tropical Medicine (Mahidol University, Bangkok, Thailand). 20ml aliquots of umbilical cord blood were collected in lithium heparin tubes immediately after delivery of the baby and the blood group determined using standard ABO antisera kit. After plasma removal and washing of the RBCs in McCoys 5A medium, white blood cells and platelets were depleted using Non-woven filters™ (Antoshin). The RBCs, diluted to 50% HCT in McCoys 5A medium, were then layered onto 70% isotonic percoll and centrifuged at 1200g for 15 minutes. The resulting band of enriched reticulocytes was carefully removed and washed twice in McCoys 5A medium. This reticulocyte rich fraction was then diluted to 50% HCT in PBS and incubated for 20 minutes with anti-CD71 MicroBeads (Miltenyi). The mixture was then passed through a large selection (LS) column (Miltenyi) to obtain a CD71-depleted (negative) fraction and a CD71-rich fraction (positive). The purity levels of these CD71+ fractions were assessed both with microscopy using new methylene blue staining (Sigma–Aldrich). The reticulocyte preparations were kept at 4°C in McCoy 5A medium at 20% hematocrit, and used for the invasion assays within 2 weeks of preparation.

2.4.3 Purification of schizonts from *ex vivo* Pv samples

5 mL samples of whole blood were collected from consenting patients presenting with *P. vivax* malaria in clinics run the Shoklo Malaria Research Unit, Thailand. They were collected in lithium heparin blood tubes and rapidly transported at room

temperature back to the laboratory, usually arriving within 4 hours of having been taken.

Samples were not taken from patients who had taken antimalarial or antimicrobial drugs within the previous month, or whose parasitemia was $< 0.1\%$ on smear microscopy. On arrival in the laboratory, the samples were processed for leukocyte-depletion using Non-woven filters™ (Antoshin), and either cultured directly or cryopreserved in Glycerolyte 57 (Baxter, USA) for later use [367]. Cryopreserved parasites were thawed by dropwise dilution in sodium chloride solution, as previously described [44]. Thawed or fresh parasites were were cultured to schizont stage in 12 mL of McCoy 5A medium (Gibco) supplemented with 2.4 g/L D-glucose, 40 mg/mL gentamycin sulfate, and 20% heat-inactivated human AB serum, in an atmosphere of 5% O2 at 37.5°C for approximately 22 hours.

Once the cultures were predominantly at schizont stage, the RBCs were recovered by centrifugation and re-suspended in McCoy 5A medium to 50% HCT before adding 3 mL of 0.125% w/v trypsin-versene in PBS and incubating for 15 minutes at 37.5°C [63]. The trypsin digestion was halted by washing the cells once in McCoy 5A medium followed by addition of 1 mL of AB serum to the pellet and incubation for 5 minutes at room temperature. McCoy 5A medium was then added to the trypsinised iRBC pellet to a total volume of 5 mL, and the suspension was overlaid on a 45% Percoll (isotonic) cushion and centrifuged for 15 minutes at 1200g. The fine band of concentrated schizonts found on the Percoll interface was carefully removed and washed twice in McCoy 5A medium.

Invasion assay

The concentrated mature schizont preparation was mixed with the enriched reticulocyte fraction at a ratio of 1:6, giving a starting schizont parasitemia of $\sim$14%. The mixture was diluted to 1.3% hematocrit in 300μL of complete McCoy 5A medium and cultured in 96-well cell culture plates in an atmosphere of 5% O2 at 37.5°C. Test antibodies and controls were buffer exchanged into Pv culture medium and added to the final invasion assay mixture at the desired concentration. In the case of

the anti-PvDBPII mAbs this was 1mg/mL. The anti-DARC nanobody, at 25μg/mL, and the recombinant IgG1 anti-Ebola mAb, at 1mg/mL, were added to all assays as positive and negative controls respectively.

Maturation was obtained after incubation for an average of 24 hours. This was extended to 30 hours or curtailed to 20 hours depending on the extent of parasite maturation, which was assessed at 20 hours by microscopy. At the end of the incubation period, thin smears (each made with 1μL packed cells) were made, and stained with Giemsa (Sigma-Aldrich). The number of ring stages and trophozoites per 4000 erythrocytes was determined by examining the Giemsa thin film smears by light microscopy. A thin smear was made before the incubation and the number of ring and trophozoite stage parasites was subtracted from that determined in the assay wells after incubation, and the resulting value was used to calculate the percentage of newly invaded RBCs.

2.4.4 Sequencing of the PvDBPII gene from Thai isolates

Genomic DNA was extracted either from an aliquot (200μL) of the initial blood sample or from a dried blood spot, using the DNeasy Blood and Tissue kit (QIAGEN). PCR amplification was performed on 1μL of the purified genomic DNA in a total volume of 50 μL, containing 1X PCR buffer, 2.5mM MgCl2, 0.2mM of each dNTP, 2μM of each primer (forward 5'-gtgactgggcatgagggaaattctcg and reverse 5'-gcgtagaatctcctggaaccttctcc) and 1.25U of AmpliTaq Gold DNA polymerase (Applied Biosystems). The cycling conditions were: 95°C for 5 minutes followed by 30 cycles at 94°C for 1 minute, 63°C for 2 minutes, and 72°C for 2 minutes. The product was purified using the QIAquick PCR purification kit (QIAGEN) and then sequenced (GATC biotech).

2.5 Chapter VI methods

2.5.1 X-ray crystallography

Protein production and Fab-antigen complex preparation

PvDBPII (Sal 1) was expressed in BL21(DE3) cells and the *E. coli* cell pellets were re-suspended in 20mM Tris-HCl pH8; 300mM NaCl; 15mM imidazole; 0.05% TRITON X-100; 10% glycerol (lysis buffer). This bacterial resuspension was lysed using a Sonicator S-400 (Misonix, USA) at a power of 60W, 3s on; 7s off, for 6 minutes total. The lysate was then spun down at 50,000g for 20 minutes and inclusion body purification carried out.

Since PvDBPII expressed in the form of inclusion bodies, the pellets were unfolded by incubation at room temperature in 6M guanidine-hydrochloride, 20mM Tris pH8, 300mM NaCl, 10mM β-mercaptoethanol for 1 hour. After centrifugation at 22,000 g for 30 min, the supernatant was filtered through a 0,22μm membrane (Millipore) and was refolded by dropwise adding to 2L flash dilution buffer (400 mM L-arginine, 10 mM EDTA, 0.1 mM phenylmethanesulfonylfluoride, 3 mM reduced glutathione, 0.3 mM oxidized glutathione, pH 8.0). After being stirred at 4°C for >36h, the precipitate was removed by spinning at 15,000g. The refolded protein was buffer exchanged using TFF and concentrated to 100ml in 20 mM Tris, 300mM NaCl, 20mM imidazole pH 8.0. This was then loaded on a NiNTA column overnight. Protein was eluted in 20mM Tris-HCl pH 8; 300mM NaCl; 200mM imidazole.

His-tagged proteins were buffer exchanged into phosphate buffered saline (ThermoFisher Scientific). TEV protease (1mg/10ml) was incubated with these proteins at room temperature for 15h. The His-tagged TEV was subsequently separated from the cleaved protein using a Ni-NTA column, collecting the cleaved product in the flow-through. This cleaved protein was then further purified by size exclusion gel chromatography through a HiLoad Superdex 75 16/60 column (GE Healthcare), into 20mM HEPES pH7.5, 150mM NaCl.

To obtain Fab fragments, the DB9 was incubated with papain beads (20341, ThermoFisher Scientific) in digestion buffer (20mM Phosphate, 10mM EDTA, 20mM fresh cysteine-HCl pH7) at 37°C for 36 hours. The Fab and Fc fragments were separated using a protein-A HiTrap column (GE Healthcare Life Sciences). The Fab fractions were gel filtered using an S75 16/60 column.

The purified PvDBPII and DB9Fab were incubated together in a 1:1 molar ratio for an hour. The complex was then separated from any excess individual components using a size exclusion chromatography S200 HiLoad 16/60 column (GE Healthcare). The peak fractions were pooled and concentrated to 10.5mg/mL.

PvDBPII:DB9 Fab crystallisation

Crystals were grown using the sitting-drop vapour-diffusion method in 96 well plates. Initial crystals were obtained through a broad screen with droplets containing 100nL of protein solution mixed with 100nl of well solution. Optimisation screens were performed on one condition (Molecular Dimensions MIDAS screen D3), with each droplet contained 100nL of protein solution, 100nl of well solution and 50nL of additive solution (Silver Bullets, Hampton Research).

Crystals grew with a reservoir solution of 45% v/v polypropylene glycol 400, 10% v/v ethanol. Crystals were cryo-cooled in their reservoir solution in liquid nitrogen for storage and data collection.

Crystallography data collection and molecular replacement

Data from crystals containing the PvDBPII:DB9Fab complex were collected at beamline I03 (Diamond Light Source, UK) using radiation with a wavelength of 0.9763A° and a Pilatus 3 6M detector. These data were indexed and refined using iMosflm, then scaled using SCALA to resolution of 2.9 A°. Molecular replacement using Phaser-MR found one copy of PvDBPII and one copy of DB9 Fab in the asymmetric unit. The models of each domains were built into the remaining electron

density using an iterative cycle of refinement using Refmac and autobuster and manual model building using Coot.

2.5.2 Rabbit immunization

Proteins used in rabbit immunization

Three groups, each of four rabbits, were immunised (Table 2.15 on page 75) with four doses of 20μg protein at two week intervals (Genscript).

- Group 1; PvDBPII,
- Group 2; Subdomain 3 (SD3) of PvDBPII
- Group 3; Interface (a variant of SD3 with five mutated amino acids, see below)

The three proteins were all based on the same strain sequence of PvDBPII (Sal 1) and were expressed in BL21 (DE3) bacteria and purified by a His-tag at the N-terminus which was cleaved off prior to immunisation, via a TEV protease site. The PvDBPII protein was refolded from inclusion body via flash dilution into a high concentration of Arginine buffer. This was followed by nickel purification, tag removal and SEC.

The SD3 protein was solubilised from insoluble pellet (post-lysis) in guanidine buffer and refolded on a nickel column by gradually reducing the amount of guanidine present. It was then nickel purified and underwent tag removal and SEC The 'Interface' construct, amino acid sequence as below, expressed in a soluble fraction so the cell lysis supernatant was passed through a nickel column. This was followed by nickel purification, tag removal and SEC.

The amino acid sequences for the three proteins used in the rabbit immunisation were:

- PvDBPII; (302 amino acids) GGSGNTVMKNCNYKRKRRERDWDCN-TKKDVCIPDRRYQLCMKELTNLVNNTDTNFHRDITFRKLYLKRKLIYDAA VEGDLLLKLNNYRYNKDFCKDIRWSLGDFGDIIMGTDMEGIGYSKVVENN

LRSIFGTDEKAQQRRKQWWNESKAQIWTAMMYSVKKRLKGNFIWICKLNV
AVNIEPQIYRWIREWGRDYVSELPTEVQKLKEKCDGKINYTDKKVCKVPP
CQNACKSYDQWITRKKNQWDVLSNKFISVKNAEKVQTAGIVTPYDILKQE
LDEFNEVAFENEINKRDGAYIELCVCS

- SD3; (121 amino acids) PQIYRWIREWGRDYVSELPTEVQKLKEKCDGKI-
AYTDKKVCKVPPCQNAC
KSYDQWITRKKNQWDVLSNKFISVK
NAEKVQTAGIVTPYDILKQELDEFNEVAFENEINKRDGAYIELCVC

- SD3 variant 'Interface'; (121 amino acids) PDIYEKIREWGRDYVSELPTEVQKLKEKCDGK
IAYTDKKVCKVPPCQNACKSYDQWITRKKNEWDELSNKFISVKNAEKVQTAG
IVTPYDILKQELDEFNEVAFENEINKRDGAYIELCVC

As highlighted in red above, the 'Interface' construct differs from SD3 by five amino acid substitutions.

Immunisation schedule

	Group 1 PvDBPII	**Group 2 PvDBPII SD3**	**Group 3 PvDBPII SD3 Interface**
Number of rabbits (NZL White)	4	4	4
Immunogen Mw	39KDa	11KDa	11KDa
Adjuvant	Freunds	Freunds	Freunds
Dose/vaccination	20µg	20µg	20µg
Schedule	4 doses 2 weeks apart	4 doses 2 weeks apart	4 doses 2 weeks apart
Route	intramuscular	Intramuscular	intramuscular

Table 2.15: Immunisation Schedule

Purification of IgG from the rabbit sera

As described in Section 2.3.2 on page 66.

2.5.3 Quantification of antigen-specific antibody

The concentration of antigen-specific antibody in each of the 12 rabbit sera, was determined using the standardised ELISA method described by Miura et al [257]. In these ELISAs, an identical dilution series of a "standard" serum sample is made on each plate. The hyperbolic relationship between IgG concentration and OD_{405} can only be approximated to a straight line in a certain range of IgG concentrations, and test samples are diluted such that they yield OD values (at 405nm) that fall in this range. In this manner, the IgG concentration in a diluted serum or purified IgG sample can be interpolated, and the IgG concentration in the original sample back-calculated. The method, allows for a relative comparison between samples by comparing "ELISA units"; the dilution at which a sample gives an OD_{405} of 1 when assayed on the antigen of interest. Previous work by the Draper group has established a link between arbitrary "ELISA units" and an absolute antibody concentration by calibration-free concentration analysis (CFCA) using a Biacore X100. This constant of proportionality was measured at: 1 ELISA unit = 0.434μg/mL.

2.5.4 GIA assays with rabbit serum

As described above in section 2.3.2 on page 66.

2.5.5 Statistical analysis

Nonlinear least-squares regression was used to approximate EC_{50} values; these were interpolated by fitting a four-parameter dose-response curve to the relationship between Log10 (dose, μg/mL)) and GIA (%). All data analysis was carried out in Prism 5.0 (GraphPad). The threshold for statistical significance (α) was set at 0.05.

2.6 Chapter VII methods

These are current and ongoing experiments using unpublished protocols, so the method outlines below are correct at the time of writing but may be amended in the future.

2.6.1 AAV-expressed DB9

The protocol is adapted from a published method [19]. Three AAV8 constructs were made for initial anti-PvDBPII mAb expression testing in mice. The first, AAV8-DB3, encoded the poorly neutralising mAb DB3 and the second two encoded the broadly-neutralising DB9. The first of the AAV8-DB9 constructs encoded the original variable chain sequences as per Figure 3.7 and in the second AAV8-DB9 construct the variable chain sequences have been codon-optimised for humans.

The DB3 and DB9 variable regions were synthesised (GeneArt) and cloned into the pENTR-VIP vector plasmid. This vector is unpublished, but its main features include the following; a CASI promoter, a secretion peptide, heavy chain variable region sequence, 2A peptide, secretion peptide, light chain variable region sequence, WPRE and a polyA tail.

Heavy chain variable regions were cloned using KpnI-SalI and light chain variable regions using BamHI-XhoI restriction enzymes. This ENTRY plasmid was then

recombined with the destination plasmid pAAV-DEST1 (unpublished; an AAV destination plasmid which works using the Invitrogen Gateway system). The resulting plasmid was then used for AAV production and the resulting viral vectors were injected intramuscularly into BALB/c mice. There are six mice per group and six groups:

1. Control vaccine
2. PvDBPII vaccine (ChAd63 MVA PvDBPII)
3. AAV8-DB3
4. AAV8-DB9-original
5. AAV8-DB9 codon-optimised
6. PvDBPII vaccine + AAV8-DB9 optimised

mAb levels in circulation will be quantified by standardised ELISA using the serum, and after 8 weeks the blood will be collected by cardiac puncture and the serum tested in ELISA and GIA assays.

2.6.2 DB9-DARC immuno-adhesin

Three DARC peptide sequences, all Fyb allele, were chosen for fusion to the DB9 Fc:

1. N-terminal 60 amino acids
2. amino acids 8-42
3. amino acids 19-30

The DNA encoding these three DARC constructs were synthesised by Twist Biosciences and cloned using XmaI and HindIII at the C-terminus of the DB9 heavy chain (HC) plasmid. HEK293A cells will be transiently co-transfected with this DB9 HC-DARC and the DB9 light chain plasmid and the resulting IgG purified and tested in GIA assays.

2.6.3 Pv-infected blood from returning travellers

Following agreements with three UK NHS Trusts a clinical protocol (LabPv001, Ethics Ref; 17/LO/0748) has established to allow the collection of blood from returning travellers diagnosed with Pv malaria. The blood, taken before the administration of anti-malarial therapy, is transported by courier to the laboratory in Oxford and processed for use in *ex vivo* invasion assays (as described in Section 2.4) and IFAT. For the assessment of antibody reactivity to native parasites by IFAT, microscopy slides will be prepared with enriched schizonts and fixed with paraformaldehyde. At this point the slides can be stored at -80°C. All slides will be stained with diluted serum, plasma or purified antibodies, followed by a secondary fluorescence antibody and DAPI as nuclear stain. Slides will be analysed by fluorescence microscopy.

Umbilical cord blood samples which are surplus to clinical requirements or unsuitable for clinical use will be obtained from NHS Blood and Transplant. Consent for use of such samples for research is obtained from mothers at the time of sample collection. Reticulocytes will be purified for use in the assay as described in Section 2.4.

2.6.4 Passive transfer mouse model

This experiment, currently underway, follows an unpublished protocol based on the *P. falciparum* humanised mouse model [134]. It has been extensively adapted for use with *P. vivax*. An outline of the experiment is given below:

- 10 liver-chimeric FRGN mice will be infected intravenously with 500 000 – 1 million *P. vivax* sporozoites.
- All mice will be repopulated with human reticulocytes to ensure presence of target cells when the parasites egress from the liver on days 8-10 post infection.
- On day 7 post infection

  - 5 mice will be administered 100mg/kg anti-PvDBPII mAb
  - 3 mice will be administered 100mg/kg anti-Ebola mAb
  - 2 mice will receive 100μL PBS

- Blood samples will be taken daily starting on day 8 post infection to monitor blood-stage infection by thin and thick blood smear as well as q-rtPCR.

3

Isolation of a vaccine-induced panel of human monoclonal antibodies against *Plasmodium vivax*

3.1 Authorship statement

The fluorescence activated cell sorting of the plasmablasts was done by Dr. Sean Elias and Andrew Worth. Dr Genevieve Labbé carried out the RT-PCR and PCR1 of one of the plates.

3.2 Introduction

Antibodies have been used as therapeutics since long before the technologies that led to the development of monoclonal antibodies (mAbs). The transfer of serum from an immunised person, or animal, to a non-immunised one was first demonstrated over 100 years ago [84] when serum therapy protected against diphtheria. Serum therapy was commonly used to treat infectious diseases until the discovery of chemotherapy in the form of sulphonamide in the 1930s [64].

First produced in the 1970s [208] by fusing mouse B cells with immortalized myeloma tumour cells to create 'hybridomas', mAbs have been licensed as therapeutics since the mid-1980s. In recent years, mAbs and related products have been the fastest

growing class of therapeutic agents [33].
There are now over thirty mAbs licensed by the FDA for clinical use but despite the potential of mAbs as powerful tools in the field of infectious diseases, during the past 25 years, only one mAb has been approved for the prevention of a viral infection (RSV) [338], and one approved in the U.S. for the treatment of bacterial toxin (anthrax) [135]. All others have been clinically designed for the treatment of cancer and autoimmune or allergic conditions [321].
The big therapeutic breakthrough came with the 'humanisation' of mAbs in the 1990s and since then various production methods for human mAbs (hmAbs) have been developed. These include; fully human hybridomas [291], EBV-immortalised human B cells [424], transgenic mice carrying a human antibody repertoire [220], proteomic methods [46, 423], human VH and VL phage libraries [242] and the single-cell cloning method [361, 381, 426] chosen for this research project.

The ability to express and characterize antigen-specific hmAbs is useful not only for producing therapeutics, but also for elucidating the interactions of particular antibodies and antigens. Malaria's main advantage over us as vaccine-makers lies in its immense diversity, its 'panacea-defying' polymorphism. This protean nature makes malaria as hard to pin-down as pathogens like Influenza and HIV. Isolating broadly neutralising human mAbs against such pathogens allows us to pinpoint the 'needle-in-a-haystack' islands of homogeneity in their immense heterogeneity and is thus a powerful tool for vaccine design.

The single-cell cloning method allows the rapid development of a library of antibodies with a range of specificities against a particular immunogen. Unlike phage display technologies in which the heavy and light chains are randomly paired *in vitro*, the single-cell cloning method preserves the cognate pairing of heavy and light chains and thus the binding properties of the antibody paratope. Work has previously been published on mouse mAbs to PvDBPII [72]; but antibodies generated in other species do not provide a true evaluation of the epitope specificities

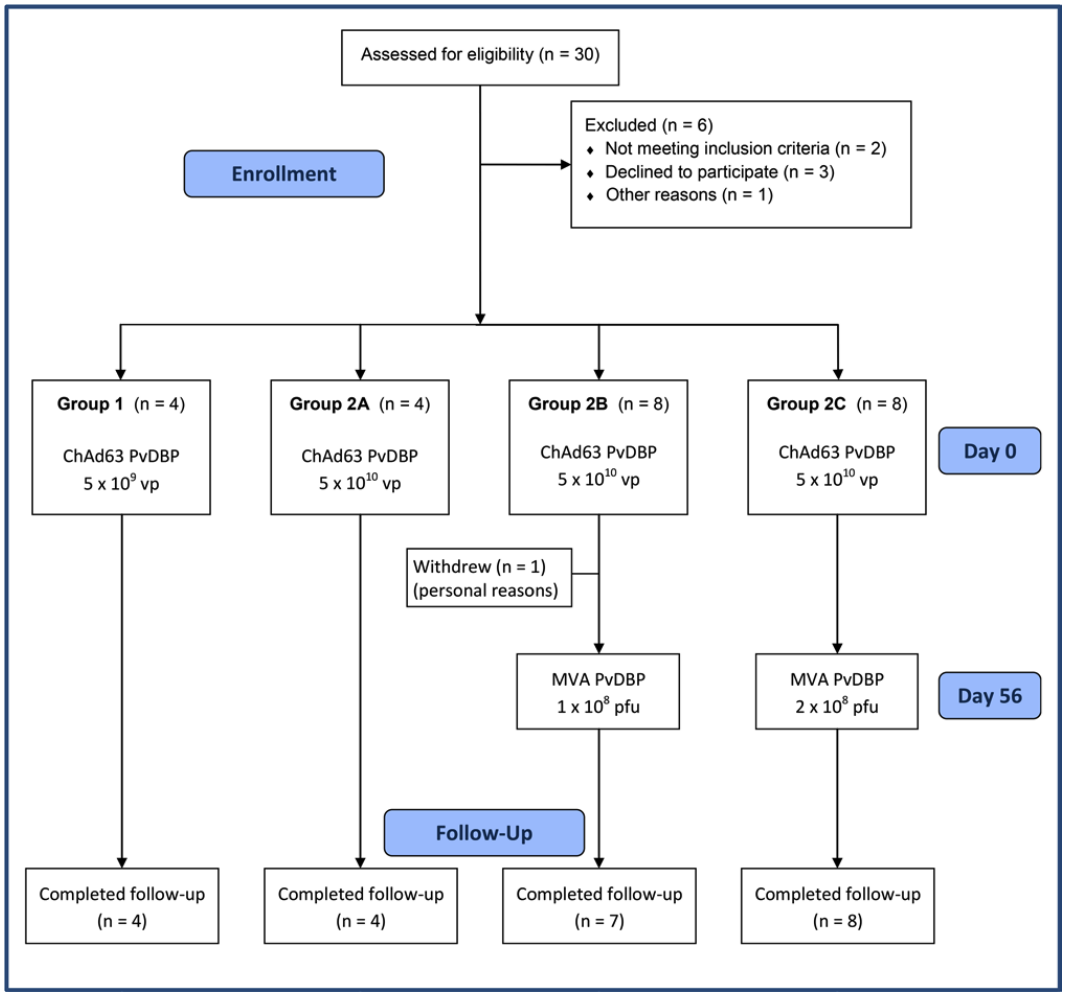


Figure 3.1: Flow chart of study design and volunteer recruitment for 'VAC051' a Phase IA clinical trial of viral vectored PvDBPII [304].

that humans generate *in vivo* and this limits their use for applications such as epitope discovery and vaccine development [8, 251, 404].

Other approaches to hmAb production are memory B cell–based; while this allows a retrospective evaluation of antigen exposures and avoids the logistical difficulties of obtaining B cells from people with active immune responses, it does not provide a window into the ongoing and active immune response to vaccination afforded by the single-cell cloning method. To date, the single-cell cloning technique has been used to produce hmAb libraries from individuals vaccinated against many viral and bacterial pathogens including influenza, anthrax toxin and pneumococcus [361].

In 2014, the first-in-human Phase Ia safety and immunogenicity clinical trial of PvDBPII (Sal1 strain) was conducted [304]. 24 healthy volunteers were enrolled

and of these, sixteen were vaccinated twice; once with 5×10^{10}vp ChAd63 PvDBPII and once with 1×10^{8}pfu (group 2B) or 2×10^{8}pfu (group 2C) MVA PvDBPII following an 8-week prime-boost interval (Figure 3.1).
Viral vectored vaccines are replication-deficient viruses containing a heterologous expression cassette encoding the vaccine antigen of choice for ectopic expression from muscle cells [130]. They typically induce a strong T cell response but a weaker humoral response [173, 346] and they avoid the need for large scale recombinant protein production to cGMP standards, which can be very difficult for certain malaria proteins [248].

This first clinical trial of a blood-stage vaccine against *Plasmodium vivax* malaria presented a unique opportunity to isolate a panel of fully human mAbs against PvDBPII, the leading blood stage vaccine candidate.

This chapter describes the production and initial characteristics of this panel of antibodies.

3.3 Production of human mAbs to PvDBPII

Following vaccination, naïve B lymphocytes in the germinal centres of lymph nodes, are antigenically stimulated and activated through their B cell receptor (BCR) with help from T cells [104]. Their affinity for the antigen matures in the secondary lymphoid organs through the processes of somatic hypermutation and clonal selection [245]; this results in proliferation of these stimulated and selected B cell clones and their differentiation into memory B cells. On repeated exposure to the same antigen, these memory B cells rapidly differentiate into antibody-secreting cells (ASC) and secrete large volumes of antibody [374]. There is typically a transient increase in these antigen-specific plasmablasts in the peripheral blood around 7 days after the booster vaccination [39, 61, 426] as they migrate from the lymph nodes to the bone marrow or spleen (Figure 3.2).

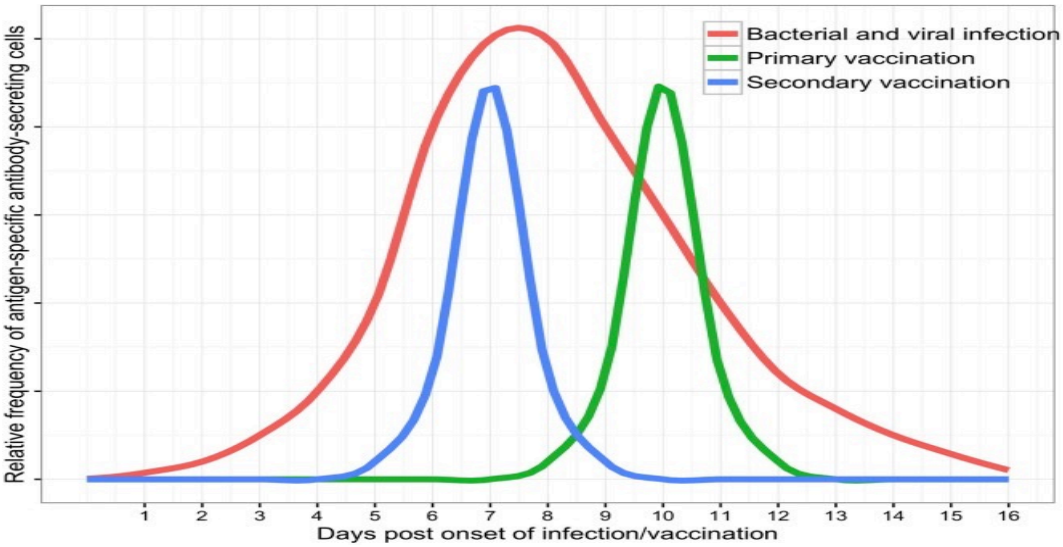


Figure 3.2: Antigen-specific ASC response after infection or vaccination [61].

These cells are characterised by their expression of CD19 (B cell marker), CD27 (memory B cell phenotype) and CD38 (plasma cell marker) and their down-regulation of CD20 (marking late stage B cell differentiation) and CD21 (absence marks B cell activation). The PBMCs taken at day 63 of the VAC051 vaccine trial, 7 days post-MVA boost, were labelled with fluorescent antibodies and flow-sorted according to this phenotype; CD19+, CD20-, CD21-, CD27hi, IgG+, CD38hi.

The protocol followed to produce mAbs from these cells, from flow sorting of PBMCs to gene cloning to expression and screening, is summarised in Figure 3.3 and was adapted from that published by *Smith et al.* [361].

Sorting yielded between 50 and 200 CD38hi plasmablasts for each sample of PBMC taken at the seven day post-boost time point. Because plasmablasts secrete large amounts of antibody [293], the antibody-encoding mRNA is in great relative abundance to the DNA and this allowed access to the antibody variable gene sequences via reverse transcription of the mRNA. The primers used in the initial RT-PCR step were designed to guide reverse transcription of the whole antibody transcript to cDNA.

The subsequent step (PCR 1) used the same primers to amplify the cDNA and yield sufficient template for the nested PCR (PCR 2). The PCR 2 primers

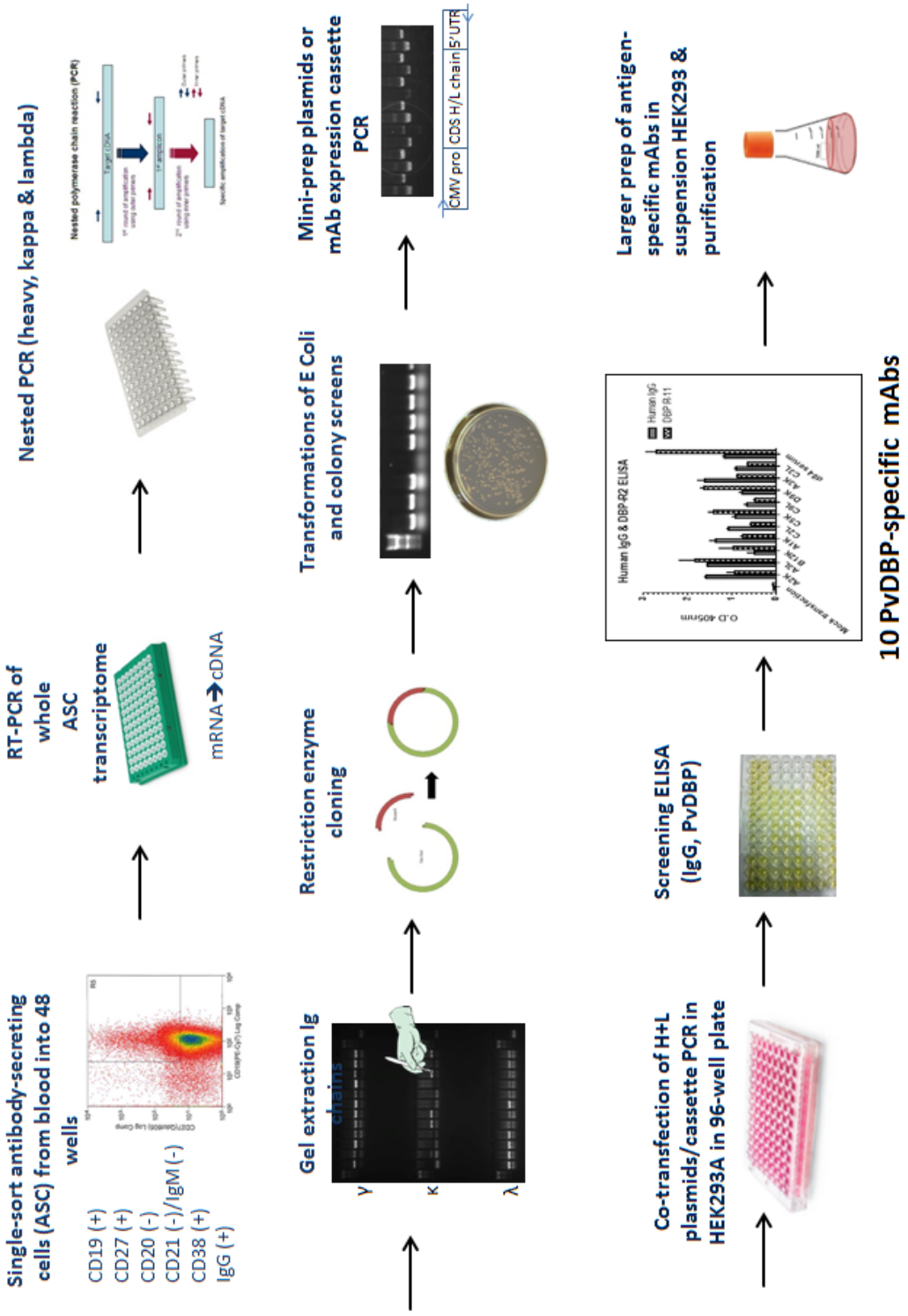


Figure 3.3: Schematic summarising the single-cell cloning protocol for producing mAbs from the PMBCs of volunteers vaccinated with PvDBPII.

were designed to put just the variable domain-coding regions in frame with the plasmid ORF with the addition of 5' and 3' adjuncts needed for cloning. Figure 3.4 shows a gel electrophoresis picture of the nested PCR product from 12 ASCs (A1-A12) from one vaccinated volunteer.

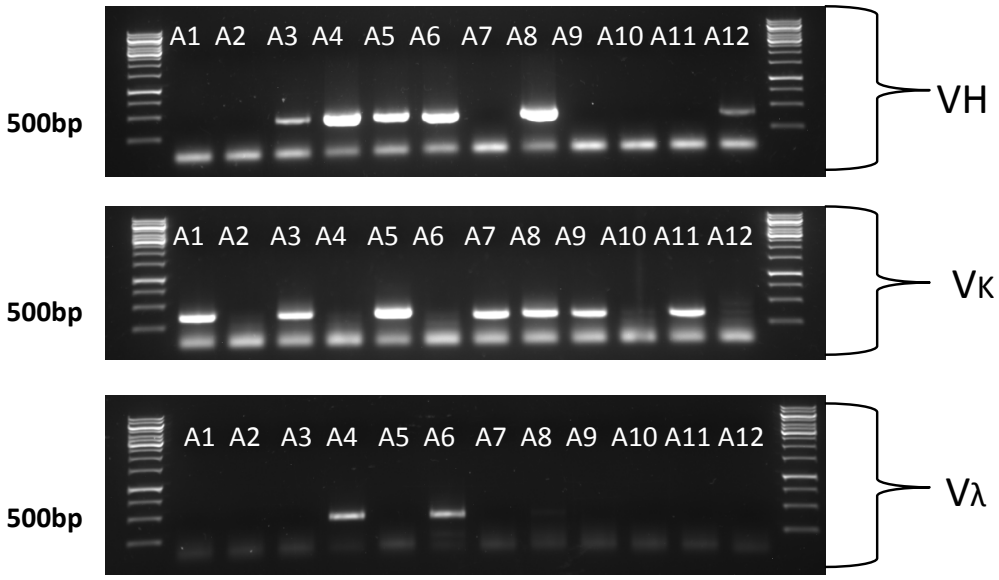


Figure 3.4: Protein gel electrophoresis showing the amplification of V_H, V_κ and V_λ exon inserts from 12 wells (A1-A12) containing a single antibody secreting cell. The expected size of the amplicons was; 420bp for V_H, 395bp for V_κ and 430bp for V_λ.

The cDNA for each matched heavy and light chain antibody pair was extracted from the gel, purified and then digested and ligated into matching Ig chain backbones. 116 out of a possible 288 antibodies (6 plates of 48 wells) were successfully cloned into expression vectors, giving the process an efficiency of $\sim$ 40% at this stage of the protocol (Table 3.1). Cognate heavy and light-chain coding plasmids were co-transfected into HEK293 cells using linear 25kDa polyethylenimine (PEI) in small volumes in single wells of a 96-well cell culture plate. This cell line was chosen as it has been shown to readily express correctly-folded, correctly-glycosylated human antibodies in large quantities when transfected using PEI [14]. Supernatant from the transfected HEK293 cells was screened by ELISA to test first for IgG (Figure 3.5 A) and then for PvDBPII-specific IgG (Figure 3.5 B).

Plates of single-cell sorted ASCs were chosen for cloning based primarily on their availability at the time, but there was also some clinical trial data to guide the choice.

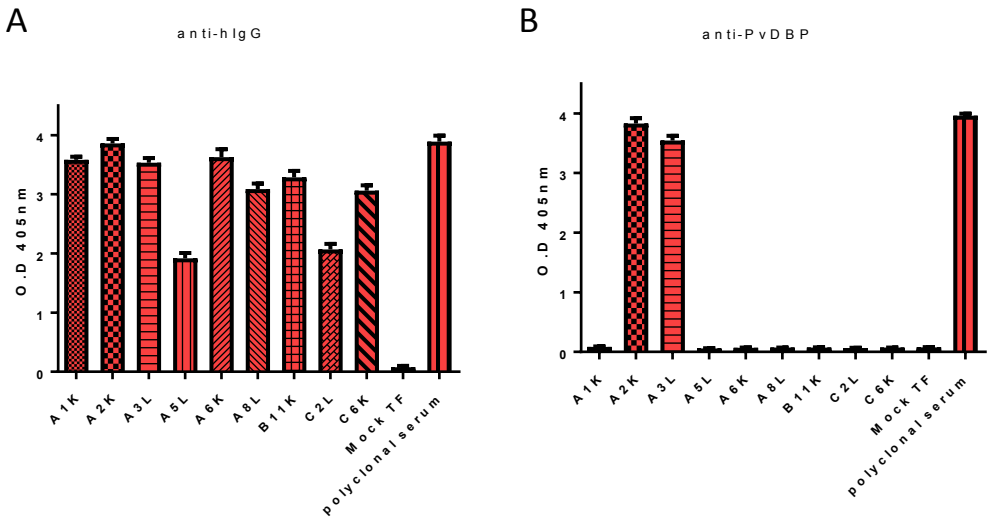


Figure 3.5: Panel A: Anti-human IgG sandwich ELISA showing IgG expression levels of 9 successfully cloned plasmids originating from plasmablasts isolated from one volunteer. Panel B: Indirect anti-PvDBPII ELISA showing two positive clones. A mock transfection (Mock TF) with no DNA, and polyclonal human immune serum from the vaccine trial, were included as negative and positive controls respectively. Data shown represent the average of three separately transfected wells and error bars are standard deviation

This included; antigen-specific ASC ELISPOT responses (Figure 3.6, A); levels of anti-PvDBPII specific IgG (Figure 3.6, B); and the DBP-DARC binding-inhibitory properties of each serum sample (Figure 3.6, C).

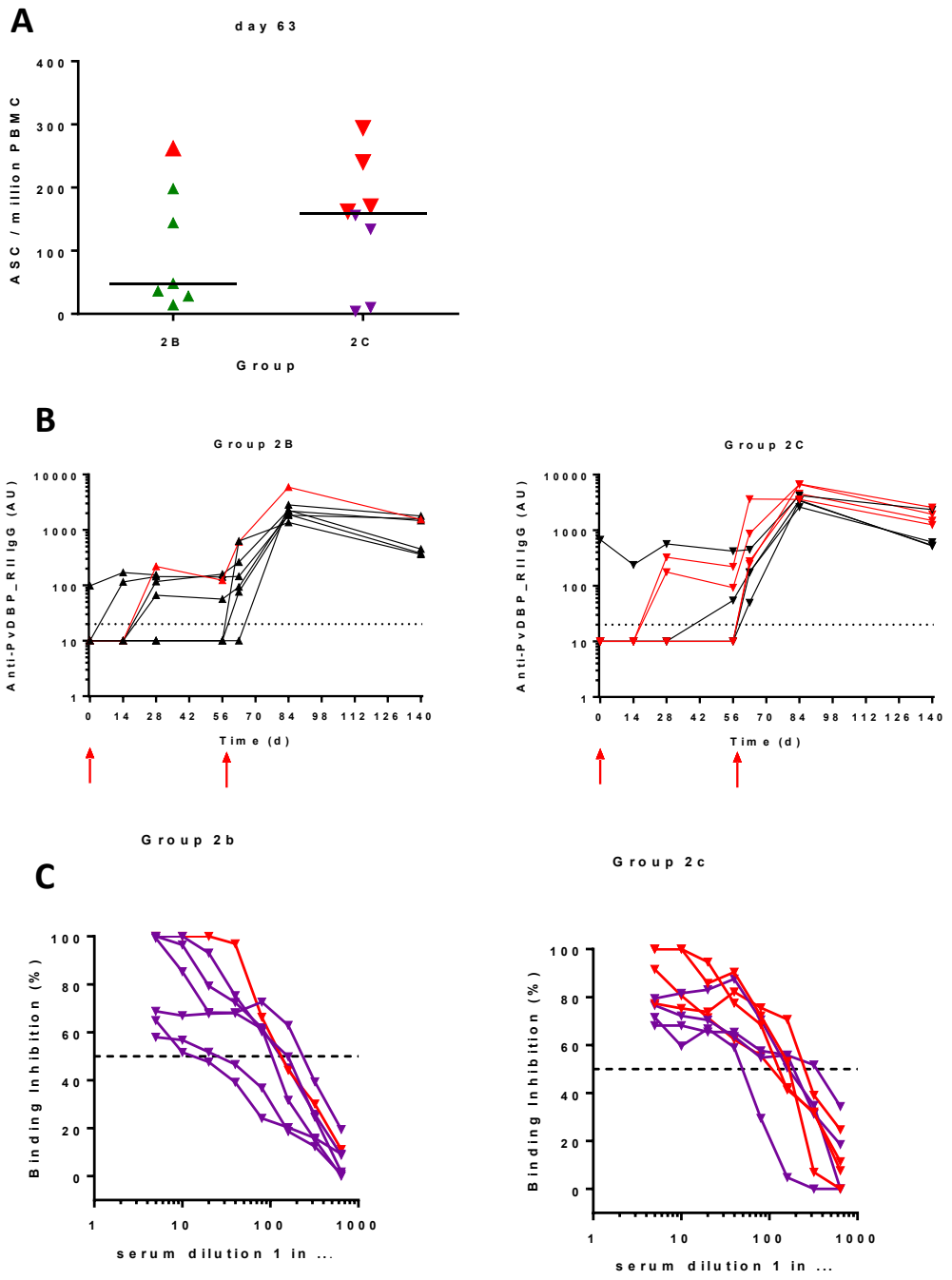


Figure 3.6: (A) B cell ELISPOT data showing the relative number of PvDBPII-specific ASC in the PBMC of each volunteer separated by dose group. The large red triangles represent the volunteers chosen for mAb production. (B) Anti-PvDBPII antibody levels over time for groups 2B and 2C. The lines in red are the volunteers whose PBMC from the day 63 timepoint were used for mAb cloning. (C) PvDBPII – DARC binding inhibition curves for the serum of individual volunteers in groups 2b and 2c. The curves highlighted in red were those of the volunteers whose PBMCs were used for mAb production.

It is unclear whether plasmablast-derived IgG reflects serum IgG [359, 406] but there was no clear relationship between individual volunteer's preliminary immunology readouts and the number of PvDBPII-specific mAbs subsequently cloned from their PBMC.

As shown in Table 3.1 below, 116 out of a possible 288 pairs of antibody genes were successfully cloned into expression vectors; 90 out of 116 plasmid pairs expressed IgG; and 10 of those 90 recombinant mAbs bound PvDBPII by ELISA.

	Cloned	IgG expressed	PvDBPII specific
V002 plate	12	9	2
V002 plate	23	18	7
V020 plate	21	16	0
V025 plate	26	18	0
V030 plate	19	15	1
V024 plate	15	14	0
Success (%)	116/288 (40.2%)	90/116 (77.5%)	10/90 (11.1%)

Table 3.1: Success rate at each bottleneck in the PvDBPII-specific mAb isolation process. 116 out of a possible 288 pairs of antibody genes were successfully cloned into expression vectors; 90 out of 116 plasmid pairs expressed IgG; and 10 of those 90 recombinant mAbs bound PvDBPII by ELISA.

Other groups, using similar protocols to clone antibody variable genes from post-vaccination plasmablasts, have reported higher yields of antigen-specific mAbs [426]; this may be related to the vaccine trial volunteers having had previous exposure to the vaccine pathogen. Any possibility of prior malaria infection was an exclusion criterion in this clinical trial.

The ten antibodies in the panel were clearly distinct as shown by their differing variable region length and use of V-gene exons (Table 3.2).

Sequencing of the antibody variable genes revealed significant clonal diversity within this relatively small panel of mAbs, (Figure 3.7).

The small amount of somatic hypermutation (SHM) of most of the mAbs was suggestive of low levels of germinal centre migration and is characteristic of early extra-follicular responses [147, 287]. Although the sample size was not large enough to draw any significant correlations, there were no clear trends to suggest a link between different levels of SHM and the characteristics, either functional or kinetic, of the antibodies.

mAb	V_H	D	J_H	CDR3 length	CDR3 sequence	% SHM
DB1	5-51	3-22	3*02	16	ARLAYDSSGYYYAFDI	1.7
DB2	4-59	6-13	3*02	14	ARHFHSSTAAAFDI	1.4
DB3	4-31	2-2	4*02	21	ARSQGYCSSSSCLLPRGYFDY	6.5
DB4	1-69	6-6	4*02	14	ARDGGHHGQLVFDY	3.1
DB5	1-46	2-21	6*02	21	ARDNSEGAAYYSYYYYYGMDV	0.7
DB6	1-2	6-19	6*02	18	ARGLRYSIAWYSDYGLDV	2.8
DB7	4-39	3-10	5*02	11	ARRSLGYFFGP	2.7
DB8	1-3	6-19	4*02	16	ARSYRSSIGWFWMFDY	2.1
DB9	4-39	1-1	2*01	10	ARDGTGALDL	1.7
DB10	3-21	3-16	6*02	17	ARDSVAGPFYYFYAMDV	2.8

Table 3.2: mAb panel list showing the heavy chain variable exon usage and the percentage amino acid deviation from germline resulting from junctional diversity and somatic hypermutation. The data were compiled using NCBI's IgBLAST [431].

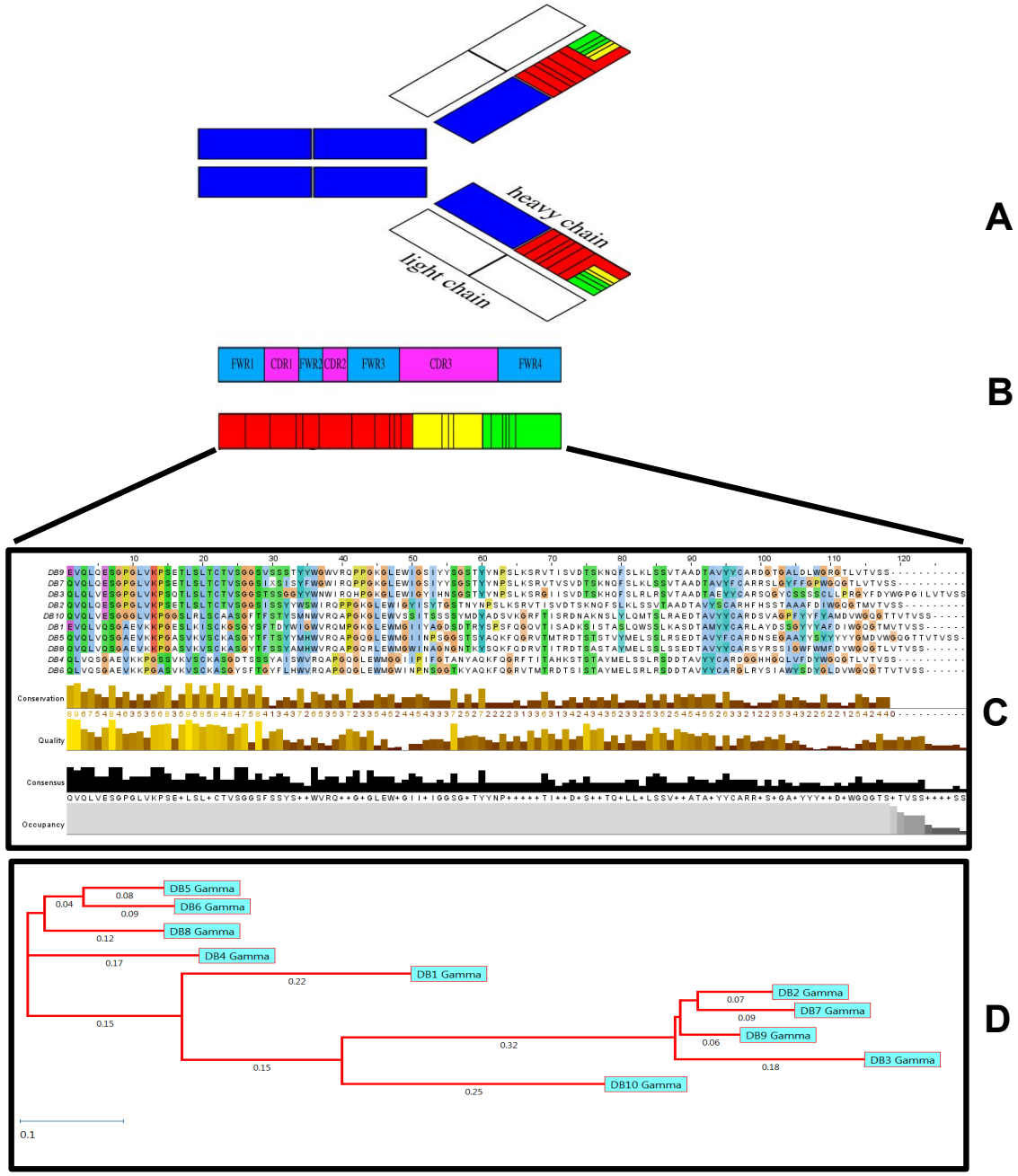


Figure 3.7: Multiple alignments of the heavy chain variable regions amino acid sequences of the ten anti-PvDBPII mAbs. (A) and (B) Cartoon of the heavy chain variable region gene showing the interspersed framework (FWR) and complementarity-determining (CDR) regions. (C) alignment of the ten mAb heavy chain variable region amino acid sequences, aligned using ClustalW and visualised with Jalview (D) Cladogram generated by NCBI's Clustal Omega after multiple sequence alignment of each mAb's V_H exon. The numbers on the lines represent sequence similarity to the closest consensus sequence; identical sequences would have values of 0.

3.4 Characterisation of the mAbs

3.4.1 Affinity and kinetics

Affinity is the strength of binding of a single molecule to its ligand and is usually measured and reported by the equilibrium dissociation constant (K_D). Antibody-antigen binding is a reversible process, and the rate of the reaction is proportional to the concentrations of the reactants. K_D is the ratio of the dissociation rate (k_{off} or k_d) to the association rate (k_{on} or k_a) of the antibody:

$$\mathrm{A} + \mathrm{B} \underset{k_\mathrm{d}}{\overset{k_\mathrm{a}}{\rightleftharpoons}} \mathrm{AB}$$

At equilibrium, the rate of antibody-antigen complex formation (k_{on}) is equal to the rate of dissociation (k_{off}) and the measurement of the reaction rate constants can be used to define an equilibrium or affinity constant ($\frac{1}{K_D}$). The smaller the K_D value the greater the affinity of the antibody for its target. Most antibodies have K_D values in the low micromolar (10^{-6}) to nanomolar (10^{-7} to 10^{-9}) range; those considered high affinity are generally in the low nanomolar range (10^{-9}) with very high affinity antibodies being in the picomolar (10^{-10}-10^{-12}) range [179]. The general view is that high affinity antibodies are better neutralisers [315, 368], however, as illustrated in Figure 3.8 antibodies with similar affinities may have very different kinetics .

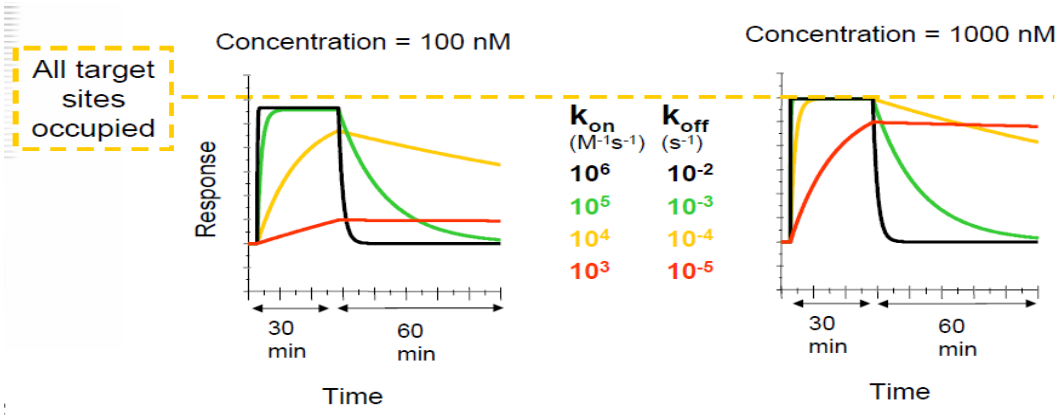


Figure 3.8: SPR binding curves for 4 imaginary antibodies (black, red, green and yellow lines) binding to their antigen. Each has a very different kinetic profile but all four have the same affinity (K_D) of $10nM$ [235].

This distinction between affinity and on- and off-rates may be of particular relevance to antibodies that disrupt merozoite invasion as will be discussed later [410]. The kinetic results for the anti-PvDBPII mAbs were calculated using Biacore X100 evaluation software using the calculated kinetic rate parameters and fitting to a 1:1 Langmuir binding model measured by SPR. The mAbs were bound to a protein A-coated chip and solutions of PvDBPII flowed over at five different concentrations (Figure 3.9).

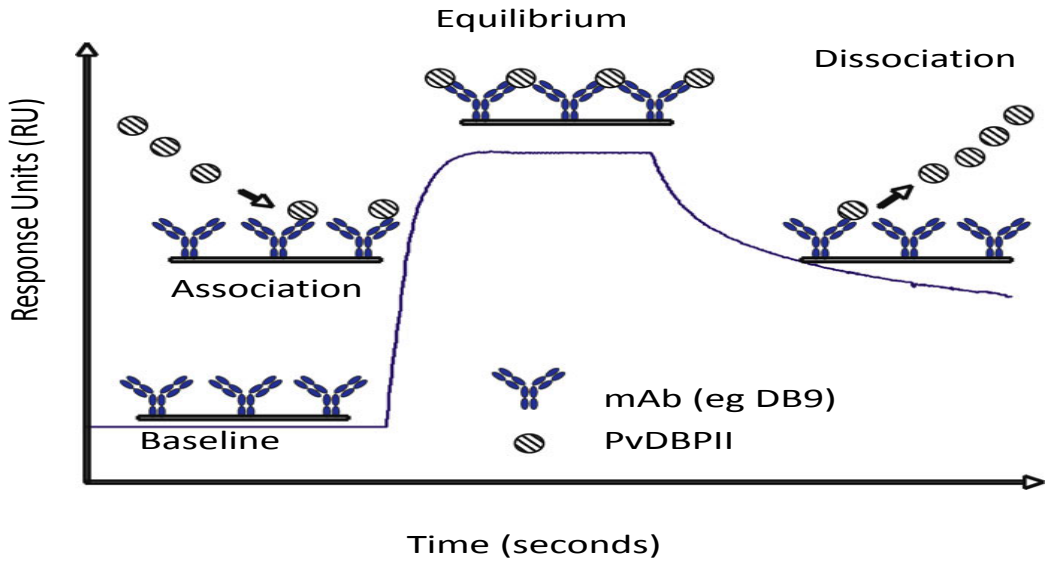


Figure 3.9: Cartoon of the SPR sensorgram profile used to measure the binding kinetics of each mAb to PvDBPII. Adapted from [169].

The ten anti-PvDBPII mAbs were all high or very high affinity antibodies, with K_D values ranging from low nanomolar to picomolar. These affinities fall within the reported range [179] for antibodies, but given the relatively low levels of somatic hypermutation, were higher than might have been expected (Table 3.3).

What is more striking, and perhaps of more relevance, are marked variations in on-rate; DB1, DB6, DB7, DB9 and DB10 have very rapid association rates (Figure 3.10,A and circled in Figure 3.10,D). This is reflected in their high affinity constant for PvDBPII (Figure 3.10,C), except in the case of DB1, whose very rapid association rate is counter-balanced by an equally rapid dissociation rate (Figure 3.10,B).

mAb	k_a ($M^{-1}.s^{-1}$)	k_d (s^{-1})	K_D (M)
DB1	$1.88E^{7}$	$6.46E^{-3}$	$3.44E^{-10}$
DB2	$9.02E^{5}$	$6.05E^{-4}$	$2.35E^{-10}$
DB3	$2.98E^{6}$	$4.27E^{-4}$	$2.07E^{-10}$
DB4	$1.30E^{6}$	$4.39E^{-4}$	$3.37E^{-10}$
DB5	$2.33E^{6}$	$4.33E^{-4}$	$2.86E^{-10}$
DB6	$8.65E^{6}$	$2.53E^{-4}$	$2.92E^{-11}$
DB7	$1.72E^{7}$	$1.13E^{-4}$	$6.55E^{-12}$
DB8	$1.73E^{6}$	$3.92E^{-4}$	$2.27E^{-10}$
DB9	$1.79E^{7}$	$3.57E^{-4}$	$2.00E^{-11}$
DB10	$1.06E^{7}$	$5.05E^{-4}$	$4.78E^{-11}$

Table 3.3: Affinity and rate constant values for the panel of 10 human anti-PvDBPII mAbs as determined by SPR. The values were calculated from injections of 5 different concentrations of PvDBPII, plus one replicate.

The significance of these diverse kinetic profiles becomes of greater interest when correlated with functional parasite assays, as discussed in later chapters.

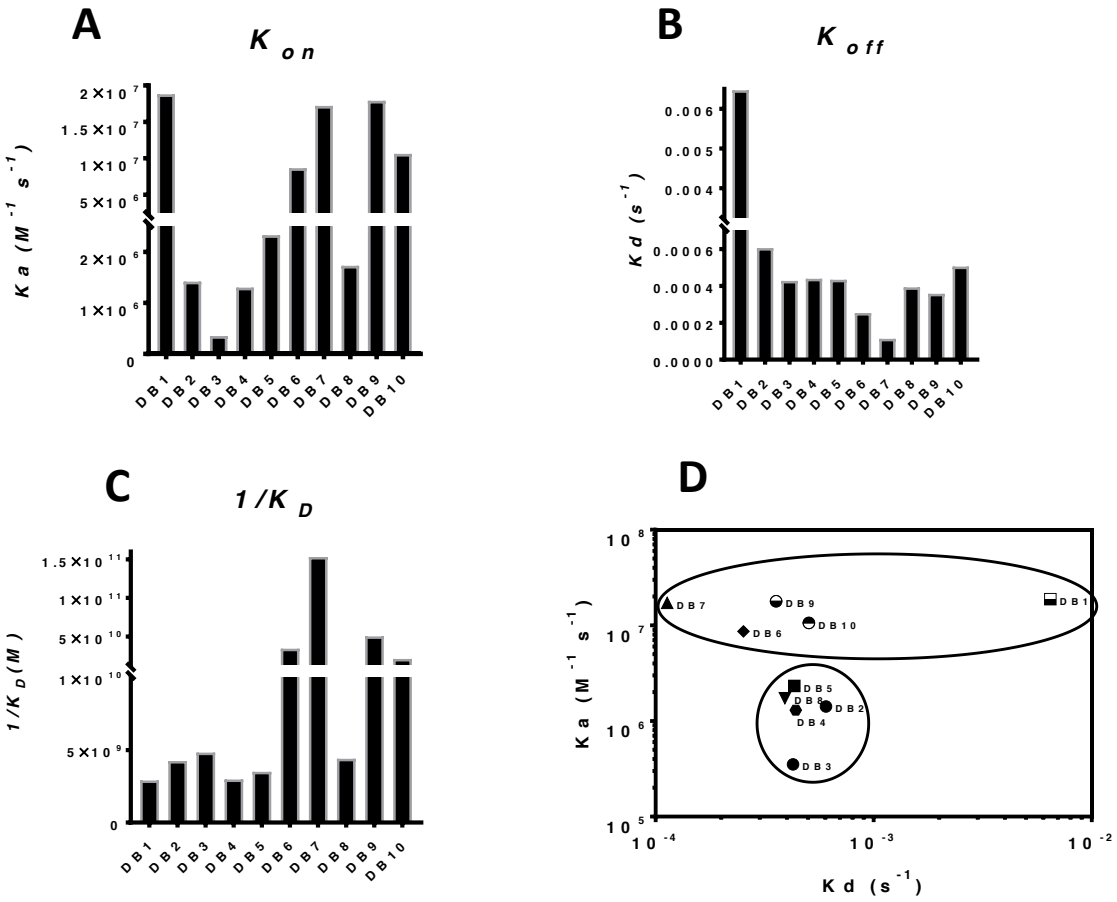


Figure 3.10: Kinetics of the ten anti-PvDBPII mAbs binding to PvDBPII as determined by SPR. Panel (A) shows the 'on-rate' or k_a/K_{on} for each mAb; panel (B) shows the 'off-rate' or K_d/k_{off} for each mAb, panel (C) shows the 'affinity constant' $(1/k_D)$ of each mAb and panel (D) plots the on-rate against the off-rate or each mAb to show clusterings of the antibodies by their association and dissociation rates. The upper oval contains the five mAbs with very rapid on-rates and the lower circle the five with slower on-rates.

3.4.2 Competition for epitopes

Having established the binding kinetics of each mAb, the next experiment sought to determine whether the mAbs compete with each other for binding sites. The spatial separation of epitopes was of particular importance given that an intended use of these mAbs was to map the antigen and re-engineer the vaccine. In order to assess competition for binding sites, a sequential real-time binding assay was used in which the binding of each mAb ('mAb1') to PvDBPII was measured in the presence of another pre-bound mAb ('mAb2'). The amount of mAb1 bound to PvDBPII which had been pre-exposed to mAb2, was compared to the signal of mAb1 binding PvDBPII alone. The following definitions were used to categorise this binding site competition between each pair of mAbs:

- "blocking"; if mAb2 reduced the binding of mAb1 to 5% or less of its binding alone
- "non-blocking"; if mAb2 did not reduce the binding of mAb1 by more than 25%
- "partially blocking"; for all values in between.

The raw data were compiled in a "relative binding" matrix, (Figure 3.11, A) and this "relative binding" profile of each mAb was then correlated with that of each other mAb to generate a correlation matrix, (Figure 3.11, B) Four of the mAbs, DB2, DB6, DB8 and DB9 consistently blocked each other's binding and so presumably have close or overlapping epitopes. DB3 competed with DB9 alone and DB1 and DB10 competed exclusively with each other. DB4, DB5 and DB7 have distinct epitopes as their binding is unaffected by prior binding of any of the other mAbs (Figure 3.11, C).

Based on this panel of mAbs, there appear to be multiple distinct antigenic sites on PvDBPII, with one site dominating and accounting for 50% of the isolated antibody response.

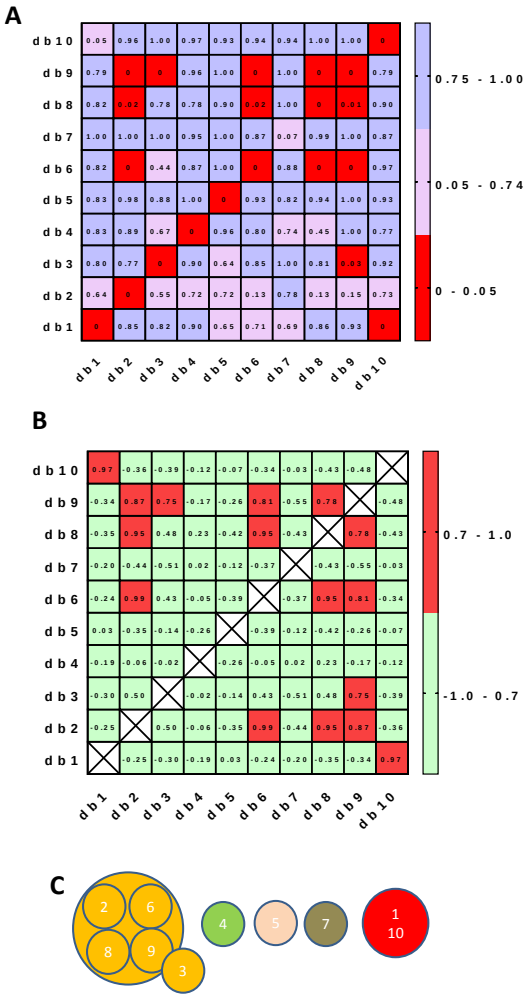


Figure 3.11: Competition between the mAbs for binding sites on PvDBPII. (A) Values represent the fractional binding of mAb 2 in the presence of mAb 1 relative to mAb 2 binding to PvDBPII alone. Values >1 were normalised to 1 and negative values were normalised to 0. Data were binned into 3 colours: blue (non-blocking) if relative binding $\geq$0.75, lilac (partially blocking) if relative binding <0.75 and $\geq$0.05 and red (blocking) if relative binding <0.05. (B) Shows a Pearson product-moment table which correlates the binding profile of every mAb against every other mAb in the panel to identify members of the same epitope bin. Similar profiles were highlighted in red with a cut-off set at 0.70. Panel (C) illustrates the competition groupings within the panel of mAbs.

3.4.3 PvDBPII-DARC binding inhibition assays

The assays described above gave detailed information on how the vaccine-induced antibodies interact with the antigen, but of most importance was to know whether they disrupt binding to its erythrocyte ligand DARC. In the case of *Plasmodium falciparum*, which is maintained in continuous *in vitro* culture in many labs, the next step would have been to test the mAbs in a Growth Inhibition Activity (GIA) assay. As discussed earlier however, this is not an option for the as yet un-cultureable *P. vivax*. As a proxy for *in vitro* assays of parasite neutralisation, recombinant protein assays have been established to assess antibody blockade of PvDBPII-DARC binding [343]. Such assays have, in the absence of functional alternatives, been considered the 'gold standard' method for assessing anti-PvDBPII antibodies. Though they provide no functional evidence of parasite neutralisation, data from such assays has, nevertheless, been used as the basis for describing anti-PvDBPII antibodies as 'broadly neutralising' [72].

Following the same protocol [343] used to evaluate mouse sera from the pre-clinical PvDBPII vaccine work [112], I first assessed the PvDBPII-DARC binding inhibition properties of the polyclonal serum from the clinical trial. The detailed methodology is described in Chapter II, but Figure 3.12 summarises the essence of the ELISA-based assay.

Polyclonal sera from the clinical trial

Dilution series of vaccinated sera from all 23 clinical trial volunteers gave encouraging results in this assay; all samples from volunteers that received both the prime and boost vaccinations (group 2B and 2C), produced antibodies that inhibited PvDBPII (Sal 1) – DARC binding (Figure 3.13).

This was, however, only indicative of a binding-inhibitory effect against the vaccine homologous strain of PvDBPII (Sal1). Given the significant global polymorphism of PvDBPII [68, 75, 279], the next assay sought to assess whether polyclonal sera raised against the Sal 1 vaccine strain, would also inhibit the DARC-binding of other alleles of PvDBPII. The assay was repeated, but this

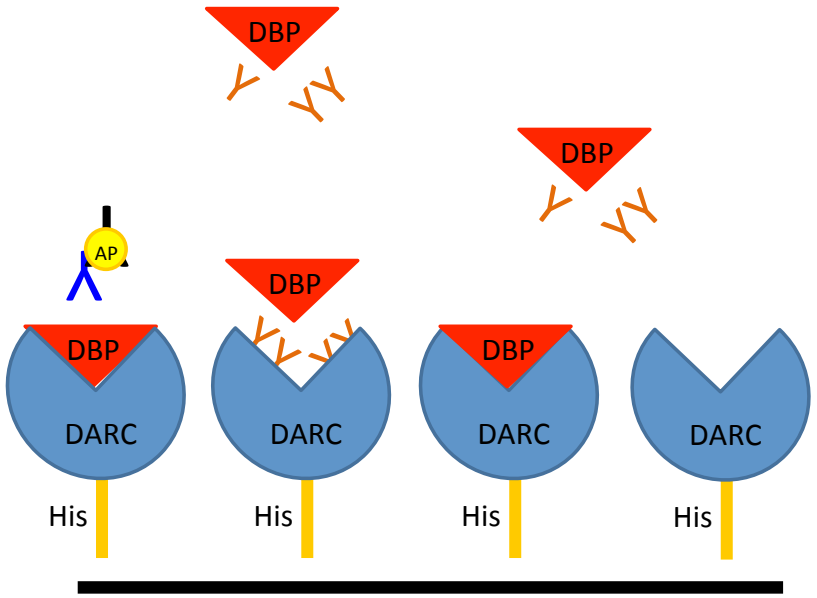


Figure 3.12: Cartoon illustrating the PvDBPII-DARC binding-inhibition ELISA. Antibodies (orange) binding to recombinant PvDBPII disrupt its binding to recombinant N-terminal DARC on the plate. The readout, detected by rabbit (blue) anti-PvDBPII sera, is the amount of PvDBPII bound to the plate

time using a panel of recombinant PvDBPII allelic variants; Sal 1, PvAH, PvO, PvP and HMP013 (Figure 3.14).

These allelic variants were sequenced from vivax patients in Indonesia [93] and Central America [60] and between them include many of the known polymorphisms in PvDBPII (Figure 3.15). The HMP013 strain was isolated from an Australian traveller returning from Indonesia and has recently been used in controlled human malaria infection (CHMI) studies [243]. It was a useful addition to the panel, in that it has polymorphisms distinct from the other alleles and thus lent more credibility to the strain transcending nature of the polyclonal response.

The results above showed that human immunisation with PvDBPII Sal I, induced antibodies that cross-react with a wide variety of PvDBPII alleles and indicate the presence of inhibitory epitopes common to all these strains. When the polymorphic residues of HMP013 (Figure 3.16), were superimposed on the structure of the PvDBPII dimer [29], it could be seen that they cluster around the dimer interface and the putative DARC binding groove. This region of subdomain 2 is

particularly polymorphic and has been referred to in the literature as a 'decoy epitope' distracting from the crucial binding sites adjacent [73].

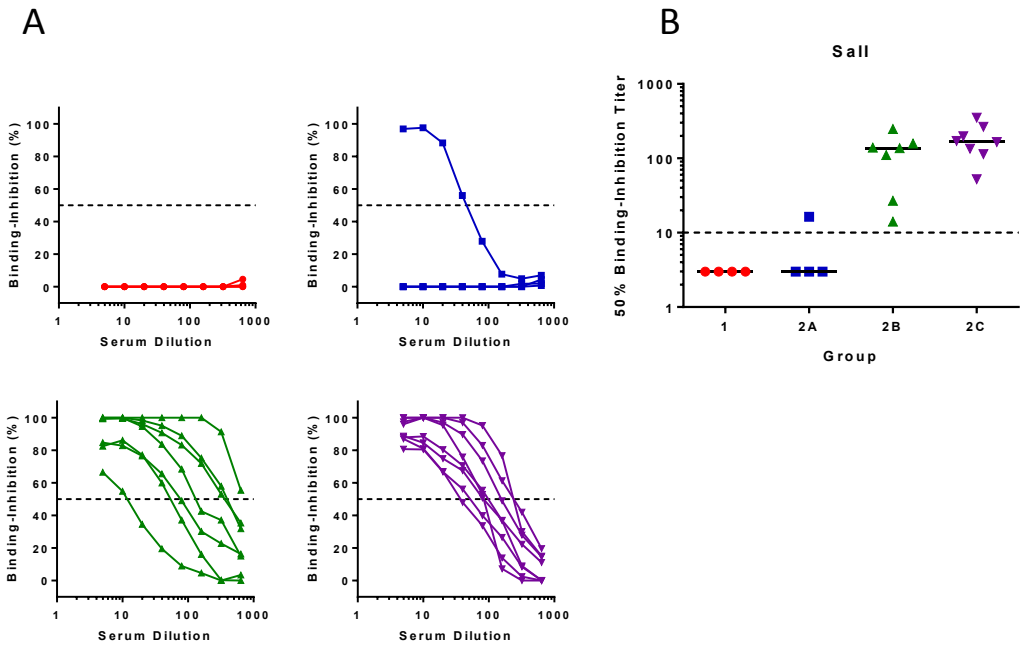


Figure 3.13: PvDBPII-DARC binding-inhibition ELISA showing (A) percentage inhibition of the sera from each individual in the four groups of the clinical trial and (B) the interpolated IC_{50} values for each group, ie the dilution of sera which inhibited 50% of PvDBPII-DARC binding in the ELISA. This assay used the Sal 1, vaccine homologous, sequence of PvDBPII.

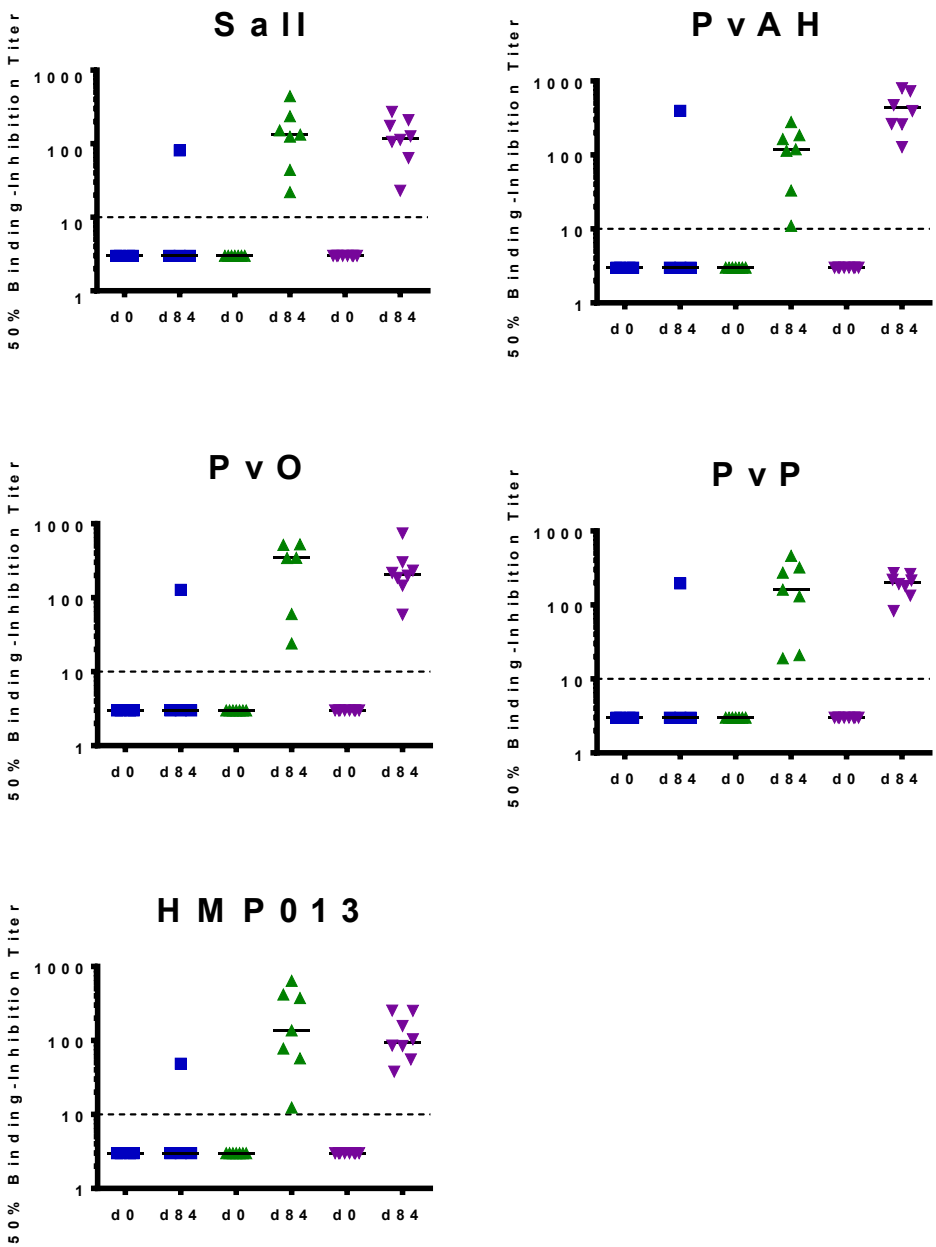


Figure 3.14: Clinical trial sera, both pre- and post-vaccination, were tested for their ability to inhibit binding of a panel of recombinant PvDBPII alleles (PvDBPII: SalI, PvAH, PvO and PvP) to DARC using an ELISA-based assay. Samples were titrated starting at 1:5 dilutions down to 1:640. Data show the interpolated dilution for each sample that gave 50% binding inhibition. The individual and median results are shown for each group. The dashed line shows an arbitrary cut-off below which negative samples are plotted.

AA residue	261	263	288	326	330	339	340	341	345	353	359	372	379	392	402	*	458	464
SalI	**F**	**R**	**L**	**K**	**N**	**D**	**E**	**K**	**R**	**S**	**T**	**N**	**L**	**W**	**S**	**–**	**I**	**E**
P	.	S	F	.	D	G	K	N	H	.	.	K	I	R	.	.	K	.
O	.	S	.	.	.	G	.	.	H	.	.	.	I	.	K	.	.	.
AH	.	S	.	E	.	G	.	Q	.	.	.	K	I	R	.	.	K	.
HMP013	L	S	.	.	.	G	K	N	.	T	R	.	I	.	.	L	.	K

Figure 3.15: Sequence polymorphisms of PvDBP_RII variants. The SalI reference sequence is shown in bold. Amino acid polymorphisms are indicated for the PvDBPII variants (P, O, AH and HMP013) described previously [417]. Amino acids that are the same as the reference sequence are indicated by a full stop, and a hyphen indicates an insertion/deletion. * HMP013 has a leucine insertion between V429 and P430 in the SalI reference sequence

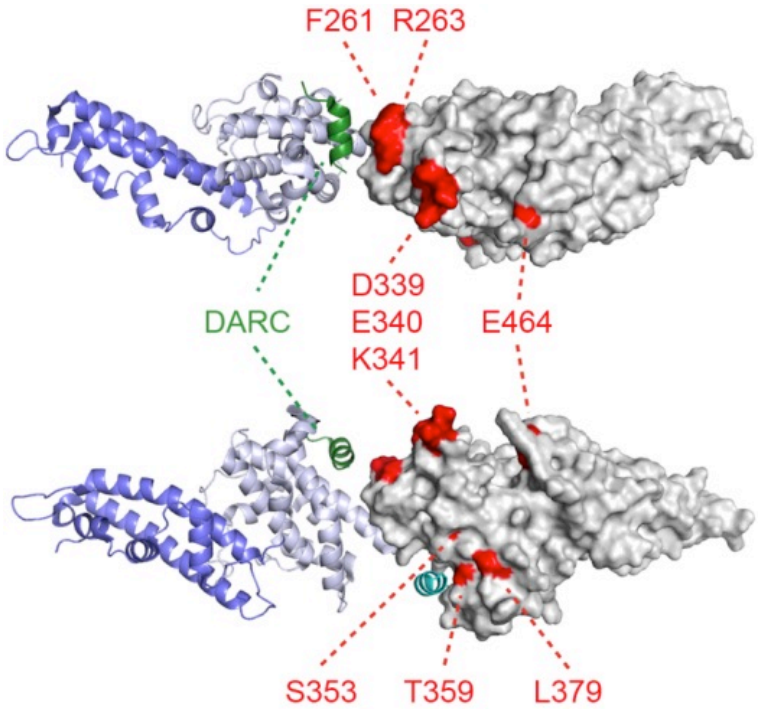


Figure 3.16: The location of polymorphic residues in the HMP013 strain of PvDBPII bound to aa 19-30 of DARC (PDB code 4NVU) [29, 304]. Two views of the dimer are shown, rotated by 90 degrees around the horizontal axis. One molecule of PvDBPII is shown in grey surface representation with polymorphic residues colored in red. The second molecule of PvDBPII is in blue cartoon representation with SD3 in a darker blue. The two helices from DARC are shown in green and cyan respectively.

The anti-PvDBPII Monoclonal antibodies in the binding-inhibition assay

In contrast to the polyclonal sera from the individual trial volunteers, the mAbs showed marked variation in binding-inhibition between different alleles when tested in the DBP-DARC binding inhibition ELISA (Figure 3.17).

DB7, for example, which inhibited the DARC-binding of the vaccine homologous Sal 1 PvDBPII strain most potently, showed no inhibition against the 'AH' and 'P' variants which differ from Sal1 sequence by only 8 and 11 amino acid substitutions respectively. Likewise, DB6 which strongly inhibited the binding of Sal1 PvDBPII, did not inhibit the binding of the O allele. DB1, DB3, DB4 and DB10 showed little DARC-binding inhibition when incubated with any of the five allelic PvDBPII variant proteins.

Only one mAb, DB9, showed consistent DARC-binding inhibition of $> 50\%$ across all five PvDBPII variants. At this initial stage of characterisation, prior to any functional assays, the data indicated six binding-inhibitory mAbs (Figure 3.18), four of which were strain-restricted and two strain-transcendent.

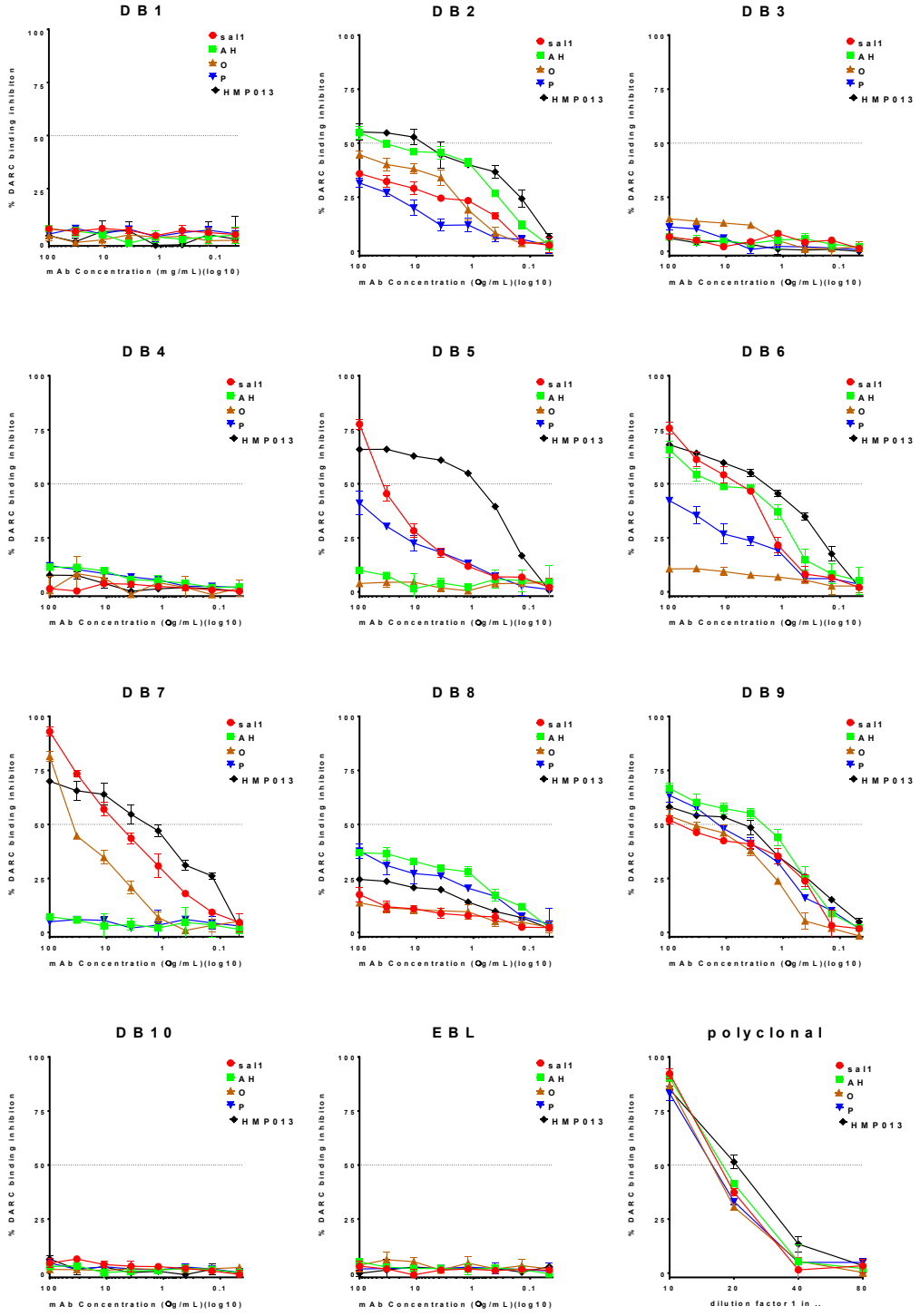


Figure 3.17: Binding inhibition of each mAb against the five variant PvDBPII alleles; Sal1 (red), AH (green), O (brown), P (blue) and HMP013 (black). The final two graphs show the positive and negative controls, EBL (an anti-Ebola recombinant human mAb) and polyclonal (polyclonal human serum) respectively.

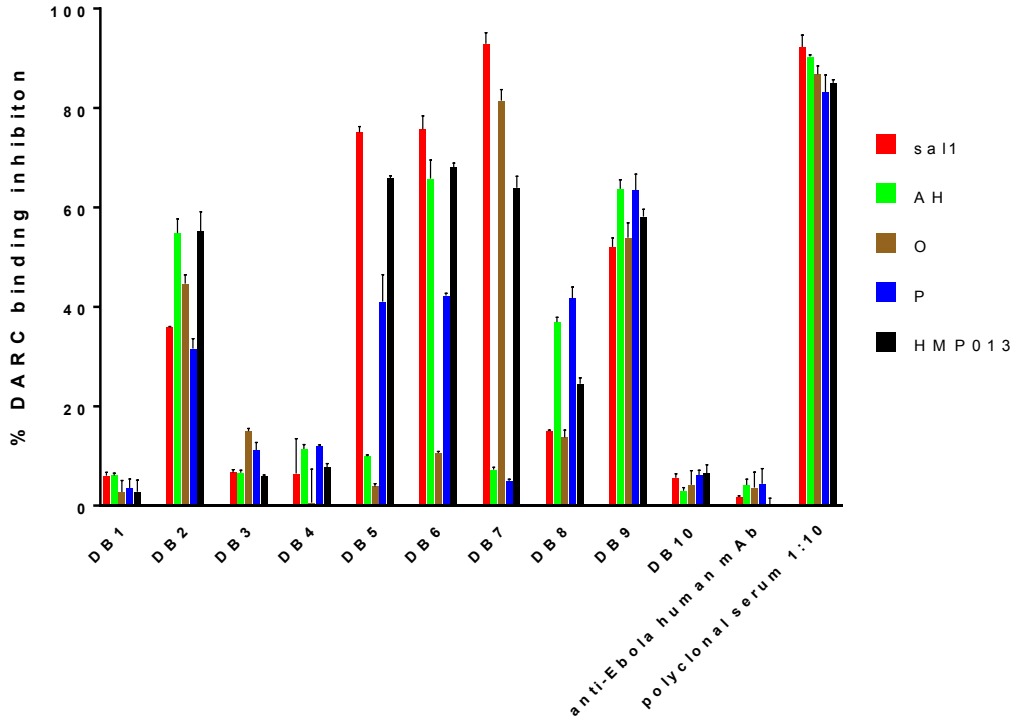


Figure 3.18: DARC binding inhibition of each PvDBPII variant allele by each mAb at 100μg/mL.

3.5 Discussion

In this Chapter I have described the cloning and initial characterisation of the first panel of fully human *Plasmodium vivax* mAbs. These antibodies, induced by viral-vectored vaccination with PvDBPII Sal1, were diverse in their variable chain sequences and showed a broad range of binding kinetics and DARC-binding inhibition. Broadly neutralizing antibodies (bnAbs) against polymorphic pathogens are rare; in the case of HIV, for example, tens of thousands of mAbs have been screened [185] to find a handful of bnAbs. Each pathogen is different, however, and the random nature of selecting B cells for cloning means that a lot of chance is involved when searching for bnAbs. At this early stage it appeared that I had been fortunate in finding one mAb in a panel of just ten which strongly inhibited the binding of multiple allelic variants of PvDBPII to recombinant DARC. Various factors may have contributed to my relatively low yield of antigen-specific mAbs. These included:

- The lack of initial selection for antigen-specificity; attempts were made to stain the PBMCs with labelled antigen to increase the yield of antigen-specific ASCs, but problems with high background levels of binding rendered this ineffective. The low levels of surface IgG on antibody secreting cells may also have frustrated this approach

- Loss of efficiency during the cloning stages; missing amplicons, both heavy and light chains, were common after the PCR steps. The degenerate primers, at the thermal cycle settings chosen, will have undoubtedly preferentially amplified certain templates. An example of this can be seen in the marked difference in band intensity between VH A9 and A10 on the gel electrophoresis picture in Figure 3.3.

- Some level of mRNA degradation was inevitable and it is also likely that errors in the process of labelling and flow-sorting of the PBMCs, occasionally led to the wrong cell type being selected.

- Bands were sometimes visible in both the V_κ and V_λ wells of a cell following PCR. This should not theoretically occur, due to the process of allelic exclusion, though it has been previously reported [337]. It is more likely, however, that this duplication of light chains was due to occasional mixing between wells or the promiscuity of some of the degenerate primers.

- The screening of the HEK293 cell supernatant for IgG by ELISA involved multiple wash steps with PBS-Tween and this may have led to certain low affinity PvDBPII-specific mAbs not being detected. In general, selecting for higher affinity and 'better' mAbs, would be considered a good thing, but as will be discussed later, low affinity mAbs may be potent neutralisers of merozoite invasion.

- The plates used to screen the supernatants for IgG and PvDBPII-specific IgG (NUNC ® Maxisorp™ polystyrene plates) are designed for very high protein-binding; this strength of binding may have distorted fragile conformational epitopes on PvDBPII or held the protein in orientations that shielded certain epitopes.

The anti-PvDBPII mAbs were all of high affinity in the context of published normal ranges [309]. As mentioned earlier, this combination of high affinity and low levels of somatic hypermutation, challenges traditional dogma [310]. It may be that the screening ELISA, with its multiple wash steps, contributed to the screening out of lower affinity mAbs.

The BLI competition assay pointed to an immunodominant region on PvDBPII, with 50% of the mAbs competing for binding. Previous attempts to map epitopes on PvDBPII [166, 398] have generally pointed to subdomain 2 (SD2) as the immunodominant region. SD2 is certainly the most polymorphic [428] of the three subdomains and is thus considered to have been under the most intense immune selection. On that basis, my initial presumption was that the clustering of five epitopes was most likely to be on subdomain 2, possibly on the highly

polymorphic regions that flank the putative PvDBPII dimer interface and DARC binding sites [73, 283, 332] The combined data from the epitope binning asay and the binding inhibition ELISA suggested the presence of a conserved, binding-inhibitory epitope within this immunodominant region.

The rationale behind a PvDBPII-based vaccine is that the induction of high-titer antibodies against PvDBPII will inhibit RBC invasion by preventing the interaction between PvDBPII and its natural ligand, DARC/Fy. In the absence of an easily available and standardized *P. vivax* assay of growth inhibition activity to assess anti-merozoite antibody function *in vitro*, a variety of *in vitro* receptor–ligand binding inhibition assays have been developed [154, 285, 343]. Given the lack of a better alternative, a lot of emphasis had been put on these recombinant protein binding inhibition assays to evaluate anti-vivax antibodies. There is clearly, however, a huge difference between the hyper-simplified context of two recombinant subunit proteins binding, or not, in a plastic plate and the *in vivo* reality. By initially evaluating the mAbs in these 'traditional' recombinant protein assays and then progressing to functional invasion assays with live parasites, I was well-placed to test the usefulness of the former. In the following chapters I report the performance of the panel of mAbs in two different functional assays.

4

Transgenic *Plasmodium knowlesi* assays

4.1 Authorship statement

The genetic modification of Pk A1H1 was performed by Professor Robert Moon's group at the London School of Hygiene and Tropical Medicine (*Mohring et al* submitted for publication).

4.2 Introduction

In the absence of long term *in vitro* culture, the preclinical development and testing of blood-stage vaccines against *P. vivax* have focused on biochemical assays [5, 78, 154, 332, 398] or in silico models [30] which do not directly demonstrate effectiveness in blocking RBC invasion by live parasites.

Having isolated and begun to characterise the panel of anti-PvDBPII mAbs in these biochemical assays, the next step was to find ways of testing their potency against live parasites.

There is clearly a big difference between an antibody binding to and interfering with a recombinant parasite protein in isolation and that same antibody interacting with that same protein as presented by the pathogen. The temporal and kinetic

aspects of the interaction will be very different as will the unknown effects of multiple other parasite and host proteins. Though the functional assays reported in the next two Chapters are still *in vitro* (or *ex vivo*), by testing the mAbs against live parasites, they move us a step closer to the *in vivo* reality.

Neutralisation, in immunology, is defined as antibodies binding to specific antigens on a pathogen to block its entry into the host cell. It is very different, therefore, from the binding-inhibition of proteins elucidated in the biochemical assays, which have sometimes been used erroneously to report antibodies as 'neutralising'.

Whilst antibodies can neutralise pathogens by various mechanisms, (antibody-dependent cellular cytotoxicity (ADCC), antibody-dependent cell phagocytosis (ADCP), and complement-dependent cytotoxicity (CDC)), invasion-blocking vaccines attempt to induce antibodies with the specific function of interfering with essential protein-protein interactions on the merozoite surface.

4.2.1 The assay of GIA

Blood-stage falciparum malaria vaccinology benefits from the use of an established in vitro assay of growth inhibition activity (GIA) [258] which correlates with a vaccine-induced protection in non-human primate (NHP) malaria infection models [122, 230, 356]. The assay is designed to quantify the change in parasite multiplication rate (PMR) over one growth cycle by measuring the endpoint activity of parasite lacatate dehydrogenase (pLDH), a plasmodial enzyme which correlates with parasite biomass. It is intended to quantify the effect of invasion-blocking antibodies and can be interpreted as a measure of the interference of merozoite attachment to, and invasion of, the erythrocyte. The assay does not contain any immune cells or active complement, discounting any growth-inhibitory effect attributable to ADCC, ADCP or CDC. It differs from physiological conditions in other ways as well; the haematocrit is very low, 2% instead of the physiological

45% and the static setup is far removed from the blood-flow through blood vessels. These differences have, of course, raised questions over the validity of such an assay as a correlate of protection for vaccine or drug screening purposes. Whilst not capable of measuring what is thought to be the mechanism of antibody-mediated NAI (see Chapter I), it does measure a conceptually-valid method of non-natural immunity which can be induced by vaccination and, as mentioned above, this has been demonstrated in NHP trials.

The two Pf studies referred to above, which report a correlative link between this GIA assay and *in vivo* PMR reduction/ protection in *Aotus* monkeys [122, 356], both indicated that $\geq 60\%$ GIA at a serum dilution of 1:4 is correlative of protection. A further study extended these findings for the protection of Rhesus macaques against *P. knowlesi* [164] and serum from a recent blood-stage human challenge of a PfAMA1 vaccine [303] showed $< 60\%$ GIA at a dilution of 1:4 and there was no protective efficacy. It is unknown whether the threshold for protection in humans is the same as for NHPs.

Given the lack of *in vitro* culture, however, a standardised *P. vivax* GIA assay was not an option for testing my panel of anti-PvDBPII mAbs, so alternative approaches had to be found. The first approach was entirely novel and evaluated for the first time in this DPhil Thesis. It involved the use of transgenic lines of the closely related species, *Plasmodium knowlesi*, which, unlike Pv, can be maintained in long term *in vitro* culture; routinely in rhesus RBC but now also in human RBC.

4.2.2 *Plasmodium knowlesi* (Pk)

Pk is a simian malaria parasite of South-East Asia and phylogenetically close to *P. vivax* [296]. First identified in a cynomolgus macaque (*Macaca fascicularis*) by Knowles and Das Gupta in 1932, they went on to demonstrate that the parasite could also infect humans by blood passage [204, 205]. The first natural human Pk

infection was identified in 1965 [76] and in 2004, a surprisingly high prevalence of *P. knowlesi* was found in humans in Malaysian Borneo when diagnostic microscopy was replaced by the more discriminatory method of nested PCR [101, 353]. This study identified that all blood samples from over 200 people reporting atypical malaria infection were *P. knowlesi*-positive but had been misdiagnosed with the morphologically similar *P. malariae*.

Although long- and pig-tailed macaques are the natural hosts for this species, *P. knowlesi* has now been described in humans across several South-East Asian countries and is the leading cause of human malaria in Malaysian Borneo [352]. While malaria cases caused by other *Plasmodium* species are on the decline in Malaysian Borneo, Pk cases increased over ten-fold between 2004 and 2011, indicating that this parasite is an emerging threat in the region [419]. There is not yet any direct evidence for human-to-human transmission by mosquitoes in the field.

Most cases are uncomplicated, with non-specific febrile illness and thrombocytopenia, but rates of severe malaria are similar to those of *P. falciparum*, reaching 6.5% in a district hospital in Sarawak, Malaysia [109]. Respiratory distress and renal failure are the most common severe complications and are usually associated with hyperparasitaemia [24].

Before *in vitro* culture of *P. falciparum* was achieved, Pk rhesus infections provided a source of highly synchronous parasites for laboratory studies. A landmark finding from these Pk animal models was the protection provided by passive immunisation of newly infected monkeys with serum from chronically infected ones [89] and not long after this, the first immunisation studies were conducted using killed blood-stage Pk or avian *P. lophurae* parasites [137]. Both studies showed protective effects and provided early evidence that a whole parasite vaccine may be a valuable tool. Antigenic variation mediated by the successive expression of variant proteins was first described in Pk [54] and led on to the identification

and characterisation of the corresponding gene family called SICAvar in Pk [180] and later the *var* genes in *P. falciparum*. The first of the RBC receptor–merozoite ligand pairs involved in erythrocyte invasion, PkDBPα/DARC, was discovered in Pk [4, 255], and later found to be shared with *P. vivax* [176]. The isolation of live Pk merozoites from infected rhesus RBCs [116], facilitated electron microscopy studies of erythrocyte invasion and identification of the moving junction between parasite and RBC [6, 22] (see Figure 1.5).

Once *P. falciparum* had been successfully cultured [388] the use of Pk diminished, but in 2002 the Pk H strain was successfully adapted to continuous culture and provided an *in vitro* system that produced enough parasites to allow transfection experiments [207]. This *in vitro* adapted line was transferrable back into rhesus monkeys, allowing genetic modification of parasites *in vitro* and the study of their phenotype *in vivo*. The need for monkey blood to culture Pk has recently been overcome with the successful adaptation of the H strain to grow in human RBCs [223, 261]. These human-adapted lines were still DARC dependent since no invasion was observed in Duffy-negative human RBCs or in cells depleted of DARC by chymotrypsin treatment [223, 261]. The first transfections in Pk were carried out in the 1990s [395] and transfections using the human-adapted line have resulted in $\sim$ 30% GFP positive parasites just one day after transfection [261]; this indicated the highest recorded transfection efficiency for any human malaria parasite. Compared to *P. falciparum*, Pk has the experimental advantages of a more balanced AT- content in its genome and vastly more efficient transfection [155, 207, 261].

The sequencing of the Pv and Pk genomes in 2008 revealed a near perfect synteny interspersed with expansions of species-specific genes [60, 296] and that the genomes share more than ninety genes with no orthologues in *P. falciparum* [136].

The Pk genome encodes three DBPs [296] and PkDBPα is pivotal for the invasion of human RBCs [350]. The functions of the other two DBPs (DBPβ and γ) are unknown but they do not bind human RBCs and are therefore likely to be

involved in rhesus RBC invasion [78]. The DARC-binding motifs of both PkDBPα and PvDBP lie in the cysteine-rich region 2 (DBPII) and share $\sim 70\%$ sequence identity [317]. Despite sharing a critical mechanism for RBC invasion, differences between Pk and Pv, most notably that Pk does not form hypnozoites and is not restricted to reticulocytes, limit the use of Pk as a more generalisable model for Pv.

A collaborating group from the London School of Hygiene and Tropical Medicine has recently established CRISPR-Cas9 genome editing in Pk (*Mohring et al* – submitted for publication) and used it to replace PkDBPα with its PvDBP orthologue. They then iteratively deleted the other two PkDBP paralogues (β and γ) to create a transgenic Pk line which relies on the PvDBP protein for invasion of erythrocytes.

In this Chapter, the neutralisation potential of the anti-PvDBPII mAbs against wild-type and transgenic Pk strains carrying the vaccine homologous PvDBPII Sal 1 sequence was assessed in a GIA assay.

4.3 *Plasmodium knowlesi* GIA

4.3.1 Setting up the assay

Detailed in Chapter II, the Pk GIA assay was adapted from the well-validated and widely used protocol for the Pf GIA assay [258]. The major differences, highlighted in the cartoon below (Figure 4.1), were; the length of the intra-erythrocytic life cycle, the method used to synchronise the culture, the growth rate, and the controls used.

The first task was to establish optimal conditions for the assay and, while awaiting the arrival of the transgenic parasite lines, standardisation assays were run with the wild-type Pk A1H1 line in human RBC.

In these standardisation assays, the haematocrit (HCT) and starting parasitaemia were varied to determine the optimal conditions for a clean readout. Based on the results shown below (Figure 4.2), the best signal:noise ratios were seen when the assays was run at 2%HCT with a starting parasitaemia of 1.5%.

Figure 4.1: Schematic of the Pk GIA assay.

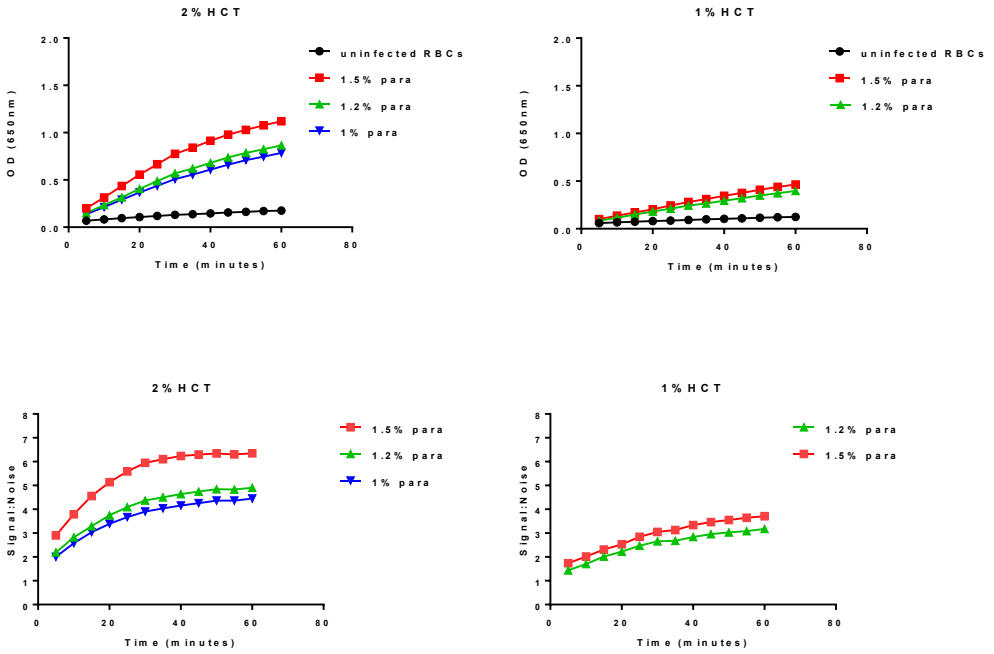


Figure 4.2: Initial assays to calibrate the growth of Pk A1H1 under various conditions; (A) 2% HCT and starting parasitaemias ranging from 1-1.5%; (B) starting parasitaemias of 1.2% and 1.5% at 1% HCT; (C) and (D) signal to noise ratios resulting from different starting parasitaemias and HCT. Signal to noise ratio is the average OD650 of the wells containing infected RBCs divided by the average OD650 of the wells containing uninfected RBCs.

4.3.2 Controls

The next step was to test potential controls reagents. I was able to obtain an anti-DARC camelid nanobody/VHH, which had been previously been shown to inhibit Pv invasion [329], as a gift from Olivier Bertrand (INSERM, Paris). Recombinant VHHs, or nanobodies, are the smallest intact antigen binding fragment derivative from the heavy chain-only antibodies present in camelids [163]. They express in high yield, have high solubility when compared to mouse or human two-chain derived antibody fragments and are in development for multiple diagnostic and therapeutic uses [3, 23]. In this case they were prepared from a dromedary immunised against DARC N-terminal extracellular domain expressed in *E. coli* [364]. This domain carries the polymorphic site responsible for the Fya/Fyb allotypes, the Fy6 epitope [387, 407] and participates in the binding of chemokines and PvDBP. The

critical PvDBPII-binding residues of DARC have been mapped to N-terminal region amino acids 8–42 [177, 308].

In addition to testing the anti-DARC nanobody, I also tested recombinant N-terminal DARC itself as a positive control.

Two antithetic antigens of DARC have been described, Fya and Fyb, which correspond to a single polymorphism in the extracellular part of the molecule [386]. The gene that encodes the Duffy antigen has two major polymorphisms; $Asp \rightarrow Gly$ amino acid substitution at codon 42 in the N-terminal region is associated with the Fyb and Fya blood-group antigens respectively and the $T \rightarrow C$ transition at nucleotide -33 in the GATA box of the Duffy gene promoter ablates Duffy expression on erythrocytes (the 'Duffy-negative' phenotype) [384]. Studies from the Brazilian Amazon region indicate that individuals expressing the Fyb compared with Fya antigen are more susceptible to Pv infection [66] and given that NHP studies suggest that Fyb is the ancestral allele [221, 383] it has been hypothesised that the Fya allele may have spread as a mutation conferring some protection against Pv. One study also showed that PkDBPα bound to Fyb-expressing erythrocytes more strongly than those expressing Fya [168].

On the basis of these reported differences between the alleles, I was keen to test both Fyb and Fya in the Pk assay, so, using site-directed mutagenesis of position 42 of the Fyb gene I transfected HEK293 cells with a plasmid containing the Fya allele and was able to express and purify Fya protein (Figure 4.3).

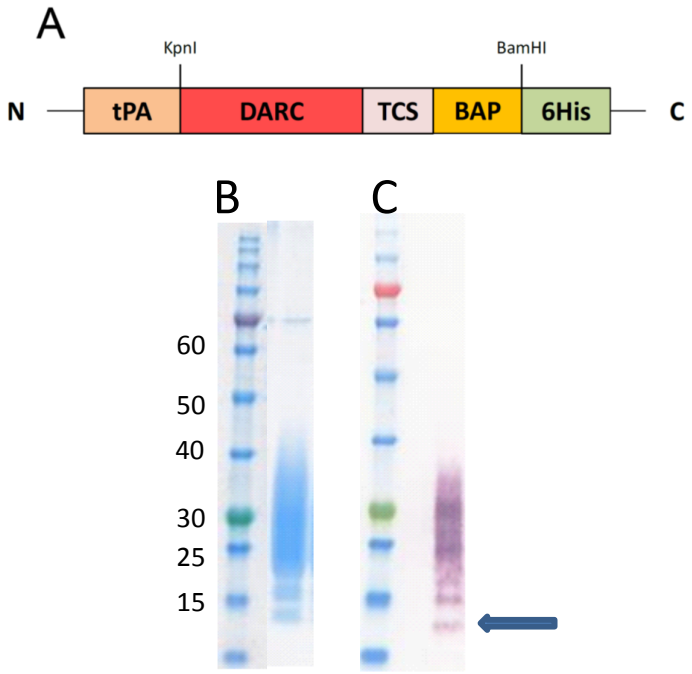


Figure 4.3: Expression of Fya DARC-His in HEK293 cells. DARC was expressed by transient transfection of HEK293E cells. (A) Amino acids 1-60 of the Fya variant of human DARC fused to a TCS, BAP and His tag were cloned into expression vector pENTR4 with a tPA leader sequence. After three days of culture, supernatants were harvested and DARC.His purified on a HisTrap column. Purified protein samples were run on SDS PAGE under non-reducing conditions and detected with (B) Coomassie Blue stain, and (C) polyclonal anti-DARC antibody. Arrow indicates monomeric DARC.

As shown in Figure 4.4, the anti-DARC camelid nanobody potently inhibited growth of PkA1H1, with an EC50 in the region of 2-3μg/mL.

Likewise, soluble N-terminal DARC also inhibited growth, with EC50 values of approximately 30μg/mL and 60μg/mL for Fyb and Fya respectively. This result was in keeping with the studies referred to above suggesting that DBP binds more strongly to the Fyb allele of DARC.

Using the host cell receptor to bind to and block entry of a pathogen is a fascinating concept that has been tested in viruses [143, 159] and, as will be discussed later, one that I intend to pursue for Pv malaria.

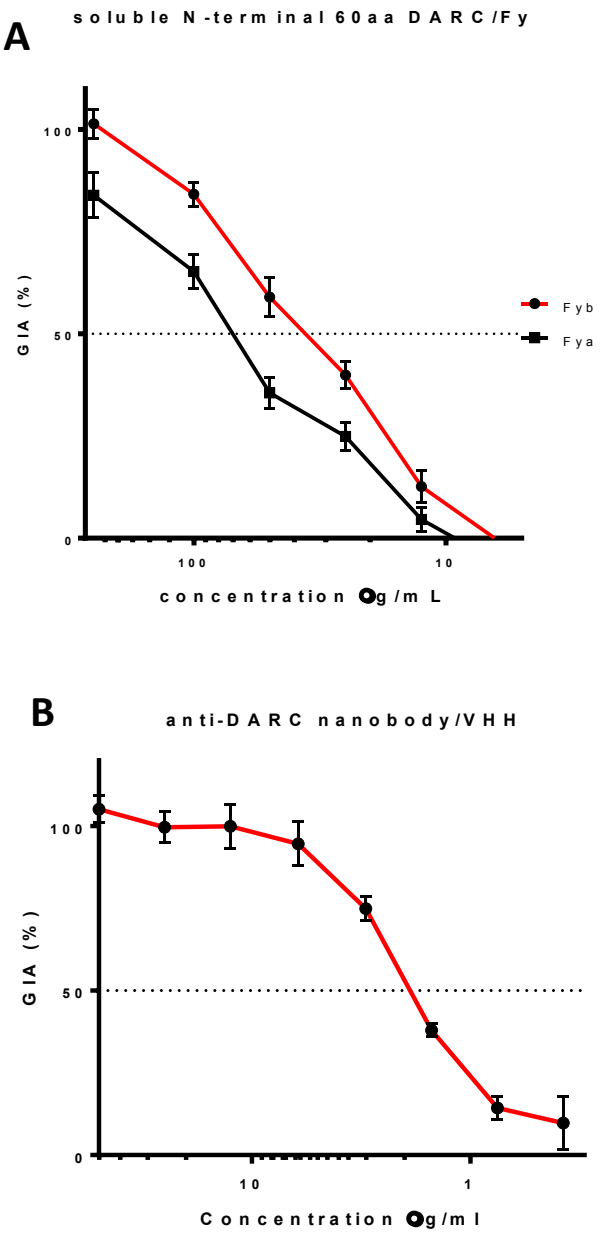


Figure 4.4: Testing of positive control reagents for the Pk GIA assays. (A) Soluble recombinant N-terminal DARC comparing the allelic variants Fya and Fyb; (B) Anti-DARC nanobody/VHH. The data points and error bars represent the median and standard deviation of three replicate wells.

4.3.3 Transgenic *Plasmodium knowlesi*

Whilst likely functionally equivalent, the PvDBP and PkDBPα orthologues are antigenically distinct with $\sim$ 70% amino acid identity in binding region II (Figure 4.10). Having established CRISPR-Cas9 genome editing in Pk, colleagues at the London School of Hygiene and Tropical Medicine replaced native PkDBPα with its PvDBP orthologue, and deleted the other two PkDBP paralogues (PkDBPβ and PkDBPγ) as illustrated in the Figure 4.5 (*Mohring et al* submitted for publication).

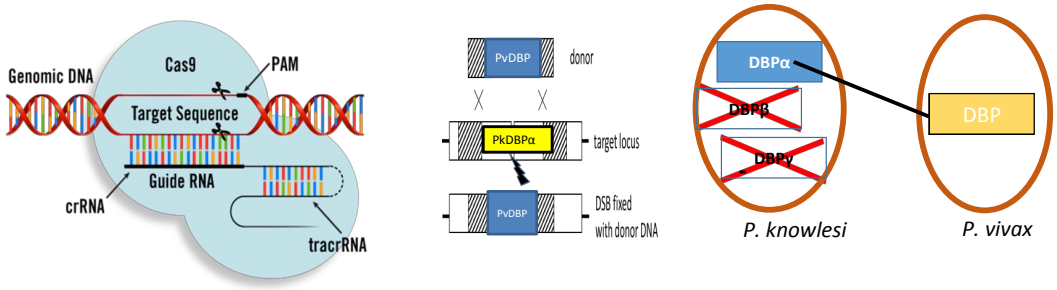


Figure 4.5: Schematic overview of the CRISPR/Cas9 genetic modification of *P. knowlesi*. PAM = protospacer adjacent motif. DSB = double-stranded break

They carried out an orthologue replacement (OR) of the full-length PkDBPα with PvDBP in the *P. knowlesi* A1H1 line (PvDBP^{OR}) using a recodonised synthetic PvDBP gene flanked by homology regions (HRs) targeting the 5' and 3'UTRs of the PkDBPα gene (Figure 4.6). Once integrated, this deletes the PkDBPα gene and places the PvDBP gene under control of the PkDBPα regulatory sequences, enabling a precisely matched expression profile. As a control they exchanged PkDBPα with a recodonised PkDBPα gene (PkDBPα^{OR}) using the same sgRNA (Figure 4.6 on page 125). Successful integration was achieved and limiting dilution cloning resulted in 100 % PkDBPα^{OR} and PvDBP^{OR} clones. The PkA1-H.1 line relies on the DARC receptor for invasion of human RBCs [261] and PkDBPα is required to mediate this interaction [350], thus the successful replacement indicated that the Pv orthologue could fully complement its role in DARC binding and parasite invasion.

Pk contains two DBPα paralogues, DBPβ and DBPγ, which are highly similar at the nucleotide (91-93% identity) and amino acid level (68-88% identity) but

are thought to bind to distinct receptors unique to macaque RBCs [110]. The PkDBPα sgRNA was designed to be distinct to equivalent PkDBPβ and PkDBPγ protospacer adjacent motif (PAM) sites, as off-target Cas9 induced DSBs are a major issue in other systems [402, 433]. They sequenced the four most similar PAM sites, including one in PkDBPγ, in the PvDBP^{OR} lines and did not detect any off-target mutations, suggesting that as for other malaria parasites [146] the absence of non-homologous end joining [202] ameliorates the potential for off-target mutations. Having established accurate targeting of the PkDBPα locus, they made use of pCas/sg plasmid recycling to additionally delete both PkDBPβ and PkDBPγ in iterative transfections.

Analysis of PkDBPα^{OR} and PvDBP^{OR} and their equivalent double knockout lines (PkDBP$\alpha^{OR}/\Delta\gamma\beta$ and PvDBP$^{OR}/\ \Delta\gamma\beta$) revealed no difference in growth rate in human RBCs, confirming that the *P. vivax* protein was able to fully complement the role of its *P. knowlesi* orthologue, and PkDBPβ and γ proteins are dispensable for invasion of humans RBCs [110]. The method and clones produced are shown in the figure below (*Mohring et al*, submitted for publication), but in summary and for clarification I used five different Pk lines in the GIA assays reported below;

1. **PkA1H1**. This is the human RBC adapted line with no genetic modification;

2. **PkDBP$\alpha^{\mathbf{OR}}$**. This has the PkDBPα^{OR} gene replaced with a recodonised version and acts as a transgenic control;

3. **PvDBP$^{\mathbf{OR}}$**. This has the PvDBP gene in place of the PkDBPα gene;

4. **PkDBP$\alpha^{\mathbf{OR}}/\mathbf{\Delta}\gamma\beta$**. As for strain 2, but with the PkDBPβ and PkDBPγ genes deleted;

5. **PvDBP$\alpha^{\mathbf{OR}}/\mathbf{\Delta}\gamma\beta$**. As for strain 3, but with the PkDBPβ and PkDBPγ genes deleted.

PvDBP$\alpha^{OR}/\Delta\gamma\beta$ is, in theory, the cleanest model for Pv as it has only the PvDBP gene with which to interact with DARC. As mentioned above, however, the fact that the PkDBP$\alpha^{OR}/\Delta\gamma\beta$ line, with its β and γ DBP genes deleted, grew just as well in human RBCs, suggests that these DBP paralogues are not involved in the invasion of human erythrocytes.

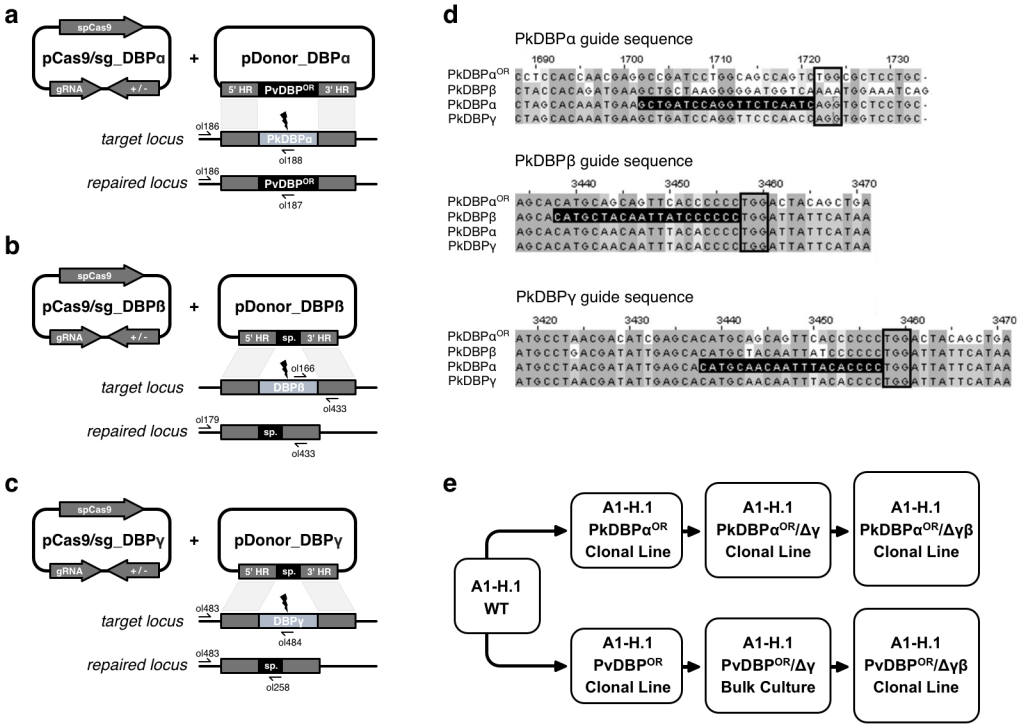


Figure 4.6: Schematic of CRISPR-Cas9 strategy. (a) Integration of the PvDBP into the target PkDBPα locus via homologous recombination. Arrows indicating oligo positions for diagnostic PCRs. (b) Integration of a spacer sequence into the target PkDBPβ. (c) Integration of a spacer sequence into the target PkDBPγ locus. (d) Nucleotide sequence alignment of PkDBPα PkDBPβ and PkDBPγ guide sequences. The chosen guide sequence for transfections are highlighted in black. The boxes highlight the PAM sites. (e) Flow chart indicating generated transgenic DBP parasite lines. First wild type parasites were edited by orthologous replacement of PkDBPα with the recodonised gene (PkDBPαOR) or *P. vivax* DBP (PvDBP^{OR}) and clonal lines established by limiting dilution cloning. Both clonal parasite lines were edited by knockout of PkDBPγ (PkDBP$\alpha^{OR}/\Delta\gamma$ and PvDBP$^{OR}/\Delta\gamma$). Knockout of PkDBPβ was carried out in a clonal PkDBP$\alpha^{OR}/\Delta\gamma$ and uncloned PvDBP$^{OR}/\Delta\gamma$ line resulting in PkDBP$\alpha^{OR}/\Delta\gamma\beta$ and PvDBP$^{OR}/\Delta\gamma\beta$ lines which were cloned before use in invasion assays and GIAs. (Figure from *Mohring et al* – submitted for publication).

4.3.4 Pk GIA assays with polyclonal rabbit serum

These first GIA assays with the transgenic Pk lines revealed that they were all equally susceptible to invasion inhibition by both the anti-DARC camelid nanobody and polyclonal rabbit anti-PkMSP1$_{19}$ antibody (Figure 4.7, E). In contrast, polyclonal rabbit sera raised against PvDBPII, demonstrated low-level growth inhibition against the PkDBPα^{OR} and PkDBP$\alpha^{OR}/\Delta\gamma\beta$ lines ($\sim$ 30% inhibition at 10 mg/mL) but significantly stronger inhibition against the PvDBP^{OR} and PvDBP$^{OR}/\Delta\gamma\beta$ lines, reaching a maximum inhibition of $\sim$ 75% at 10 mg/mL and around 50% at 4 mg/mL (Figure 4.7, A-D).

The PvDBP^{OR} could thus be readily inhibited by antibodies against the *P. vivax* protein and the PkDBPα orthologues γ and β appeared to play no interactive role.

Whilst running these initial assays using rabbit antisera to ascertain the robustness of the new Pk GIA model, I also tested IgG from rabbits vaccinated with Pk cysteine rich protective antigen (PkCyRPA). (*Knuepffer and Wright et al*, submitted for publication).

Plasmodium falciparum RH5 (PfRH5) is an atypical RBL family ligand which, being essential for invasion and conserved in all isolates tested [32, 320, 389] and having recently shown protection of Aotus monkeys against a vaccine-heterologous *P. falciparum* challenge [122], is currently the leading Pf blood-stage vaccine candidate. PfRH5 forms a heterotrimeric complex with cysteine rich protective antigen (PfCyRPA) and RH5 interacting protein (PfRIPR), two micronemal proteins [74, 319]. Both PfCyRPA and PfRIPR are essential for invasion, and antibodies against either of them have shown invasion-blocking potential [401]. No direct orthologue of PfRH5 has been identified in the genomes of Pv or Pk, but genes orthologous to PfRIPR and PfCyRPA are found in all or most *Plasmodium* species.

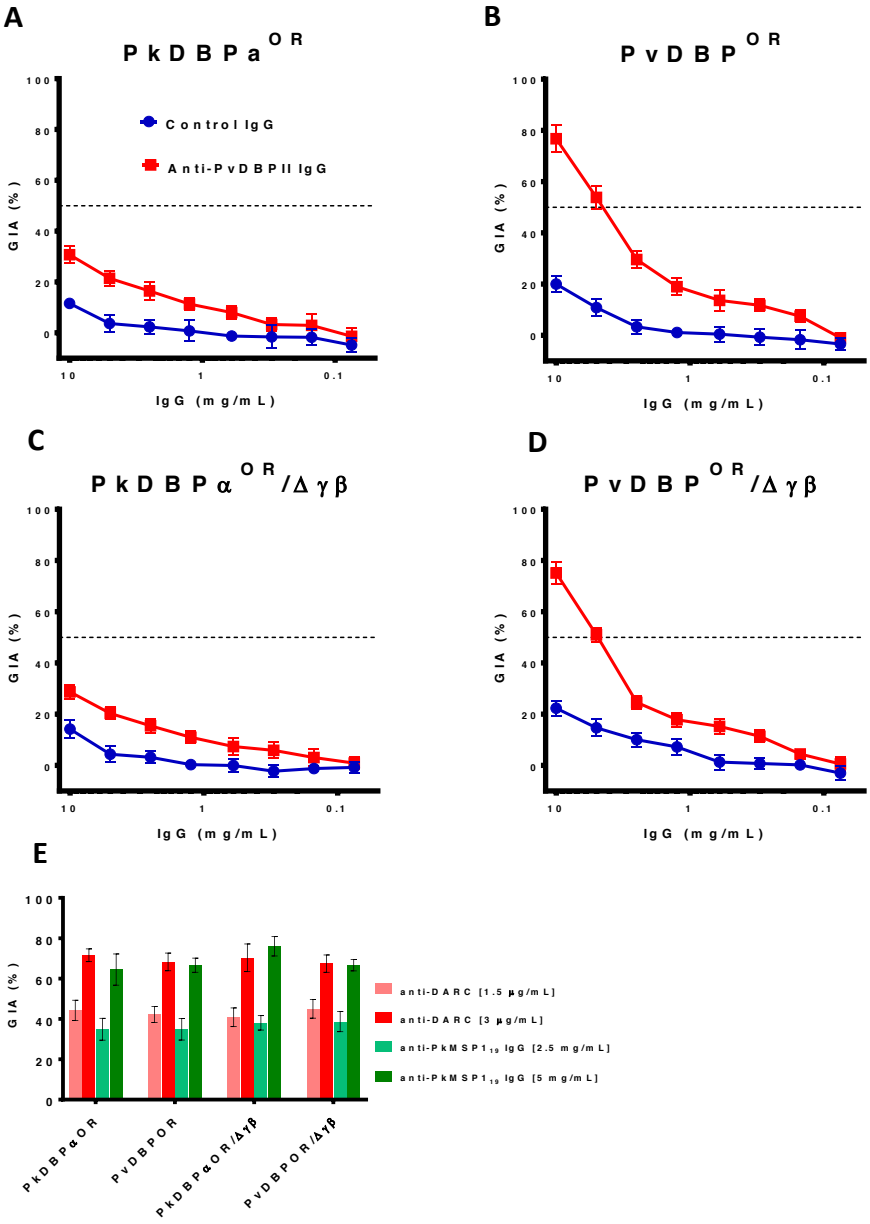


Figure 4.7: Growth inhibition activity of polyclonal rabbit anti-PvDBPII IgG and controls on four different transgenic *Plasmodium knowlesi* lines. Panels A-D show the % GIA of a dilution series of total IgG purified from sera of PvDBPII (SalI)-immunised rabbits as well as control IgG purified from the pre-immunisation sera of the same rabbits. (A) PkDBPα^{OR} line. (B) PvDBP^{OR}. (C) PkDBP$\alpha^{OR}/\Delta\gamma\beta$. (D) PvDBP$^{OR}/\Delta\gamma\beta$ Data points represent the mean and error bars indicate ± 1 SD of 6 replicates. (E) GIA of anti-DARC VHH nanobody and anti-PkMSP119 purified total rabbit IgG against each transgenic line. Data points represent the mean and SD of triplicate test wells.

It was on this basis that anti-PkCyRPA antibodies were tested against PkA1H1 in this assay, but disappointingly they showed no inhibitory effect (Figure 4.8).

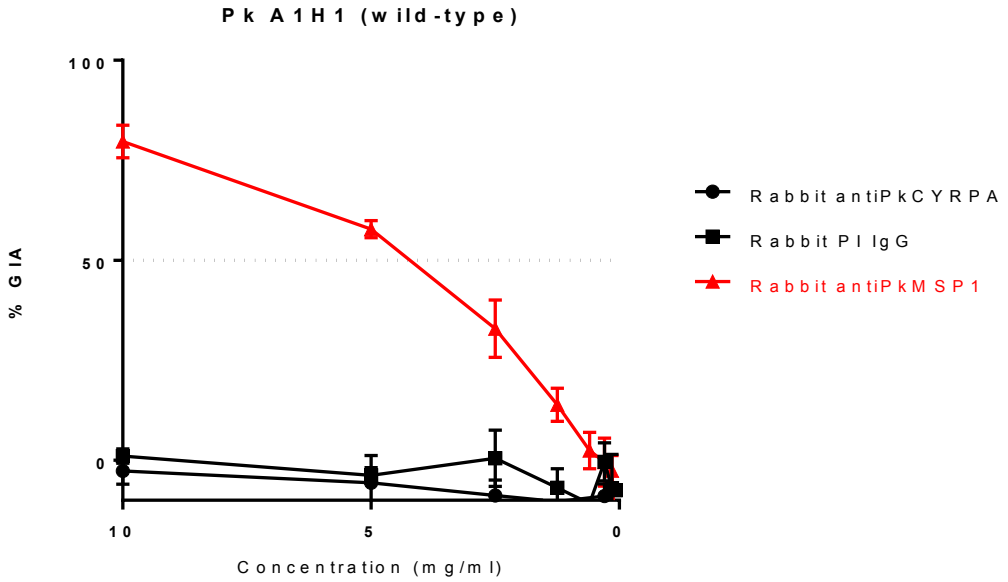


Figure 4.8: Pk A1H1 GIA of dilution series of IgG purified from rabbits immunised with PkCyRPA and PkMSP1$_{19}$. Data points represent the mean and SD of triplicate wells.

Further studies into the function of CyRPA in Pk have shown that its role appears to be very divergent from that in Pf (*Knuepffer and Wright et al*, submitted for publication).

4.3.5 Anti-PvDBPII mAbs in the Pk GIA assays

As seen in panels A,B and D of Figure 4.9, one of the ten anti-PvDBPII mAbs, DB7, inhibited growth of the wild type (and control) Pk lines. The polyclonal rabbit anti-PvDBPII serum showed some species cross-reactivity and given the high sequence homology (Figure 4.10) between PvDBP and PkDBPα, it is perhaps not surprising that one of the mAbs would cross react, albeit with low potency (EC_{50} of $>500\mu$g/mL).

As shown in panels C and E of Figure 4.9, all of the mAbs inhibited growth of the Pk lines containing the PvDBP transgene, with seven of the ten mAbs exhibiting GIA of >50% at concentrations below 250μg/mL. The mAbs clustered into 3 growth inhibitory groups.

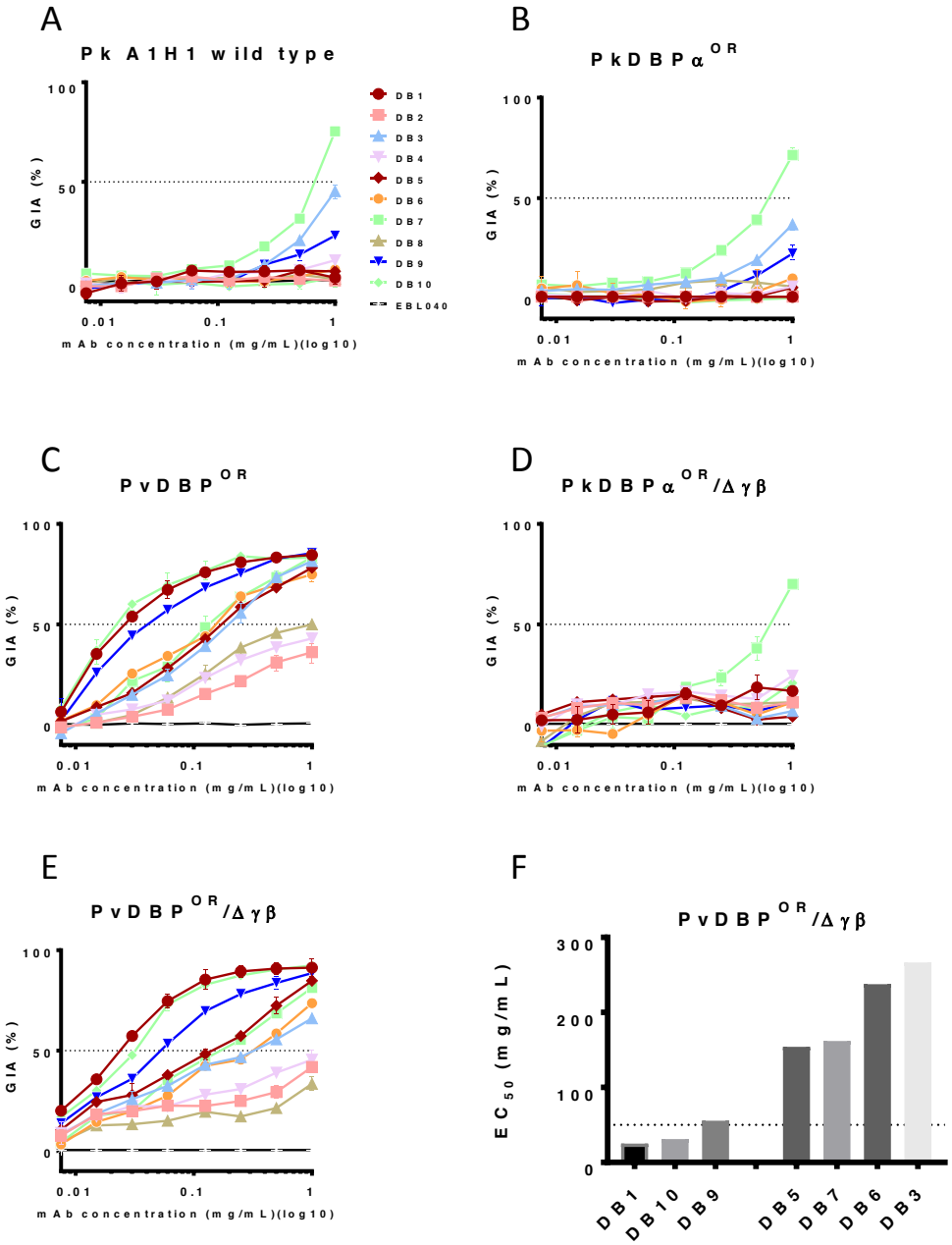


Figure 4.9: Assays of GIA by the ten anti-PvDBPII human mAbs against 5 different Pk lines. (A) 'Wild type' Pk A1H1; (B) PkDBPα^{OR}; (C) PvDBP^{OR}; (D) PkDBP$\alpha^{OR}/\Delta\gamma\beta$; and (E) PvDBP$^{OR}/\Delta\gamma\beta$. In all the assays the mAbs were tested in a doubling dilution series starting at 1mg/mL. Data points represent the mean and SD of triplicate test wells. Panel (F) shows the interpolated EC_{50} for the 7 mAbs which reached 50% inhibition against the PvDBP$^{OR}/\Delta\gamma\beta$ line at the maximum concentration. They are shown in ascending rank order. EC_{50} values were interpolated from a non-linear regression curves generated by GraphPad Prism software

- Potent growth inhibition (EC_{50} <50μg/mL); DB1, DB9 and DB10
- Moderate growth inhibition (EC_{50} <250μg/mL); DB3, DB5,DB6, and DB7
- Poor growth inhibition (EC_{50} > 1mg/mL) DB2, DB4 and DB8

The most inhibitory mAbs (DB1, DB10 and DB9), with EC_{50} values of ∼25, ∼30 and ∼50μg/mL respectively against PvDBP^{OR}/$\Delta\gamma\beta$, were on a par with some of the most potent anti-Pf mAbs as assessed in GIA assays [123, 294].

When the GIA of each mAb was considered in light of the epitope binning assays (Figure 4.11) described in the last Chapter it could be seen that DB1 and DB10, which competed for binding on PvDBPII, must target a neutralising epitope on the Sal1 strain. The largest cluster of binding sites on the antigen, however (Figure 3.11), within which five of the ten mAbs competed, contains antibodies with a broad spectrum of neutralisation; from DB9, one of the most potent, to DB2, one of the least potent.

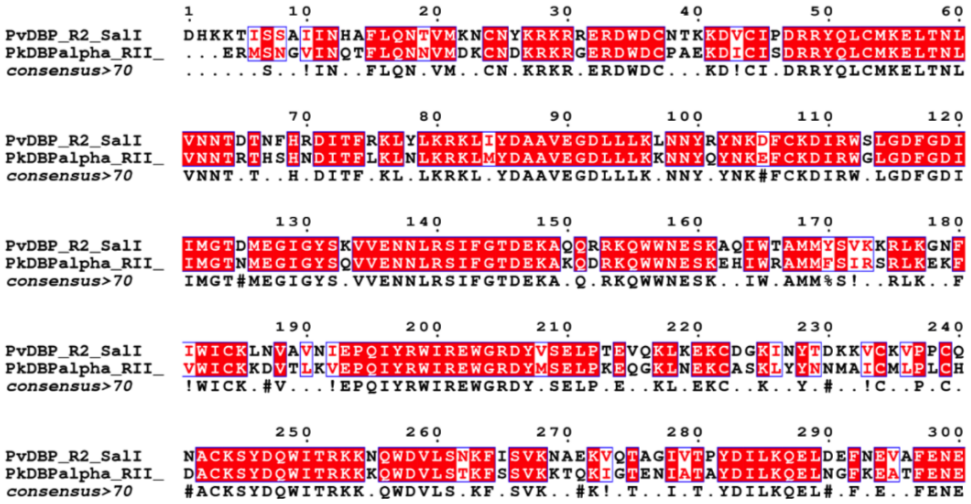


Figure 4.10: Amino acid sequences of region II of PkDBPα (H strain) and PvDBP (Sal 1 strain) aligned using Clustal Omega, showing >70% sequence homology. Red boxes show preserved amino-acids.

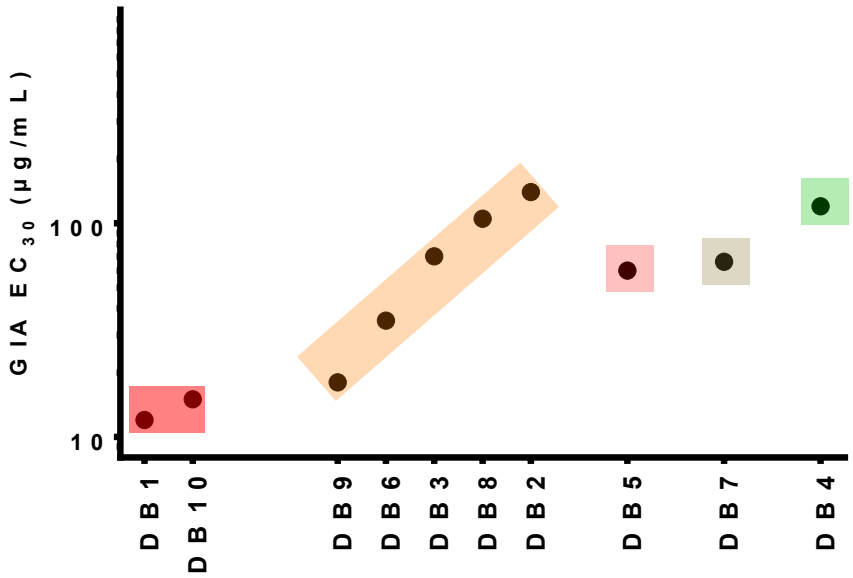


Figure 4.11: mAb epitope bins by neutralisation phenotype. Epitope bins, as determined by a matrix of sequential binding assays are shown by the different coloured boxes and these are plotted against the interpolated EC_{30} of the mAbs. The data used to construct the epitope bins are shown in Figure 3.11 and EC_{30} values are interpolated from Figure 4.9.

4.3.6 Correlation between antibody kinetics and neutralisation

While the link between epitope bin and neutralization was not clear cut at this stage, a correlation between the kinetic profiles of the individual mAbs and their growth inhibition of the PvDBP$^{OR}/\Delta\gamma\beta$ transgenic Pk was striking. The affinity (KD), on-rate (K_{on}) and off-rate (K_{off}) of each mAb was plotted against their percentage inhibition in the transgenic Pk assay (Figure 4.12).

There was a strong correlation between the on-rate of the mAbs and their neutralisation in the Pk transgenic GIA assay (R= -0.95; p=0.002) but no correlation between the off-rate or the affinity constants and parasite neutralisation.

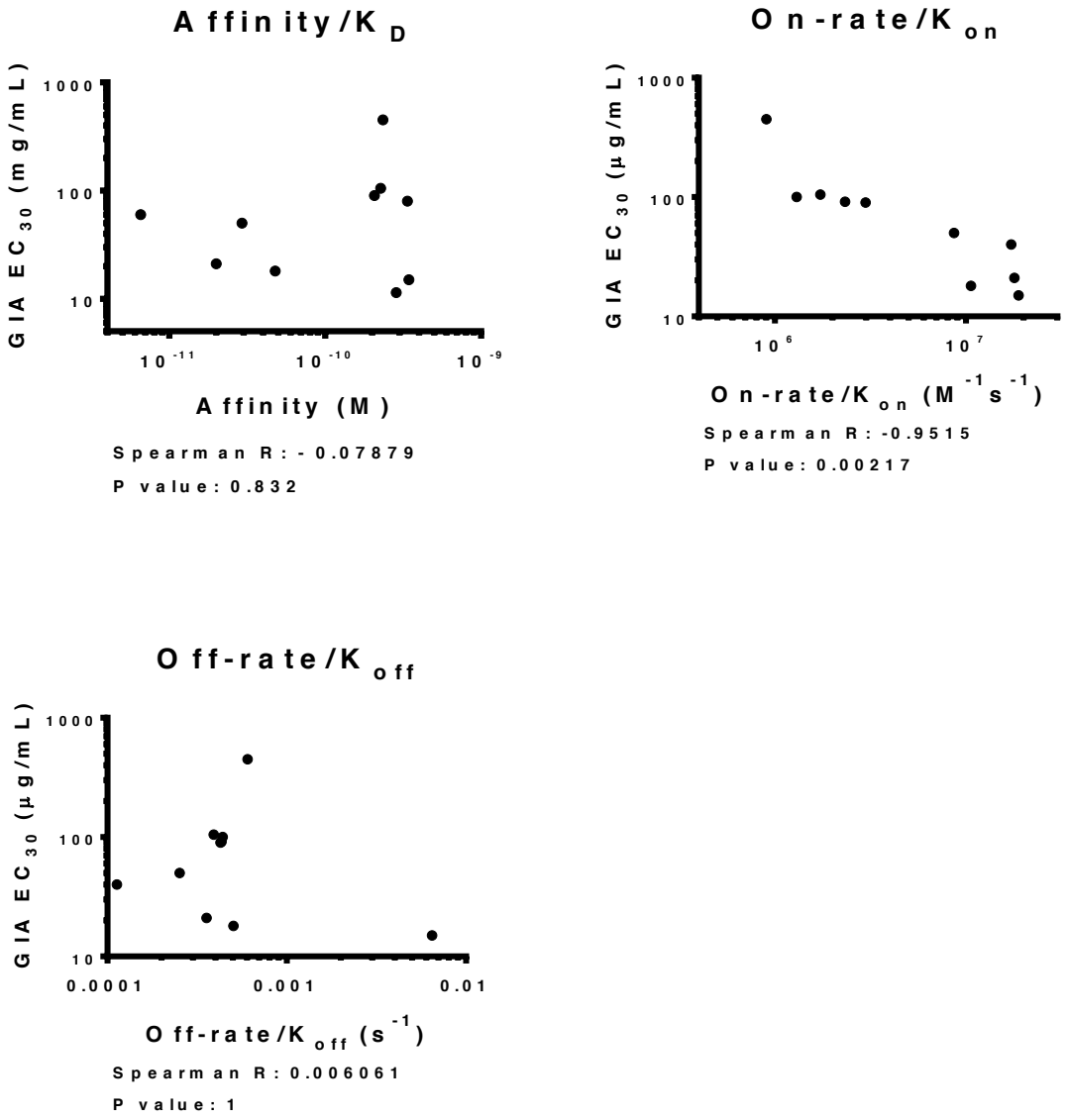


Figure 4.12: Correlations of the kinetic binding constants Kon (on-rate), Koff (off-rate) and KD (affinity) with growth inhibition for the 10 anti-PvDBPII mAbs. EC_{30} values, chosen as the neutralisation readout in order to include weaker-neutralising mAbs, were interpolated from non-linear regression curves generated by GraphPad Prism software and based on the data in Figure 4.9 and the kinetic values taken from Table 3.3.

4.4 Discussion

This Chapter describes the first use of a Pk transgenic model to assess anti-*P. vivax* antibodies. The results were encouraging in two respects; the model appeared robust in its response to polyclonal rabbit anti-Pv sera and a panel of human anti-PvDBPII mAbs elicited a broad range of growth inhibition.

This was good proof of concept for the new Pk model, which will undoubtedly be widely adopted as a proxy to study Pv; until that is, Pv itself can be cultured successfully. The main limitation in these first assays was that I was only able to test the mAbs against the vaccine homologous Sal 1 strain of Pv. Our collaborators at the London School of Hygiene and Tropical Medicine are currently working on inserting other allelic variants of PvDBP into their Pk lines. This will open up the exciting opportunity to test for strain transcendence using this model. In the meantime, the technically challenging *ex vivo* Pv assays, described in the next Chapter, remain the only option to assess for functional strain transcendence.

In the light of this first round of functional invasion data, some discrepancies with the recombinant protein binding-inhibition assays were clear. The two most potently neutralising mAbs in the transgenic Pk GIA assay, DB1 and DB10, had consistently shown the least DBP-DARC binding inhibition against all five allelic variants of recombinant PvDBPII. It should be noted that these transgenic Pk lines contained the full-length PvDBP gene, not just region II as used in the recombinant protein assays. Likewise, the binding-inhibition ELISAs assessed binding to only the N-terminal 60 amino acids of DARC. It is possible that in the functional assays the antibodies also interact with protein domains other than those in region II of DBP or the N-terminal 60 aa of DARC.

This major disconnect casts doubt on the validity of the recombinant protein assays to predict neutralisation.

The very rapid invasion of RBCs by the merozoite is a major obstacle to the effectiveness of antibodies. In comparison to many other antibody-susceptible pathogens, against which neutralising antibodies are afforded the time to reach equilibrium, anti-merozoite antibodies have only seconds to act. The realisation that association rate (K_{on}) is important for invasion-blocking antibodies is not new [123, 336].

RBC invasion in *in vitro* culture is achieved in less than 1 min by most (77%) *P. falciparum* merozoites, and once contact is made with the RBC, invasion usually takes ∼20 seconds to complete [411].

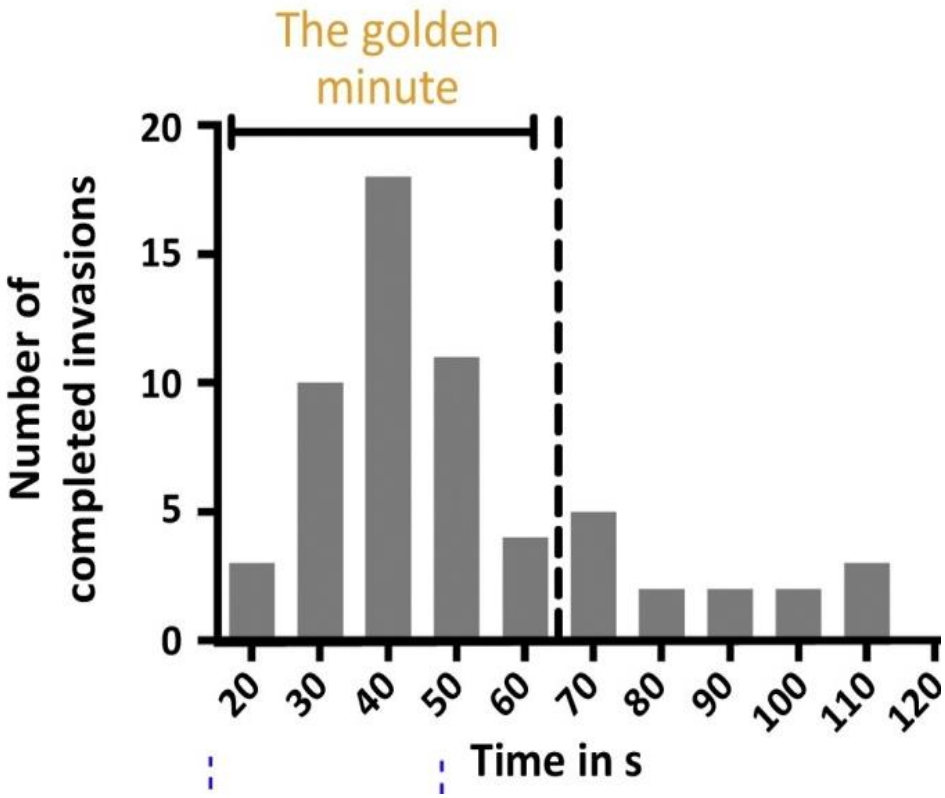


Figure 4.13: Histogram from *Weiss et al.* [410] showing the average invasion speed of Pf merozoites in culture.

Merozoites only remain infective for a few minutes *in vitro*, and almost certainly less than this *in vivo* when under attack from the host immune responses [51, 103]. The 'naked' merozoite in this momentary extracellular stage is arguably at the most

vulnerable point of its life cycle.

These assessments of the 'golden minute' are, however, based on live microscopy of Pf merozoites invading erythrocytes [410]. Given that Pv merozoites can only invade ∼1% of circulating erythrocytes, it may be that the time frame is longer for Pv. If this is the case, and this crucial window of opportunity is indeed longer for Pv, it may significantly improve the chances of inducing effective antibody blockade of the Pv merozoite.

5

Plasmodium vivax assays

5.1 Authorship statement

I was assisted in the Pv invasion assays by Dr Jee Sun Cho (SIgN, Singapore) and Dr Varakorn Kosaisavee (Shoklo Malaria Research Unit, Mae Sot, Thailand).

5.2 Introduction

In the experiments described in Chapter IV, I showed some of the anti-PvDBPII mAbs to be potent neutralisers of transgenic Pk parasites; but, however robust the Pk model, the gold standard was to test the mAbs against vivax herself. With this intent I travelled to South-East Asia.

5.2.1 *Plasmodium vivax in vitro*

Unlike *P. falciparum*, *P. vivax* cannot be reliably kept alive in long-term *in vitro* culture [38, 281, 380]. This has been a major impediment to research and it will be a significant breakthrough when the missing pieces of the jigsaw are finally found. It may turn out to be something as simple as a candle jar, as was the case with *Plasmodium falciparum* in the 1970s [388]. The first attempt to cultivate Pv was published over a hundred years ago, in 1912 [28], but despite the author's

optimism and a century of trying, we have still not succeeded. The main difficulty seems to be the host cell, the reticulocyte.

5.2.2 The reticulocyte

Of the malaria species with a tropism for reticulocytes, *P. vivax* may be the best known, but the young erythrocytes are attractive to many parasites. Haemoprotozoans, such as *Babesia* spp., *Haemogregarina* spp. and *Plasmodium* spp., which grow and reproduce in the nutrient rich and immunologically protected environment inside red blood cells, are some of the most successful and diverse parasites and found in almost every class of vertebrate. A disadvantage, however, of targeting red blood cells is that they are short-lived (∼120 days); invading a mature erythrocyte could result in premature clearance and it is not surprising, therefore, that most *Plasmodium* spp. prefer to invade younger erythrocytes [86, 88, 238]. Most primate malaria parasites have a tropism for immature erythrocytes [88] and even those species with the capacity to invade a wide range of erythrocytes, such as *P. falciparum*, will preferentially invade reticulocytes if given the chance [299, 421].

Reticulocytes, broadly defined as a group of immature erythrocytes which no longer contain a nucleus, undergo significant membrane and cytoplasmic remodelling. It is the degenerate intracellular network (substantia reticulo-filamentosa), visualised with stains such as the RNA-precipitating dye new methylene blue, that remains the key diagnostic of the reticulocyte population [125]. While reticulocytes only represent 0.6% to 2.9% of erythrocytes in adult blood and 1.7% to 5.0% in cord blood [300], they are central to the understanding of erythropoiesis and the pathophysiology of diseases such as sickle cell anaemia and malaria [259]. The four day time-span of a reticulocyte's development is characterised by a wide range of biochemical and immunological changes as well as alterations in shape and deformability [69, 70]. Early stage reticulocytes found in bone marrow are large, rigid, irregular spherical cells and as they mature they become smaller, biconcave and lose membrane proteins [234]. These early stages are restricted to the bone

marrow and only the most mature reticulocytes are common in the peripheral blood supply [341]. Recent work has shown the bone marrow to be an important reservoir for *P. vivax* [289].

The transferrin receptor (CD71) is sequentially lost as the reticulocyte matures and the distinction between CD71+ and CD71- reticulocytes is important as *P. vivax* merozoites have a strong preference for CD71+ reticulocytes [234]. Very soon after invasion the parasite effects changes in the RBC immunophenotype, including the loss of these CD71 receptors; it has been suggested that this might represent a strategy to block the invasion of other merozoites [233]. The fact that DARC is expressed on both immature and mature erythrocytes [234] means it is not the reticulocyte-specific receptor. The search for this reticulocyte-specific receptor has focused on two families of merozoite proteins; the reticulocyte-binding proteins (RBPs) and erythrocyte-binding proteins (EBPs) [141, 172, 318]. CD71 (also known as Transferrin receptor 1/TfR1) has recently been proposed as a reticulocyte-specific ligand which binds PvRBP2b [156].
Reticulocytes, although enucleated, still express MHC class I molecules which remain from the nucleated reticuloblast stage; this is in contrast to mature erythrocytes that have completely lost expression of MHC molecules [140]. Recent CHMI studies have shown that *P. vivax*, but not *P. falciparum*, infection led to the expansion of a specific subset of CD8+ T cells which were associated with an activated phenotype and cytotoxic potential [55]. Previous work using a genetically engineered mouse model of murine malaria has also shown that CD8+ T cells can be activated by parasitised erythroblasts (but not parasitised mature red blood cells) through MHC class I dependent mechanisms [188]. This CD8+ T cell killing of Pv-infected reticulocytes may have important implications for Pv blood-stage vaccine efficacy.

Despite all the logistical difficulties there are some advantages to studying a parasite that has not yet been adapted to *in vitro* culture. There are major differences in phenotype between lab-adapted and wild type malaria strains. A

transcriptomic study of *P. knowlesi* [218] showed significant differences in gene expression between lab-adapted and wild-type strains. Many of the Pf strains used regularly in drug and vaccine assays have been maintained in blood-stage lab culture for decades. They will have undoubtedly adapted to this artificial environment and may have epigenetically 'forgotten' the wild-type existence of their ancestors. Living only in the blood-stage (and a very artificial form of it at that) they will have had no use for their skin-, liver- or mosquito-stage genes for decades, so may have switched many of them off.

So, being obliged, through the lack of an *in vitro* culture, to go out into the field and experiment on wild-type parasites *ex vivo* does have the advantage that the data, though more difficult to acquire, may be more reflective of the 'wild-type' reality out there and thus more predictive of vaccine efficacy.

5.2.3 *Plasmodium vivax ex vivo*

Ex vivo studies involve the manipulation of primary clinical samples of *Plasmodium* spp. in an artificial environment for no longer than 48 hours. They are a kind of half-way house between the complex *in vivo* environment and the hyper-simplified *in vitro* one. Despite the regular addition of reticulocytes, only relatively short-term *ex vivo* cultures have so far been achieved. These are summarised in Table 5.1.

Reticulocytes have generally been purified from either umbilical cord blood [392] or haemochromatosis patients [148], though some have been derived from hematopoietic stem cells isolated from cord blood [297]. Cord blood contains a higher percentage of reticulocytes (4–5%) than peripheral blood and has been used, even without a concentration step, for short-term *P. vivax* cultures [392]. Reticulocyte concentration can be increased up to approximately 60% by centrifugation on a 60-70% isotonic Percoll [329, 367]. Using these purified reticulocytes the parasite can now be kept alive long enough to allow invasion assays and thus assess antibody inhibition of merozoites [154, 329].

Table 5.1: Summary of the published *ex vivo* invasion assays adapted from [281]. The assay highlighted in pink is the one used in the assays described below.

Year	Source of Pv	Pv concentration	Retic concentration	Culture medium	Max parasitaemia	Refs
1987	Belem strain from *Saimiri* monkey	54% Percoll	65% Percoll	Not provided	Not provided	[276]
1988	Palo Alto strain from *Aotus nancymai*	58% nicodenz	Monkey blood/induced anemia	RPM1 1640 with HEPES $NaHCO_3$, neomycin + 20% serum	11.9%	[260]
1989	Belem strain from *Saimiri* monkey	54% Percoll	65% Percoll	RPMI 1640 with HEPES, hypoxanthine, D-glucose + 15% serum	15.0%	[26]
2007	Infected patients	No concentration	No concentration	McCoy's 5A medium with HEPES, $NaHCO_3$, L-glutamine, gentamicin + 25% serum	0.1%	[154]
2011	**Infected patients**	**45% Percoll**	**60% Percoll + CD71 selection**	**McCoy's 5A medium with L-glutamine, gentamicin, glucose + 20% serum**	**22.3%**	**[329]**
2012	Infected patients (cryopreserved isolates)	45% Percoll	HSC-derived reticulocytes	McCoy's 5A medium with L-glutamine, glucose + 20% serum	2.5%	[282]

A major limitation, which has restricted these *ex vivo* assays to laboratories in endemic areas, has been the need for freshly isolated *P. vivax* from humans (or NHPs). It has recently been reported, however, that cryopreserved Pv parasites and reticulocytes perform equally well in these assays [44]. The successful use of cryopreserved parasites and reticulocytes in these assays means that in future such experiments will no longer be limited to endemic areas with access to fresh samples.

To test my panel of human mAbs, I collaborated with the Russel/Renia group who had established the assays in Mae Sot, Thailand.

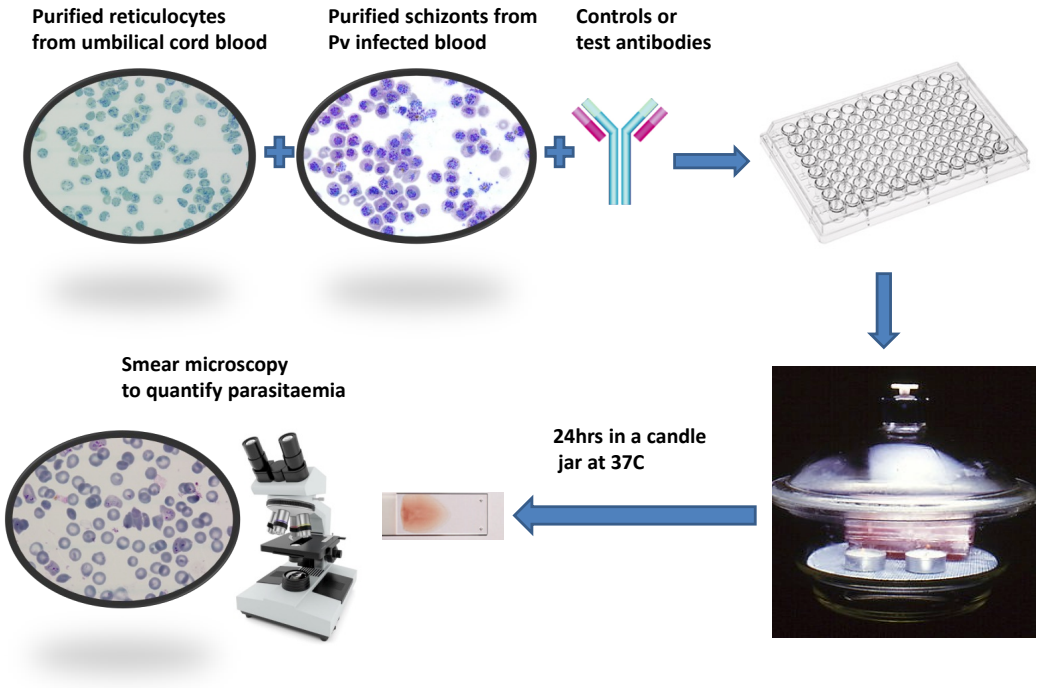


Figure 5.1: Schematic of the Pv *ex vivo* invasion assays carried out in Mae Sot, Thailand.

5.3 The human anti-PvDBPII mAbs in the *ex vivo* invasion assay

5.3.1 Reticulocyte purification

Fresh samples of umbilical cord blood were collected from consenting mothers in the labour wards run by the Shoklo Malaria Research Unit and rapidly transported to the lab for processing. The samples were first filtered to deplete leukocytes in order to minimise phagocytosis of merozoite or iRBCs during the assay [197]. In the past, repeated powdered cellulose filtration was necessary to deplete leukocytes, however the introduction of non-woven fabric filter now allows for faster processing of blood [373].

The reticulocyte purification process, as detailed in Chapter II, essentially involved two steps; firstly a density gradient centrifugation to obtain an enriched fraction and secondly, labelling with anti-CD71 coated microbeads and magnetic cell sorting, to further purify. The results were impressive; light microscopy of smears of the purified cells stained with new methylene blue revealed over 90% reticulocytes (Figure 5.2).

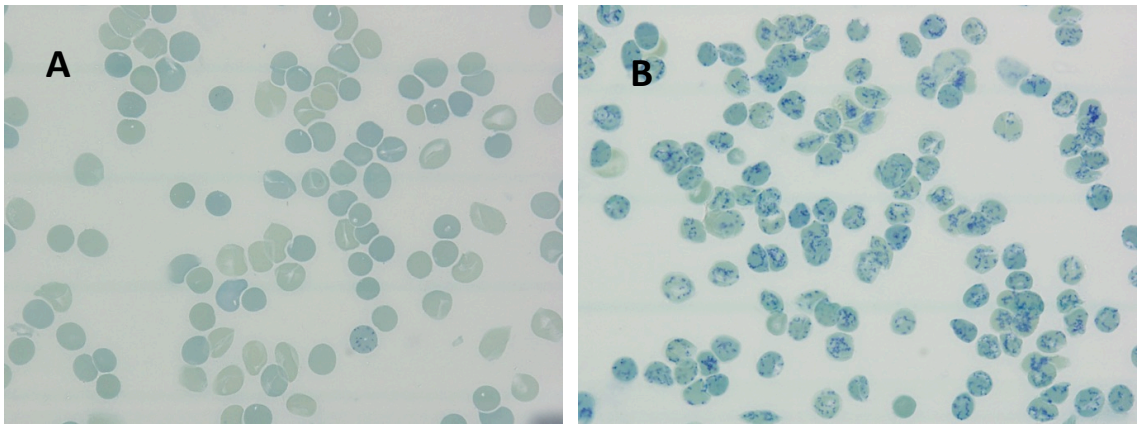


Figure 5.2: Purification of reticulocytes from umbilical cord blood. Thin smears stained with methylene blue (A) pre-purification and (B) post-purification.

5.3.2 Schizont purification

The fresh *P. vivax* blood samples received from the clinics were mostly at low parasitemia (mean 0.4%) and most often contained predominantly late ring-stage parasites. This is presumably because patients tend to present in clinic soon after a bout of fever. During periods when no fresh *P. vivax* samples arrived, cryopreserved samples were used. *P. vivax* isolates with >80% early ring stage had been previously frozen down in Glycerolyte 57 (Baxter, Belgium). Glycerolyte 57 was originally used to preserve RBCs [241, 340, 379], and is now widely used in the cryopreservation of *Plasmodium* spp. [85, 118, 240, 327]. The thawing method used was a stepwise NaCl method which has been successfully used in previous *P. vivax* studies [210, 345].

As the assay requires the parasites to be synchronised at the schizont stage, a maturation step was needed to maximise the proportion of schizonts prior to purifying out these haemozoin-rich late stages (Figure 5.3) using magnetic-activated cell sorting (MACS).

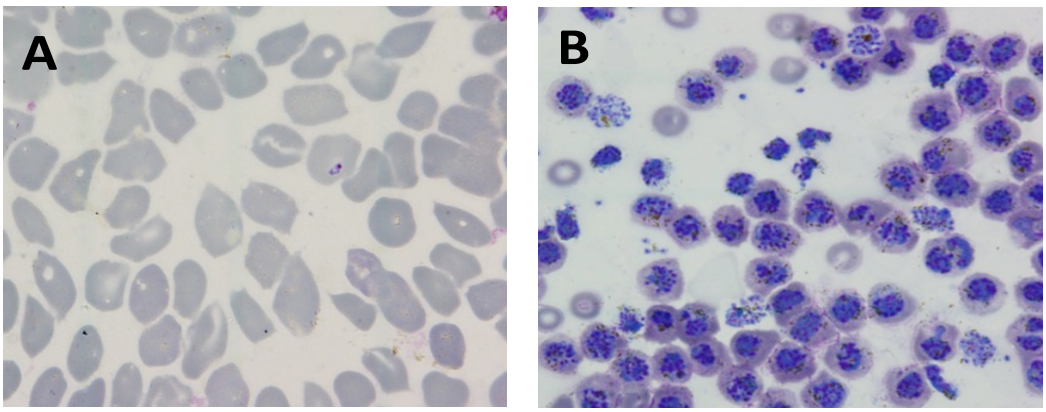


Figure 5.3: Giemsa-stained thin smears showing (A) the very low ring-stage parasitemia of the initial blood sample and (B) the almost pure schizont inoculum used in the assay.

A drawback was that after maturation and purification, the final amount of schizont was usually very small; in the range of 4-8μL from an initial 5mL whole blood sample. This greatly limited the number of test wells available for each isolate and meant that I was unable to test the mAbs in dilution series as I had

done with the transgenic Pk GIA assays. The simplest way to increase the yield of schizont available would have been to take larger volumes of blood, but his was not possible in the Thai assays. It will be, however, in the protocol just underway in Oxford, where 50mL of blood will be collected from returning travellers diagnosed with Pv; this will allow testing antibodies at various concentrations and in combination with each other.

5.3.3 Controls

As shown in Figure 5.4, an anti-Ebola glycoprotein human mAb at 1mg/mL used as a negative control, did not inhibit invasion; whereas the anti-DARC nanobody did so potently, with a median invasion inhibition of ∼80% when added at 25μg/mL.

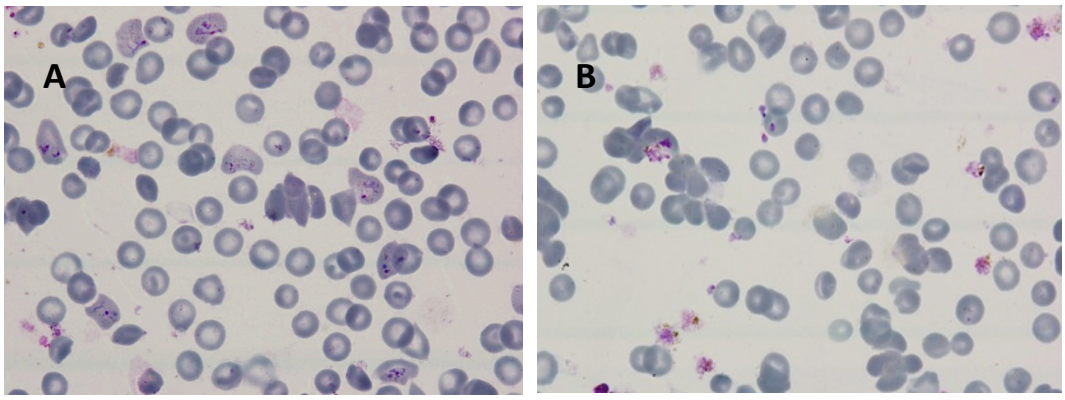


Figure 5.4: Smear microscopy showing Giemsa-stained thin smears taken at the end of the assay. (A) Negative control wells in which the parasites were free to invade the reticulocytes uninhibited or with the addition of a human anti-Ebola mAb, showing large numbers of ring stage parasites and (B) positive control wells in which the anti-DARC camelid nanodody, was added at a final concentration of 25μg/mL, showing free merozoites and schizont 'Ghost' cells, but no (or very scanty) invasion.

5.3.4 The anti-PvDBPII human mAbs

In total, I was able to run the *ex vivo* invasion assay with thirteen different Pv isolates. Because of the low yield of purified schizont from each 5mL blood sample, it was not possible to test each mAb against each isolate. Therefore those mAbs which showed signs of potency and strain-transcendence in early assays were prioritised for testing against these scarce wild type isolates. All of the mAbs were tested against

at least three Pv isolates and Figure 5.5 summarises the results of all thirteen *ex vivo* assays. As DB9 showed potent neutralisation in the initial assays, it was prioritised for testing against the majority of subsequent isolates.

As expected most of the mAbs exhibited different neutralisation activity against different isolates, but strikingly, one of the antibodies, DB9, consistently and potently inhibited invasion against multiple isolates. It gave a mean inhibition of 77% against ten isolates and this compared to 79% mean inhibition for the anti-DARC VHH positive control.

mAbs DB1 and DB10, which were the top performers in the Pk transgenic GIA assays, showed marked differences in their invasion inhibition between isolates. They potently inhibited invasion of Pv isolates seven and four, but failed to inhibit invasion by isolates five and eight.

mAbs DB2, DB4 and DB8 showed little potency against any of the isolates and mAbs DB3, DB5, DB6 and DB7 were intermediate, with inhibition ranging from ∼30-70%.

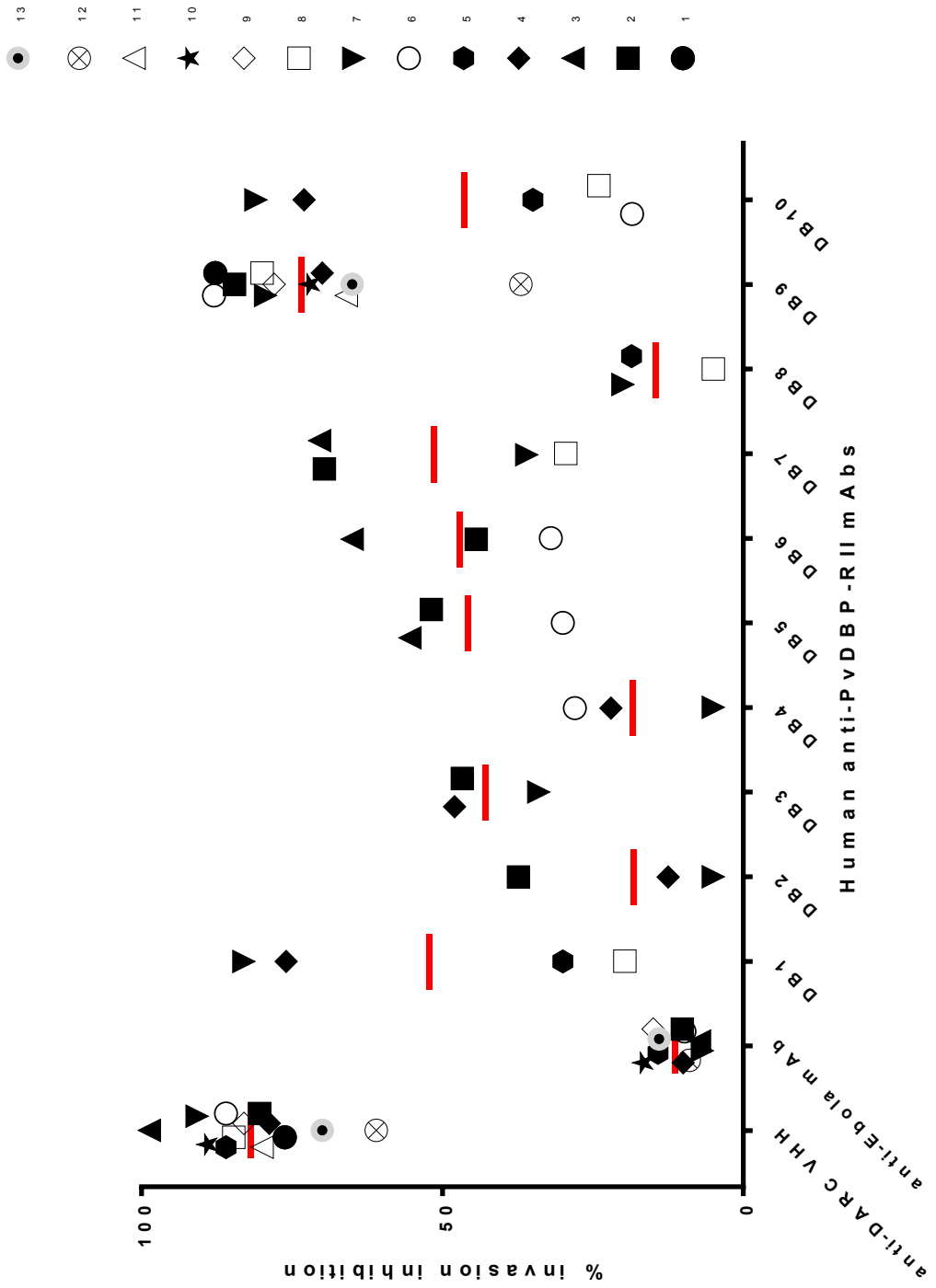


Figure 5.5: Pv *ex vivo* invasion assays performed with thirteen separate isolates of Pv-infected blood from local patients. Each data point represents the % inhibition of each antibody against one of the thirteen isolates. All antibodies were tested at a final concentration of 1mg/mL, except the positive control anti-DARC VHH which was assayed at 25μg/mL. The red bars represent the median % inhibition for each antibody.

5.4 Sequencing the strains

I was able to obtain sequence data of region II of the PvDBP gene from eight of the thirteen Thai isolates; this is shown below (Figure 5.6) with the reference vaccine strain (Sal1) for comparison.

The region where the samples were taken is on the porous border between Northern Thailand and Myanmar and the clinics are in or nearby to large refugee camps. Given the flux of peoples and their close confinement in forest camps, it is not surprising that there is a wide variety of strains circulating. Such a mixed and mobile human population, harbouring an equally diverse parasite population, is an ideal place to screen for strain-transcendent antibodies [81].

Two of the eight isolates had no amino acid polymorphisms within region II of their PVDBP gene and another two just a single change. The other four sequenced isolates, however, contained multiple polymorphic residues, ranging from four to ten, when compared to the vaccine homologous Sal 1 reference sequence. The DEK sequence, amino acids 339-341, in sub domain 2, is notoriously polymorphic and has been the focus of much attention as a possible 'decoy' epitope distracting the immune response from nearby conserved and critical regions [73, 332]. Three of the eight isolates sequenced had a complete switch of the 'DEK' epitope to 'GKN'.

DB9 was assayed against six of the eight sequenced isolates (all except isolates 3 and 5) and neutralised strains ranging from the Sal 1 vaccine homologous (isolates 4 and 7) to those with very highly polymorphic DBPII sequences (isolates 6 and 8). This was a very exciting result, suggesting that DB9's epitope was critical and conserved across multiple highly diverse wild-type strains.

These data indicated that the very potent GIA of DB1 and DB10 in the transgenic Pk assay, was specific to the Sal1 strain. DB1 and DB10 both showed high levels of invasion blocking against Thai Pv isolates 7 and 4 which have identical

DBPII amino acid sequences to Sal1, whereas they failed to block invasion by Thai isolates 5 and 8 which both had multiple polymorphic residues. Isolates 5 and 8 had the same substitutions at amino acids 372, 379 and 390 (NLW to KIR) in subdomain 2 of PvDBPII. This suggests that the epitopes of DB1 and DB10, which compete for binding sites (see Chapter III) are disrupted by mutation at these residues. Polymorphisms at positions 372 and 392 either singly or in combination have previously been shown to change PvDBP's antigenic character and sensitivity to inhibitory antibodies [397].

Figure 5.6: Amino acid polymorphisms of the PvDBPII gene segment of eight of the Thai Pv isolates. The Salvador I (SalI) reference sequence is shown in the bottom row. Amino acids that are the same as the reference sequence are indicated by a period, and a hyphen indicates an insertion/deletion. * Isolate 6 has a leucine insertion between V429 and P430 in the SalI reference sequence. Also shown are the mAbs tested against each sequenced isolated and their percentage invasion inhibition when added at 1mg/mL. Red shading represents $\geq 65\%$ inhibition, green shading represents $30 - 65\%$ inhibition, and blue shading represents $\leq 30\%$ inhibition. The positive control was the camelid anti-DARC nanobody (VHH) always assayed at 25μg/mL and the negative control was a recombinant human anti-Ebola mAb (EBL) at a concentration of 1mg/mL.

5.5 Combining the mAbs

Two of the major limitations of single mAb preparations, their low neutralising potency and potential failure to treat mutants or subtypes, could be overcome by combining several mAbs. Recent studies have shown that such mAb cocktails may exhibit synergistic neutralisation; i.e. the combination displays substantially elevated neutralising activity that exceeds the level of improvement expected by the independent contribution of each mAb in the mixture. The neutralising activity of such mAb cocktails can be similar to the potency of polyclonal Ab-based preparations [34, 117, 181]. Cooperativity between non-neutralising mAbs and neutralising mAbs has been described in HIV [178, 334], Ebola virus [181] and *Neisseria* meningitidis neutralisation [34, 231]. Immune interference in the form of antagonism between antibodies binding the same merozoite protein has been reported in the field of blood-stage malaria vaccines [158, 288]. Investigating the interplay between mAbs specific for the same pathogen protein also has major implications for vaccine engineering. When combining two or more mAbs, three outcomes can be expected:

- an additive effect, i.e., the summation of individual independent neutralising activities;
- antagonism, a reduction in efficacy;
- synergism, in which the protective properties of the combined mAb preparation significantly exceeds the independent and additive effect of the components in the mixture.

Attempts to estimate the combined effect of multiple drugs have been documented for more than a century [83]. A widely used proposal that describes how independent effects combine and serves as reference model to determine synergy or antagonism is Bliss independence or Bliss additivity. Bliss additivity is based on probabilistic arguments that the combined effect of two inhibitors on the survival is defined as the probability of being affected by at least one of the

inhibitors [87]. In the specific case of malaria parasite growth rates, Bliss additivity is equivalent to adding all single effects of the various inhibitors. Applying this to a combination of two mAbs added together to the same GIA assay, the equation used to calculate Bliss additivity was;

$$GIA_{[A+B]Bliss} = [1 - (1 - \frac{GIA_A}{100}) * (1 - \frac{GIA_B}{,}100)] * 100$$

where A is one mAb and B the other.

Having identified DB9 as a broadly neutralising mAb, I sought to assess whether its effects would be enhanced or diminished by combining it with the other nine mAbs in the panel. Antibodies are large 150kDa molecules interacting with a small parasite protein region (PvDBPII is approx. 40KDa), so intuitively, one would expect some degree of steric hindrance between the mAbs. This was seen in the BLI competition assay, described in Chapter 3, which showed that 50% of the mAbs including DB9 competed with each other for binding sites on recombinant PvDBPII.

While the yields of Pv schizont available for use in Thai *ex vivo* assays were insufficient to run synergy assays, on my return to the lab in Oxford I had the transgenic Pk model at my disposal. In the assays shown below, using the PvDBP^{OR}/$\Delta\gamma\beta$ line of transgenic Pk, DB9 was added at a fixed concentration of 25μg/mL in combination with a doubling dilution series, of each of the other nine mAbs (Figure 5.7).

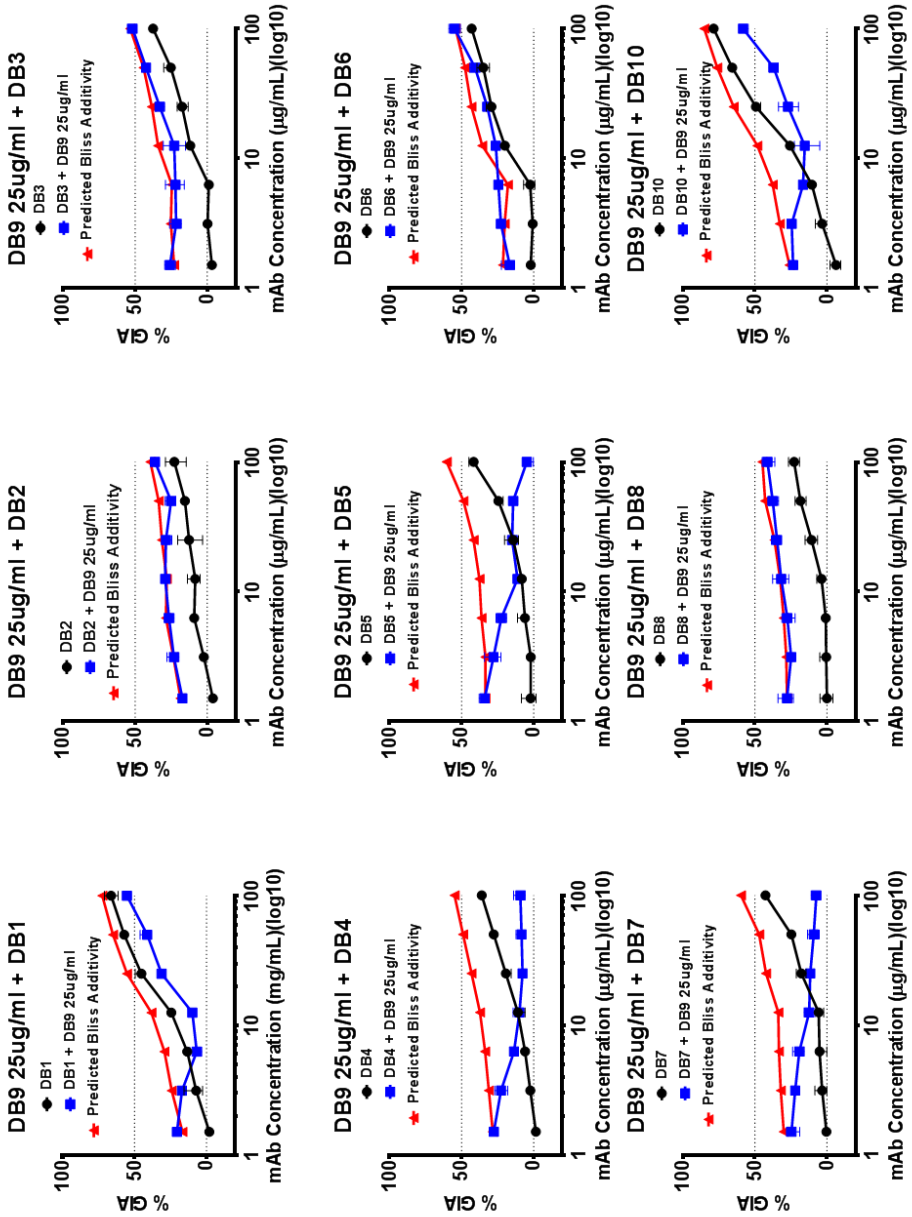


Figure 5.7: Synergy GIA assays with the PvDBP^{OR}/$\Delta\gamma\beta$ transgenic Pk line. Each graph shows DB9 in combination with one of the other 9 mAbs. DB9 was added at a fixed concentration of 25µg/mL to all wells while the other mAbs were run in a doubling dilution concentration series starting at 100μg/mL. The black line shows the % inhibition of the mAb alone, the red line shows the predicted inhibition (Bliss additivity as calculated in the equation above) of the mAb plus DB9 at 25μg/mL. The blue line shows the actual % inhibition of the combined mAbs. Data points and error bars represent the mean and standard deviation of triplicate wells.

There was no synergy detected between DB9 and any of the other mAbs, but interestingly there was antagonism between DB9 and five of the others. These were the five mAbs (DB1, DB4, DB5, DB7 and DB10) which, according to the BLI competition assay reported in Chapter III, did not compete with DB9 for binding.

In the case of DB1 and DB10, there is initial antagonism, but as their concentration increases above that of DB9 (which was fixed at 25μg/mL) the level of inhibition recovers. In the case of DB4, DB5 and DB7, however, the growth inhibition is completely reversed by combining them with DB9, at least within the concentration limits of the assay (100μg/mL).

The growth inhibition curves for the combinations of DB9 with the four mAbs that did compete with it in the BLI assay (DB2, DB3, DB6 and DB8) ran approximately along the predicted Bliss additivity line.

5.6 Discussion

Extreme polymorphism is common among malaria antigens [372] and PvDBPII is no exception; DBPII alleles have a very high ratio of nonsynonymous to synonymous mutation, consistent with high selection pressure driving allelic diversity as a means to evade the host immune response [91, 391, 428]. One study in Papua New Guinea found the substitution rate within region II of DBP to be ten-fold greater than within the DBP gene overall [391] and that over 90% of the polymorphisms were within the central segment of DBPII, between cysteines 4 and 7 [391]. Polymorphism at specific residues, such as at positions 372, 392 and 458 have been shown to change the antigenic character of PvDBPII and the parasite strain's sensitivity to inhibitory anti-PvDBPII antibodies [397].

Some polymorphic residues in DBPII appear to be unique to one population or region, whereas others including; K326E, D339G, E340K, K341N, N372K, L379I, W302R and I458K are commonly found throughout global isolates [13, 186, 195, 196].

Only a few individuals however have been found to produce anti-PvDBPII responses that broadly inhibit against multiple allelic variants [82, 201] and thus the polymorphic nature of PvDBPII is considered a major impediment to a widely protective PvDBPII vaccine.

I was delighted, therefore, to have found within this first and relatively small panel of human mAbs, a clone that blocked over 90% of the wild-type isolates tested. The sequencing of the PvDBPII gene region showed these Thai parasites to be highly polymorphic and between them they contained variation in most of the known polymorphic regions.

The fact that DB1 and DB10 blocked invasion of the Sal 1 homologous Thai Pv strains, in concordance with their blocking of the Sal 1 Pk transgenic line, was further validation of the Pk transgenic model. The applicability of the Pk model will, however, need further testing by the insertion of other allelic versions of PvDBP. This is planned for the near future.

It would have been preferable to have had access to larger volumes of blood, as this would have enabled all the mAbs to be tested against all the Pv isolates. This would have allowed more direct comparison, as well as allowing the antibodies to be run in dilution series (as per the Pk GIA assay) and in combination, to test for synergy or antagonism. As it was, however, constrained by very the low yield, I was limited to testing each mAb at a fixed concentration. As already mentioned, this problem of low parasite yield for use in *ex vivo* invasion assays, should soon be overcome. A new clinical protocol has just launched in Oxford, whereby Pv infected blood will be collected from returning travellers; in this case 50mL, rather than 5mL, thereby providing much more parasite material per assay.

Whereas the GIA assay has been correlated with *in vivo* protection for *Plasmodium falciparum* [122, 164, 356], this *ex vivo* vivax assay has not and in my opinion

it is best suited as a screen for strain-transcendence rather than a quantitative test for antibody potency. I say this, because the context of the assay is, as it has to be, highly skewed in favour of the parasite. The purified schizont is added to an almost pure target cell population of reticulocytes. *In vivo* the merozoites can invade only about 2% of the RBCs they make contact with, whereas in the assay it is almost 100%. It could be argued that any invasion blocking by an antibody in this assay is highly significant, given the scale of the job asked of it. As is the case for the GIA assays, all the other mechanisms by which antibodies neutralise pathogens, antibody-dependent cellular cytotoxicity (ADCC), antibody-dependent cell phagocytosis (ADCP), and complement-dependent cytotoxicity (CDC), do not apply in this context.

The low yield of parasites did not allow for replicate test wells so there was always the possibility of spurious results or contamination (though contamination by bacteria or yeast would be detected on smear microscopy – and it was on one occasion, leading to abandonment of the assay). The fact remains however, that DB9 was tested repeatedly against many wild-type parasites and inhibited invasion in all of them. The other 9 mAbs whose invasion inhibition was low, medium or variable between strains, themselves acted as controls for the strain-transcendent effects of DB9. *A priori*, given the enormous inter-strain variation in PvDBPII sequences, I would have expected all the mAbs to have shown the variable inhibition demonstrated by DB1 and DB10.

The apparent antagonism between DB9 and five of the other mAbs in the panel (Figure 5.7), suggested by the GIA assays with the Pk PvDBP$^{OR}/\Delta\gamma\beta$ line, was interesting. As mentioned above, the mAbs whose growth inhibitory effect was diminished when combined with DB9, were those which, according to the competition assay, do not compete for binding sites with DB9. The antagonism between DB9 and DB1 and DB10 which both potently inhibit Pk PvDBP$^{OR}/\Delta\gamma\beta$, was dose-dependent, but that between DB9 and DB4, DB5 and DB7 was absolute;

with the combined inhibitory effect reducing to almost zero despite the increasing dose of antibody.

Without knowing the epitopes of all the mAbs and how their binding affects the structure of PvDBPII, explaining this antagonism is speculative. Steric hindrance is always a likely candidate, but it is also possible that conformational changes occur when one mAb is bound which then compromises the epitope of the other. While the explanation is not known, such antagonism would be of great importance when considering how to redesign PvDBPII as a vaccine antigen. Clearly it would not be desirable to induce mAbs that antagonise each other's inhibitory effects. The good news, however, is that based on the data from the BLI assay (Figure 3.11), the binding site of DB9 is distinct from those of the five mAbs it appears to antagonise, which might, in theory, allow scope to excise their antagonistic epitopes.

In Chapter VI I present the X-ray crystal structure of DB9 bound to PvDBPII and define its epitope.

6

A broadly-neutralising epitope on PvDBPII

6.1 Authorship statement

The X-ray crystallography work and production of the subdomain-3 proteins was performed by Natalie Barber and Matt Higgins.

6.2 Introduction

6.2.1 Epitope mapping

Mapping the epitope of DB9, the first broadly-neutralising human mAb against Pv, was now the top priority. If the PvDBPII vaccine was to be re-designed to induce DB9-like antibodies we needed to know precisely where it bound.

An epitope can be defined as the collection of atoms that directly contact or bind an antibody. Electrostatic attractions, water-mediated hydrogen-bond networks, and long-range forces such as ionic and hydrophobic interactions contribute to the overall binding affinity between an antigen and an antibody [21, 342, 396]. Epitope mapping is the determination of which residues directly contact the antibody and

such a detailed understanding of the epitope is required for antibody engineering and vaccine design [222].

Many techniques are now available for epitope mapping, including; peptide display technologies [132], NMR spectroscopy [25], mass spectrometry [292], and X-ray crystallography. While each method has its own pros and cons, the specific nature of the epitope recognised by the antibody must be considered. Antibody epitopes fall into two possible categories; linear epitopes, which are short peptides of continuous amino acid sequence; and conformational epitopes, which are discontinuous in sequence and are formed from the 3D fold of the protein or peptide segment. The vast majority of B cell epitopes ($> 90\%$) are thought to be conformational epitopes, and therefore can only properly be characterised by structural approaches [405]. X-ray crystallography is considered the gold standard of epitope mapping as it provides an unequivocal, atomic resolution picture of the antibody-antigen interaction and it is especially valuable when the antibody epitope is a complex 3D conformational epitope.

Because antibodies are large, glycosylated, multi-domain proteins they are not readily amenable to structure determination by X-ray crystallography, so typically, antibody fragments such as the Fab fragment or single chain antibodies (ScFv) are used for X-ray structure determination. X-ray crystallography cannot, however, be considered a universal solution to epitope mapping. There are many potential limiting factors; the generation of crystals often requires large amounts of sample material; the lack of certainty that any protein, or antigen-antibody complex, will produce high-quality crystals; and the unpredictable timelines for the crystallisation and structure determination processes which can stretch from days to months to never.

6.2.2 Epitope-focused vaccine design

Pathogens that rapidly change their antigenic profiles include RNA viruses such as HIV, influenza and hepatitis C; bacteria such as *Streptococcus pneumoniae*; and

protozoa such as *Plasmodium* and *Trypanosoma* spp. The antigenic diversity of such pathogens pose major challenges for vaccine design [58]. The discovery of broadly neutralising antibodies (bNAbs) that neutralise diverse strains of HIV, influenza, or HCV gave rise to a strategy in which bNAbs are employed to guide design of immunogens in the hope of inducing responses similar in structural recognition, breadth and potency [56]. This strategy has been variously termed 'reverse vaccine engineering' or 'antibody-guided' or 'epitope-focused' vaccine design.

One general approach to focus responses on protective epitopes is to generate stable sub-domains of larger pathogen proteins that contain the epitopes of interest but lack other non-protective or potentially undesirable epitopes. This type of 'antigen minimisation' work is best done with a detailed knowledge of the relevant protein structure to guide selection of stable domains or to design stabilising features that compensate for domain isolation. This approach has been widely used in immunogen design for lyme disease [209], influenza [43, 369], HIV [194, 305, 430], ricin [98], and chlamydia [365]. The immune-dominance of antigenic sites that do not confer broad and potent neutralisation over those that can be targeted by potent bNAbs is a poorly understood phenomenon, but it is well established that non-neutralising antibodies can facilitate virus entry into host cells between different serotypes of certain pathogens (e.g. dengue virus), thereby causing antibody-dependent disease enhancement (ADE) [114].

A key challenge for next-generation vaccines, then, is to place neutralising epitopes in the immune system's spotlight for efficient recognition and enhanced epitope-specific antibody elicitation. Such vaccines are sometimes referred to as 'precision vaccines' given their extremely well-defined epitope-directed antibody response. An essential pre-requisite for precision vaccines is to encode the structural information of epitopes targeted by broad and potently neutralising antibodies in the designed immunogens.

There are various structure-based immunogen design approaches that aim to elicit focused antibody responses (Figure 6.1). Four of the major techniques used, with examples cited, are listed below.

1. **Silencing non-neutralising epitopes** by excising antigen domains mainly targeted by non-neutralising antibodies [189] or reducing the accessibility of non-neutralising epitopes through glycan masking [324, 332];

2. **Conformational stabilisation**; which aims to stabilise the antigen in its pre-fusion state by introducing disulphide bonds and cavity-filling hydrophobic mutations [246];

3. **Germline targeting**; which aims to engage the un-mutated precursors of the bNAbs, and drive their maturation towards a bNAb [53];

4. **Epitope scaffolding**; the design of heterologous proteins that mimic the structure of the epitope and are structurally compatible with the antibody binding mode [157].

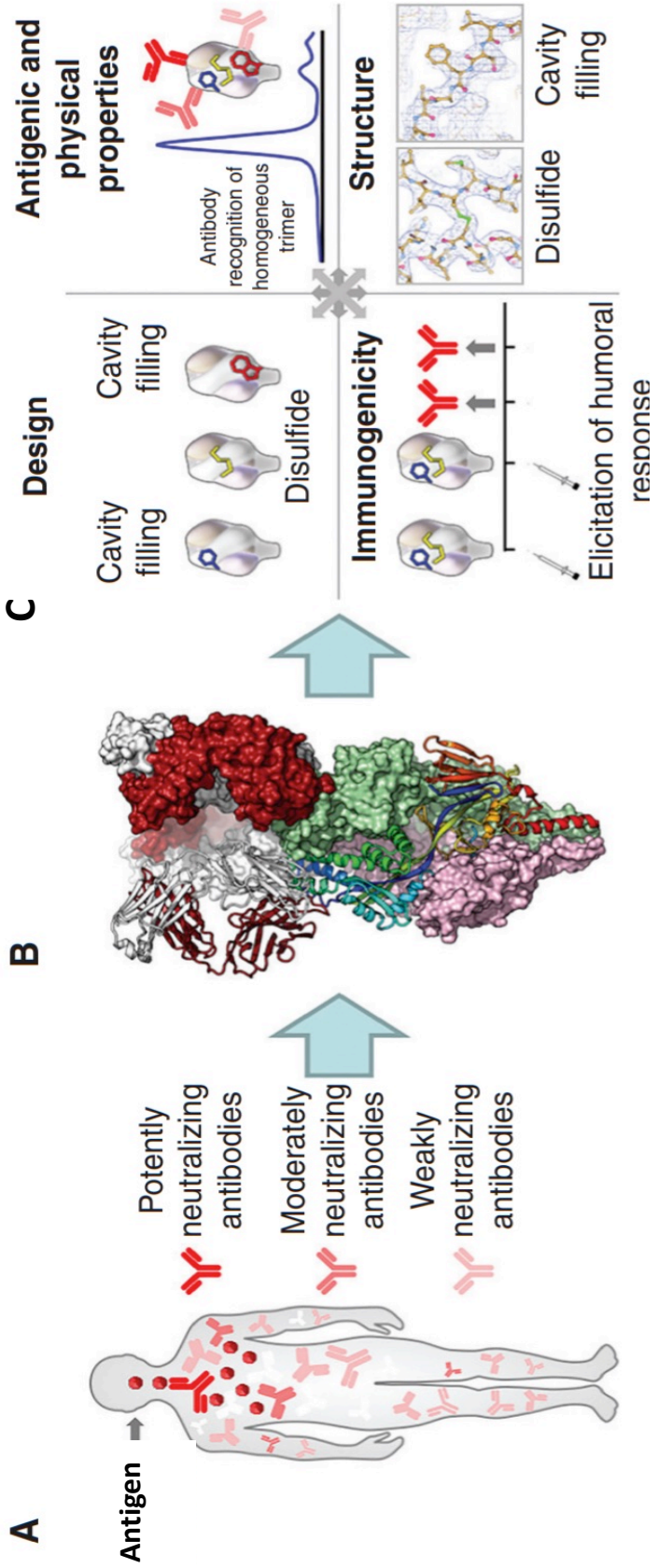


Figure 6.1: Schematic giving an overview of epitope-focused vaccine design and antigen engineering, adapted from [222].

The structure of the Duffy binding proteins of both Pk and Pv, have been solved [30, 357], and so, before presenting our crystal structure, the first of PvDBPII bound to a human bNAb, it is worth reviewing what is known, or thought to be known, about the protein and the prevailing ideas about where neutralising epitopes lie.

PvDBPII is an elongated boomerang shaped molecule, composed primarily of α helices, with an antiparallel β hairpin near the N-terminus. It is similar in sequence and structure to the DBL domains of region II of PfEBA-175 and PkDBPα [30]. The PvDBPII DBL domain is composed of three subdomains that are stabilised by intra-subdomain disulfide bridges. Subdomain 1 (SD1) is composed of residues Asn211–Leu253 and has two intra-subdomain disulfides, Cys217–Cys246 and Cys230–Cys237. Subdomain 2 (SD2) is composed of residues Tyr271–Glu386 and has one intra-subdomain disulfide, Cys300–Cys377. Subdomain 3 (SD3) is composed of residues Pro387–Ser508 and has three intra-subdomain disulfides, Cys415–Cys432, Cys427–Cys507, and Cys436–Cys505 [30]. There are the fourteen common polymorphic amino acid residues within PvDBPII [94], twelve of which are expressed on the surface of the molecule. The majority are in SD2, with none in SD1 and only three in SD3, the largest sub-domain of the protein.
When the structure of PvDBPII was published in 2011 [30], the authors proposed the formation of a hetero-tetrameric structure (panel E, Figure 6.2 on the next page) involving two PvDBPII and two N-terminal DARC moieties [30]. Their model suggested that the engagement of DARC by one PvDBPII protein was essential for PvDBPII dimerization and the subsequent binding of the second N-terminal DARC ligand (Figure 6.2 panel E). Neutralising epitopes were said to map to the PvDBPII dimer interface and their putative DARC binding sites (Panels B, C and D Figure 6.2). The neutralising epitopes shown in red and brown in panel D refer to the binding of polyclonal antibodies whose epitopes were inferred by linear peptide array and mapped onto the structure of Plasmodium knowlesi DBPα [82].

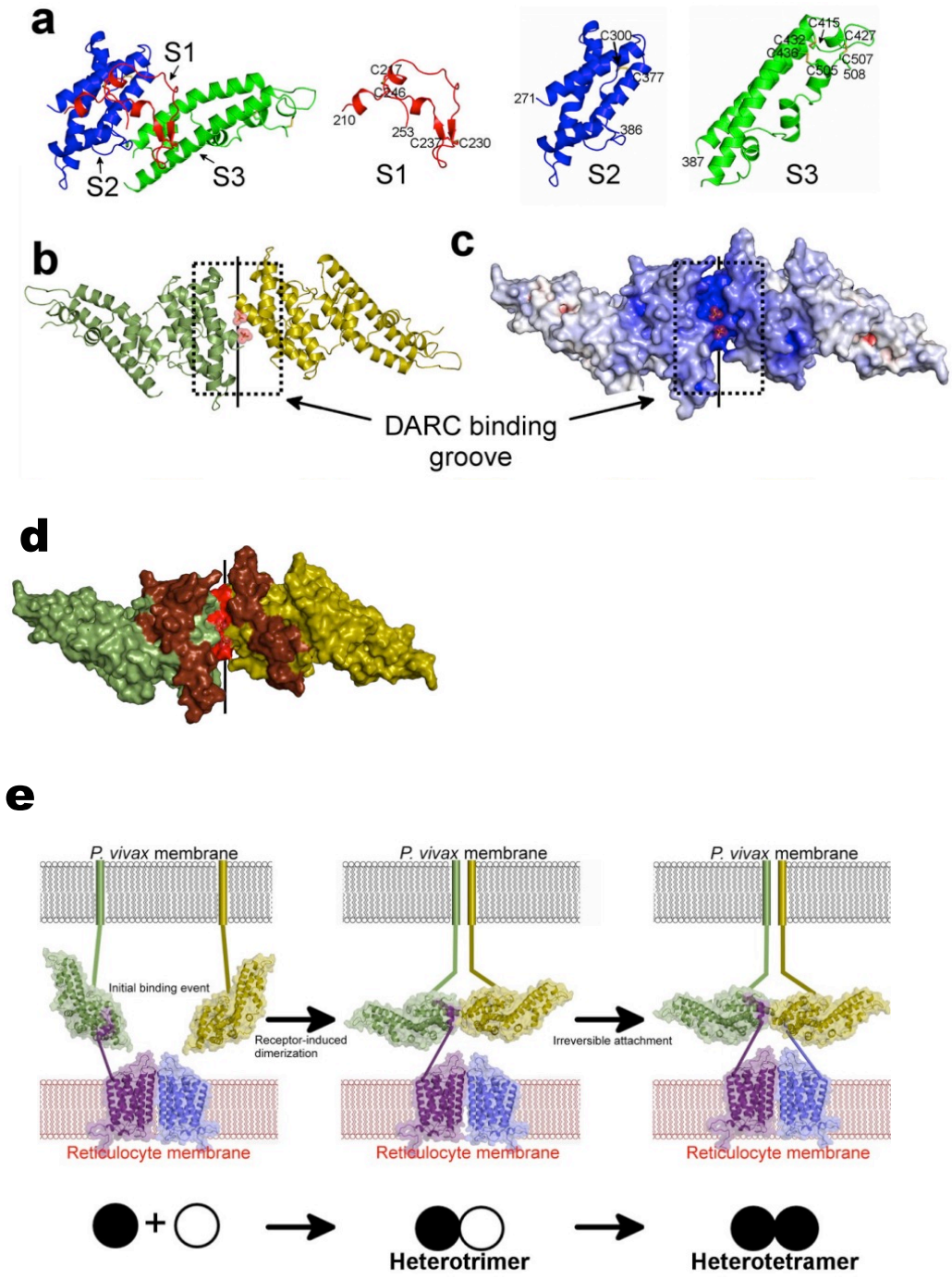


Figure 6.2: Crystal structure of PvDBPII dimer solved in 2011, figure is adapted from [30] and shows (A) the 3 subdomains of PvDBPII, S1 (red), S2 (blue) and S3 (green); (B) The PvDBPII dimer in ribbon representation; (C) electrostatic of the dimer to illustrate the positive charge in the putative DARC binding groove; (D) Epitopes recognised by blocking-antibodies [82] (red – most significant, brown – significant) map to the functional regions of PvDBPII which include the dimer interface and DARC binding groove, and (E) proposed heterotetrameric model for PvDBP-DARC interaction [29].

The 'neutralisation' referred to is based on recombinant protein binding-inhibition assays rather than invasion of inhibition. This published structure of PvDBPII-DARC [30] was not, however, based on the co-crystallization of PvDBPII and DARC proteins. Ammoniun phosphate or sodium selenate were used as the nidus for dimerisation, without the presence of DARC. Phosphate and selenate are structurally similar to sulphate and the purpose of using selenate was structure determination by anomalous dispersion. A previous study, using a protein construct comprising the N-terminal 60 aa of Fy linked to human IgG heavy chain, indicated that sulphation of Tyrosine 41 in the N-terminal portion of DARC was critical for binding to PvDBPII [80]. It is uncertain whether this chimeric construct fully represents native DARC on erythrocytes.

A few years later, in 2016, the same research group reported the location of broadly neutralising epitopes to be on SD3 rather than SD2 [72]. These were, however, the epitopes of murine mAbs, not human mAbs and the 'neutralisation' reported was PvDBPII-DARC binding-inhibition rather than functional invasion blocking. The 'broadly' part of the 'broadly neutralising' title was based on the lack of polymorphisms on sequence alignment of the epitopes of the mouse mAbs, rather than any functional assays to demonstrate strain transcendence.

As appealingly symmetrical as this hetero-tetrameric model shown above is, it is almost certainly incomplete and an over-simplification as will be discussed later. To my knowledge, the structure presented below (Figure 6.3), is the first to show a broadly-neutralizing human antibody bound to PvDBPII.

6.3 The crystal structure of DB9 bound to PvDBPII

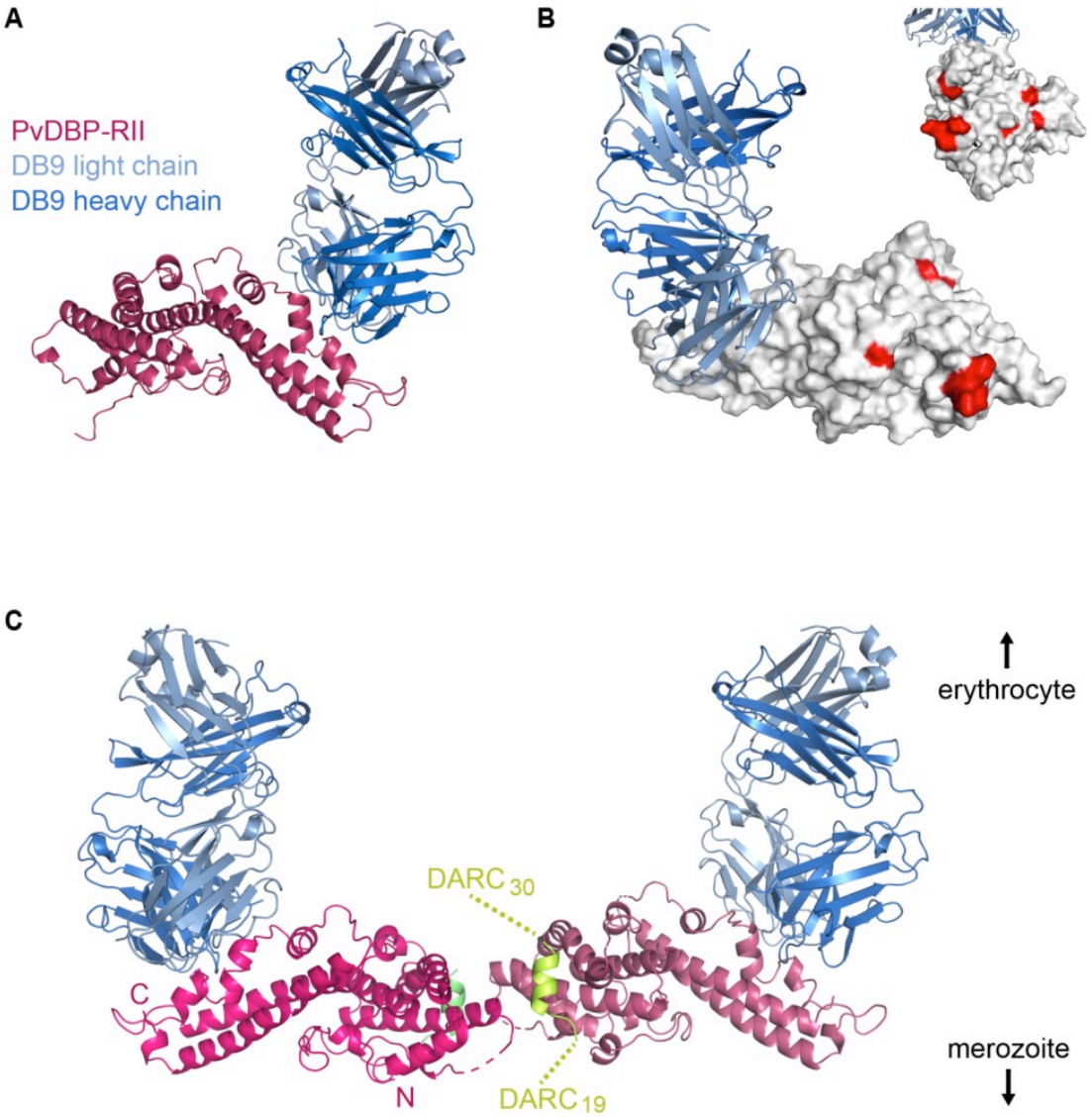


Figure 6.3: Crystal structure of the PvDBPII/DB9Fab complex. (A) Overall structure of the PvDBPII/DB9 Fab complex shown in ribbon representation. The PvDBPII domain is coloured in purple. The DB9 Fab heavy chain (VH) is in dark blue, and the light chain (VL) is in pale blue. (B) Two views of the complex with ribbon representation of the DB9 Fab showing it binding to subdomain 3 of PvDBPII shown in surface representation. The areas shaded red on the surface of PvDBPII are areas known to be highly polymorphic [304]. (C) Illustrates the orientation of DB9 relative to the DBPII dimer and the erythrocyte and merozoite surfaces. This is based on the orientation of the DARC 19-30 peptide in the model, shown in green.

Fab Chain	Residue	Group	PvDBP-RII residue	Group	Interaction
Light Chain	W51	Side Chain	R497	Side Chain	Cation-pi
Light Chain	Y68	Side Chain	E487	Side Chain	Hydrogen bond
Light Chain	Y68	Side Chain	V488	Side Chain	Hydrophobic
Light Chain	L74	Side Chain	V488	Side Chain	Hydrophobic
Light Chain	S75	Side Chain	D476	Side Chain	Hydrogen bond
Light Chain	S75	Main Chain	E487	Side Chain	Hydrogen bond
Heavy Chain	E20	Main Chain	E484	Side Chain	Hydrogen bond
Heavy Chain	G45	Main Chain	E484	Side Chain	Hydrogen bond
Heavy Chain	S51	Main Chain	A500	Main Chain	Hydrogen bond
Heavy Chain	T52	Main Chain	G499	Main Chain	Hydrogen bond
Heavy Chain	T52	Side Chain	E493	Side Chain	Hydrogen bond
Heavy Chain	Y54	Side Chain	E503	Side Chain	Hydrogen bond
Heavy Chain	Y74	Side Chain	K412	Side Chain	Hydrogen bond
Heavy Chain	Y79	Side Chain	E503	Side Chain	Hydrogen bond
Heavy Chain	R118	Side Chain	N486	Side Chain	Hydrogen bond
Heavy Chain	T121	Main Chain	N492	Side Chain	Hydrogen bond
Heavy Chain	T121	Side Chain	R497	Main Chain	Hydrogen bond
Heavy Chain	T121	Main Chain	R497	Side Chain	Hydrogen bond

Table 6.1: Contact residues between the DB9 Fab and PvDBPII

PvDBPII:DB9	
Data collection	
Space group	$P6_222$
Cell dimensions	
a, b, c (Å)	173.58, 173.58, 169.88
$\alpha, \beta, \gamma(^\circ)$	90.0, 90.0, 120.0
Wavelength	0.97625
Resolution (Å)	84.94 – 3.04 (3.09 – 3.04)
Total Observations	58086 (2896)
Total Unique	29628 (1442)
R_{pim} (%)	4.0 (46.9)
$CC_{1/2}$	0.999 (0.670)
$I/\sigma(I)$	12.8 (1.2)
Completeness (%)	100.0 (100.0)
Multiplicity	19.6 (20.1)
Refinement	
Number of reflections	30703
R_{work} / R_{free}	17.7 / 22.0
Number of residues	
Protein	648
R.m.s deviations	
Bond lengths (Å)	0.01
Bond angles (°)	1.24
Ramachandran plot	
Favored (%)	95.0%
Allowed (%)	5.0%
Disallowed (%)	0.0%

Table 6.2: Data collection and refinement statistics for DB9 Fab/PvDBPII complex. All structures were determined from one crystal. Values in parentheses are for highest-resolution shell

As shown in Figure 6.3 and Tables 6.1 and 6.2, the crystal structure of DB9 Fab in complex with PvDBPII was solved to a resolution of 3.0 Å. At this resolution, the mAb epitope can be clearly identified; mAb DB9 binds to a conformational epitope composed of amino acids K412 and D476 to E503 at the end of a three-helix bundle within sub-domain 3 (SD3).

Contacts are made with amino acids in all the three CDR loops of the DB9 heavy chain and CDR1 and CDR2 of the light chain (Figure 6.4).

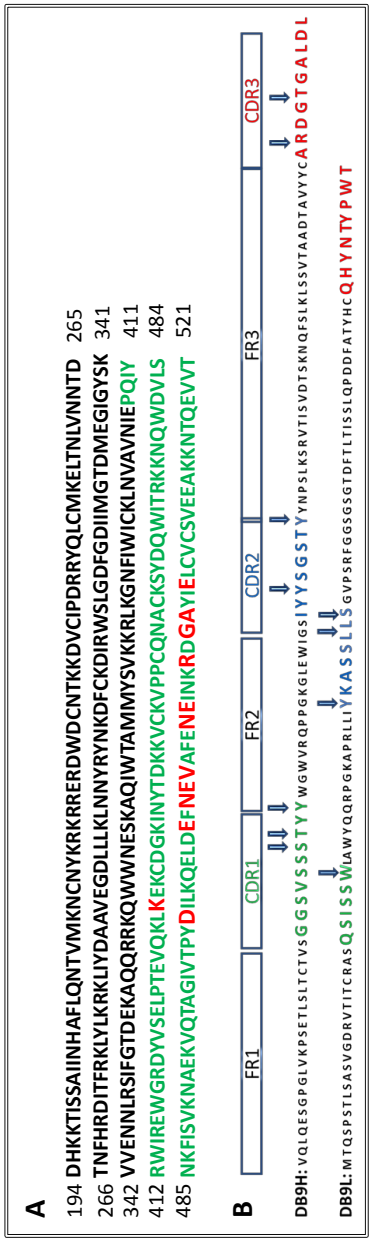


Figure 6.4: (A) Amino acid sequence of PvDBPII Sal 1 strain, amino acids 194 - 521 as used in the vaccine trial. Subdomain 3 is highlighted in green and the amino acids making contact with DB9 are shown in large red letters. (B) Amino acid sequence of DB9 heavy (DB9H) and light (DB9L) chain variable regions. The three framework regions (FR1 – FR3) are shown in black text with CDR1 in green, CDR2 in blue and CDR3 in red. The blue arrows indicated the amino acids that make contact with PvDBPII. These contact residues are located in all three CDR regions in the DB9H and CDR1 and 2 in DB9L.

The full amino acid sequence of PvDBPII Sal 1 strain, as used in the vaccine trial from which these mAbs derived, is shown in Figure 6.4 with SD3 highlighted in green and the amino acids contacted by the DB9 Fab shown in large red letters.

Binding of DB9 does not change the structure of DBPII, with an RMSD of 0.523Å between bound and unbound PvDBPII. Thus, the inhibitory effects of DB9 are not due to disruption of the DBL fold, but rather to the epitope location and disruption of protein function.

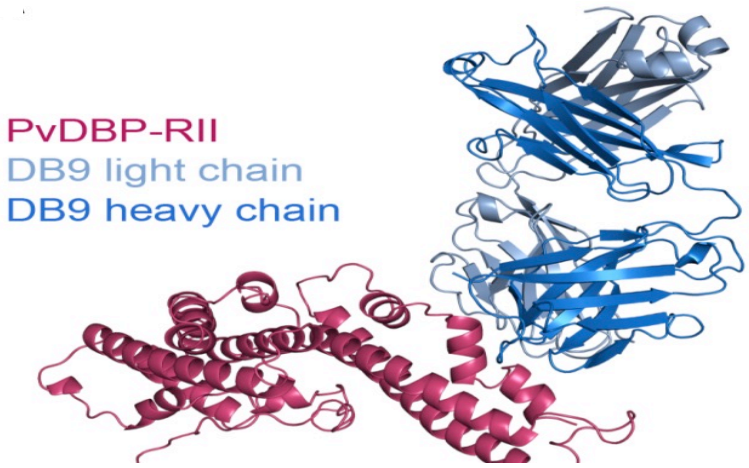
6.4 Subdomain three

The twelve conserved cysteine residues within PvDBPII form intra-domain disulphide bridges and can be used to subdivide the protein into three sub-domains. Subdomain 3 is the largest of the three and includes cysteines 7 to 12.

As already stated, PvDBPII is known to be highly polymorphic; the largest alignment of globally disparate sequences of PvDBPII looked at 511 sequences and found over 120 polymorphic sites with nucleotide diversity varying between 0.006 and 0.0109, resulting in 193 haplotypes [279].

To assess the sequence preservation of the epitope of DB9, I retrieved amino acid sequences spanning the epitope, from K412 to E503, for 284 globally diverse strains from Genbank and aligned them using Clustal Omega (Figure 6.5). As can be seen, even among this large panel from many different countries, there are no documented substitutions at any of the twelve PvDBPII residues that contact DB9. Complete preservation of contact residues does not necessarily correlate with complete preservation of a conformational epitope, but this sequence preservation when combined with DB9's potent inhibition of multiple diverse strains in the functional assays does suggest a highly conserved and critical epitope.

A



B

DHKKTISSAIINHAFLQNTVMKNCNYKRKRRERDWDCNTKKDVCIPDRRYQL
CMKELTNLVNNTDTNFHRDITFRKLYLKRKLIYDAAVEGDLLLKLNNYRYNKDF
CKDIRWSLGDFGDIIMGTDMEGIGYSKVVENNLRSIFGTDEKAQQRRKQWW
NESKAQIWTAMMYSVKKRLKGNFIWICKLNVAVNIEPQIYRWIREWGRDYVS
ELPTEVQKLKEKCDGKINYTDKKVCKVPPCQNACKSYDQWITRKKNQWDVL
SNKFISVKNAEKVQTAGIVTPYDILKQELDEFNEVAFENEINKRDGAYIELCVC
SVEEAKKNTQEVVT

C

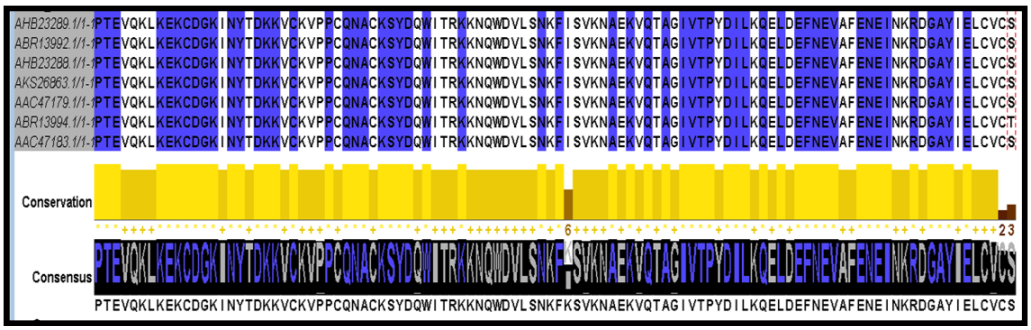


Figure 6.5: The epitope of DB9. Panel (A) shows in ribbon representation the binding of the DB9 Fab near the C-terminal end of SD3. Panel (B) shows the full amino acid sequence of PvDBPII Sal I strain. SD3 is highlighted in green and the epitope of DB9 is within the red rectangle. The letters in red are the residues that make contact with DB9. The black rectangles with pink shading show the epitopes of two inhibitory mouse mAbs mapped in a previous study [30]. Panel C shows an excerpt of the output from the multiple sequence alignment of 284 sequences of the region of PvDBPII spanned by the DB9 epitope. These sequences were retrieved from GenBank, aligned using Clustal Omega and visualised with JalView. The colour coding was set so that those amino acid sequences in blue were 100% conserved among the 284 sequences aligned. In the consensus histogram at the bottom of panel C, amino acid residues that are 100% conserved are shown in blue and those with any polymorphisms are in white.

Antigen engineering can, due to the complex internal architecture of proteins, be very fiddly; but serendipitously, DB9 bound SD3 and it proved relatively straightforward to express SD3 as a stand-alone protein. As discussed earlier, there are many different ways to engineer antigens in order to maximise epitope-specific responses and optimise immunogenicity. But I decided to start simply with just the basic SD3 subdomain itself, and one minor variant of SD3.

There was no guarantee, of course, that immunising with the whole of SD3 would induce a high proportion of DB9-like super-clones, but, in full expectation that iterations would be needed, it seemed a sensible first approach. The minor variant of SD3, named 'Interface' (SD3-int) was the SD3 sequence with 5 amino acids that would normally be buried in the interface with SD2, mutated to ensure solubility and correct folding, as detailed in Chapter II.

E. coli were transfected with plasmids containing the genes for full-length PvDBPII, SD3 and SD3-Int. They all expressed in sufficient yield and after purification and tag removal were sent for a rabbit immunisation (GenScript) with the plan to test and compare the anti-sera against the three different proteins in the transgenic Pk GIA assay. Whilst awaiting the rabbit anti-sera, I used the small amount of spare SD3 protein to conduct an ELISA binding assay to see which of the 10 human anti-PvDBPII mAbs bound SD3 (Figure 6.6).

This SD3-binding ELISA showed clearly that 6 of the 10 mAbs bound SD3. With the exception of DB4, the mAbs binding SD3 were the same cluster that competed for binding on PvDBPII in the BLI competition assay described in Chapter III.

It was now clear that these six mAbs were all competing for epitopes on SD3. This was intriguing in the context of the Pk GIA synergy experiments described in Chapter IV. In those assays, the combinations of DB9 with the other mAbs that bind SD3 (DB2, DB3, DB6 and DB8) were additive in their inhibition, whereas the

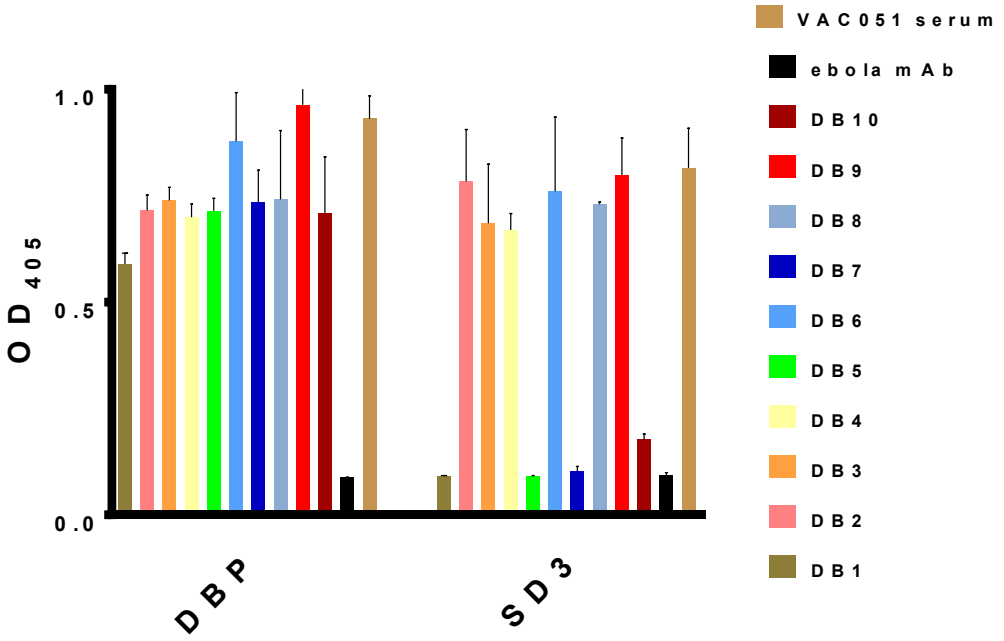


Figure 6.6: ELISA showing the binding of the ten anti-PvDBPII mAbs to PvDBPII (left) and SD3 (right). The column heights and error bars represent the mean and SD of triplicate wells. Human polyclonal serum from the VAC051 PvDBPII trial and a human anti-Ebola mAb were used as positive and negative controls respectively.

combination of DB9 with the non-SD3 binding mAbs (DB1, DB5, DB7 and DB10) was antagonistic. This suggests that in the context of the protein as presented by the parasite and DARC as presented on the RBC membrane, antibodies binding SD3 combine in their inhibitory effect whereas antibodies against different PvDBPII domains appear to antagonise anti-SD3 antibodies.

6.4.1 Immunising with SD3

Twelve rabbits were immunised. All the proteins were given with Freund's adjuvant and the schedules and doses were identical. To recap, the three protein constructs were;

1. Full-length PvDBPII (DBPII)
2. Sub-domain 3 of PvDBPII (SD3)
3. A subdomain 3 variant with five amino acid substitutions, called Interface (SD3-int)

	Group 1 PvDBPII	**Group 2 PvDBPII SD3**	**Group 3 PvDBPII SD3 Interface**
Number of rabbits (NZL White)	4	4	4
Immunogen Mw	39KDa	11KDa	11KDa
Adjuvant	Freunds	Freunds	Freunds
Dose/vaccination	20μg	20μg	20μg
Schedule	4 doses apart 2 weeks	4 doses 2 weeks	4 doses 2 weeks
Route	Intramuscular	Intramuscular	Intramuscular

Table 6.3: Rabbit immunisation schedule

All twelve serum samples were assayed by ELISA for binding to the PvDBPII and SD3 recombinant proteins used for the immunisations to confirm reactivity with the vaccine antigens (Figure 6.7).

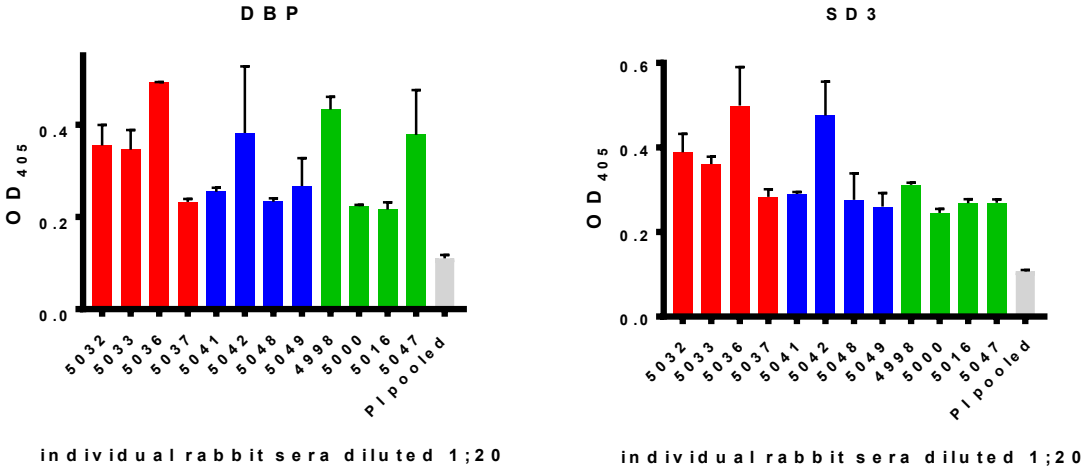


Figure 6.7: ELISA reactivity to PvDBPII and SD3 plotted as raw optical density at 405nm of 1:20 dilutions of serum samples from each of the 12 rabbits. Columns in red are the 4 rabbits immunised with DBPII, those in blue are the rabbits immunised with SD3 and those in green SD3-int. The data and error bars represent the mean and standard deviation of triplicate wells.

IgG was then purified from each serum sample and the purified IgG used in the Pk transgenic GIA assay (Figure 6.8).

The results of this rabbit immunisation study were a little difficult to interpret as, despite all 12 sera binding to PvDBPII and SD3 by ELISA (Figure 6.7), only two of the twelve samples showed significant growth inhibition. These 2 samples were from one rabbit immunised with DBPII (rabbit #5032) and one rabbit immunised with SD3 (rabbit #5041).

Of these two rabbits who did respond with neutralising IgG, the anti-SD3 response was much more potent. The interpolated EC_{50} value for the anti-SD3 rabbit IgG (1.16×10^7 AU) was approximately 7-fold lower than that for the anti-DBPII IgG (6.99×10^7 AU). However, the lack of inhibition in the other samples makes interpretation difficult. The major differences in GIA potency between the individual rabbit sera, may simply be due to inter-individual variation and the presence of particularly inhibitory clones in the IgG of rabbits #5032 and #5041. It is also possible that, despite all twelve samples binding PvDBPII and SD3 by ELISA, there had been some protein degradation within the samples; the immunisations

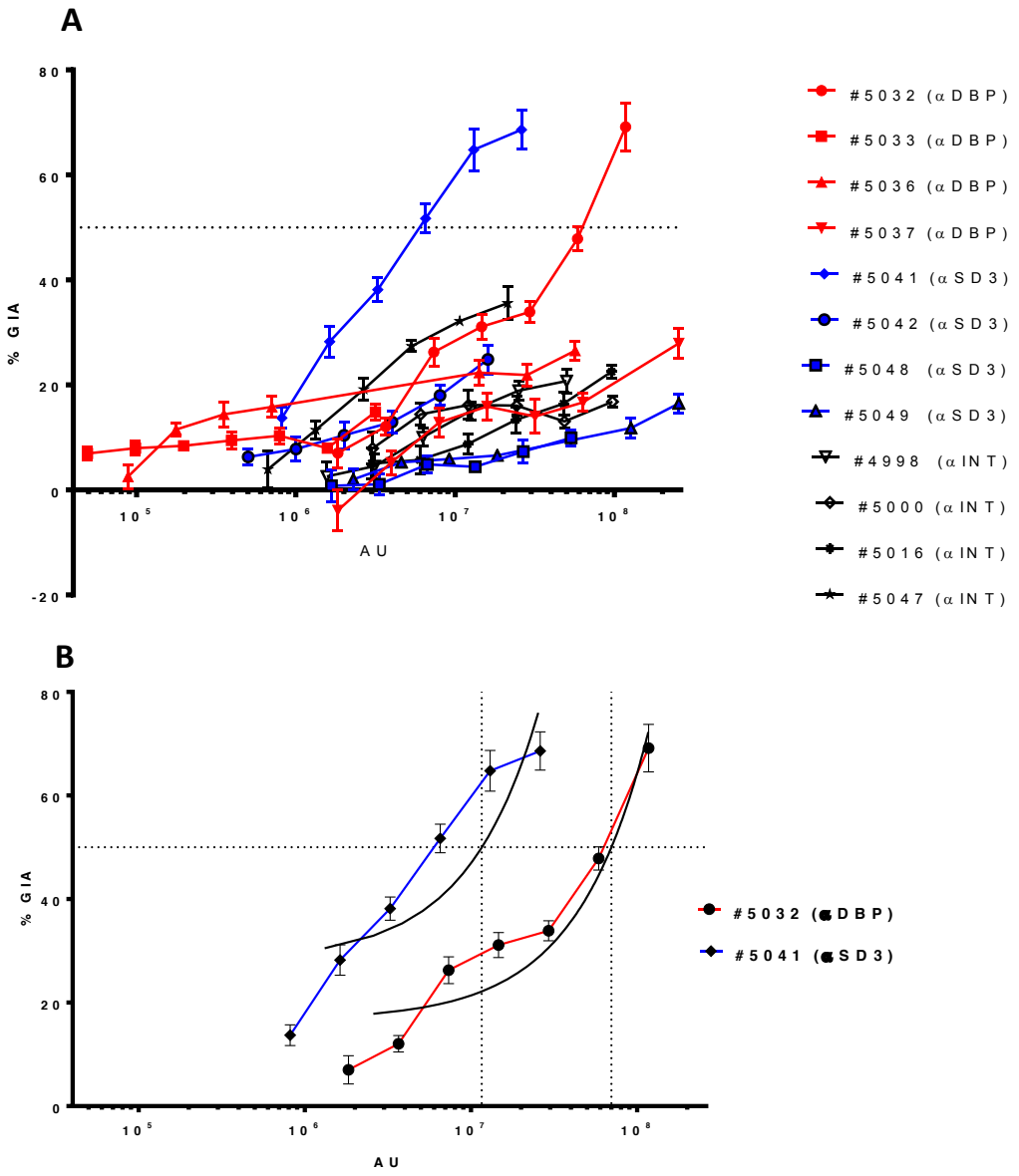


Figure 6.8: Pk transgenic GIA assay of a dilution series of purified rabbit anti-PvDBPII, anti-SD3 and anti-SD3-int IgG, concentration-adjusted and starting at 10mg/mL. Results for purified IgG from 4 rabbits immunised with PvDBPII are shown as red lines, the 4 rabbits immunised with SD3 as blue lines and the 4 rabbits immunised with SD3-int as black lines. Concentration of total IgG was converted from mg/mL to AU to adjust for differences in amount of antigen-specific IgG and allow direct comparison of antibody quality [257]. Pre-immune serum from each rabbit was also tested for growth inhibition; all were negative (data not shown). Panel (B) shows the growth Inhibition in the Pk transgenic GIA assay of purified IgG from rabbit #5032 immunised with PvDBPII (red line) and #5041 immunised with SD3 (blue line). The corresponding black lines represent linear regression lines plotted with GraphPad Prism software and used to interpolate EC50 values.

were performed commercially in China (GenScript) and the frozen sera sent to the UK.

It is important to remember that this transgenic Pk GIA assay used to test the anti-SD3 rabbit sera, currently just encodes the Sal I strain of PvDBPII. What makes SD3, or more accurately, a future iteration of it, exciting as a potential vaccine candidate is that we now know that it contains the epitope of a broadly-neutralising antibody, DB9. It will be interesting therefore, once variant PvDBPII alleles have been successfully introduced into the transgenic Pk model, to test the IgG from rabbit #5041 against alleles of PvDBPII very different to the Sal1 strain sequence. If the IgG of rabbit #5041, raised against SD3, contains clones with the breadth of neutralisation of DB9, then it should be expected to inhibit Pk lines with multiple and allelically-diverse PvDBPII transgenes.

6.5 Discussion

There are two basic approaches to overcoming the problem of polymorphism in an otherwise promising vaccine candidate; multi-allele vaccines and artificially engineered synthetic immunogens [73, 283, 284, 286]. Both approaches require the identification of broadly neutralising epitopes.

In this Chapter I report the first broadly-neutralizing epitope of a human antibody on PvDBPII, which remains the most promising blood-stage vaccine candidate against vivax malaria. It is also the first epitope whose claim to be 'broadly-neutralising' is based on data from functional invasion assays.

Of the three sub-domains of PvDBPII, SD2 is known to be highly polymorphic, whereas the other subdomains are relatively conserved [428]. This has been interpreted to suggest that SD2 is the major target of immune selection. The 2011 paper which presented the crystal structure of PvDBPII [30] proposed that PvDBPII forms a dimer on initial engagement with DARC and that SD2, which is

directly involved in this dimerisation and DARC engagement, contains the critical binding residues [30]. Alanine mutagenesis of residues in PvDBPII has demonstrated critical binding residues in SD2, but mutagenesis of residues outside the SD2 have also been shown to impair DARC binding [166, 398].

In this published structure of PvDBPII, however, it was not co-crystallized with DARC, but rather the DARC binding site was inferred; it may not, therefore, represent the true conformation of PvDBPII when complexed with its natural RBC ligand. Co-crystallisation of the DBL3x domain of *P. falciparum* erythrocyte membrane protein 1 (Pfemp1), which shares close structural homology with PvDBPII, with its ligand chondroitin A sulphate (CSA), showed that it was SD3 of DBL3x that contained the minimal binding region [354, 355]. Colleagues in the Biochemistry Department in Oxford are currently working on the co-crystallization of DARC and DBP; but for the moment the actual binding mechanism is not known. The fact that the epitope of our broadly-neutralising human mAb, lies towards the tip of SD3 suggests that a secondary receptor-binding event may be occurring outside of the previously identified primary DARC-binding sites in SD2 [29, 30]. The tail end of SD3 may contact extracellular loops linking the seven transmembrane regions of DARC and this might play a role in DBP binding [385].

The authors of the 2011 PvDBPII structure paper, which posited the hetero-tetrameric model and suggested SD2 as the site of neutralising epitopes, published another paper in 2016 in which they report broadly-neutralising epitopes in SD3. A 2012 paper from a different group working on PvDBP, also claimed to have shown that SD3 contained broadly neutralising epitopes [348]. Both of these studies were with murine mAbs and neither had functional evidence of parasite invasion blocking. Despite the limits of their methodology, however, it is encouraging that different groups using different approaches are reaching similar conclusions about SD3.

Figure 6.3 shows that the predicted orientation of DB9 when bound to PvDBPII is with its long axis interposing directly between the merozoite and RBC membrane. This suggests a possible mechanism of action; that DB9 blocks erythrocyte approach and prevents DARC engagement. If the heterodimeric model is correct, then preventing initial DARC engagement would prevent the subsequent dimerisation of DBPII and thus complex formation.

Exciting though it is, mapping a broadly-neutralising epitope is just the start of another long journey. The next conundrum is how to engineer the vaccine antigen so that it induces maximal response against this epitope. As previously mentioned, broadly neutralising epitopes have been mapped on vaccine candidate antigens for many other proteins, but translating this into the desired vaccine-induced immune response is not proving easy. There is, however, an ever-expanding array of antigen engineering methods intended to optimise responses to pre-determined epitopes.

It was perhaps overly optimistic to hope that by expressing SD3 alone and immunising with it, we would induce a high proportion of 'DB9-like' super-antibodies. As shown in earlier Chapters, over half of the panel of mAbs against full-length PvDBPII bind SD3, so it will undoubtedly have induced a broad repertoire of antibodies with highly variable potency. It may be that the most immunogenic regions of SD3 elicit the least neutralizing antibodies. It may also be that there is significant antagonism between anti-SD3 antibodies, as was shown by the interaction of DB9 and DB4 in the synergy assays described in Chapter V. If an SD3-based construct is to progress as a vaccine candidate, then more work is needed to define its various epitopes and how they interact.

Over 90% of the DB9 epitope is within a twenty amino acid stretch in the distal third of SD3. If this small region could be expressed intact, or stabilised and arrayed on a scaffold, and used as an immunogen, it may induce a much more DB9-like polyclonal response. There are, of course, problems and difficulties

with trimming down protein antigens more and more tightly around a particular epitope. Conformational epitopes are often stabilised by distant residues and by minimizing the size of the antigen there is often major loss of immunogenicity. Full-length PvDBPII, for example, contains strong T cell epitopes primarily in SD2 and SD1 [429]. An antigen based tightly around the DB9 epitope might well need strong T cell epitopes to be engineered in. One option I am currently exploring is to deliver a PvDBPII- SD3 construct on a virus-like particle (VLP).

7

Conclusions and future directions

7.1 Summary of output

7.1.1 Human mAbs against *Plasmodium vivax*

The isolation of the mAbs described in this Thesis is, to my knowledge, the first report of fully-human mAbs specific for *P. vivax*. These mAbs were elicited in response to a human-compatible vaccine, and thus shed light on the human immune response to a PvDBPII; a vaccine candidate antigen that has been the subject of pre-clinical speculation for decades.

7.1.2 Proof of concept of a transgenic *Plasmodium knowlesi* model for testing anti-*P. vivax* antibodies

Perhaps the single biggest hindrance to *P. vivax* research remains the lack of long term *in vitro* culture. This first demonstration of the utility of a transgenic *P. knowlesi* model to assess inhibition by anti-*P. vivax* antibodies, will lead to it being widely adopted by the *P. vivax* research community. Showing that the *P. knowlesi* model correctly predicted the neutralisation of the mAbs against wild-type Thai Pv strains in the *ex vivo* assays adds greatly to its validation. I will soon be receiving

further transgenic *P. knowlesi* lines with variant PvDBPII allelic inserts and will then be able to screen anti-*P. vivax* antibodies for strain-variable inhibition in Oxford.

7.1.3 Isolating the first human broadly-neutralising antibody against *P. vivax*

Finding, among this first panel of human anti-PvDBPII mAbs, one that potently inhibits the RBC invasion of a genetically diverse sample of wild-type Pv isolates is an exciting breakthrough. Experience with other pathogens has shown that such bnAbs are few and far between and a precious resource for vaccine design.

The failure of the biochemical assays described in Chapter III to predict the functional data in the subsequent two Chapters is an important finding in itself. These biochemical assays have been the most widely used method to characterise anti-vivax antibodies, so demonstrating a lack of correlation between DARC-binding inhibition and parasite neutralisation should trigger a re-think of the usefulness of the biochemical assays.

7.1.4 Mapping the broadly-neutralising epitope on PvDBPII

The mapping of a broadly-neutralising epitope to subdomain 3 of PvDBPII is of great significance and demands a re-think of the current model which suggests that neutralising epitopes are on the PvDBPII dimer interface and the DARC-binding site [30]. It may be that the neutralising potency of DB9 relates primarily to steric hindrance caused by the orientation of its long axis directly interposing between merozoite and erythrocyte; or it may be that it is interfering with other, as yet unknown, points of interaction between PvDBP and DARC.

While the process of re-engineering PvDBPII around the epitope of DB9 has only just begun, if it proves possible to elicit a predominantly 'DB9-like' antibody response, then an SD3-based antigen may have potential as a next-generation vaccine candidate. This Thesis has also shown that antagonism between antibodies is a feature of the polyclonal response to PvDBPII and is likely to play a significant role in influencing the potency of vaccine-induced polyclonal antibody.

7.2 Future directions

7.2.1 *In vivo* data

My first priority is to test DB9, in an *in vivo* model. A newly-developed and as yet unpublished humanised mouse model for supporting *P. vivax* blood-stage growth has been made available to me at the Center for Infection Disease Research (CIDR, Seattle, USA). The model is based on the FRG mouse on a NOD background (FRGN) supplied by Yecuris™ and is able to be engrafted with human hepatocytes and red blood cells which are maintained due to severe immunodeficiency [134]. Ten liver-chimeric FRGN mice will be infected intravenously with 500,000 – 1 million *P. vivax* sporozoites. The mice will be repopulated with human reticulocytes to ensure presence of target cells when the parasites egress from the liver on days eight to ten post-infection. On day seven post-infection the mice will be administered either an anti-PvDBPII mAb or a control mAb and blood samples will be taken daily to monitor blood-stage infection by thin and thick blood smear as well as q-rtPCR.

I have also started discussions with colleagues about the possibility of a passive transfer study of the anti-PvDBPII mAb 'DB9' in Aotus monkeys. The most exciting *in vivo* data on the very near horizon at The Jenner Institute are those which will come from the *P. vivax* controlled human malaria infection (CHMI) studies. These are already underway: Two volunteers were successfully infected by mosquito bite earlier this year, their blood has been screened and banked and it will be used in an efficacy study of the PvDBPII vaccine next year. This will be the first human efficacy trial of a blood-stage vaccination against *P. vivax* and its

results will guide future work on a PvDBPII-based vaccine. If it shows an inhibitory effect on the parasite multiplication rate there will be a strong rationale to develop new and better iterations based on the work in this DPhil Thesis.

7.2.2 AAV-vectored DB9

In recent years the concept of "vectored immuno-prophylaxis" or VIP has been described [18, 19, 113, 192]. To date this approach has primarily utilised an adeno-associated virus (AAV) vector to deliver a mAb, or antibody-like immuno-adhesin, which is expressed *in situ* into the plasma from virally-transduced cells following intramuscular immunisation. Studies have shown these vectors can lead to circulating serum levels of 100-1000μg/mL mAb which persist for up to a year and confer protection against challenge in mouse models of HIV-1 [19] and influenza [18], rodent malaria sporozoite infection [113] and against SIV in rhesus macaques [192]. A Phase I trial in healthy UK male adults using an AAV1 vector encoding the PG9 anti-HIV mAb has initiated at the University of Surrey, UK in 2014 (Clinicaltrials.gov NCT01937455) [20]. The approach of VIP could revolutionise the concept of human vaccination, bypassing the adaptive immune system by delivering highly effective immunity against a target antigen using optimally defined human mAbs. This cost-effective approach to antibody delivery opens up possibilities for the prophylactic use of mAbs against diseases of poverty such as malaria.

It is not currently clear whether delivery of a single mAb is an efficient way of protecting against the blood-stage of malaria. A highly-neutralising mAb against a *P. falciparum* blood-stage antigen (PfRH5) was recently passively transferred in monkeys prior to an Aotus-adapted *P. falciparum* challenge (*Douglas et al.*, submitted and personal communications). A dose of 33mg/kg was insufficient for protection but 100mg/kg was successful, although serum mAb levels were in the order of hundreds of μg/mL, which is higher than can currently be achieved by vaccination. The concern over escape mutants aside, it may be that efficient neutralisation requires cooperativity between different clones of mAb. Using vectored delivery, specific

combinations of cooperative mAbs could be delivered, thus removing the problem of vaccine-induced antagonistic antibodies, and leading to a more potent response than could be achieved with one mAb. It may also be that Fabs, camelid nanobodies, single-chain variable fragments (ScFvs) or other small protein constructs would show sufficiently reduced antagonism from interfering antibodies to outweigh the loss in half-life conferred by Fc in whole IgG molecules [393].

We have immunised mice with AAVs encoding DB9 and other mAbs from the panel, and the resultant IgG will be tested in the Pk transgenic GIA assays.

7.2.3 Immuno-adhesins

Recently, a chimeric antibody construct called 'eCD4-Ig' was described [143], a fusion of an anti-HIVCD4 IgG with a small CCR5-mimetic sulfopeptide. This binds avidly and cooperatively to the HIV-1 envelope glycoprotein and is more potent and broader than the best 'broadly neutralising antibodies' against HIV-1, HIV-2 and SIV. Following VIP delivery by AAV, rhesus macaques expressed eCD4-Ig at levels of up to 77μg/mL for more than 40 weeks, and were protected from infectious challenges [143].
Figure 7.1 taken from [159], summarises the principle; at the same time as the antibody Fab binds the CD4-binding site on the HIV envelope protein, the CCR5-mimetic tail binds to the CCR5 binding site. This leads to the blocking of two critical and conserved epitopes at the same time, by the same chimeric antibody.

In Chapter IV, I describe the use of recombinant DARC (the N-terminal sixty amino acids) as a positive control in the transgenic *P. knowlesi* GIA assays. It worked well and potently inhibited invasion even at low concentration (Figure 4.4). N-terminal DARC, which binds PvDBPII, is, like CCR5, a small sulfopeptide.

As outlined in Chapter II, we are currently working on a DB9:DARC immuno-adhesin in which N-terminal DARC is fused to the Fc portion of DB9. We plan to express the DB9-DARC immuno-adhesin, and test it both in transgenic *P. knowlesi*

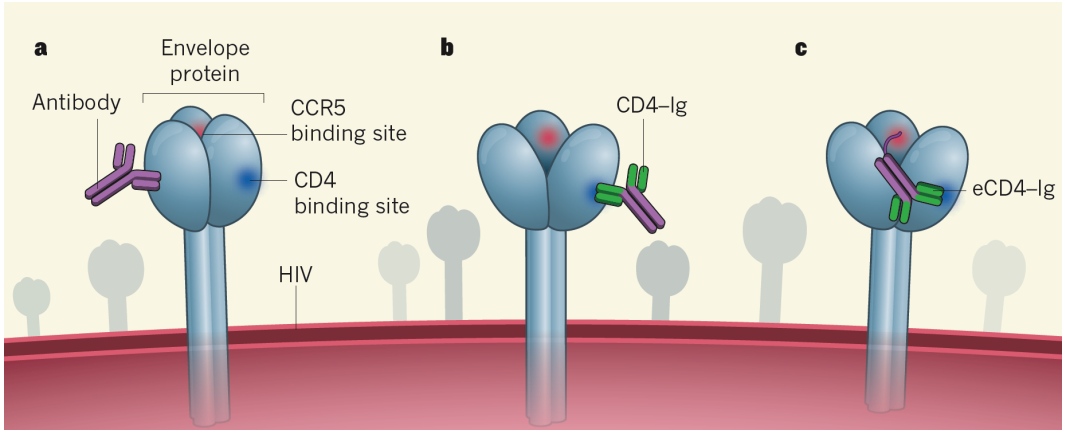


Figure 7.1: Cartoon illustrating the double binding of an immuno-adhesin against the HIV envelope protein. Taken from [159]

GIA assays and in *P. vivax* invasion assays using samples from returning travellers. If this DB9-DARC immuno-adhesin shows potent inhibition in these assays, we plan to encode it in an AAV vector and test expression in mice.

7.2.4 Other antigens

There is a growing consensus that an effective vaccine against a pathogen as protean as *Plasmodium* will need to target more than one antigen and probably antigens in more than one life-cycle stage [42, 295, 390]. A sub-domain 3 construct of PvDBPII may well be one of those antigens, but there has also been a lot of recent interest in PvRBP2b as a blood-stage Pv vaccine candidate [156]. I have immunised rabbits with a novel PvRBP2b C-terminal construct and, using *P. vivax* samples obtained from returning travellers to the UK, I will be testing this rabbit anti-PvRBP2b IgG in *P. vivax* invasion assays in the coming months. I will also test these anti-PvRBP2b antibodies in combination with anti-PvDBPII antibodies to look for possible synergy.

7.3 Final thoughts

As is often the case, things start to get really interesting right at the end of a DPhil. *P. vivax* research in Oxford is certainly entering a very exciting period. For the first time we have the parasite in house; both in the form of cryopreserved samples from returning travellers and as a screened biobank for CHMI studies.

The samples from returning travellers will give us a globally diverse library of wild-type strains (in decent volumes) for use in invasion assays, and the biobank will allow us to conduct human infection studies with *P. vivax*; for the first time in Europe since the era of malariotherapy. Although thousands were intentionally infected with *P. vivax* as treatment for neurosyphilis in the first half of the twentieth century, we now have powerful tools to minutely dissect the host immune response. As well as enabling molecular-level scrutiny of the *in vivo* interactions between human and parasite, it will allow us to test the efficacy of our candidate vivax vaccines. The first candidate to be tested, scheduled for next year, will be the ChAd-MVA encoded PvDBPII from whose phase Ia trial [304], the mAbs studied in this project derived.

As already mentioned, blood-stage malaria vaccines do not need to induce sterile protection to be efficacious; to some extent, the less efficacious vaccine, the more it should benefit from boosting by natural infection. Given that a robust naturally-acquired immunity to *P. vivax* usually develops with the first few years of life, a PvDBPII-based vaccine that conferred some clinical protection in these early years could be a useful intervention.

Having been so overshadowed by *P. falciparum* in the research agenda, there are still huge gaps in our understanding of *P. vivax*; but with these come great scope for breakthroughs. Having spent the last few years mulling over this parasite, I think there are reasons to be optimistic and suspect that, as we now move to testing vaccine efficacy in humans, we're going to be in for some surprises. Pleasant ones, I hope.

Bibliography

[1] APLMA. East Asia Summit adopts unprecedented regional malaria goal; 2014.

[2] PAHO. Central America and Hispaniola seek to eliminate malaria by 2025;2013.

[3] Abderrazek, R. B., Hmila, I., Vincke, C., Benlasfar, Z., Pellis, M., Dabbek, H., Saerens, D., El Ayeb, M., Muyldermans, S., and Bouhaouala-Zahar, B. (2009). Identification of potent nanobodies to neutralize the most poisonous polypeptide from scorpion venom. *Biochem J*, 424(2):263–72.

[4] Adams, J. H., Hudson, D. E., Torii, M., Ward, G. E., Wellems, T. E., Aikawa, M., and Miller, L. H. (1990). The Duffy receptor family of *Plasmodium knowlesi* is located within the micronemes of invasive malaria merozoites. *Cell*, 63(1):141–53.

[5] Adams, J. H., Sim, B. K., Dolan, S. A., Fang, X., Kaslow, D. C., and Miller, L. H. (1992). A family of erythrocyte binding proteins of malaria parasites. *Proc Natl Acad Sci U S A*, 89(15):7085–9.

[6] Aikawa, M., Miller, L. H., Johnson, J., and Rabbege, J. (1978). Erythrocyte entry by malarial parasites. a moving junction between erythrocyte and parasite. *J Cell Biol*, 77(1):72–82.

[7] Akinyi, S., Hanssen, E., Meyer, E. V., Jiang, J., Korir, C. C., Singh, B., Lapp, S., Barnwell, J. W., Tilley, L., and Galinski, M. R. (2012). A 95 kda protein of *Plasmodium vivax* and *P. cynomolgi* visualized by three-dimensional tomography in the caveola-vesicle complexes (Schuffner's dots) of infected erythrocytes is a member of the PHIST family. *Mol Microbiol*, 84(5):816–31.

[8] Ala'Aldeen, D. A., Stevenson, P., Griffiths, E., Gorringe, A. R., Irons, L. I., Robinson, A., Hyde, S., and Borriello, S. P. (1994). Immune responses in humans and animals to meningococcal transferrin-binding proteins: implications for vaccine design. *Infect Immun*, 62(7):2984–90.

[9] Alonso, P. L. and Tanner, M. (2013). Public health challenges and prospects for malaria control and elimination. *Nat Med*, 19(2):150–5.

[10] Anonymous (1922.). General paralysis. *Br. Med. J. 2, 1120–1121.*

[11] Ashley, E. A., Dhorda, M., Fairhurst, R. M., Amaratunga, C., Lim, P., Suon, S., Sreng, S., Anderson, J. M., Mao, S., Sam, B., Sopha, C., Chuor, C. M., Nguon, C., Sovannaroth, S., Pukrittayakamee, S., Jittamala, P., Chotivanich, K., Chutasmit, K., Suchatsoonthorn, C., Runcharoen, R., Hien, T. T., Thuy-Nhien, N. T., Thanh, N. V., Phu, N. H., Htut, Y., Han, K. T., Aye, K. H., Mokuolu, O. A., Olaosebikan, R. R., Folaranmi, O. O., Mayxay, M., Khanthavong, M., Hongvanthong, B., Newton, P. N., Onyamboko, M. A., Fanello, C. I., Tshefu, A. K., Mishra, N., Valecha, N., Phyo, A. P., Nosten, F., Yi, P., Tripura, R., Borrmann, S., Bashraheil, M., Peshu, J., Faiz, M. A., Ghose, A., Hossain, M. A., Samad, R., Rahman, M. R., Hasan, M. M., Islam, A., Miotto, O., Amato, R., MacInnis, B., Stalker, J., Kwiatkowski, D. P., Bozdech, Z., Jeeyapant, A., Cheah, P. Y., Sakulthaew, T., Chalk, J., Intharabut, B., Silamut, K., Lee, S. J., Vihokhern, B., Kunasol, C., Imwong, M., Tarning, J., Taylor, W. J., Yeung, S., Woodrow, C. J., Flegg, J. A., Das, D., Smith, J., Venkatesan, M., Plowe, C. V., Stepniewska, K., Guerin, P. J., Dondorp, A. M., Day, N. P., White, N. J., and Tracking Resistance to Artemisinin, C. (2014). Spread of artemisinin resistance in *Plasmodium falciparum* malaria. *N Engl J Med*, 371(5):411–23.

[12] Ayala, F. J., Escalante, A. A., Lal, A. A., and Rich, S. M. (1998). Evolutionary relationships of human malaria parasites. In *Malaria Parasite Biology, Pathogenesis, and Protection*, pages 285–300. ASM press, Washington DC.

[13] Babaeekho, L., Zakeri, S., and Djadid, N. D. (2009). Genetic mapping of the Duffy binding protein (DBP) ligand domain of *Plasmodium vivax* from unstable malaria region in the Middle East. *Am J Trop Med Hyg*, 80(1):112–8.

[14] Backliwal, G., Hildinger, M., Chenuet, S., Wulhfard, S., De Jesus, M., and Wurm, F. M. (2008). Rational vector design and multi-pathway modulation of HEK 293E cells yield recombinant antibody titers exceeding 1 g/l by transient transfection under serum-free conditions. *Nucleic Acids Res*, 36(15):e96.

[15] Baer, K., Klotz, C., Kappe, S. H., Schnieder, T., and Frevert, U. (2007). Release of hepatic *Plasmodium yoelii* merozoites into the pulmonary microvasculature. *PLoS Pathog*, 3(11):e171.

[16] Baird, J. K. (2010). Eliminating malaria–all of them. *Lancet*, 376(9756):1883–5.

[17] Baird, J. K., Leksana, B., Masbar, S., Fryauff, D. J., Sutanihardja, M. A., Suradi, Wignall, F. S., and Hoffman, S. L. (1997). Diagnosis of resistance to chloroquine by *Plasmodium vivax*: timing of recurrence and whole blood chloroquine levels. *Am J Trop Med Hyg*, 56(6):621–6.

[18] Balazs, A. B., Bloom, J. D., Hong, C. M., Rao, D. S., and Baltimore, D. (2013). Broad protection against influenza infection by vectored immunoprophylaxis in mice. *Nat Biotechnol*, 31(7):647–52.

[19] Balazs, A. B., Chen, J., Hong, C. M., Rao, D. S., Yang, L., and Baltimore, D. (2011). Antibody-based protection against HIV infection by vectored immunoprophylaxis. *Nature*, 481(7379):81–4.

[20] Balazs, A. B. and West, A. P., J. (2013). Antibody gene transfer for HIV immunoprophylaxis. *Nat Immunol*, 14(1):1–5.

[21] Ball, P. (2008). Water as an active constituent in cell biology. *Chem Rev*, 108(1):74–108.

[22] Bannister, L. H., Butcher, G. A., Dennis, E. D., and Mitchell, G. H. (1975). Structure and invasive behaviour of *Plasmodium knowlesi* merozoites in vitro. *Parasitology*, 71(3):483–91.

[23] Baral, T. N., Magez, S., Stijlemans, B., Conrath, K., Vanhollebeke, B., Pays, E., Muyldermans, S., and De Baetselier, P. (2006). Experimental therapy of African *trypanosomiasis* with a nanobody-conjugated human trypanolytic factor. *Nat Med*, 12(5):580–4.

[24] Barber, B. E., William, T., Grigg, M. J., Menon, J., Auburn, S., Marfurt, J., Anstey, N. M., and Yeo, T. W. (2013). A prospective comparative study of *knowlesi*, *falciparum*, and *vivax* malaria in Sabah, Malaysia: high proportion with severe disease from *Plasmodium knowlesi* and *Plasmodium vivax* but no mortality with early referral and artesunate therapy. *Clin Infect Dis*, 56(3):383–97.

[25] Bardelli, M., Livoti, E., Simonelli, L., Pedotti, M., Moraes, A., Valente, A. P., and Varani, L. (2015). Epitope mapping by solution NMR spectroscopy. *J Mol Recognit*, 28(6):393–400.

[26] Barnwell, J. W., Nichols, M. E., and Rubinstein, P. (1989). In vitro evaluation of the role of the Duffy blood group in erythrocyte invasion by *Plasmodium vivax*. *J Exp Med*, 169(5):1795–802.

[27] Baruch, D. I., Pasloske, B. L., Singh, H. B., Bi, X., Ma, X. C., Feldman, M., Taraschi, T. F., and Howard, R. J. (1995). Cloning the *P. falciparum* gene encoding PfEMP1, a malarial variant antigen and adherence receptor on the surface of parasitized human erythrocytes. *Cell*, 82(1):77–87.

[28] Bass, C. C. and Johns, F. M. (1912). The Cultivation of Malarial *Plasmodia* (*Plasmodium vivax* and *Plasmodium falciparum*) in vitro. *J Exp Med*, 16(4):567–79.

[29] Batchelor, J. D., Malpede, B. M., Omattage, N. S., DeKoster, G. T., Henzler-Wildman, K. A., and Tolia, N. H. (2014). Red blood cell invasion by *Plasmodium vivax*: structural basis for DBP engagement of DARC. *PLoS Pathog*, 10(1):e1003869.

[30] Batchelor, J. D., Zahm, J. A., and Tolia, N. H. (2011). Dimerization of *Plasmodium vivax* DBP is induced upon receptor binding and drives recognition of DARC. *Nat Struct Mol Biol*, 18(8):908–14.

[31] Battle, K. E., Gething, P. W., Elyazar, I. R., Moyes, C. L., Sinka, M. E., Howes, R. E., Guerra, C. A., Price, R. N., Baird, K. J., and Hay, S. I. (2012). The global public health significance of *Plasmodium vivax*. *Adv Parasitol*, 80:1–111.

[32] Baum, J., Chen, L., Healer, J., Lopaticki, S., Boyle, M., Triglia, T., Ehlgen, F., Ralph, S. A., Beeson, J. G., and Cowman, A. F. (2009). Reticulocyte-binding protein homologue 5 - an essential adhesin involved in invasion of human erythrocytes by *Plasmodium falciparum*. *Int J Parasitol*, 39(3):371–80.

[33] Beck, A., Wurch, T., Bailly, C., and Corvaia, N. (2010). Strategies and challenges for the next generation of therapeutic antibodies. *Nat Rev Immunol*, 10(5):345–52.

[34] Beernink, P. T., Welsch, J. A., Bar-Lev, M., Koeberling, O., Comanducci, M., and Granoff, D. M. (2008). Fine antigenic specificity and cooperative bactericidal activity of monoclonal antibodies directed at the meningococcal vaccine candidate factor h-binding protein. *Infect Immun*, 76(9):4232–40.

[35] Beg, M., Khan, R., Baig, S., Gulzar, Z., Hussain, R., and Smego Jr, R. (2002). Cerebral involvement in benign tertian malaria. *The American journal of tropical medicine and hygiene*, 67(3):230–232.

[36] Bell, D. and Peeling, R. W. (2006). Evaluation of rapid diagnostic tests: malaria. *Nature Reviews Microbiology*, 4:S34–S38.

[37] Bennett, J. W., Yadava, A., Tosh, D., Sattabongkot, J., Komisar, J., Ware, L. A., McCarthy, W. F., Cowden, J. J., Regules, J., Spring, M. D., Paolino, K., Hartzell, J. D., Cummings, J. F., Richie, T. L., Lumsden, J., Kamau, E., Murphy, J., Lee, C., Parekh, F., Birkett, A., Cohen, J., Ballou, W. R., Polhemus, M. E., Vanloubbeeck, Y. F., Vekemans, J., and Ockenhouse, C. F. (2016). Phase 1/2a trial of *Plasmodium vivax* malaria vaccine candidate vmp001/AS01b in malaria-naive adults: Safety, immunogenicity, and efficacy. *PLoS Negl Trop Dis*, 10(2):e0004423.

[38] Bermudez, M., Moreno-Perez, D. A., Arevalo-Pinzon, G., Curtidor, H., and Patarroyo, M. A. (2018). *Plasmodium vivax* in vitro continuous culture: the spoke in the wheel. *Malar J*, 17(1):301.

[39] Bernasconi, N. L., Traggiai, E., and Lanzavecchia, A. (2002). Maintenance of serological memory by polyclonal activation of human memory B cells. *Science*, 298(5601):2199–202.

[40] Bignami, A. (2010). [atti della societa per gli studi della malaria. vol. xi. 1910. on the pathogenesis of recurrence in malarial fever]. *Parassitologia*, 52(3-4):441, 443–57.

[41] Bockarie, M. J. and Dagoro, H. (2006). Are insecticide-treated bednets more protective against *Plasmodium falciparum* than *Plasmodium vivax*-infected mosquitoes? *Malar J*, 5:15.

[42] Boes, A., Spiegel, H., Voepel, N., Edgue, G., Beiss, V., Kapelski, S., Fendel, R., Scheuermayer, M., Pradel, G., Bolscher, J. M., Behet, M. C., Dechering, K. J., Hermsen, C. C., Sauerwein, R. W., Schillberg, S., Reimann, A., and Fischer, R. (2015). Analysis of a multi-component multi-stage malaria vaccine candidate–tackling the cocktail challenge. *PLoS One*, 10(7):e0131456.

[43] Bommakanti, G., Lu, X., Citron, M. P., Najar, T. A., Heidecker, G. J., ter Meulen, J., Varadarajan, R., and Liang, X. (2012). Design of *Escherichia*

coli-expressed stalk domain immunogens of H1N1 hemagglutinin that protect mice from lethal challenge. *J Virol*, 86(24):13434–44.

[44] Borlon, C., Russell, B., Sriprawat, K., Suwanarusk, R., Erhart, A., Renia, L., Nosten, F., and D'Alessandro, U. (2012). Cryopreserved *Plasmodium vivax* and cord blood reticulocytes can be used for invasion and short term culture. *Int J Parasitol*, 42(2):155–60.

[45] Bousema, T. and Drakeley, C. (2011). Epidemiology and infectivity of *Plasmodium falciparum* and *Plasmodium vivax* gametocytes in relation to malaria control and elimination. *Clin Microbiol Rev*, 24(2):377–410.

[46] Boutz, D. R., Horton, A. P., Wine, Y., Lavinder, J. J., Georgiou, G., and Marcotte, E. M. (2014). Proteomic identification of monoclonal antibodies from serum. *Anal Chem*, 86(10):4758–66.

[47] Boyd, M. F. (1941). An historical sketch of the prevalence of malaria in North America. *Am. J. Trop. Med. 21:223-244.*

[48] Boyd, M. F. (1947). A review of studies on immunity to *vivax* malaria. *J Natl Malar Soc*, 6(1):12–31.

[49] Boyd, M.F., S.-T. W. (1933). Studies on benign tertian malaria. 4. on the refractoriness of negroes to inoculation with *Plasmodium vivax. Am. J. Hyg. 18, 485–489.*

[50] Boyd, M., S.-T. W. M. H. (1936). The occurrence of gametocytes of *Plasmodium vivax* during the primary attack. *Am. J. Trop. Med. Hyg. s1–16, 133–138.*

[51] Boyle, M. J., Wilson, D. W., Richards, J. S., Riglar, D. T., Tetteh, K. K., Conway, D. J., Ralph, S. A., Baum, J., and Beeson, J. G. (2010). Isolation of viable *Plasmodium falciparum* merozoites to define erythrocyte invasion events and advance vaccine and drug development. *Proc Natl Acad Sci U S A*, 107(32):14378–83.

[52] Bray, R. S. (1958). The susceptibility of Liberians to the Madagascar strain of *Plasmodium vivax*. *J Parasitol*, 44(4, Section 1):371–3.

[53] Briney, B., Sok, D., Jardine, J. G., Kulp, D. W., Skog, P., Menis, S., Jacak, R., Kalyuzhniy, O., de Val, N., Sesterhenn, F., Le, K. M., Ramos, A., Jones, M., Saye-Francisco, K. L., Blane, T. R., Spencer, S., Georgeson, E., Hu, X., Ozorowski, G., Adachi, Y., Kubitz, M., Sarkar, A., Wilson, I. A., Ward, A. B., Nemazee, D., Burton, D. R., and Schief, W. R. (2016). Tailored immunogens direct affinity maturation toward HIV neutralizing antibodies. *Cell*, 166(6):1459–1470 e11.

[54] Brown, K. N. and Brown, I. N. (1965). Immunity to malaria: antigenic variation in chronic infections of *Plasmodium knowlesi*. *Nature*, 208(5017):1286–8.

[55] Burel, J. G., Apte, S. H., McCarthy, J. S., and Doolan, D. L. (2016). *Plasmodium vivax* but not *Plasmodium falciparum* blood-stage infection in humans is associated with the expansion of a CD8+ T cell population with cytotoxic potential. *PLoS Negl Trop Dis*, 10(12):e0005031.

[56] Burton, D. R. (2002). Antibodies, viruses and vaccines. *Nat Rev Immunol*, 2(9):706–13.

[57] Burton, D. R., Desrosiers, R. C., Doms, R. W., Koff, W. C., Kwong, P. D., Moore, J. P., Nabel, G. J., Sodroski, J., Wilson, I. A., and Wyatt, R. T. (2004). HIV vaccine design and the neutralizing antibody problem. *Nat Immunol*, 5(3):233–6.

[58] Burton, D. R., Poignard, P., Stanfield, R. L., and Wilson, I. A. (2012). Broadly neutralizing antibodies present new prospects to counter highly antigenically diverse viruses. *Science*, 337(6091):183–6.

[59] Butler, N. S., Nolz, J. C., and Harty, J. T. (2011). Immunologic considerations for generating memory CD8 T cells through vaccination. *Cell Microbiol*, 13(7):925–33.

[60] Carlton, J. M., Adams, J. H., Silva, J. C., Bidwell, S. L., Lorenzi, H., Caler, E., Crabtree, J., Angiuoli, S. V., Merino, E. F., Amedeo, P., Cheng, Q., Coulson, R. M., Crabb, B. S., Del Portillo, H. A., Essien, K., Feldblyum, T. V., Fernandez-Becerra, C., Gilson, P. R., Gueye, A. H., Guo, X., Kang'a, S., Kooij, T. W., Korsinczky, M., Meyer, E. V., Nene, V., Paulsen, I., White, O., Ralph, S. A., Ren, Q., Sargeant, T. J., Salzberg, S. L., Stoeckert, C. J., Sullivan, S. A., Yamamoto, M. M., Hoffman, S. L., Wortman, J. R., Gardner, M. J., Galinski, M. R., Barnwell, J. W., and Fraser-Liggett, C. M. (2008). Comparative genomics of the neglected human malaria parasite *Plasmodium vivax*. *Nature*, 455(7214):757–63.

[61] Carter, M. J., Mitchell, R. M., Meyer Sauteur, P. M., Kelly, D. F., and Truck, J. (2017). The antibody-secreting cell response to infection: Kinetics and clinical applications. *Front Immunol*, 8:630.

[62] Carter, R. and Mendis, K. N. (2002). Evolutionary and historical aspects of the burden of malaria. *Clin Microbiol Rev*, 15(4):564–94.

[63] Carvalho, B. O., Lopes, S. C., Nogueira, P. A., Orlandi, P. P., Bargieri, D. Y., Blanco, Y. C., Mamoni, R., Leite, J. A., Rodrigues, M. M., Soares, I. S., Oliveira, T. R., Wunderlich, G., Lacerda, M. V., del Portillo, H. A., Araujo, M. O., Russell, B., Suwanarusk, R., Snounou, G., Renia, L., and Costa, F. T. (2010). On the cytoadhesion of *Plasmodium vivax*-infected erythrocytes. *J Infect Dis*, 202(4):638–47.

[64] Casadevall, A. (2006). The third age of antimicrobial therapy. *Clin Infect Dis*, 42(10):1414–6.

[65] Cavalli-Sforza, L. L., P. M. and Piazza., A. (1994). The history and geography of human genes. *Princeton University Press, Princeton, N.J.*

[66] Cavasini, C. E., de Mattos, L. C., Couto, A. A., Couto, V. S., Gollino, Y., Moretti, L. J., Bonini-Domingos, C. R., Rossit, A. R., Castilho, L., and Machado, R. L. (2007). Duffy blood group gene polymorphisms among malaria *vivax* patients in four areas of the Brazilian Amazon region. *Malar J*, 6:167.

[67] Celli, A. (1933). The history of malaria in the Roman Campagna from ancient times. *John Bales, Danielsson, London, United Kingdom*.

[68] Chan, E. R., Menard, D., David, P. H., Ratsimbasoa, A., Kim, S., Chim, P., Do, C., Witkowski, B., Mercereau-Puijalon, O., Zimmerman, P. A., and Serre, D. (2012). Whole genome sequencing of field isolates provides robust characterization of genetic diversity in *Plasmodium vivax*. *PLoS Negl Trop Dis*, 6(9):e1811.

[69] Chasis, J. A., Prenant, M., Leung, A., and Mohandas, N. (1989). Membrane assembly and remodeling during reticulocyte maturation. *Blood*, 74(3):1112–20.

[70] Chasis, J. A. and Schrier, S. L. (1989). Membrane deformability and the capacity for shape change in the erythrocyte. *Blood*, 74(7):2562–8.

[71] Chaudhuri, A., Polyakova, J., Zbrzezna, V., and Pogo, A. O. (1995). The coding sequence of Duffy blood group gene in humans and simians: restriction fragment length polymorphism, antibody and malarial parasite specificities, and expression in nonerythroid tissues in Duffy-negative individuals. *Blood*, 85(3):615–21.

[72] Chen, E., Salinas, N. D., Huang, Y., Ntumngia, F., Plasencia, M. D., Gross, M. L., Adams, J. H., and Tolia, N. H. (2016). Broadly neutralizing epitopes in the *Plasmodium vivax* vaccine candidate Duffy binding protein. *Proc Natl Acad Sci U S A*, 113(22):6277–82.

[73] Chen, E., Salinas, N. D., Ntumngia, F. B., Adams, J. H., and Tolia, N. H. (2015). Structural analysis of the synthetic Duffy binding protein (DBP) antigen

DEKnull relevant for *Plasmodium vivax* malaria vaccine design. *PLoS Negl Trop Dis*, 9(3):e0003644.

[74] Chen, L., Lopaticki, S., Riglar, D. T., Dekiwadia, C., Uboldi, A. D., Tham, W. H., O'Neill, M. T., Richard, D., Baum, J., Ralph, S. A., and Cowman, A. F. (2011). An EGF-like protein forms a complex with PfRh5 and is required for invasion of human erythrocytes by *Plasmodium falciparum*. *PLoS Pathog*, 7(9):e1002199.

[75] Chenet, S. M., Tapia, L. L., Escalante, A. A., Durand, S., Lucas, C., and Bacon, D. J. (2012). Genetic diversity and population structure of genes encoding vaccine candidate antigens of *Plasmodium vivax*. *Malar J*, 11:68.

[76] Chin, W., Contacos, P. G., Coatney, G. R., and Kimball, H. R. (1965). A naturally acquited quotidian-type malaria in man transferable to monkeys. *Science*, 149(3686):865.

[77] Chitnis, C. E., Chaudhuri, A., Horuk, R., Pogo, A. O., and Miller, L. H. (1996). The domain on the Duffy blood group antigen for binding *Plasmodium vivax* and *P. knowlesi* malarial parasites to erythrocytes. *J Exp Med*, 184(4):1531–6.

[78] Chitnis, C. E. and Miller, L. H. (1994). Identification of the erythrocyte binding domains of *Plasmodium vivax* and *Plasmodium knowlesi* proteins involved in erythrocyte invasion. *J Exp Med*, 180(2):497–506.

[79] Cho, J. S., Russell, B., Kosaisavee, V., Zhang, R., Colin, Y., Bertrand, O., Chandramohanadas, R., Chu, C. S., Nosten, F., Renia, L., and Malleret, B. (2016). Unambiguous determination of *Plasmodium vivax* reticulocyte invasion by flow cytometry. *Int J Parasitol*, 46(1):31–9.

[80] Choe, H., Moore, M. J., Owens, C. M., Wright, P. L., Vasilieva, N., Li, W., Singh, A. P., Shakri, R., Chitnis, C. E., and Farzan, M. (2005). Sulphated tyrosines mediate association of chemokines and *Plasmodium vivax* Duffy

binding protein with the Duffy antigen/receptor for chemokines (DARC). *Mol Microbiol*, 55(5):1413–22.

[81] Chootong, P., McHenry, A. M., Ntumngia, F. B., Sattabongkot, J., and Adams, J. H. (2014). The association of Duffy binding protein region ii polymorphisms and its antigenicity in *Plasmodium vivax* isolates from Thailand. *Parasitol Int*, 63(6):858–64.

[82] Chootong, P., Ntumngia, F. B., VanBuskirk, K. M., Xainli, J., Cole-Tobian, J. L., Campbell, C. O., Fraser, T. S., King, C. L., and Adams, J. H. (2010). Mapping epitopes of the *Plasmodium vivax* Duffy binding protein with naturally acquired inhibitory antibodies. *Infect Immun*, 78(3):1089–95.

[83] Chou, T. C. and Talalay, P. (1984). Quantitative analysis of dose-effect relationships: the combined effects of multiple drugs or enzyme inhibitors. *Adv Enzyme Regul*, 22:27–55.

[84] Chow, S. K. and Casadevall, A. (2012). Monoclonal antibodies and toxins–a perspective on function and isotype. *Toxins (Basel)*, 4(6):430–54.

[85] Christofinis, G. J. and Miller, H. (1983). A simplified method for cryopreservation of *Plasmodium falciparum* from continuous in vitro cultures. *Ann Trop Med Parasitol*, 77(2):123–6.

[86] Chwatt, L. J. (1948). Infection of reticulocytes by *Plasmodium falciparum* and *Plasmodium malariae* in hyperendemic indigenous malaria. *Ann Trop Med Parasitol*, 42(1):101–12.

[87] CI., B. (1939.). The toxicity of poisons applied jointly. *Ann. Appl. Biol. 26, 585–615.*

[88] Coatney, G., Collins, W., Warren, M., and Contacos, P. (1971). The primate malarias. *Government Printing Office, Washington DC, U.S.A.*.

[89] Coggeshall, L. T. and Kumm, H. W. (1937). Demonstration of passive immunity in experimental monkey malaria. *J Exp Med*, 66(2):177–90.

[90] Cohen, S., McGregor, I. A., and Carrington, S. (1961). Gamma-globulin and acquired immunity to human malaria. *Nature*, 192:733–7.

[91] Cole-Tobian, J. and King, C. L. (2003). Diversity and natural selection in *Plasmodium vivax* Duffy binding protein gene. *Mol Biochem Parasitol*, 127(2):121–32.

[92] Cole-Tobian, J. L., Michon, P., Biasor, M., Richards, J. S., Beeson, J. G., Mueller, I., and King, C. L. (2009). Strain-specific Duffy binding protein antibodies correlate with protection against infection with homologous compared to heterologous *Plasmodium vivax* strains in Papua New Guinean children. *Infect Immun*, 77(9):4009–17.

[93] Cole-Tobian, J. L., Michon, P., Dabod, E., Mueller, I., and King, C. L. (2007a). Dynamics of asymptomatic *Plasmodium vivax* infections and Duffy binding protein polymorphisms in relation to parasitemia levels in Papua New Guinean children. *Am J Trop Med Hyg*, 77(5):955–62.

[94] Cole-Tobian, J. L., Zimmerman, P. A., and King, C. L. (2007b). High-throughput identification of the predominant malaria parasite clone in complex blood stage infections using a multi-snp molecular haplotyping assay. *Am J Trop Med Hyg*, 76(1):12–9.

[95] Collins, W. E., Jeffery, G. M., and Roberts, J. M. (2004a). A retrospective examination of reinfection of humans with *Plasmodium vivax*. *Am J Trop Med Hyg*, 70(6):642–4.

[96] Collins, W. E., Jeffery, G. M., and Roberts, J. M. (2004b). A retrospective examination of the effect of fever and microgametocyte count on mosquito infection on humans infected with *Plasmodium vivax*. *Am J Trop Med Hyg*, 70(6):638–41.

[97] Coluzzi, M. (1999). The clay feet of the malaria giant and its African roots: hypotheses and inferences about origin, spread and control of *Plasmodium falciparum*. *Parassitologia*, 41(1-3):277–83.

[98] Compton, J. R., Legler, P. M., Clingan, B. V., Olson, M. A., and Millard, C. B. (2011). Introduction of a disulfide bond leads to stabilization and crystallization of a ricin immunogen. *Proteins*, 79(4):1048–60.

[99] Conway, D. J., Machado, R. L., Singh, B., Dessert, P., Mikes, Z. S., Povoa, M. M., Oduola, A. M., and Roper, C. (2001). Extreme geographical fixation of variation in the *Plasmodium falciparum* gamete surface protein gene pfs48/45 compared with microsatellite loci. *Mol Biochem Parasitol*, 115(2):145–56.

[100] Covell G, . (1955). Spontaneous rupture of the spleen. *Trop Dis Bull 52: 705–723.*

[101] Cox-Singh, J., Davis, T. M., Lee, K. S., Shamsul, S. S., Matusop, A., Ratnam, S., Rahman, H. A., Conway, D. J., and Singh, B. (2008). *Plasmodium knowlesi* malaria in humans is widely distributed and potentially life threatening. *Clin Infect Dis*, 46(2):165–71.

[102] Coxon, R. and Hayes, W. (1945). Investigation into the efficacy of sulphadiazine in the treatment of malaria. *Transactions of the Royal Society of Tropical Medicine and Hygiene*, 39(3):195–205.

[103] Crick, A. J., Theron, M., Tiffert, T., Lew, V. L., Cicuta, P., and Rayner, J. C. (2014). Quantitation of malaria parasite-erythrocyte cell-cell interactions using optical tweezers. *Biophys J*, 107(4):846–53.

[104] Crotty, S. (2015). A brief history of T cell help to B cells. *Nat Rev Immunol*, 15(3):185–9.

[105] Culleton, R., Ndounga, M., Zeyrek, F. Y., Coban, C., Casimiro, P. N., Takeo, S., Tsuboi, T., Yadava, A., Carter, R., and Tanabe, K. (2009). Evidence for the

transmission of *Plasmodium vivax* in the Republic of the Congo, West central Africa. *J Infect Dis*, 200(9):1465–9.

[106] Culleton, R. L., Mita, T., Ndounga, M., Unger, H., Cravo, P. V., Paganotti, G. M., Takahashi, N., Kaneko, A., Eto, H., Tinto, H., Karema, C., D'Alessandro, U., do Rosario, V., Kobayakawa, T., Ntoumi, F., Carter, R., and Tanabe, K. (2008). Failure to detect *Plasmodium vivax* in West and central Africa by PCR species typing. *Malar J*, 7:174.

[107] Curtin, P. D. (1989). Death by migration: Europe's encounter with the tropics in the nineteenth century. *Cambridge University Press, New York, N.Y.*

[108] Cutbush, M. and Mollison, P. L. (1950). The Duffy blood group system. *Heredity (Edinb)*, 4(3):383–9.

[109] Daneshvar, C., Davis, T. M., Cox-Singh, J., Rafa'ee, M. Z., Zakaria, S. K., Divis, P. C., and Singh, B. (2009). Clinical and laboratory features of human *Plasmodium knowlesi* infection. *Clin Infect Dis*, 49(6):852–60.

[110] Dankwa, S., Lim, C., Bei, A. K., Jiang, R. H., Abshire, J. R., Patel, S. D., Goldberg, J. M., Moreno, Y., Kono, M., Niles, J. C., and Duraisingh, M. T. (2016). Ancient human sialic acid variant restricts an emerging zoonotic malaria parasite. *Nat Commun*, 7:11187.

[111] Darbonne, W. C., Rice, G. C., Mohler, M. A., Apple, T., Hebert, C. A., Valente, A. J., and Baker, J. B. (1991). Red blood cells are a sink for interleukin 8, a leukocyte chemotaxin. *J Clin Invest*, 88(4):1362–9.

[112] de Cassan, S. C., Shakri, A. R., Llewellyn, D., Elias, S. C., Cho, J. S., Goodman, A. L., Jin, J., Douglas, A. D., Suwanarusk, R., Nosten, F. H., Renia, L., Russell, B., Chitnis, C. E., and Draper, S. J. (2015). Preclinical assessment of viral vectored and protein vaccines targeting the Duffy-binding protein region ii of *Plasmodium vivax*. *Front Immunol*, 6:348.

[113] Deal, C., Balazs, A. B., Espinosa, D. A., Zavala, F., Baltimore, D., and Ketner, G. (2014). Vectored antibody gene delivery protects against *Plasmodium falciparum* sporozoite challenge in mice. *Proc Natl Acad Sci U S A*, 111(34):12528–32.

[114] Dejnirattisai, W., Jumnainsong, A., Onsirisakul, N., Fitton, P., Vasanawathana, S., Limpitikul, W., Puttikhunt, C., Edwards, C., Duangchinda, T., Supasa, S., Chawansuntati, K., Malasit, P., Mongkolsapaya, J., and Screaton, G. (2010). Cross-reacting antibodies enhance dengue virus infection in humans. *Science*, 328(5979):745–8.

[115] del Portillo, H. A., Fernandez-Becerra, C., Bowman, S., Oliver, K., Preuss, M., Sanchez, C. P., Schneider, N. K., Villalobos, J. M., Rajandream, M. A., Harris, D., Pereira da Silva, L. H., Barrell, B., and Lanzer, M. (2001). A superfamily of variant genes encoded in the subtelomeric region of *Plasmodium vivax*. *Nature*, 410(6830):839–42.

[116] Dennis, E. D., Mitchell, G. H., Butcher, G. A., and Cohen, S. (1975). In vitro isolation of *Plasmodium knowlesi* merozoites using polycarbonate sieves. *Parasitology*, 71(3):475–81.

[117] Diamant, E., Lachmi, B. E., Keren, A., Barnea, A., Marcus, H., Cohen, S., David, A. B., and Zichel, R. (2014). Evaluating the synergistic neutralizing effect of anti-botulinum oligoclonal antibody preparations. *PLoS One*, 9(1):e87089.

[118] Diggs, C., Joseph, K., Flemmings, B., Snodgrass, R., and Hines, F. (1975). Protein synthesis in vitro by cryopreserved *Plasmodium falciparum*. *Am J Trop Med Hyg*, 24(5):760–3.

[119] Dobson, M. J. (1994). Malaria in England: a geographical and historical perspective. *Parassitologia*, 36(1-2):35–60.

[120] Dobson, M. J., Malowany, M., and Snow, R. W. (2000). Malaria control in East Africa: the Kampala conference and the pare-taveta scheme: a meeting of common and high ground. *Parassitologia*, 42(1-2):149–66.

[121] Dondorp, A. M., Fanello, C. I., Hendriksen, I. C., Gomes, E., Seni, A., Chhaganlal, K. D., Bojang, K., Olaosebikan, R., Anunobi, N., Maitland, K., Kivaya, E., Agbenyega, T., Nguah, S. B., Evans, J., Gesase, S., Kahabuka, C., Mtove, G., Nadjm, B., Deen, J., Mwanga-Amumpaire, J., Nansumba, M., Karema, C., Umulisa, N., Uwimana, A., Mokuolu, O. A., Adedoyin, O. T., Johnson, W. B., Tshefu, A. K., Onyamboko, M. A., Sakulthaew, T., Ngum, W. P., Silamut, K., Stepniewska, K., Woodrow, C. J., Bethell, D., Wills, B., Oneko, M., Peto, T. E., von Seidlein, L., Day, N. P., White, N. J., and group, A. (2010). Artesunate versus quinine in the treatment of severe *falciparum* malaria in African children (aquamat): an open-label, randomised trial. *Lancet*, 376(9753):1647–57.

[122] Douglas, A. D., Baldeviano, G. C., Lucas, C. M., Lugo-Roman, L. A., Crosnier, C., Bartholdson, S. J., Diouf, A., Miura, K., Lambert, L. E., Ventocilla, J. A., Leiva, K. P., Milne, K. H., Illingworth, J. J., Spencer, A. J., Hjerrild, K. A., Alanine, D. G., Turner, A. V., Moorhead, J. T., Edgel, K. A., Wu, Y., Long, C. A., Wright, G. J., Lescano, A. G., and Draper, S. J. (2015). A PFRH5-based vaccine is efficacious against heterologous strain blood-stage *Plasmodium falciparum* infection in *Aotus* monkeys. *Cell Host Microbe*, 17(1):130–9.

[123] Douglas, A. D., Williams, A. R., Knuepfer, E., Illingworth, J. J., Furze, J. M., Crosnier, C., Choudhary, P., Bustamante, L. Y., Zakutansky, S. E., Awuah, D. K., Alanine, D. G., Theron, M., Worth, A., Shimkets, R., Rayner, J. C., Holder, A. A., Wright, G. J., and Draper, S. J. (2014). Neutralization of *Plasmodium falciparum* merozoites by antibodies against PFRH5. *J Immunol*, 192(1):245–58.

[124] Draper, S. J., Sack, B. K., King, C. R., Nielsen, C. M., Rayner, J. C., Higgins, M. K., Long, C. A., and Seder, R. A. (2018). Malaria vaccines: Recent advances and new horizons. *Cell Host Microbe*, 24(1):43–56.

[125] Ehrlich (1881). Uber einige Beobachtungen am anamischen Blut. *Berl Klin Wschr 18: 43.*

[126] Ekiert, D. C. and Wilson, I. A. (2012). Broadly neutralizing antibodies against influenza virus and prospects for universal therapies. *Curr Opin Virol*, 2(2):134–41.

[127] Escalante, A. A. and Ayala, F. J. (1995). Evolutionary origin of *Plasmodium* and other *Apicomplexa* based on rRNA genes. *Proc Natl Acad Sci U S A*, 92(13):5793–7.

[128] Escalante, A. A., Barrio, E., and Ayala, F. J. (1995). Evolutionary origin of human and primate malarias: evidence from the circumsporozoite protein gene. *Mol Biol Evol*, 12(4):616–26.

[129] Escalante, A. A., Freeland, D. E., Collins, W. E., and Lal, A. A. (1998). The evolution of primate malaria parasites based on the gene encoding cytochrome b from the linear mitochondrial genome. *Proc Natl Acad Sci U S A*, 95(14):8124–9.

[130] Ewer, K. J., Lambe, T., Rollier, C. S., Spencer, A. J., Hill, A. V., and Dorrell, L. (2016). Viral vectors as vaccine platforms: from immunogenicity to impact. *Curr Opin Immunol*, 41:47–54.

[131] Feachem, R. G., Phillips, A. A., Hwang, J., Cotter, C., Wielgosz, B., Greenwood, B. M., Sabot, O., Rodriguez, M. H., Abeyasinghe, R. R., Ghebreyesus, T. A., and Snow, R. W. (2010). Shrinking the malaria map: progress and prospects. *Lancet*, 376(9752):1566–78.

[132] Fiore-Gartland, A., Manso, B. A., Friedrich, D. P., Gabriel, E. E., Finak, G., Moodie, Z., Hertz, T., De Rosa, S. C., Frahm, N., Gilbert, P. B., and McElrath, M. J. (2016). Pooled-peptide epitope mapping strategies are efficient and highly

sensitive: An evaluation of methods for identifying human T cell epitope specificities in large-scale HIV vaccine efficacy trials. *PLoS One*, 11(2):e0147812.

[133] Fong, T. (1937). A study of the mortality rate and complications following therapeutic malaria. *South. Med. J. 30, 1084–1088.*

[134] Foquet, L., Schafer, C., Minkah, N. K., Alanine, D. G. W., Flannery, E. L., Steel, R. W. J., Sack, B. K., Camargo, N., Fishbaugher, M., Betz, W., Nguyen, T., Billman, Z. P., Wilson, E. M., Bial, J., Murphy, S. C., Draper, S. J., Mikolajczak, S. A., and Kappe, S. H. I. (2018). *Plasmodium falciparum* liver stage infection and transition to stable blood stage infection in liver-humanized and blood-humanized FRGN KO mice enables testing of blood stage inhibitory antibodies (reticulocyte-binding protein homolog 5) in vivo. *Front Immunol*, 9:524.

[135] Fox, J. L. (2013). Anthrax drug first antibacterial mAb to win approval. *Nat Biotechnol*, 31(1):8.

[136] Frech, C. and Chen, N. (2011). Genome comparison of human and non-human malaria parasites reveals species subset-specific genes potentially linked to human disease. *PLoS Comput Biol*, 7(12):e1002320.

[137] Freund, J., Thomson, K. J., Sommer, H. E., Walter, A. W., and Schenkein, E. L. (1945). Immunization of *Rhesus* monkeys against malarial infection (*P. knowlesi*) with killed parasites and adjuvants. *Science*, 102(2643):202–4.

[138] Fryauff, D. J., Tuti, S., Mardi, A., Masbar, S., Patipelohi, R., Leksana, B., Kain, K. C., Bangs, M. J., Richie, T. L., and Baird, J. K. (1998). Chloroquine-resistant *Plasmodium vivax* in transmigration settlements of West Kalimantan, Indonesia. *Am J Trop Med Hyg*, 59(4):513–8.

[139] Fukuma, N., Akimitsu, N., Hamamoto, H., Kusuhara, H., Sugiyama, Y., and Sekimizu, K. (2003). A role of the Duffy antigen for the maintenance of plasma chemokine concentrations. *Biochem Biophys Res Commun*, 303(1):137–9.

[140] Galinski, M. R. and Barnwell, J. W. (1996). *Plasmodium vivax*: Merozoites, invasion of reticulocytes and considerations for malaria vaccine development. *Parasitol Today*, 12(1):20–9.

[141] Galinski, M. R., Medina, C. C., Ingravallo, P., and Barnwell, J. W. (1992). A reticulocyte-binding protein complex of *Plasmodium vivax* merozoites. *Cell*, 69(7):1213–26.

[142] Galinski, M. R., Meyer, E. V., and Barnwell, J. W. (2013). *Plasmodium vivax*: modern strategies to study a persistent parasite's life cycle. *Adv Parasitol*, 81:1–26.

[143] Gardner, M. R., Kattenhorn, L. M., Kondur, H. R., von Schaewen, M., Dorfman, T., Chiang, J. J., Haworth, K. G., Decker, J. M., Alpert, M. D., Bailey, C. C., Neale, E. S., J., Fellinger, C. H., Joshi, V. R., Fuchs, S. P., Martinez-Navio, J. M., Quinlan, B. D., Yao, A. Y., Mouquet, H., Gorman, J., Zhang, B., Poignard, P., Nussenzweig, M. C., Burton, D. R., Kwong, P. D., Piatak, M., J., Lifson, J. D., Gao, G., Desrosiers, R. C., Evans, D. T., Hahn, B. H., Ploss, A., Cannon, P. M., Seaman, M. S., and Farzan, M. (2015). AAV-expressed eCD4-Ig provides durable protection from multiple SIV challenges. *Nature*, 519(7541):87–91.

[144] Garnham, P. C. C. (1996.). Malaria parasites and other *Haemosporidia. Blackwell, London, United Kingdom.*

[145] Gething, P. W., Elyazar, I. R., Moyes, C. L., Smith, D. L., Battle, K. E., Guerra, C. A., Patil, A. P., Tatem, A. J., Howes, R. E., Myers, M. F., George, D. B., Horby, P., Wertheim, H. F., Price, R. N., Mueller, I., Baird, J. K., and Hay, S. I. (2012). A long neglected world malaria map: *Plasmodium vivax* endemicity in 2010. *PLoS Negl Trop Dis*, 6(9):e1814.

[146] Ghorbal, M., Gorman, M., Macpherson, C. R., Martins, R. M., Scherf, A., and Lopez-Rubio, J. J. (2014). Genome editing in the human malaria parasite

Plasmodium falciparum using the CRISPR-Cas9 system. *Nat Biotechnol*, 32(8):819–21.

[147] Godoy-Lozano, E. E., Tellez-Sosa, J., Sanchez-Gonzalez, G., Samano-Sanchez, H., Aguilar-Salgado, A., Salinas-Rodriguez, A., Cortina-Ceballos, B., Vivanco-Cid, H., Hernandez-Flores, K., Pfaff, J. M., Kahle, K. M., Doranz, B. J., Gomez-Barreto, R. E., Valdovinos-Torres, H., Lopez-Martinez, I., Rodriguez, M. H., and Martinez-Barnetche, J. (2016). Lower IgG somatic hypermutation rates during acute dengue virus infection is compatible with a germinal center-independent B cell response. *Genome Med*, 8(1):23.

[148] Golenda, C. F., Li, J., and Rosenberg, R. (1997). Continuous in vitro propagation of the malaria parasite *Plasmodium vivax*. *Proc Natl Acad Sci U S A*, 94(13):6786–91.

[149] Goller, J. L., Jolley, D., Ringwald, P., and Biggs, B. A. (2007). Regional differences in the response of *Plasmodium vivax* malaria to primaquine as anti-relapse therapy. *Am J Trop Med Hyg*, 76(2):203–7.

[150] Grassi, B., Bignami, A., and Bastianelli, G. (1899). Medical zoology: Further researches upon the cycle of human malaria in the body of the mosquito. *Ind Med Gaz*, 34(3):104–107.

[151] Greenwood, B. (2014). The contribution of vaccination to global health: past, present and future. *Philos Trans R Soc Lond B Biol Sci*, 369(1645):20130433.

[152] Greenwood, B. and Targett, G. (2009). Do we still need a malaria vaccine? *Parasite Immunol*, 31(9):582–6.

[153] Griffin, J. T., Hollingsworth, T. D., Okell, L. C., Churcher, T. S., White, M., Hinsley, W., Bousema, T., Drakeley, C. J., Ferguson, N. M., Basanez, M. G., and Ghani, A. C. (2010). Reducing *Plasmodium falciparum* malaria transmission in Africa: a model-based evaluation of intervention strategies. *PLoS Med*, 7(8).

[154] Grimberg, B. T., Udomsangpetch, R., Xainli, J., McHenry, A., Panichakul, T., Sattabongkot, J., Cui, L., Bockarie, M., Chitnis, C., Adams, J., Zimmerman, P. A., and King, C. L. (2007). *Plasmodium vivax* invasion of human erythrocytes inhibited by antibodies directed against the Duffy binding protein. *PLoS Med*, 4(12):e337.

[155] Gruring, C., Moon, R. W., Lim, C., Holder, A. A., Blackman, M. J., and Duraisingh, M. T. (2014). Human red blood cell-adapted *Plasmodium knowlesi* parasites: a new model system for malaria research. *Cell Microbiol*, 16(5):612–20.

[156] Gruszczyk, J., Kanjee, U., Chan, L. J., Menant, S., Malleret, B., Lim, N. T. Y., Schmidt, C. Q., Mok, Y. F., Lin, K. M., Pearson, R. D., Rangel, G., Smith, B. J., Call, M. J., Weekes, M. P., Griffin, M. D. W., Murphy, J. M., Abraham, J., Sriprawat, K., Menezes, M. J., Ferreira, M. U., Russell, B., Renia, L., Duraisingh, M. T., and Tham, W. H. (2018). Transferrin receptor 1 is a reticulocyte-specific receptor for *Plasmodium vivax*. *Science*, 359(6371):48–55.

[157] Guenaga, J., Dosenovic, P., Ofek, G., Baker, D., Schief, W. R., Kwong, P. D., Karlsson Hedestam, G. B., and Wyatt, R. T. (2011). Heterologous epitope-scaffold prime:boosting immuno-focuses B cell responses to the HIV-1 gp41 2f5 neutralization determinant. *PLoS One*, 6(1):e16074.

[158] Guevara Patino, J. A., Holder, A. A., McBride, J. S., and Blackman, M. J. (1997). Antibodies that inhibit malaria merozoite surface protein-1 processing and erythrocyte invasion are blocked by naturally acquired human antibodies. *J Exp Med*, 186(10):1689–99.

[159] Haigwood, N. L. (2015). HIV: tied down by its own receptor. *Nature*, 519(7541):36–7.

[160] Halbroth, B. R. and Draper, S. J. (2015). Recent developments in malaria vaccinology. *Adv Parasitol*, 88:1–49.

[161] Haldane, J. B. S. (1948). The rate of mutation of human genes. *Hereditas 35(Suppl.):267-273.*

[162] Hamblin, M. T. and Di Rienzo, A. (2000). Detection of the signature of natural selection in humans: evidence from the Duffy blood group locus. *Am J Hum Genet*, 66(5):1669–79.

[163] Hamers-Casterman, C., Atarhouch, T., Muyldermans, S., Robinson, G., Hamers, C., Songa, E. B., Bendahman, N., and Hamers, R. (1993). Naturally occurring antibodies devoid of light chains. *Nature*, 363(6428):446–8.

[164] Hamid, M. M., Remarque, E. J., El Hassan, I. M., Hussain, A. A., Narum, D. L., Thomas, A. W., Kocken, C. H., Weiss, W. R., and Faber, B. W. (2011). Malaria infection by sporozoite challenge induces high functional antibody titres against blood stage antigens after a DNA prime, poxvirus boost vaccination strategy in rhesus macaques. *Malar J*, 10:29.

[165] Handayani, S., Chiu, D. T., Tjitra, E., Kuo, J. S., Lampah, D., Kenangalem, E., Renia, L., Snounou, G., Price, R. N., Anstey, N. M., and Russell, B. (2009). High deformability of *Plasmodium vivax*-infected red blood cells under microfluidic conditions. *J Infect Dis*, 199(3):445–50.

[166] Hans, D., Pattnaik, P., Bhattacharyya, A., Shakri, A. R., Yazdani, S. S., Sharma, M., Choe, H., Farzan, M., and Chitnis, C. E. (2005). Mapping binding residues in the *Plasmodium vivax* domain that binds Duffy antigen during red cell invasion. *Mol Microbiol*, 55(5):1423–34.

[167] Harris, I., Sharrock, W. W., Bain, L. M., Gray, K. A., Bobogare, A., Boaz, L., Lilley, K., Krause, D., Vallely, A., Johnson, M. L., Gatton, M. L., Shanks, G. D., and Cheng, Q. (2010). A large proportion of asymptomatic *Plasmodium* infections with low and sub-microscopic parasite densities in the low transmission setting of Temotu Province, Solomon Islands: challenges for malaria diagnostics in an elimination setting. *Malar J*, 9:254.

[168] Haynes, J. D., Dalton, J. P., Klotz, F. W., McGinniss, M. H., Hadley, T. J., Hudson, D. E., and Miller, L. H. (1988). Receptor-like specificity of a *Plasmodium knowlesi* malarial protein that binds to Duffy antigen ligands on erythrocytes. *J Exp Med*, 167(6):1873–81.

[169] Hearty, S., Leonard, P., and O'Kennedy, R. (2012). Measuring antibody-antigen binding kinetics using surface plasmon resonance. *Methods Mol Biol*, 907:411–42.

[170] Hemmer, C. J., Holst, F. G., Kern, P., Chiwakata, C. B., Dietrich, M., and Reisinger, E. C. (2006). Stronger host response per parasitized erythrocyte in *Plasmodium vivax* or ovale than in *Plasmodium falciparum* malaria. *Trop Med Int Health*, 11(6):817–23.

[171] Herrera, S., Fernandez, O. L., Vera, O., Cardenas, W., Ramirez, O., Palacios, R., Chen-Mok, M., Corradin, G., and Arevalo-Herrera, M. (2011). Phase i safety and immunogenicity trial of *Plasmodium vivax* CS derived long synthetic peptides adjuvanted with montanide ISA 720 or montanide ISA 51. *Am J Trop Med Hyg*, 84(2 Suppl):12–20.

[172] Hester, J., Chan, E. R., Menard, D., Mercereau-Puijalon, O., Barnwell, J., Zimmerman, P. A., and Serre, D. (2013). De novo assembly of a field isolate genome reveals novel *Plasmodium vivax* erythrocyte invasion genes. *PLoS Negl Trop Dis*, 7(12):e2569.

[173] Hodgson, S. H., Choudhary, P., Elias, S. C., Milne, K. H., Rampling, T. W., Biswas, S., Poulton, I. D., Miura, K., Douglas, A. D., Alanine, D. G., Illingworth, J. J., de Cassan, S. C., Zhu, D., Nicosia, A., Long, C. A., Moyle, S., Berrie, E., Lawrie, A. M., Wu, Y., Ellis, R. D., Hill, A. V., and Draper, S. J. (2014). Combining viral vectored and protein-in-adjuvant vaccines against the blood-stage malaria antigen ama1: report on a phase 1a clinical trial. *Mol Ther*, 22(12):2142–54.

[174] Hoeppli, R. (1959). Parasites and parasitic infections in early medicine and science. *University of Malaya, Singapore, Singapore.*

[175] Hollingdale, M. R., Nardin, E. H., Tharavanij, S., Schwartz, A. L., and Nussenzweig, R. S. (1984). Inhibition of entry of *Plasmodium falciparum* and *P. vivax* sporozoites into cultured cells; an in vitro assay of protective antibodies. *J Immunol*, 132(2):909–13.

[176] Horuk, R., Chitnis, C. E., Darbonne, W. C., Colby, T. J., Rybicki, A., Hadley, T. J., and Miller, L. H. (1993). A receptor for the malarial parasite *Plasmodium vivax*: the erythrocyte chemokine receptor. *Science*, 261(5125):1182–4.

[177] Horuk, R., Wang, Z. X., Peiper, S. C., and Hesselgesser, J. (1994). Identification and characterization of a promiscuous chemokine-binding protein in a human erythroleukemic cell line. *J Biol Chem*, 269(26):17730–3.

[178] Horwitz, J. A., Bar-On, Y., Lu, C. L., Fera, D., Lockhart, A. A. K., Lorenzi, J. C. C., Nogueira, L., Golijanin, J., Scheid, J. F., Seaman, M. S., Gazumyan, A., Zolla-Pazner, S., and Nussenzweig, M. C. (2017). Non-neutralizing antibodies alter the course of HIV-1 infection in vivo. *Cell*, 170(4):637–648 e10.

[179] Houk, K. N., Leach, A. G., Kim, S. P., and Zhang, X. (2003). Binding affinities of host-guest, protein-ligand, and protein-transition-state complexes. *Angew Chem Int Ed Engl*, 42(40):4872–97.

[180] Howard, R. J., Barnwell, J. W., and Kao, V. (1983). Antigenic variation of *Plasmodium knowlesi* malaria: identification of the variant antigen on infected erythrocytes. *Proc Natl Acad Sci U S A*, 80(13):4129–33.

[181] Howell, K. A., Brannan, J. M., Bryan, C., McNeal, A., Davidson, E., Turner, H. L., Vu, H., Shulenin, S., He, S., Kuehne, A., Herbert, A. S., Qiu, X., Doranz, B. J., Holtsberg, F. W., Ward, A. B., Dye, J. M., and Aman, M. J. (2017). Cooperativity enables non-neutralizing antibodies to neutralize ebolavirus. *Cell Rep*, 19(2):413–424.

[182] Howes, R. E., Patil, A. P., Piel, F. B., Nyangiri, O. A., Kabaria, C. W., Gething, P. W., Zimmerman, P. A., Barnadas, C., Beall, C. M., Gebremedhin, A., Menard, D., Williams, T. N., Weatherall, D. J., and Hay, S. I. (2011). The global distribution of the Duffy blood group. *Nat Commun*, 2:266.

[183] Howes, R. E., Piel, F. B., Patil, A. P., Nyangiri, O. A., Gething, P. W., Dewi, M., Hogg, M. M., Battle, K. E., Padilla, C. D., Baird, J. K., and Hay, S. I. (2012). G6PD deficiency prevalence and estimates of affected populations in malaria endemic countries: a geostatistical model-based map. *PLoS Med*, 9(11):e1001339.

[184] Hu, S. L., Abrams, K., Barber, G. N., Moran, P., Zarling, J. M., Langlois, A. J., Kuller, L., Morton, W. R., and Benveniste, R. E. (1992). Protection of macaques against SIV infection by subunit vaccines of SIV envelope glycoprotein gp160. *Science*, 255(5043):456–9.

[185] Huang, J., Kang, B. H., Pancera, M., Lee, J. H., Tong, T., Feng, Y., Imamichi, H., Georgiev, I. S., Chuang, G. Y., Druz, A., Doria-Rose, N. A., Laub, L., Sliepen, K., van Gils, M. J., de la Pena, A. T., Derking, R., Klasse, P. J., Migueles, S. A., Bailer, R. T., Alam, M., Pugach, P., Haynes, B. F., Wyatt, R. T., Sanders, R. W., Binley, J. M., Ward, A. B., Mascola, J. R., Kwong, P. D., and Connors, M. (2014). Broad and potent HIV-1 neutralization by a human antibody that binds the gp41-gp120 interface. *Nature*, 515(7525):138–42.

[186] Hwang, S. Y., Kim, S. H., and Kho, W. G. (2009). Genetic characteristics of polymorphic antigenic markers among Korean isolates of *Plasmodium vivax*. *Korean J Parasitol*, 47 Suppl:S51–8.

[187] Ikin, E. W., Mourant, A. E., Pettenkofer, H. J., and Blumenthal, G. (1951). Discovery of the expected haemagglutinin, anti-fyb. *Nature*, 168(4288):1077–8.

[188] Imai, T., Ishida, H., Suzue, K., Hirai, M., Taniguchi, T., Okada, H., Suzuki, T., Shimokawa, C., and Hisaeda, H. (2013). CD8(+) T cell activation by murine erythroblasts infected with malaria parasites. *Sci Rep*, 3:1572.

[189] Impagliazzo, A., Milder, F., Kuipers, H., Wagner, M. V., Zhu, X., Hoffman, R. M., van Meersbergen, R., Huizingh, J., Wanningen, P., Verspuij, J., de Man, M., Ding, Z., Apetri, A., Kukrer, B., Sneekes-Vriese, E., Tomkiewicz, D., Laursen, N. S., Lee, P. S., Zakrzewska, A., Dekking, L., Tolboom, J., Tettero, L., van Meerten, S., Yu, W., Koudstaal, W., Goudsmit, J., Ward, A. B., Meijberg, W., Wilson, I. A., and Radosevic, K. (2015). A stable trimeric influenza hemagglutinin stem as a broadly protective immunogen. *Science*, 349(6254):1301–6.

[190] Imwong, M., Snounou, G., Pukrittayakamee, S., Tanomsing, N., Kim, J. R., Nandy, A., Guthmann, J. P., Nosten, F., Carlton, J., Looareesuwan, S., Nair, S., Sudimack, D., Day, N. P., Anderson, T. J., and White, N. J. (2007). Relapses of *Plasmodium vivax* infection usually result from activation of heterologous hypnozoites. *J Infect Dis*, 195(7):927–33.

[191] Jin, J., Hjerrild, K. A., Silk, S. E., Brown, R. E., Labbe, G. M., Marshall, J. M., Wright, K. E., Bezemer, S., Clemmensen, S. B., Biswas, S., Li, Y., El-Turabi, A., Douglas, A. D., Hermans, P., Detmers, F. J., de Jongh, W. A., Higgins, M. K., Ashfield, R., and Draper, S. J. (2017). Accelerating the clinical development of protein-based vaccines for malaria by efficient purification using a four amino acid C-terminal 'C-tag'. *Int J Parasitol*, 47(7):435–446.

[192] Johnson, P. R., Schnepp, B. C., Zhang, J., Connell, M. J., Greene, S. M., Yuste, E., Desrosiers, R. C., and Clark, K. R. (2009). Vector-mediated gene transfer engenders long-lived neutralizing activity and protection against SIV infection in monkeys. *Nat Med*, 15(8):901–6.

[193] Jones, W. H. S. et al. (1886). Airs, waters and places. *The genuine works of Hippocrates*, page 171.

[194] Joyce, M. G., Kanekiyo, M., Xu, L., Biertumpfel, C., Boyington, J. C., Moquin, S., Shi, W., Wu, X., Yang, Y., Yang, Z. Y., Zhang, B., Zheng, A., Zhou, T., Zhu, J., Mascola, J. R., Kwong, P. D., and Nabel, G. J. (2013). Outer

domain of HIV-1 gp120: antigenic optimization, structural malleability, and crystal structure with antibody vrc-pg04. *J Virol*, 87(4):2294–306.

[195] Ju, H. L., Kang, J. M., Moon, S. U., Bahk, Y. Y., Cho, P. Y., Sohn, W. M., Park, Y. K., Park, J. W., Kim, T. S., and Na, B. K. (2013). Genetic diversity and natural selection of Duffy binding protein of *Plasmodium vivax* korean isolates. *Acta Trop*, 125(1):67–74.

[196] Ju, H. L., Kang, J. M., Moon, S. U., Kim, J. Y., Lee, H. W., Lin, K., Sohn, W. M., Lee, J. S., Kim, T. S., and Na, B. K. (2012). Genetic polymorphism and natural selection of Duffy binding protein of *Plasmodium vivax* Myanmar isolates. *Malar J*, 11:60.

[197] Kaewpongsri, S., Sriprawat, K., Suwanarusk, R., Kyle, D. E., Lek-Uthai, U., Leimanis, M., Lwin, K. M., Phyo, A. P., Zwang, J., Russell, B., Nosten, F., and Renia, L. (2011). The presence of leukocytes in ex vivo assays significantly increases the 50-percent inhibitory concentrations of artesunate and chloroquine against *Plasmodium vivax* and *Plasmodium falciparum*. *Antimicrob Agents Chemother*, 55(3):1300–4.

[198] Karunajeewa, H. A., Mueller, I., Senn, M., Lin, E., Law, I., Gomorrai, P. S., Oa, O., Griffin, S., Kotab, K., Suano, P., Tarongka, N., Ura, A., Lautu, D., Page-Sharp, M., Wong, R., Salman, S., Siba, P., Ilett, K. F., and Davis, T. M. (2008). A trial of combination antimalarial therapies in children from Papua New Guinea. *N Engl J Med*, 359(24):2545–57.

[199] Kennedy, M. C., Wang, J., Zhang, Y., Miles, A. P., Chitsaz, F., Saul, A., Long, C. A., Miller, L. H., and Stowers, A. W. (2002). In vitro studies with recombinant *Plasmodium falciparum* apical membrane antigen 1 (ama1): production and activity of an ama1 vaccine and generation of a multiallelic response. *Infect Immun*, 70(12):6948–60.

[200] King, C. L., Adams, J. H., Xianli, J., Grimberg, B. T., McHenry, A. M., Greenberg, L. J., Siddiqui, A., Howes, R. E., da Silva-Nunes, M., Ferreira, M. U., and Zimmerman, P. A. (2011). Fy(a)/fy(b) antigen polymorphism in human erythrocyte Duffy antigen affects susceptibility to *Plasmodium vivax* malaria. *Proc Natl Acad Sci U S A*, 108(50):20113–8.

[201] King, C. L., Michon, P., Shakri, A. R., Marcotty, A., Stanisic, D., Zimmerman, P. A., Cole-Tobian, J. L., Mueller, I., and Chitnis, C. E. (2008). Naturally acquired Duffy-binding protein-specific binding inhibitory antibodies confer protection from blood-stage *Plasmodium vivax* infection. *Proc Natl Acad Sci U S A*, 105(24):8363–8.

[202] Kirkman, L. A., Lawrence, E. A., and Deitsch, K. W. (2014). Malaria parasites utilize both homologous recombination and alternative end joining pathways to maintain genome integrity. *Nucleic Acids Res*, 42(1):370–9.

[203] Kitchen, S. (1949). Symptomatology: general considerations. *In: Boyd, M.F. (Ed.), Malariology, W.B. Saunders, Philadelphia, pp. 966–994.*

[204] Knowles, R. and Gupta, B. M. D. (1932a). Clinical studies in malaria by cultural and enumerative methods. second series. *Ind Med Gaz*, 67(8):432–446.

[205] Knowles, R. and Gupta, B. M. D. (1932b). A study of monkey-malaria, and its experimental transmission to man. *Ind Med Gaz*, 67(6):301–320.

[206] Koch, R. (1900). Professor Koch's Investigations on Malaria: Fourth report to the colonial department of the German colonial office. *Br Med J*, 1(2061):1597–8.

[207] Kocken, C. H., Ozwara, H., van der Wel, A., Beetsma, A. L., Mwenda, J. M., and Thomas, A. W. (2002). *Plasmodium knowlesi* provides a rapid in vitro and in vivo transfection system that enables double-crossover gene knockout studies. *Infect Immun*, 70(2):655–60.

[208] Kohler, G. and Milstein, C. (1975). Continuous cultures of fused cells secreting antibody of predefined specificity. *Nature*, 256(5517):495–7.

[209] Koide, S., Yang, X., Huang, X., Dunn, J. J., and Luft, B. J. (2005). Structure-based design of a second-generation lyme disease vaccine based on a c-terminal fragment of *Borrelia burgdorferi* ospA. *J Mol Biol*, 350(2):290–9.

[210] Kosaisavee, V., Suwanarusk, R., Nosten, F., Kyle, D. E., Barrends, M., Jones, J., Price, R., Russell, B., and Lek-Uthai, U. (2006). *Plasmodium vivax*: isotopic, picogreen, and microscopic assays for measuring chloroquine sensitivity in fresh and cryopreserved isolates. *Exp Parasitol*, 114(1):34–9.

[211] Krogstad, D. J., Gluzman, I. Y., Kyle, D. E., Oduola, A. M., Martin, S. K., Milhous, W. K., and Schlesinger, P. H. (1987). Efflux of chloroquine from *Plasmodium falciparum*: mechanism of chloroquine resistance. *Science*, 238(4831):1283–5.

[212] Krotoski, W. A., Collins, W. E., Bray, R. S., Garnham, P. C., Cogswell, F. B., Gwadz, R. W., Killick-Kendrick, R., Wolf, R., Sinden, R., Koontz, L. C., and Stanfill, P. S. (1982). Demonstration of hypnozoites in sporozoite-transmitted *Plasmodium vivax* infection. *Am J Trop Med Hyg*, 31(6):1291–3.

[213] Krotoski, W. A., Krotoski, D. M., Garnham, P. C., Bray, R. S., Killick-Kendrick, R., Draper, C. C., Targett, G. A., and Guy, M. W. (1980). Relapses in primate malaria: discovery of two populations of exoerythrocytic stages. preliminary note. *Br Med J*, 280(6208):153–4.

[214] Kudo, R. R. (1971). Protozoology. *Charles C. Thomas, Springfield, Ill.*

[215] Kumar, S. and Hedges, S. B. (1998). A molecular timescale for vertebrate evolution. *Nature*, 392(6679):917–20.

[216] Kwong, P. D., Mascola, J. R., and Nabel, G. J. (2011). Rational design of vaccines to elicit broadly neutralizing antibodies to HIV-1. *Cold Spring Harb Perspect Med*, 1(1):a007278.

[217] Lacerda, M. V., Fragoso, S. C., Alecrim, M. G., Alexandre, M. A., Magalhaes, B. M., Siqueira, A. M., Ferreira, L. C., Araujo, J. R., Mourao, M. P., Ferrer, M., Castillo, P., Martin-Jaular, L., Fernandez-Becerra, C., del Portillo, H., Ordi, J., Alonso, P. L., and Bassat, Q. (2012). Postmortem characterization of patients with clinical diagnosis of *Plasmodium vivax* malaria: to what extent does this parasite kill? *Clin Infect Dis*, 55(8):e67–74.

[218] Lapp, S. A., Mok, S., Zhu, L., Wu, H., Preiser, P. R., Bozdech, Z., and Galinski, M. R. (2015). *Plasmodium knowlesi* gene expression differs in ex vivo compared to in vitro blood-stage cultures. *Malar J*, 14:110.

[219] Laveran, C. (1880). Note sur un nouveau parasite trouvé dans le sang de plusieurs malades atteints de fièvre palustres. *Bull. Acad. Natl. Med. (Paris)*.

[220] Lee, E. C., Liang, Q., Ali, H., Bayliss, L., Beasley, A., Bloomfield-Gerdes, T., Bonoli, L., Brown, R., Campbell, J., Carpenter, A., Chalk, S., Davis, A., England, N., Fane-Dremucheva, A., Franz, B., Germaschewski, V., Holmes, H., Holmes, S., Kirby, I., Kosmac, M., Legent, A., Lui, H., Manin, A., O'Leary, S., Paterson, J., Sciarrillo, R., Speak, A., Spensberger, D., Tuffery, L., Waddell, N., Wang, W., Wells, S., Wong, V., Wood, A., Owen, M. J., Friedrich, G. A., and Bradley, A. (2014). Complete humanization of the mouse immunoglobulin loci enables efficient therapeutic antibody discovery. *Nat Biotechnol*, 32(4):356–63.

[221] Li, J., Iwamoto, S., Sugimoto, N., Okuda, H., and Kajii, E. (1997). Dinucleotide repeat in the 3' flanking region provides a clue to the molecular evolution of the Duffy gene. *Hum Genet*, 99(5):573–7.

[222] Liljeroos, L., Malito, E., Ferlenghi, I., and Bottomley, M. J. (2015). Structural and computational biology in the design of immunogenic vaccine antigens. *J Immunol Res*, 2015:156241.

[223] Lim, C., Hansen, E., DeSimone, T. M., Moreno, Y., Junker, K., Bei, A., Brugnara, C., Buckee, C. O., and Duraisingh, M. T. (2013). Expansion of host

cellular niche can drive adaptation of a zoonotic malaria parasite to humans. *Nat Commun*, 4:1638.

[224] Lin, E., Kiniboro, B., Gray, L., Dobbie, S., Robinson, L., Laumaea, A., Schopflin, S., Stanisic, D., Betuela, I., Blood-Zikursh, M., Siba, P., Felger, I., Schofield, L., Zimmerman, P., and Mueller, I. (2010). Differential patterns of infection and disease with *P. falciparum* and *P. vivax* in young Papua New Guinean children. *PLoS One*, 5(2):e9047.

[225] Liu, W., Li, Y., Learn, G. H., Rudicell, R. S., Robertson, J. D., Keele, B. F., Ndjango, J. B., Sanz, C. M., Morgan, D. B., Locatelli, S., Gonder, M. K., Kranzusch, P. J., Walsh, P. D., Delaporte, E., Mpoudi-Ngole, E., Georgiev, A. V., Muller, M. N., Shaw, G. M., Peeters, M., Sharp, P. M., Rayner, J. C., and Hahn, B. H. (2010). Origin of the human malaria parasite *Plasmodium falciparum* in gorillas. *Nature*, 467(7314):420–5.

[226] Liu, W., Li, Y., Shaw, K. S., Learn, G. H., Plenderleith, L. J., Malenke, J. A., Sundararaman, S. A., Ramirez, M. A., Crystal, P. A., Smith, A. G., Bibollet-Ruche, F., Ayouba, A., Locatelli, S., Esteban, A., Mouacha, F., Guichet, E., Butel, C., Ahuka-Mundeke, S., Inogwabini, B. I., Ndjango, J. B., Speede, S., Sanz, C. M., Morgan, D. B., Gonder, M. K., Kranzusch, P. J., Walsh, P. D., Georgiev, A. V., Muller, M. N., Piel, A. K., Stewart, F. A., Wilson, M. L., Pusey, A. E., Cui, L., Wang, Z., Farnert, A., Sutherland, C. J., Nolder, D., Hart, J. A., Hart, T. B., Bertolani, P., Gillis, A., LeBreton, M., Tafon, B., Kiyang, J., Djoko, C. F., Schneider, B. S., Wolfe, N. D., Mpoudi-Ngole, E., Delaporte, E., Carter, R., Culleton, R. L., Shaw, G. M., Rayner, J. C., Peeters, M., Hahn, B. H., and Sharp, P. M. (2014). African origin of the malaria parasite *Plasmodium vivax*. *Nat Commun*, 5:3346.

[227] Loy, D. E., Liu, W., Li, Y., Learn, G. H., Plenderleith, L. J., Sundararaman, S. A., Sharp, P. M., and Hahn, B. H. (2017). Out of Africa: origins and evolution of the human malaria parasites *Plasmodium falciparum* and *Plasmodium vivax*. *International journal for parasitology*, 47(2-3):87–97.

[228] Luxemburger, C., Perea, W. A., Delmas, G., Pruja, C., Pecoul, B., and Moren, A. (1994). Permethrin-impregnated bed nets for the prevention of malaria in schoolchildren on the thai-burmese border. *Trans R Soc Trop Med Hyg*, 88(2):155–9.

[229] Luxemburger, C., Thwai, K., White, N., Webster, H., Kyle, D., Maelankirri, L., Chongsuphajaisiddhi, T., and Nosten, F. (1996). The epidemiology of malaria in a Karen population on the Western border of Thailand. *Trans R Soc Trop Med Hyg 90: 105–111.*

[230] Mahdi Abdel Hamid, M., Remarque, E. J., van Duivenvoorde, L. M., van der Werff, N., Walraven, V., Faber, B. W., Kocken, C. H., and Thomas, A. W. (2011). Vaccination with *Plasmodium knowlesi* AMA1 formulated in the novel adjuvant co-vaccine HT protects against blood-stage challenge in rhesus macaques. *PLoS One*, 6(5):e20547.

[231] Malito, E., Lo Surdo, P., Veggi, D., Santini, L., Stefek, H., Brunelli, B., Luzzi, E., Bottomley, M. J., Beernink, P. T., and Scarselli, M. (2016). *Neisseria meningitidis* factor H-binding protein bound to monoclonal antibody JAR5: implications for antibody synergy. *Biochem J*, 473(24):4699–4713.

[232] Malkin, E. M., Durbin, A. P., Diemert, D. J., Sattabongkot, J., Wu, Y., Miura, K., Long, C. A., Lambert, L., Miles, A. P., Wang, J., Stowers, A., Miller, L. H., and Saul, A. (2005). Phase 1 vaccine trial of Pvs25h: a transmission blocking vaccine for *Plasmodium vivax* malaria. *Vaccine*, 23(24):3131–8.

[233] Malleret, B., Li, A., Zhang, R., Tan, K. S., Suwanarusk, R., Claser, C., Cho, J. S., Koh, E. G., Chu, C. S., Pukrittayakamee, S., Ng, M. L., Ginhoux, F., Ng, L. G., Lim, C. T., Nosten, F., Snounou, G., Renia, L., and Russell, B. (2015). *Plasmodium vivax*: restricted tropism and rapid remodeling of CD71-positive reticulocytes. *Blood*, 125(8):1314–24.

[234] Malleret, B., Xu, F., Mohandas, N., Suwanarusk, R., Chu, C., Leite, J. A., Low, K., Turner, C., Sriprawat, K., Zhang, R., Bertrand, O., Colin, Y., Costa, F. T., Ong, C. N., Ng, M. L., Lim, C. T., Nosten, F., Renia, L., and Russell, B. (2013). Significant biochemical, biophysical and metabolic diversity in circulating human cord blood reticulocytes. *PLoS One*, 8(10):e76062.

[235] Malmqvist, M. (1999). Biacore: an affinity biosensor system for characterization of biomolecular interactions.

[236] Manson, P. (1900). Experimental proof of the mosquito malaria theory. *Br Med J*, 2(2074):949–51.

[237] Manwell, R. D. and Goldstein, F. (1940). Passive immunity in avian malaria. *J Exp Med*, 71(3):409–23.

[238] Martin-Jaular, L., Elizalde-Torrent, A., Thomson-Luque, R., Ferrer, M., Segovia, J. C., Herreros-Aviles, E., Fernandez-Becerra, C., and Del Portillo, H. A. (2013). Reticulocyte-prone malaria parasites predominantly invade CD71hi immature cells: implications for the development of an in vitro culture for *Plasmodium vivax*. *Malar J*, 12:434.

[239] Mascola, J. R., Sambor, A., Beaudry, K., Santra, S., Welcher, B., Louder, M. K., Vancott, T. C., Huang, Y., Chakrabarti, B. K., Kong, W. P., Yang, Z. Y., Xu, L., Montefiori, D. C., Nabel, G. J., and Letvin, N. L. (2005). Neutralizing antibodies elicited by immunization of monkeys with DNA plasmids and recombinant adenoviral vectors expressing human immunodeficiency virus type 1 proteins. *J Virol*, 79(2):771–9.

[240] Mathai, E. and Singh, B. (1989). A comparative study of two methods for the cryopreservation of *Plasmodium falciparum*. *Trans R Soc Trop Med Hyg*, 83(4):469–70.

[241] Mazur, P. (1970). Cryobiology: the freezing of biological systems. *Science*, 168(3934):939–49.

[242] McCafferty, J., Griffiths, A. D., Winter, G., and Chiswell, D. J. (1990). Phage antibodies: filamentous phage displaying antibody variable domains. *Nature*, 348(6301):552–4.

[243] McCarthy, J. S., Griffin, P. M., Sekuloski, S., Bright, A. T., Rockett, R., Looke, D., Elliott, S., Whiley, D., Sloots, T., Winzeler, E. A., and Trenholme, K. R. (2013). Experimentally induced blood-stage *Plasmodium vivax* infection in healthy volunteers. *J Infect Dis*, 208(10):1688–94.

[244] McGregor, I. A. (1964). The passive transfer of human malarial immunity. *Am J Trop Med Hyg*, 13:SUPPL 237–9.

[245] McHeyzer-Williams, L. J. and McHeyzer-Williams, M. G. (2005). Antigen-specific memory B cell development. *Annu Rev Immunol*, 23:487–513.

[246] McLellan, J. S., Chen, M., Joyce, M. G., Sastry, M., Stewart-Jones, G. B., Yang, Y., Zhang, B., Chen, L., Srivatsan, S., Zheng, A., Zhou, T., Graepel, K. W., Kumar, A., Moin, S., Boyington, J. C., Chuang, G. Y., Soto, C., Baxa, U., Bakker, A. Q., Spits, H., Beaumont, T., Zheng, Z., Xia, N., Ko, S. Y., Todd, J. P., Rao, S., Graham, B. S., and Kwong, P. D. (2013). Structure-based design of a fusion glycoprotein vaccine for respiratory syncytial virus. *Science*, 342(6158):592–8.

[247] McLellan, J. S., Correia, B. E., Chen, M., Yang, Y., Graham, B. S., Schief, W. R., and Kwong, P. D. (2011). Design and characterization of epitope-scaffold immunogens that present the motavizumab epitope from respiratory syncytial virus. *J Mol Biol*, 409(5):853–66.

[248] Mehlin, C., Boni, E., Buckner, F. S., Engel, L., Feist, T., Gelb, M. H., Haji, L., Kim, D., Liu, C., Mueller, N., Myler, P. J., Reddy, J. T., Sampson, J. N., Subramanian, E., Van Voorhis, W. C., Worthey, E., Zucker, F., and Hol, W. G. (2006). Heterologous expression of proteins from *Plasmodium falciparum*: results from 1000 genes. *Mol Biochem Parasitol*, 148(2):144–60.

[249] Menard, D., Barnadas, C., Bouchier, C., Henry-Halldin, C., Gray, L. R., Ratsimbasoa, A., Thonier, V., Carod, J. F., Domarle, O., Colin, Y., Bertrand, O., Picot, J., King, C. L., Grimberg, B. T., Mercereau-Puijalon, O., and Zimmerman, P. A. (2010). *Plasmodium vivax* clinical malaria is commonly observed in Duffy-negative Malagasy people. *Proc Natl Acad Sci U S A*, 107(13):5967–71.

[250] Mendis, K., Sina, B. J., Marchesini, P., and Carter, R. (2001). The neglected burden of *Plasmodium vivax* malaria. *Am J Trop Med Hyg*, 64(1-2 Suppl):97–106.

[251] Mestas, J. and Hughes, C. C. (2004). Of mice and not men: differences between mouse and human immunology. *J Immunol*, 172(5):2731–8.

[252] Michon, P., Cole-Tobian, J. L., Dabod, E., Schoepflin, S., Igu, J., Susapu, M., Tarongka, N., Zimmerman, P. A., Reeder, J. C., Beeson, J. G., Schofield, L., King, C. L., and Mueller, I. (2007). The risk of malarial infections and disease in Papua New Guinean children. *Am J Trop Med Hyg*, 76(6):997–1008.

[253] Miller, L. H., Aikawa, M., Johnson, J. G., and Shiroishi, T. (1979). Interaction between cytochalasin b-treated malarial parasites and erythrocytes. attachment and junction formation. *J Exp Med*, 149(1):172–84.

[254] Miller, L. H., Mason, S. J., Clyde, D. F., and McGinniss, M. H. (1976). The resistance factor to *Plasmodium vivax* in blacks. the Duffy-blood-group genotype, fyfy. *N Engl J Med*, 295(6):302–4.

[255] Miller, L. H., Mason, S. J., Dvorak, J. A., McGinniss, M. H., and Rothman, I. K. (1975). Erythrocyte receptors for (*Plasmodium knowlesi*) malaria: Duffy blood group determinants. *Science*, 189(4202):561–3.

[256] Milne, L. M., Kyi, M. S., Chiodini, P. L., and Warhurst, D. C. (1994). Accuracy of routine laboratory diagnosis of malaria in the united kingdom. *J Clin Pathol*, 47(8):740–2.

[257] Miura, K., Orcutt, A. C., Muratova, O. V., Miller, L. H., Saul, A., and Long, C. A. (2008). Development and characterization of a standardized elISA including a reference serum on each plate to detect antibodies induced by experimental malaria vaccines. *Vaccine*, 26(2):193–200.

[258] Miura, K., Zhou, H., Diouf, A., Moretz, S. E., Fay, M. P., Miller, L. H., Martin, L. B., Pierce, M. A., Ellis, R. D., Mullen, G. E., and Long, C. A. (2009). Anti-apical-membrane-antigen-1 antibody is more effective than anti-42-kilodalton-merozoite-surface-protein-1 antibody in inhibiting *Plasmodium falciparum* growth, as determined by the in vitro growth inhibition assay. *Clin Vaccine Immunol*, 16(7):963–8.

[259] Mohandas, N. and Gallagher, P. G. (2008). Red cell membrane: past, present, and future. *Blood*, 112(10):3939–48.

[260] Mons, B., Collins, W. E., Skinner, J. C., van der Star, W., Croon, J. J., and van der Kaay, H. J. (1988). *Plasmodium vivax*: in vitro growth and reinvasion in red blood cells of *Aotus nancymai*. *Exp Parasitol*, 66(2):183–8.

[261] Moon, R. W., Hall, J., Rangkuti, F., Ho, Y. S., Almond, N., Mitchell, G. H., Pain, A., Holder, A. A., and Blackman, M. J. (2013). Adaptation of the genetically tractable malaria pathogen *Plasmodium knowlesi* to continuous culture in human erythrocytes. *Proc Natl Acad Sci U S A*, 110(2):531–6.

[262] Moon, R. W., Sharaf, H., Hastings, C. H., Ho, Y. S., Nair, M. B., Rchiad, Z., Knuepfer, E., Ramaprasad, A., Mohring, F., Amir, A., Yusuf, N. A., Hall, J., Almond, N., Lau, Y. L., Pain, A., Blackman, M. J., and Holder, A. A. (2016). Normocyte-binding protein required for human erythrocyte invasion by the zoonotic malaria parasite *Plasmodium knowlesi*. *Proc Natl Acad Sci U S A*, 113(26):7231–6.

[263] Moorthy, V. S., Newman, R. D., and Okwo-Bele, J. M. (2013). Malaria vaccine technology roadmap. *Lancet*, 382(9906):1700–1.

[264] Moreno, A., Caro-Aguilar, I., Yazdani, S., Shakri, A., Lapp, S., Strobert, E., McClure, H., Chitnis, C., and Galinski, M. (2008). Preclinical assessment of the receptor-binding domain of *Plasmodium vivax* Duffy-binding protein as a vaccine candidate in rhesus macaques. *Vaccine*, 26(34):4338–4344.

[265] Mueller, I., Galinski, M. R., Tsuboi, T., Arevalo-Herrera, M., Collins, W. E., and King, C. L. (2013). Natural acquisition of immunity to *Plasmodium vivax*: epidemiological observations and potential targets. *Adv Parasitol*, 81:77–131.

[266] Mueller, I., Shakri, A. R., and Chitnis, C. E. (2015). Development of vaccines for *Plasmodium vivax* malaria. *Vaccine*, 33(52):7489–95.

[267] Muhlberger, N., Jelinek, T., Gascon, J., Probst, M., Zoller, T., Schunk, M., Beran, J., Gjorup, I., Behrens, R. H., Clerinx, J., Bjorkman, A., McWhinney, P., Matteelli, A., Lopez-Velez, R., Bisoffi, Z., Hellgren, U., Puente, S., Schmid, M. L., Myrvang, B., Holthoff-Stich, M. L., Laferl, H., Hatz, C., Kollaritsch, H., Kapaun, A., Knobloch, J., Iversen, J., Kotlowski, A., Malvy, D. J., Kern, P., Fry, G., Siikamaki, H., Schulze, M. H., Soula, G., Paul, M., Gomez i Prat, J., Lehmann, V., Bouchaud, O., da Cunha, S., Atouguia, J., and Boecken, G. (2004). Epidemiology and clinical features of *vivax* malaria imported to Europe: sentinel surveillance data from tropneteurop. *Malar J*, 3:5.

[268] Murphy, P. M. (1996). Chemokine receptors: structure, function and role in microbial pathogenesis. *Cytokine Growth Factor Rev*, 7(1):47–64.

[269] Nabel, G. J. (2013). Designing tomorrow's vaccines. *N Engl J Med*, 368(6):551–60.

[270] Nabel, G. J. and Fauci, A. S. (2010). Induction of unnatural immunity: prospects for a broadly protective universal influenza vaccine. *Nat Med*, 16(12):1389–91.

[271] Nabel, G. J., Kwong, P. D., and Mascola, J. R. (2011). Progress in the rational design of an AIDS vaccine. *Philos Trans R Soc Lond B Biol Sci*, 366(1579):2759–65.

[272] Ndiath, M. O., Mazenot, C., Sokhna, C., and Trape, J. F. (2014). How the malaria vector *Anopheles gambiae* adapts to the use of insecticide-treated nets by African populations. *PLoS One*, 9(6):e97700.

[273] Nevill, C. G., Some, E. S., Mung'ala, V. O., Mutemi, W., New, L., Marsh, K., Lengeler, C., and Snow, R. W. (1996). Insecticide-treated bednets reduce mortality and severe morbidity from malaria among children on the Kenyan coast. *Trop Med Int Health*, 1(2):139–46.

[274] Newby, G., Bennett, A., Larson, E., Cotter, C., Shretta, R., Phillips, A. A., and Feachem, R. G. (2016). The path to eradication: a progress report on the malaria-eliminating countries. *Lancet*, 387(10029):1775–84.

[275] Nibbs, R., Graham, G., and Rot, A. (2003). Chemokines on the move: control by the chemokine "interceptors" Duffy blood group antigen and d6. *Semin Immunol*, 15(5):287–94.

[276] Nichols, M. E., Rubinstein, P., Barnwell, J., Rodriguez de Cordoba, S., and Rosenfield, R. E. (1987). A new human Duffy blood group specificity defined by a murine monoclonal antibody. immunogenetics and association with susceptibility to *Plasmodium vivax*. *J Exp Med*, 166(3):776–85.

[277] Nicolajev, B. (1939). The duration and course of malaria infection in man. *Med. Parasitol.Parasit Dis. 8, 191.*

[278] Nicolete, V. C., Frischmann, S., Barbosa, S., King, C. L., and Ferreira, M. U. (2016). Naturally acquired binding-inhibitory antibodies to *Plasmodium vivax* Duffy binding protein and clinical immunity to malaria in rural Amazonians. *The Journal of infectious diseases*, 214(10):1539–1546.

[279] Nobrega de Sousa, T., Carvalho, L. H., and Alves de Brito, C. F. (2011). Worldwide genetic variability of the Duffy binding protein: insights into *Plasmodium vivax* vaccine development. *PLoS One*, 6(8):e22944.

[280] Nogueira, P. A., Alves, F. P., Fernandez-Becerra, C., Pein, O., Santos, N. R., Pereira da Silva, L. H., Camargo, E. P., and del Portillo, H. A. (2006). A reduced risk of infection with *Plasmodium vivax* and clinical protection against malaria are associated with antibodies against the n terminus but not the c terminus of merozoite surface protein 1. *Infect Immun*, 74(5):2726–33.

[281] Noulin, F., Borlon, C., Van Den Abbeele, J., D'Alessandro, U., and Erhart, A. (2013). 1912-2012: a century of research on *Plasmodium vivax* in vitro culture. *Trends Parasitol*, 29(6):286–94.

[282] Noulin, F., Borlon, C., van den Eede, P., Boel, L., Verfaillie, C. M., D'Alessandro, U., and Erhart, A. (2012). Cryopreserved reticulocytes derived from hematopoietic stem cells can be invaded by cryopreserved *Plasmodium vivax* isolates. *PLoS One*, 7(7):e40798.

[283] Ntumngia, F. B. and Adams, J. H. (2012). Design and immunogenicity of a novel synthetic antigen based on the ligand domain of the *Plasmodium vivax* Duffy binding protein. *Clin Vaccine Immunol*, 19(1):30–6.

[284] Ntumngia, F. B., Barnes, S. J., McHenry, A. M., George, M. T., Schloegel, J., and Adams, J. H. (2014). Immunogenicity of a synthetic vaccine based on *Plasmodium vivax* Duffy binding protein region ii. *Clin Vaccine Immunol*, 21(9):1215–23.

[285] Ntumngia, F. B., Schloegel, J., Barnes, S. J., McHenry, A. M., Singh, S., King, C. L., and Adams, J. H. (2012). Conserved and variant epitopes of *Plasmodium vivax* Duffy binding protein as targets of inhibitory monoclonal antibodies. *Infect Immun*, 80(3):1203–8.

[286] Ntumngia, F. B., Schloegel, J., McHenry, A. M., Barnes, S. J., George, M. T., Kennedy, S., and Adams, J. H. (2013). Immunogenicity of single versus mixed allele vaccines of *Plasmodium vivax* Duffy binding protein region ii. *Vaccine*, 31(40):4382–8.

[287] Nutt, S. L., Hodgkin, P. D., Tarlinton, D. M., and Corcoran, L. M. (2015). The generation of antibody-secreting plasma cells. *Nat Rev Immunol*, 15(3):160–71.

[288] Nwuba, R. I., Sodeinde, O., Anumudu, C. I., Omosun, Y. O., Odaibo, A. B., Holder, A. A., and Nwagwu, M. (2002). The human immune response to *Plasmodium falciparum* includes both antibodies that inhibit merozoite surface protein 1 secondary processing and blocking antibodies. *Infect Immun*, 70(9):5328–31.

[289] Obaldia, N., Meibalan, E., Sa, J. M., Ma, S., Clark, M. A., Mejia, P., Moraes Barros, R. R., Otero, W., Ferreira, M. U., Mitchell, J. R., Milner, D. A., Huttenhower, C., Wirth, D. F., Duraisingh, M. T., Wellems, T. E., and Marti, M. (2018). Bone marrow is a major parasite reservoir in *Plasmodium vivax* infection. *MBio*, 9(3).

[290] Oliveira, T. Y., Harris, E. E., Meyer, D., Jue, C. K., and Silva, W. A., J. (2012). Molecular evolution of a malaria resistance gene (DARC) in primates. *Immunogenetics*, 64(7):497–505.

[291] Olsson, L. and Kaplan, H. S. (1980). Human-human hybridomas producing monoclonal antibodies of predefined antigenic specificity. *Proc Natl Acad Sci U S A*, 77(9):5429–31.

[292] Opuni, K. F. M., Al-Majdoub, M., Yefremova, Y., El-Kased, R. F., Koy, C., and Glocker, M. O. (2018). Mass spectrometric epitope mapping. *Mass Spectrom Rev*, 37(2):229–241.

[293] Oracki, S. A., Walker, J. A., Hibbs, M. L., Corcoran, L. M., and Tarlinton, D. M. (2010). Plasma cell development and survival. *Immunol Rev*, 237(1):140–59.

[294] Ord, R. L., Caldeira, J. C., Rodriguez, M., Noe, A., Chackerian, B., Peabody, D. S., Gutierrez, G., and Lobo, C. A. (2014). A malaria vaccine candidate based on an epitope of the *Plasmodium falciparum* RH5 protein. *Malar J*, 13:326.

[295] Osier, F. H., Mackinnon, M. J., Crosnier, C., Fegan, G., Kamuyu, G., Wanaguru, M., Ogada, E., McDade, B., Rayner, J. C., Wright, G. J., and Marsh, K. (2014). New antigens for a multicomponent blood-stage malaria vaccine. *Sci Transl Med*, 6(247):247ra102.

[296] Pain, A., Bohme, U., Berry, A. E., Mungall, K., Finn, R. D., Jackson, A. P., Mourier, T., Mistry, J., Pasini, E. M., Aslett, M. A., Balasubrammaniam, S., Borgwardt, K., Brooks, K., Carret, C., Carver, T. J., Cherevach, I., Chillingworth, T., Clark, T. G., Galinski, M. R., Hall, N., Harper, D., Harris, D., Hauser, H., Ivens, A., Janssen, C. S., Keane, T., Larke, N., Lapp, S., Marti, M., Moule, S., Meyer, I. M., Ormond, D., Peters, N., Sanders, M., Sanders, S., Sargeant, T. J., Simmonds, M., Smith, F., Squares, R., Thurston, S., Tivey, A. R., Walker, D., White, B., Zuiderwijk, E., Churcher, C., Quail, M. A., Cowman, A. F., Turner, C. M., Rajandream, M. A., Kocken, C. H., Thomas, A. W., Newbold, C. I., Barrell, B. G., and Berriman, M. (2008). The genome of the simian and human malaria parasite *Plasmodium knowlesi*. *Nature*, 455(7214):799–803.

[297] Panichakul, T., Sattabongkot, J., Chotivanich, K., Sirichaisinthop, J., Cui, L., and Udomsangpetch, R. (2007). Production of erythropoietic cells in vitro for continuous culture of *Plasmodium vivax*. *Int J Parasitol*, 37(14):1551–7.

[298] Parashar, A., Aikat, B. K., Sehgal, S., and Naik, S. (1977). Cell mediated and humoral immunity in experimental *Plasmodium berghei* infection. *Trans R Soc Trop Med Hyg*, 71(6):474–80.

[299] Pasvol, G., Weatherall, D. J., and Wilson, R. J. (1980). The increased susceptibility of young red cells to invasion by the malarial parasite *Plasmodium falciparum*. *Br J Haematol*, 45(2):285–95.

[300] Paterakis, G. S., Lykopoulou, L., Papassotiriou, J., Stamulakatou, A., Kattamis, C., and Loukopoulos, D. (1993). Flow-cytometric analysis of reticulocytes in normal cord blood. *Acta Haematol*, 90(4):182–5.

[301] PATH (2011). Staying the course? malaria research and development in a time of economic uncertainty.

[302] Pattanasin, S., Proux, S., Chompasuk, D., Luwiradaj, K., Jacquier, P., Looareesuwan, S., and Nosten, F. (2003). Evaluation of a new *Plasmodium* lactate dehydrogenase assay (optimal-it) for the detection of malaria. *Trans R Soc Trop Med Hyg*, 97(6):672–4.

[303] Payne, R. O., Milne, K. H., Elias, S. C., Edwards, N. J., Douglas, A. D., Brown, R. E., Silk, S. E., Biswas, S., Miura, K., Roberts, R., Rampling, T. W., Venkatraman, N., Hodgson, S. H., Labbe, G. M., Halstead, F. D., Poulton, I. D., Nugent, F. L., de Graaf, H., Sukhtankar, P., Williams, N. C., Ockenhouse, C. F., Kathcart, A. K., Qabar, A. N., Waters, N. C., Soisson, L. A., Birkett, A. J., Cooke, G. S., Faust, S. N., Woods, C., Ivinson, K., McCarthy, J. S., Diggs, C. L., Vekemans, J., Long, C. A., Hill, A. V., Lawrie, A. M., Dutta, S., and Draper, S. J. (2016). Demonstration of the blood-stage *Plasmodium falciparum* controlled human malaria infection model to assess efficacy of the *P. falciparum* apical membrane antigen 1 vaccine, fmp2.1/AS01. *J Infect Dis*, 213(11):1743–51.

[304] Payne, R. O., Silk, S. E., Elias, S. C., Milne, K. H., Rawlinson, T. A., Llewellyn, D., Shakri, A. R., Jin, J., Labbe, G. M., Edwards, N. J., Poulton, I. D., Roberts, R., Farid, R., Jorgensen, T., Alanine, D. G., de Cassan, S. C., Higgins, M. K., Otto, T. D., McCarthy, J. S., de Jongh, W. A., Nicosia, A., Moyle, S., Hill, A. V., Berrie, E., Chitnis, C. E., Lawrie, A. M., and Draper, S. J.

(2017). Human vaccination against *Plasmodium vivax* Duffy-binding protein induces strain-transcending antibodies. *JCI Insight*, 2(12).

[305] Pejchal, R., Doores, K. J., Walker, L. M., Khayat, R., Huang, P. S., Wang, S. K., Stanfield, R. L., Julien, J. P., Ramos, A., Crispin, M., Depetris, R., Katpally, U., Marozsan, A., Cupo, A., Maloveste, S., Liu, Y., McBride, R., Ito, Y., Sanders, R. W., Ogohara, C., Paulson, J. C., Feizi, T., Scanlan, C. N., Wong, C. H., Moore, J. P., Olson, W. C., Ward, A. B., Poignard, P., Schief, W. R., Burton, D. R., and Wilson, I. A. (2011). A potent and broad neutralizing antibody recognizes and penetrates the HIV glycan shield. *Science*, 334(6059):1097–103.

[306] Phimpraphi, W., Paul, R. E., Yimsamran, S., Puangsa-art, S., Thanyavanich, N., Maneeboonyang, W., Prommongkol, S., Sornklom, S., Chaimungkun, W., Chavez, I. F., Blanc, H., Looareesuwan, S., Sakuntabhai, A., and SinghaSIVanon, P. (2008). Longitudinal study of *Plasmodium falciparum* and *Plasmodium vivax* in a Karen population in Thailand. *Malar J*, 7:99.

[307] Plotkin, S. (2014). History of vaccination. *Proceedings of the National Academy of Sciences*, 111(34):12283–12287.

[308] Pogo, A. O. and Chaudhuri, A. (2000). The Duffy protein: a malarial and chemokine receptor. *Semin Hematol*, 37(2):122–9.

[309] Poulsen, T. R., Jensen, A., Haurum, J. S., and Andersen, P. S. (2011). Limits for antibody affinity maturation and repertoire diversification in hypervaccinated humans. *J Immunol*, 187(8):4229–35.

[310] Poulsen, T. R., Meijer, P. J., Jensen, A., Nielsen, L. S., and Andersen, P. S. (2007). Kinetic, affinity, and diversity limits of human polyclonal antibody responses against tetanus toxoid. *J Immunol*, 179(6):3841–50.

[311] Prasad, C. S., Aparna, N., and Harendra Kumar, M. L. (2011). Exflagellated microgametes of *Plasmodium vivax* in human peripheral blood: an uncommon feature of malaria. *Indian J Hematol Blood Transfus*, 27(2):104–6.

[312] Price, R. N., Douglas, N. M., and Anstey, N. M. (2009). New developments in *Plasmodium vivax* malaria: severe disease and the rise of chloroquine resistance. *Curr Opin Infect Dis*, 22(5):430–5.

[313] Price, R. N., Tjitra, E., Guerra, C. A., Yeung, S., White, N. J., and Anstey, N. M. (2007). *Vivax* malaria: neglected and not benign. *Am J Trop Med Hyg*, 77(6 Suppl):79–87.

[314] Price, R. N., von Seidlein, L., Valecha, N., Nosten, F., Baird, J. K., and White, N. J. (2014). Global extent of chloroquine-resistant *Plasmodium vivax*: a systematic review and meta-analysis. *Lancet Infect Dis*, 14(10):982–91.

[315] Puschnik, A., Lau, L., Cromwell, E. A., Balmaseda, A., Zompi, S., and Harris, E. (2013). Correlation between dengue-specific neutralizing antibodies and serum avidity in primary and secondary dengue virus 3 natural infections in humans. *PLoS Negl Trop Dis*, 7(6):e2274.

[316] Rahimi, B. A., Thakkinstian, A., White, N. J., Sirivichayakul, C., Dondorp, A. M., and Chokejindachai, W. (2014). Severe *vivax* malaria: a systematic review and meta-analysis of clinical studies since 1900. *Malar J*, 13:481.

[317] Ranjan, A. and Chitnis, C. E. (1999). Mapping regions containing binding residues within functional domains of *Plasmodium vivax* and *Plasmodium knowlesi* erythrocyte-binding proteins. *Proc Natl Acad Sci U S A*, 96(24):14067–72.

[318] Rayner, J. C., Vargas-Serrato, E., Huber, C. S., Galinski, M. R., and Barnwell, J. W. (2001). A *Plasmodium falciparum* homologue of *Plasmodium vivax* reticulocyte binding protein (pvrbp1) defines a trypsin-resistant erythrocyte invasion pathway. *J Exp Med*, 194(11):1571–81.

[319] Reddy, K. S., Amlabu, E., Pandey, A. K., Mitra, P., Chauhan, V. S., and Gaur, D. (2015). Multiprotein complex between the GPI-anchored CyRPA with PFRH5 and PfRipr is crucial for *Plasmodium falciparum* erythrocyte invasion. *Proc Natl Acad Sci U S A*, 112(4):1179–84.

[320] Reddy, K. S., Pandey, A. K., Singh, H., Sahar, T., Emmanuel, A., Chitnis, C. E., Chauhan, V. S., and Gaur, D. (2014). Bacterially expressed full-length recombinant *Plasmodium falciparum* RH5 protein binds erythrocytes and elicits potent strain-transcending parasite-neutralizing antibodies. *Infect Immun*, 82(1):152–64.

[321] Reichert, J. M. (2011). Antibody-based therapeutics to watch in 2011. *MAbs*, 3(1):76–99.

[322] Reininger, L., Garcia, M., Tomlins, A., Muller, S., and Doerig, C. (2012). The *Plasmodium falciparum*, nima-related kinase Pfnek-4: a marker for asexual parasites committed to sexual differentiation. *Malar J*, 11:250.

[323] Rieckmann, K. H., Davis, D. R., and Hutton, D. C. (1989). *Plasmodium vivax* resistance to chloroquine? *Lancet*, 2(8673):1183–4.

[324] Ringe, R. P., Ozorowski, G., Rantalainen, K., Struwe, W. B., Matthews, K., Torres, J. L., Yasmeen, A., Cottrell, C. A., Ketas, T. J., LaBranche, C. C., Montefiori, D. C., Cupo, A., Crispin, M., Wilson, I. A., Ward, A. B., Sanders, R. W., Klasse, P. J., and Moore, J. P. (2017). Reducing V3 antigenicity and immunogenicity on soluble, native-like HIV-1 env SOSIP trimers. *J Virol*, 91(15).

[325] Roberts, D. R. and Andre, R. G. (1994). Insecticide resistance issues in vector-borne disease control. *Am J Trop Med Hyg*, 50(6 Suppl):21–34.

[326] Ross, R. (1897). On some peculiar pigmented cells found in two mosquitos fed on malarial blood. *Br Med J*, 2(1929):1786–8.

[327] Rossan, R. N. (1985). Cryopreservation of the blood stages of *Plasmodium falciparum* and *Plasmodium vivax* for in vivo studies. *Am J Trop Med Hyg*, 34(2):207–8.

[328] Roush, S. W., Murphy, T. V., and Vaccine-Preventable Disease Table Working, G. (2007). Historical comparisons of morbidity and mortality for vaccine-preventable diseases in the united states. *JAMA*, 298(18):2155–63.

[329] Russell, B., Suwanarusk, R., Borlon, C., Costa, F. T., Chu, C. S., Rijken, M. J., Sriprawat, K., Warter, L., Koh, E. G., Malleret, B., Colin, Y., Bertrand, O., Adams, J. H., D'Alessandro, U., Snounou, G., Nosten, F., and Renia, L. (2011). A reliable ex vivo invasion assay of human reticulocytes by *Plasmodium vivax*. *Blood*, 118(13):e74–81.

[330] Russell, P. F. (1955). Man's mastery of malaria. *Oxford University Press, London, United Kingdom*.

[331] Ryan, J. R., Stoute, J. A., Amon, J., Dunton, R. F., Mtalib, R., Koros, J., Owour, B., Luckhart, S., Wirtz, R. A., Barnwell, J. W., and Rosenberg, R. (2006). Evidence for transmission of *Plasmodium vivax* among a Duffy antigen negative population in Western Kenya. *Am J Trop Med Hyg*, 75(4):575–81.

[332] Sampath, S., Carrico, C., Janes, J., Gurumoorthy, S., Gibson, C., Melcher, M., Chitnis, C. E., Wang, R., Schief, W. R., and Smith, J. D. (2013). Glycan masking of *Plasmodium vivax* Duffy binding protein for probing protein binding function and vaccine development. *PLoS Pathog*, 9(6):e1003420.

[333] Sanger, R., Race, R. R., and Jack, J. (1955). The Duffy blood groups of New York negroes: the phenotype Fy (a-b-). *Br J Haematol*, 1(4):370–4.

[334] Santra, S., Tomaras, G. D., Warrier, R., Nicely, N. I., Liao, H. X., Pollara, J., Liu, P., Alam, S. M., Zhang, R., Cocklin, S. L., Shen, X., Duffy, R., Xia, S. M., Schutte, R. J., Pemble Iv, C. W., Dennison, S. M., Li, H., Chao, A., Vidnovic, K., Evans, A., Klein, K., Kumar, A., Robinson, J., Landucci, G., Forthal, D. N.,

Montefiori, D. C., Kaewkungwal, J., Nitayaphan, S., Pitisuttithum, P., Rerks-Ngarm, S., Robb, M. L., Michael, N. L., Kim, J. H., Soderberg, K. A., Giorgi, E. E., Blair, L., Korber, B. T., Moog, C., Shattock, R. J., Letvin, N. L., Schmitz, J. E., Moody, M. A., Gao, F., Ferrari, G., Shaw, G. M., and Haynes, B. F. (2015). Human non-neutralizing HIV-1 envelope monoclonal antibodies limit the number of founder viruses during sHIV mucosal infection in rhesus macaques. *PLoS Pathog*, 11(8):e1005042.

[335] Sarton, G. (1959.). A history of science. *Harvard University Press, Cambridge, Mass.*

[336] Saul, A. (1987). Kinetic constraints on the development of a malaria vaccine. *Parasite Immunol*, 9(1):1–9.

[337] Sauter, H. and Paige, C. J. (1987). Detection of normal B-cell precursors that give rise to colonies producing both kappa and lambda light immunoglobulin chains. *Proc Natl Acad Sci U S A*, 84(14):4989–93.

[338] Saylor, C., Dadachova, E., and Casadevall, A. (2009). Monoclonal antibody-based therapies for microbial diseases. *Vaccine*, 27 Suppl 6:G38–46.

[339] Scarselli, M., Arico, B., Brunelli, B., Savino, S., Di Marcello, F., Palumbo, E., Veggi, D., Ciucchi, L., Cartocci, E., Bottomley, M. J., Malito, E., Lo Surdo, P., Comanducci, M., Giuliani, M. M., Cantini, F., Dragonetti, S., Colaprico, A., Doro, F., Giannetti, P., Pallaoro, M., Brogioni, B., Tontini, M., Hilleringmann, M., Nardi-Dei, V., Banci, L., Pizza, M., and Rappuoli, R. (2011). Rational design of a meningococcal antigen inducing broad protective immunity. *Sci Transl Med*, 3(91):91ra62.

[340] Scott, K. L., Lecak, J., and Acker, J. P. (2005). Biopreservation of red blood cells: past, present, and future. *Transfus Med Rev*, 19(2):127–42.

[341] Seip, M. (1953). The reticulocyte maturation in the peripheral blood. *Chapter V:. Acta Med. Scand. 146, 49–69.*

[342] Sela-Culang, I., Kunik, V., and Ofran, Y. (2013). The structural basis of antibody-antigen recognition. *Front Immunol*, 4:302.

[343] Shakri, A. R., Rizvi, M. M., and Chitnis, C. E. (2012). Development of quantitative receptor-ligand binding assay for use as a tool to estimate immune responses against *Plasmodium vivax* Duffy binding protein Region ii. *J Immunoassay Immunochem*, 33(4):403–13.

[344] Sharma, V. P. (1996). Re-emergence of malaria in India. *Indian J Med Res*, 103:26–45.

[345] Sharrock, W. W., Suwanarusk, R., Lek-Uthai, U., Edstein, M. D., Kosaisavee, V., Travers, T., Jaidee, A., Sriprawat, K., Price, R. N., Nosten, F., and Russell, B. (2008). *Plasmodium vivax* trophozoites insensitive to chloroquine. *Malar J*, 7:94.

[346] Sheehy, S. H., Duncan, C. J., Elias, S. C., Collins, K. A., Ewer, K. J., Spencer, A. J., Williams, A. R., Halstead, F. D., Moretz, S. E., Miura, K., Epp, C., Dicks, M. D., Poulton, I. D., Lawrie, A. M., Berrie, E., Moyle, S., Long, C. A., Colloca, S., Cortese, R., Gilbert, S. C., Nicosia, A., Hill, A. V., and Draper, S. J. (2011). Phase ia clinical evaluation of the *Plasmodium falciparum* blood-stage antigen MSP1 in ChAd63 and MVA vaccine vectors. *Mol Ther*, 19(12):2269–76.

[347] Shute, P. G. and Maryon, M. (1974). Malaria in England past, present and future. *R Soc Health J*, 94(1):23–9.

[348] Siddiqui, A. A., Xainli, J., Schloegel, J., Carias, L., Ntumngia, F., Shoham, M., Casey, J. L., Foley, M., Adams, J. H., and King, C. L. (2012). Fine specificity of *Plasmodium vivax* Duffy binding protein binding engagement of the Duffy antigen on human erythrocytes. *Infect Immun*, 80(8):2920–8.

[349] Sigerist, H. E. (1960). Problems of historical-geographical pathology. *p. 299. In M. I. Roemer (ed.), Henry E. Sigerist on the sociology of medicine. MD Publications, New York, N.Y.*

[350] Singh, A. P., Ozwara, H., Kocken, C. H., Puri, S. K., Thomas, A. W., and Chitnis, C. E. (2005). Targeted deletion of *Plasmodium knowlesi* Duffy binding protein confirms its role in junction formation during invasion. *Mol Microbiol*, 55(6):1925–34.

[351] Singh, A. P., Puri, S. K., and Chitnis, C. E. (2002). Antibodies raised against receptor-binding domain of *Plasmodium knowlesi* Duffy binding protein inhibit erythrocyte invasion. *Molecular and biochemical parasitology*, 121(1):21–31.

[352] Singh, B. and Daneshvar, C. (2013). Human infections and detection of *Plasmodium knowlesi*. *Clin Microbiol Rev*, 26(2):165–84.

[353] Singh, B., Kim Sung, L., Matusop, A., Radhakrishnan, A., Shamsul, S. S., Cox-Singh, J., Thomas, A., and Conway, D. J. (2004). A large focus of naturally acquired *Plasmodium knowlesi* infections in human beings. *Lancet*, 363(9414):1017–24.

[354] Singh, K., Gitti, R. K., Diouf, A., Zhou, H., Gowda, D. C., Miura, K., Ostazeski, S. A., Fairhurst, R. M., Garboczi, D. N., and Long, C. A. (2010). Subdomain 3 of *Plasmodium falciparum* var2csa dbl3x is identified as a minimal chondroitin sulfate a-binding region. *J Biol Chem*, 285(32):24855–62.

[355] Singh, K., Gittis, A. G., Nguyen, P., Gowda, D. C., Miller, L. H., and Garboczi, D. N. (2008). Structure of the dbl3x domain of pregnancy-associated malaria protein var2csa complexed with chondroitin sulfate a. *Nat Struct Mol Biol*, 15(9):932–8.

[356] Singh, S., Miura, K., Zhou, H., Muratova, O., Keegan, B., Miles, A., Martin, L. B., Saul, A. J., Miller, L. H., and Long, C. A. (2006a). Immunity to recombinant *Plasmodium falciparum* merozoite surface protein 1 (MSP1):

protection in *Aotus nancymai* monkeys strongly correlates with anti-MSP1 antibody titer and in vitro parasite-inhibitory activity. *Infect Immun*, 74(8):4573–80.

[357] Singh, S. K., Hora, R., Belrhali, H., Chitnis, C. E., and Sharma, A. (2006b). Structural basis for Duffy recognition by the malaria parasite Duffy-binding-like domain. *Nature*, 439(7077):741–4.

[358] Sinha, A., Singh, G., Bhat, A. S., Mohapatra, S., Gulati, A., Hari, P., Samantaray, J. C., Dinda, A. K., Agarwal, S. K., and Bagga, A. (2013). Thrombotic microangiopathy and acute kidney injury following *vivax* malaria. *Clin Exp Nephrol*, 17(1):66–72.

[359] Slifka, M. K., Antia, R., Whitmire, J. K., and Ahmed, R. (1998). Humoral immunity due to long-lived plasma cells. *Immunity*, 8(3):363–72.

[360] Smith, J. D., Chitnis, C. E., Craig, A. G., Roberts, D. J., Hudson-Taylor, D. E., Peterson, D. S., Pinches, R., Newbold, C. I., and Miller, L. H. (1995). Switches in expression of *Plasmodium falciparum* var genes correlate with changes in antigenic and cytoadherent phenotypes of infected erythrocytes. *Cell*, 82(1):101–10.

[361] Smith, K., Garman, L., Wrammert, J., Zheng, N. Y., Capra, J. D., Ahmed, R., and Wilson, P. C. (2009). Rapid generation of fully human monoclonal antibodies specific to a vaccinating antigen. *Nat Protoc*, 4(3):372–84.

[362] Smith, T., Killeen, G. F., Maire, N., Ross, A., Molineaux, L., Tediosi, F., Hutton, G., Utzinger, J., Dietz, K., and Tanner, M. (2006). Mathematical modeling of the impact of malaria vaccines on the clinical epidemiology and natural history of *Plasmodium falciparum* malaria: Overview. *Am J Trop Med Hyg*, 75(2 Suppl):1–10.

[363] Smith, T., Ross, A., Maire, N., Chitnis, N., Studer, A., Hardy, D., Brooks, A., Penny, M., and Tanner, M. (2012). Ensemble modeling of the likely public health impact of a pre-erythrocytic malaria vaccine. *PLoS Med*, 9(1):e1001157.

[364] Smolarek, D., Hattab, C., Hassanzadeh-Ghassabeh, G., Cochet, S., Gutierrez, C., de Brevern, A. G., Udomsangpetch, R., Picot, J., Grodecka, M., Wasniowska, K., Muyldermans, S., Colin, Y., Le Van Kim, C., Czerwinski, M., and Bertrand, O. (2010). A recombinant dromedary antibody fragment (vhh or nanobody) directed against human Duffy antigen receptor for chemokines. *Cell Mol Life Sci*, 67(19):3371–87.

[365] Soriani, M., Petit, P., Grifantini, R., Petracca, R., Gancitano, G., Frigimelica, E., Nardelli, F., Garcia, C., Spinelli, S., Scarabelli, G., Fiorucci, S., Affentranger, R., Ferrer-Navarro, M., Zacharias, M., Colombo, G., Vuillard, L., Daura, X., and Grandi, G. (2010). Exploiting antigenic diversity for vaccine design: the chlamydia artj paradigm. *J Biol Chem*, 285(39):30126–38.

[366] Soto, J., Toledo, J., Gutierrez, P., Luzz, M., Llinas, N., Cedeno, N., Dunne, M., and Berman, J. (2001). *Plasmodium vivax* clinically resistant to chloroquine in Colombia. *Am J Trop Med Hyg*, 65(2):90–3.

[367] Sriprawat, K., Kaewpongsri, S., Suwanarusk, R., Leimanis, M. L., Lek-Uthai, U., Phyo, A. P., Snounou, G., Russell, B., Renia, L., and Nosten, F. (2009). Effective and cheap removal of leukocytes and platelets from *Plasmodium vivax* infected blood. *Malar J*, 8:115.

[368] Steckbeck, J. D., Orlov, I., Chow, A., Grieser, H., Miller, K., Bruno, J., Robinson, J. E., Montelaro, R. C., and Cole, K. S. (2005). Kinetic rates of antibody binding correlate with neutralization sensitivity of variant simian immunodeficiency virus strains. *J Virol*, 79(19):12311–20.

[369] Steel, J., Lowen, A. C., Wang, T. T., Yondola, M., Gao, Q., Haye, K., Garcia-Sastre, A., and Palese, P. (2010). Influenza virus vaccine based on the conserved hemagglutinin stalk domain. *MBio*, 1(1).

[370] Stokes, J. (1918). The third great plague: A discussion of syphilis for everyday people. *W.B. Saunders Company, Philadelphia.*

[371] Su, X. Z., Heatwole, V. M., Wertheimer, S. P., Guinet, F., Herrfeldt, J. A., Peterson, D. S., Ravetch, J. A., and Wellems, T. E. (1995). The large diverse gene family var encodes proteins involved in cytoadherence and antigenic variation of *Plasmodium falciparum*-infected erythrocytes. *Cell*, 82(1):89–100.

[372] Takala, S. L., Coulibaly, D., Thera, M. A., Batchelor, A. H., Cummings, M. P., Escalante, A. A., Ouattara, A., Traore, K., Niangaly, A., Djimde, A. A., Doumbo, O. K., and Plowe, C. V. (2009). Extreme polymorphism in a vaccine antigen and risk of clinical malaria: implications for vaccine development. *Sci Transl Med*, 1(2):2ra5.

[373] Tao, Z. Y., Xia, H., Cao, J., and Gao, Q. (2011). Development and evaluation of a prototype non-woven fabric filter for purification of malaria-infected blood. *Malar J*, 10:251.

[374] Tarlinton, D. and Good-Jacobson, K. (2013). Diversity among memory B cells: origin, consequences, and utility. *Science*, 341(6151):1205–11.

[375] Tatem, A. J., Smith, D. L., Gething, P. W., Kabaria, C. W., Snow, R. W., and Hay, S. I. (2010). Ranking of elimination feasibility between malaria-endemic countries. *Lancet*, 376(9752):1579–91.

[376] Tham, W. H., Beeson, J. G., and Rayner, J. C. (2017). *Plasmodium vivax* vaccine research - we've only just begun. *Int J Parasitol*, 47(2-3):111–118.

[377] Thiberge, S., Blazquez, S., Baldacci, P., Renaud, O., Shorte, S., Menard, R., and Amino, R. (2007). In vivo imaging of malaria parasites in the murine liver. *Nat Protoc*, 2(7):1811–8.

[378] Thomas, J. A., Collins, C. R., Das, S., Hackett, F., Graindorge, A., Bell, D., Deu, E., and Blackman, M. J. (2016). Development and application of a simple

plaque assay for the human malaria parasite *Plasmodium falciparum*. *PLoS One*, 11(6):e0157873.

[379] Thomas, M. J. and Bell, S. H. (1995). Cryopreservation of human red blood cells. *Methods Mol Biol*, 38:235–50.

[380] Thomson-Luque, R., Shaw Saliba, K., Kocken, C. H. M., and Pasini, E. M. (2017). A continuous, long-term *Plasmodium vivax* in vitro blood-stage culture: What are we missing? *Trends Parasitol*, 33(12):921–924.

[381] Tiller, T., Meffre, E., Yurasov, S., Tsuiji, M., Nussenzweig, M. C., and Wardemann, H. (2008). Efficient generation of monoclonal antibodies from single human B cells by single cell rt-PCR and expression vector cloning. *J Immunol Methods*, 329(1-2):112–24.

[382] Tomaras, G. D. and Haynes, B. F. (2010). Strategies for eliciting HIV-1 inhibitory antibodies. *Curr Opin HIV AIDS*, 5(5):421–7.

[383] Tournamille, C., Blancher, A., Le Van Kim, C., Gane, P., Apoil, P. A., Nakamoto, W., Cartron, J. P., and Colin, Y. (2004). Sequence, evolution and ligand binding properties of mammalian Duffy antigen/receptor for chemokines. *Immunogenetics*, 55(10):682–94.

[384] Tournamille, C., Colin, Y., Cartron, J. P., and Le Van Kim, C. (1995a). Disruption of a gata motif in the Duffy gene promoter abolishes erythroid gene expression in Duffy-negative individuals. *Nat Genet*, 10(2):224–8.

[385] Tournamille, C., Le Van Kim, C., Gane, P., Blanchard, D., Proudfoot, A. E., Cartron, J. P., and Colin, Y. (1997). Close association of the first and fourth extracellular domains of the Duffy antigen/receptor for chemokines by a disulfide bond is required for ligand binding. *J Biol Chem*, 272(26):16274–80.

[386] Tournamille, C., Le Van Kim, C., Gane, P., Cartron, J. P., and Colin, Y. (1995b). Molecular basis and PCR-DNA typing of the fya/fyb blood group polymorphism. *Hum Genet*, 95(4):407–10.

[387] Tournamille, C., Le Van Kim, C., Gane, P., Le Pennec, P. Y., Roubinet, F., Babinet, J., Cartron, J. P., and Colin, Y. (1998). Arg89cys substitution results in very low membrane expression of the Duffy antigen/receptor for chemokines in fy(x) individuals. *Blood*, 92(6):2147–56.

[388] Trager, W. and Jensen, J. B. (1976). Human malaria parasites in continuous culture. *Science*, 193(4254):673–5.

[389] Tran, T. M., Ongoiba, A., Coursen, J., Crosnier, C., Diouf, A., Huang, C. Y., Li, S., Doumbo, S., Doumtabe, D., Kone, Y., Bathily, A., Dia, S., Niangaly, M., Dara, C., Sangala, J., Miller, L. H., Doumbo, O. K., Kayentao, K., Long, C. A., Miura, K., Wright, G. J., Traore, B., and Crompton, P. D. (2014). Naturally acquired antibodies specific for *Plasmodium falciparum* reticulocyte-binding protein homologue 5 inhibit parasite growth and predict protection from malaria. *J Infect Dis*, 209(5):789–98.

[390] Tran, T. M., Portugal, S., Draper, S. J., and Crompton, P. D. (2015). Malaria vaccines: Moving forward after encouraging first steps. *Curr Trop Med Rep*, 2(1):1–3.

[391] Tsuboi, T., Kappe, S. H., al Yaman, F., Prickett, M. D., Alpers, M., and Adams, J. H. (1994). Natural variation within the principal adhesion domain of the *Plasmodium vivax* Duffy binding protein. *Infect Immun*, 62(12):5581–6.

[392] Udomsangpetch, R., Somsri, S., Panichakul, T., Chotivanich, K., Sirichaisinthop, J., Yang, Z., Cui, L., and Sattabongkot, J. (2007). Short-term in vitro culture of field isolates of *Plasmodium vivax* using umbilical cord blood. *Parasitol Int*, 56(1):65–9.

[393] Unciti-Broceta, J. D., Del Castillo, T., Soriano, M., Magez, S., and Garcia-Salcedo, J. A. (2013). Novel therapy based on camelid nanobodies. *Ther Deliv*, 4(10):1321–36.

[394] Valecha, N., Pinto, R. G., Turner, G. D., Kumar, A., Rodrigues, S., Dubhashi, N. G., Rodrigues, E., Banaulikar, S. S., Singh, R., Dash, A. P., and Baird, J. K. (2009). Histopathology of fatal respiratory distress caused by *Plasmodium vivax* malaria. *Am J Trop Med Hyg*, 81(5):758–62.

[395] van der Wel, A. M., Tomas, A. M., Kocken, C. H., Malhotra, P., Janse, C. J., Waters, A. P., and Thomas, A. W. (1997). Transfection of the primate malaria parasite *Plasmodium knowlesi* using entirely heterologous constructs. *J Exp Med*, 185(8):1499–503.

[396] Van Oss, C. J. (1995). Hydrophobic, hydrophilic and other interactions in epitope-paratope binding. *Mol Immunol*, 32(3):199–211.

[397] VanBuskirk, K. M., Cole-Tobian, J. L., Baisor, M., Sevova, E. S., Bockarie, M., King, C. L., and Adams, J. H. (2004a). Antigenic drift in the ligand domain of *Plasmodium vivax* Duffy binding protein confers resistance to inhibitory antibodies. *J Infect Dis*, 190(9):1556–62.

[398] VanBuskirk, K. M., Sevova, E., and Adams, J. H. (2004b). Conserved residues in the *Plasmodium vivax* Duffy-binding protein ligand domain are critical for erythrocyte receptor recognition. *Proc Natl Acad Sci U S A*, 101(44):15754–9.

[399] Vanloubbeeck, Y., Pichyangkul, S., Bayat, B., Yongvanitchit, K., Bennett, J. W., Sattabongkot, J., Schaecher, K., Ockenhouse, C. F., Cohen, J., Yadava, A., and group, P. t. v. s. (2013). Comparison of the immune responses induced by soluble and particulate *Plasmodium vivax* circumsporozoite vaccine candidates formulated in AS01 in rhesus macaques. *Vaccine*, 31(52):6216–24.

[400] Volkman, S. K., Barry, A. E., Lyons, E. J., Nielsen, K. M., Thomas, S. M., Choi, M., Thakore, S. S., Day, K. P., Wirth, D. F., and Hartl, D. L. (2001). Recent origin of *Plasmodium falciparum* from a single progenitor. *Science*, 293(5529):482–4.

[401] Volz, J. C., Yap, A., Sisquella, X., Thompson, J. K., Lim, N. T., Whitehead, L. W., Chen, L., Lampe, M., Tham, W. H., Wilson, D., Nebl, T., Marapana, D., Triglia, T., Wong, W., Rogers, K. L., and Cowman, A. F. (2016). Essential role of the pfrh5/pfripr/cyrpa complex during *Plasmodium falciparum* invasion of erythrocytes. *Cell Host Microbe*, 20(1):60–71.

[402] Wagner, J. C., Platt, R. J., Goldfless, S. J., Zhang, F., and Niles, J. C. (2014). Efficient CRISPR-Cas9-mediated genome editing in *Plasmodium falciparum*. *Nat Methods*, 11(9):915–8.

[403] Wagner-Jauregg, J. and Bruetsch, W. L. (1946). The history of the malaria treatment of general paralysis. *Am J Psychiatry*, 102:577–82.

[404] Wahala, W. M. and Silva, A. M. (2011). The human antibody response to dengue virus infection. *Viruses*, 3(12):2374–95.

[405] Walter, G. (1986). Production and use of antibodies against synthetic peptides. *J Immunol Methods*, 88(2):149–61.

[406] Wang, X., Jiang, Y., Zhu, Y., Zhang, M., Li, M., Wang, H., and Gao, P. (2016). Circulating memory B cells and plasmablasts are associated with the levels of serum immunoglobulin in patients with ulcerative colitis. *J Cell Mol Med*, 20(5):804–14.

[407] Wasniowska, K., Petit-LeRoux, Y., Tournamille, C., Le van Kim, C., Cartron, J. P., Colin, Y., Lisowska, E., and Blanchard, D. (2002). Structural characterization of the epitope recognized by the new anti-fy6 monoclonal antibody nam 185-2c3. *Transfus Med*, 12(3):205–11.

[408] Weatherall, D. J. and Clegg, J. B. (2001). Inherited haemoglobin disorders: an increasing global health problem. *Bull World Health Organ*, 79(8):704–12.

[409] Wei, C. J., Boyington, J. C., McTamney, P. M., Kong, W. P., Pearce, M. B., Xu, L., Andersen, H., Rao, S., Tumpey, T. M., Yang, Z. Y., and Nabel, G. J.

(2010). Induction of broadly neutralizing H1N1 influenza antibodies by vaccination. *Science*, 329(5995):1060–4.

[410] Weiss, G. E., Crabb, B. S., and Gilson, P. R. (2016). Overlaying molecular and temporal aspects of malaria parasite invasion. *Trends Parasitol*, 32(4):284–295.

[411] Weiss, G. E., Gilson, P. R., Taechalertpaisarn, T., Tham, W. H., de Jong, N. W., Harvey, K. L., Fowkes, F. J., Barlow, P. N., Rayner, J. C., Wright, G. J., Cowman, A. F., and Crabb, B. S. (2015). Revealing the sequence and resulting cellular morphology of receptor-ligand interactions during *Plasmodium falciparum* invasion of erythrocytes. *PLoS Pathog*, 11(2):e1004670.

[412] Wells, T. N., Burrows, J. N., and Baird, J. K. (2010). Targeting the hypnozoite reservoir of *Plasmodium vivax*: the hidden obstacle to malaria elimination. *Trends Parasitol*, 26(3):145–51.

[413] Wertheimer, S. P. and Barnwell, J. W. (1989). *Plasmodium vivax* interaction with the human Duffy blood group glycoprotein: identification of a parasite receptor-like protein. *Exp Parasitol*, 69(4):340–50.

[414] White, N. J. (2011). Determinants of relapse periodicity in *Plasmodium vivax* malaria. *Malar J*, 10:297.

[415] WHO (1948). Report of the second session. Malarial control survey and recommendations. *Bulletin WHO*, pages 1:213–252.

[416] WHO (1999). The World Health Report. Rolling Back Malaria. *World Health Organization, Geneva, Switzerland.*, pages 49–63.

[417] WHO (2014). World Malaria Report.

[418] WHO (2017). World Malaria Report.

[419] William, T., Rahman, H. A., Jelip, J., Ibrahim, M. Y., Menon, J., Grigg, M. J., Yeo, T. W., Anstey, N. M., and Barber, B. E. (2013). Increasing incidence of *Plasmodium knowlesi* malaria following control of *P. falciparum* and *P. vivax* malaria in Sabah, Malaysia. *PLoS Negl Trop Dis*, 7(1):e2026.

[420] Williams, T. N., Maitland, K., Phelps, L., Bennett, S., Peto, T., Viji, J., Timothy, R., Clegg, J. B., Weatherall, D., and Bowden, D. (1997). *Plasmodium vivax*: a cause of malnutrition in young children. *QJM 90: 751–757.*

[421] Wilson, R. J., Pasvol, G., and Weatherall, D. J. (1977). Invasion and growth of *Plasmodium falciparum* in different types of human erythrocyte. *Bull World Health Organ*, 55(2-3):179–86.

[422] Wilson, R. J. and Williamson, D. H. (1997). Extrachromosomal DNA in the *Apicomplexa*. *Microbiol Mol Biol Rev*, 61(1):1–16.

[423] Wine, Y., Boutz, D. R., Lavinder, J. J., Miklos, A. E., Hughes, R. A., Hoi, K. H., Jung, S. T., Horton, A. P., Murrin, E. M., Ellington, A. D., Marcotte, E. M., and Georgiou, G. (2013). Molecular deconvolution of the monoclonal antibodies that comprise the polyclonal serum response. *Proc Natl Acad Sci U S A*, 110(8):2993–8.

[424] Winger, L., Winger, C., Shastry, P., Russell, A., and Longenecker, M. (1983). Efficient generation in vitro, from human peripheral blood cells, of monoclonal Epstein-Barr virus transformants producing specific antibody to a variety of antigens without prior deliberate immunization. *Proc Natl Acad Sci U S A*, 80(14):4484–8.

[425] Woolley, I. J., Wood, E. M., Sramkoski, R. M., Zimmerman, P. A., Miller, J. P., and Kazura, J. W. (2005). Expression of Duffy antigen receptor for chemokines during reticulocyte maturation: using a CD71 flow cytometric technique to identify reticulocytes. *Immunohematology*, 21(1):15–20.

[426] Wrammert, J., Smith, K., Miller, J., Langley, W. A., Kokko, K., Larsen, C., Zheng, N. Y., Mays, I., Garman, L., Helms, C., James, J., Air, G. M., Capra, J. D., Ahmed, R., and Wilson, P. C. (2008). Rapid cloning of high-affinity human monoclonal antibodies against influenza virus. *Nature*, 453(7195):667–71.

[427] Wu, Y., Ellis, R. D., Shaffer, D., Fontes, E., Malkin, E. M., Mahanty, S., Fay, M. P., Narum, D., Rausch, K., Miles, A. P., Aebig, J., Orcutt, A., Muratova, O., Song, G., Lambert, L., Zhu, D., Miura, K., Long, C., Saul, A., Miller, L. H., and Durbin, A. P. (2008). Phase 1 trial of malaria transmission blocking vaccine candidates Pfs25 and Pvs25 formulated with montanide ISA 51. *PLoS One*, 3(7):e2636.

[428] Xainli, J., Adams, J. H., and King, C. L. (2000). The erythrocyte binding motif of *Plasmodium vivax* Duffy binding protein is highly polymorphic and functionally conserved in isolates from Papua New Guinea. *Mol Biochem Parasitol*, 111(2):253–60.

[429] Xainli, J., Baisor, M., Kastens, W., Bockarie, M., Adams, J. H., and King, C. L. (2002). Age-dependent cellular immune responses to *Plasmodium vivax* Duffy binding protein in humans. *J Immunol*, 169(6):3200–7.

[430] Yang, X., Tomov, V., Kurteva, S., Wang, L., Ren, X., Gorny, M. K., Zolla-Pazner, S., and Sodroski, J. (2004). Characterization of the outer domain of the gp120 glycoprotein from human immunodeficiency virus type 1. *J Virol*, 78(23):12975–86.

[431] Ye, J., Ma, N., Madden, T. L., and Ostell, J. M. (2013). IgBLAST: an immunoglobulin variable domain sequence analysis tool. *Nucleic Acids Res*, 41(Web Server issue):W34–40.

[432] Zimmerman, P. A., Ferreira, M. U., Howes, R. E., and Mercereau-Puijalon, O. (2013). Red blood cell polymorphism and susceptibility to *Plasmodium vivax*. *Adv Parasitol*, 81:27–76.

[433] Zischewski, J., Fischer, R., and Bortesi, L. (2017). Detection of on-target and off-target mutations generated by CRISPR/Cas9 and other sequence-specific nucleases. *Biotechnol Adv*, 35(1):95–104.